SEDIMENTOLOGICAL STUDIES OF THE PALEOGENE SANDSTONES AROUND BOTSA, KOHIMA DISTRICT, NAGALAND

THESIS SUBMITTED IN FULFILMENT OF THE DEGREE OF DOCTOR OF PHILOSOPHY

GLENN. THOMAS THONG

1993

<u>CERTIFICATE</u>

The thesis presented by Mr. G.T. Thong, M.Sc., Lecturer, Deptt. of Geology, Kohima Science College, Jotsoma, embodies the results of investigations carried out by him under my supervision and guidance.

I certify that this work has not been presented for any degree elsewhere and that the candidate has fulfilled all conditions laid down by the University.

24.2.93
(Dr. R.N. SARMAH)
Reader and Head,
Deptt. of Geology,
North-Eastern Hill University,
Nagaland Campus, Kohima.

Forwarded
01.3.93
HEAD
Department of Geology
NEHU, Nagaland Campus : Kohima

ACKNOWLEDGEMENT

I am indebted to Dr. R.N. Sarmah, Reader and Head of the Department of Geology, North-Eastern Hill University, Nagaland Campus, Kohima, for his constant guidance and valuable advice throughout the work. My sincerest thanks to Prof. S.K.Dutta, Ph.D., D.Sc., Prof. T. Kataki, Ph.D., and Mr. Ranjan Sarma, M.Tech., Lecturer, all of the Department of Applied Geology, Dibrugarh University, for their help. I am equally grateful to Dr. N. Pandey, Lecturer, Department of Geology, NEHU and to Dr. J.C. Das, Lecturer in Chemistry, Mr. G. Kalita, Head of the Department of Geology and Mr. B.N. Baishya, Lecturer in Geology, all of the Kohima Science College, Jotsoma, for their useful suggestions and contributions. Thanks are also due to Mr. J. Raibaruah, Department of Census, Government of India, Nagaland, Kohima, for his immense contribution. The chemical and clay mineral analyses by the Geological Survey of India, Calcutta, is gratefully acknowledged.

It would not be out of place here to mention the help rendered by Mrs. R.N. Sarmah. Mr. M. Sarmah, my wife Rosemary, and my father-in-law, Mr. P.S. Dzüvichü, who have contributed much in bringing out this thesis.

G.T.Thong
24/2/93

(GLENN THOMAS THONG)
Lecturer,
Deptt. of Geology,
Kohima Science College,
Jotsoma, Nagaland.

CONTENTS

PART I

PART II

DISANG GROUP

LIST OF FIGURES

(Figures follow relevant pages)

LIST OF TABLES

(Tables follow relevant pages)

GEOGRAPHIC LOCATIONS OF SOME IMPORTANT PLACES OF NAGALAND

PLACE	LATITUDE	LONGITUDE
Kohima	25°40' N	94°66' E
Mokokchung	26°19' N	94°31' E
Tuensang	26°15' N	94°49' E
Zunheboto	25°52' N	94°32' E
Phek	25°20' N	94°30' E
Mon	26°35' N	95°05' E
Wokha	26°06' N	94°15' E
Dimapur	25°54' N	93°45' E

PART I

CHAPTER I

INTRODUCTION

Nagaland, the sixteenth state of the Indian Union, lies on the north-eastern border of India with Myanmar in the east, Manipur in the south, Arunachal Pradesh on the north-west and Assam covering the entire west (Fig. 1.1).

Geographically, Nagaland constitutes the northern part of the Indo-Burmese range, being the western-most morphotectonic unit of the Burmese orogen. To the north it continues into the eastern syntaxial bend of the Himalayas. The central lowlands of Burma lie on its east and the Mikir Hill Precambrian Massif and the Brahmaputra trough containing Miocene to Quaternary sediments lie in the west.

1.1. LOCATION OF THE AREA :

The area under investigation includes Botsa and its surroundings, in Kohima district. Botsa lies on the Kohima-Wokha state highway, about 37 kms. to the north of Kohima town (Fig. 1.2). The total area under investigation is approximately 100 sq.kms. It is incorporated in toposheet no. 83 K/1 of the Survey of India and is bounded by latitudes 25°50' & 26°00' and longitudes 94°05' & 94°15'.

1.2. REVIEW OF THE GEOLOGY OF NAGALAND :

The stratigraphy of Assam and Nagaland (Fig. 1.3), as established by Mathur and Evans (1964), is shown in table 1.1.

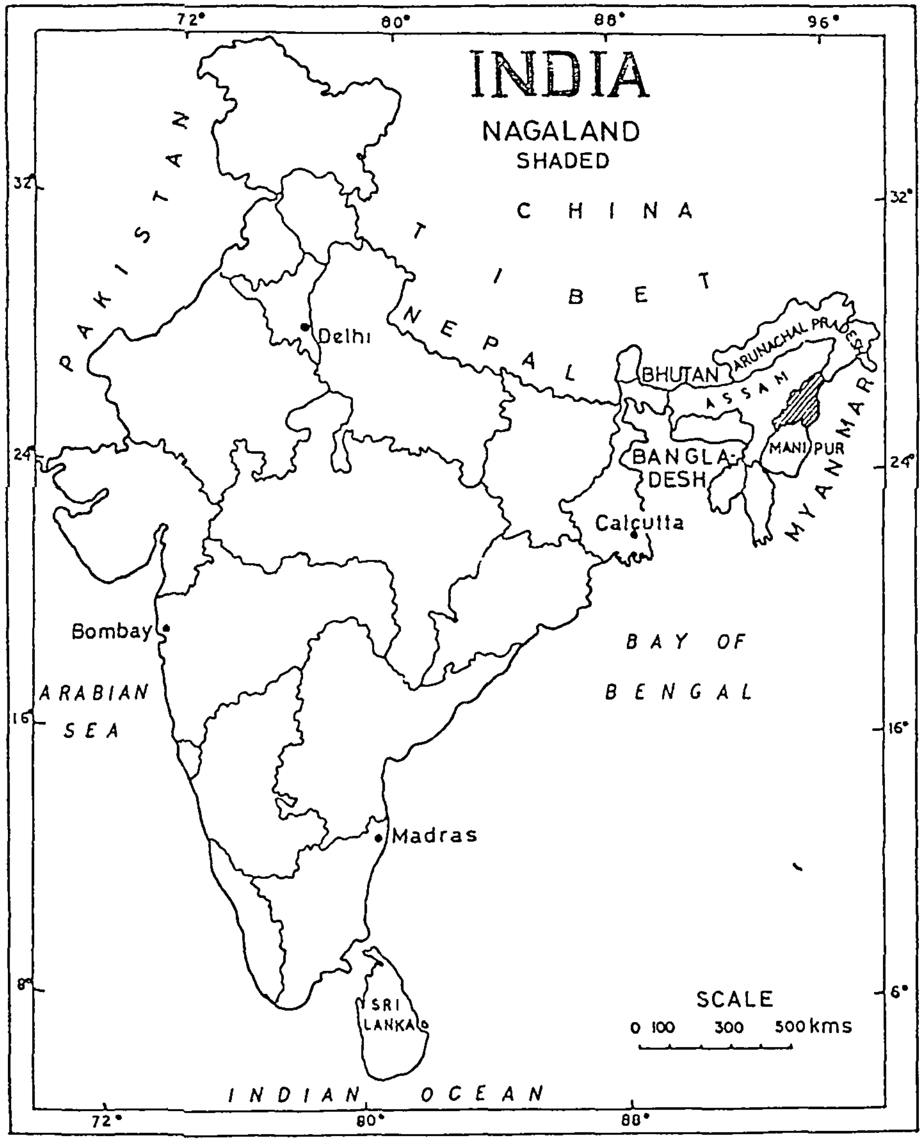
INDIA
NAGALAND
SHADED
CHINA
TIBET
PAKISTAN
NEPAL
BHUTAN
ARUNACHAL PRADESH
ASSAM
MANIPUR
MYANMAR
BANGLA-DESH
Delhi
Calcutta
Bombay
Madras
SRI LANKA
ARABIAN SEA
BAY OF BENGAL
INDIAN OCEAN
SCALE
0 100 300 500kms

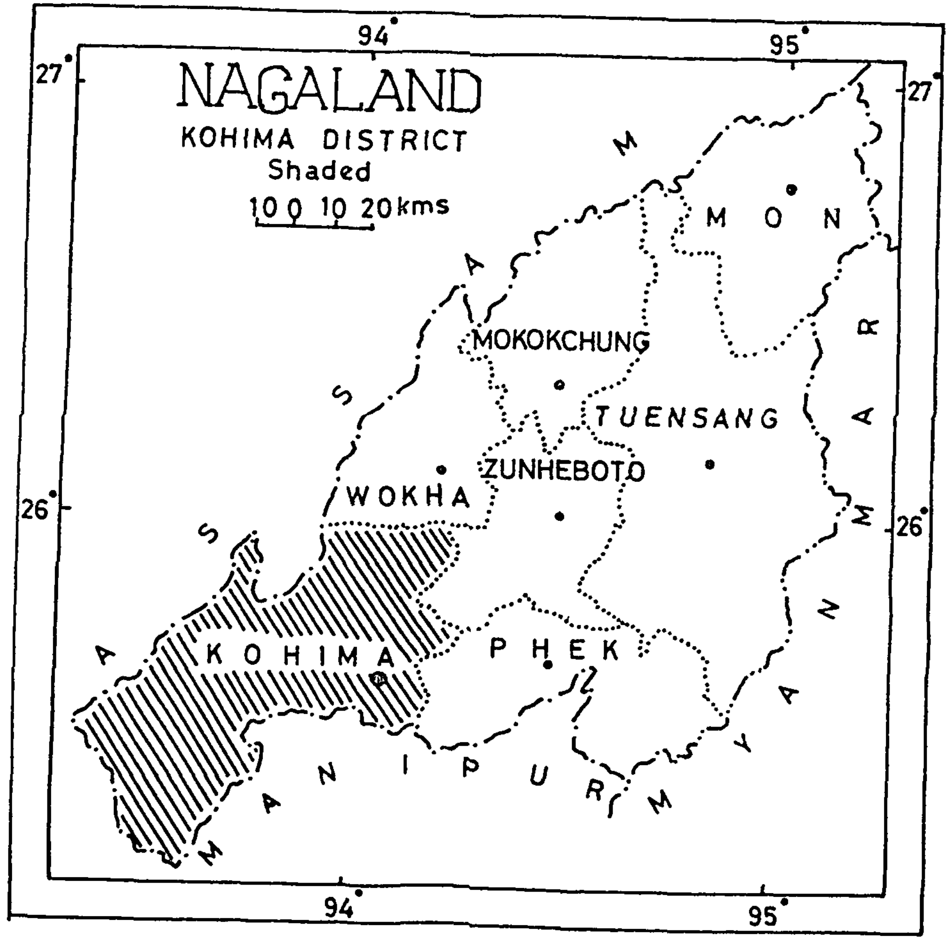
NAGALAND
KOHIMA DISTRICT
Shaded
10 0 10 20kms
MON
MOKOKCHUNG
TUENSANG
ZUNHEBOTO
WOKHA
KOHIMA
PHEK
ASSAM
MANIPUR
MYANMAR

FIG: 1·1

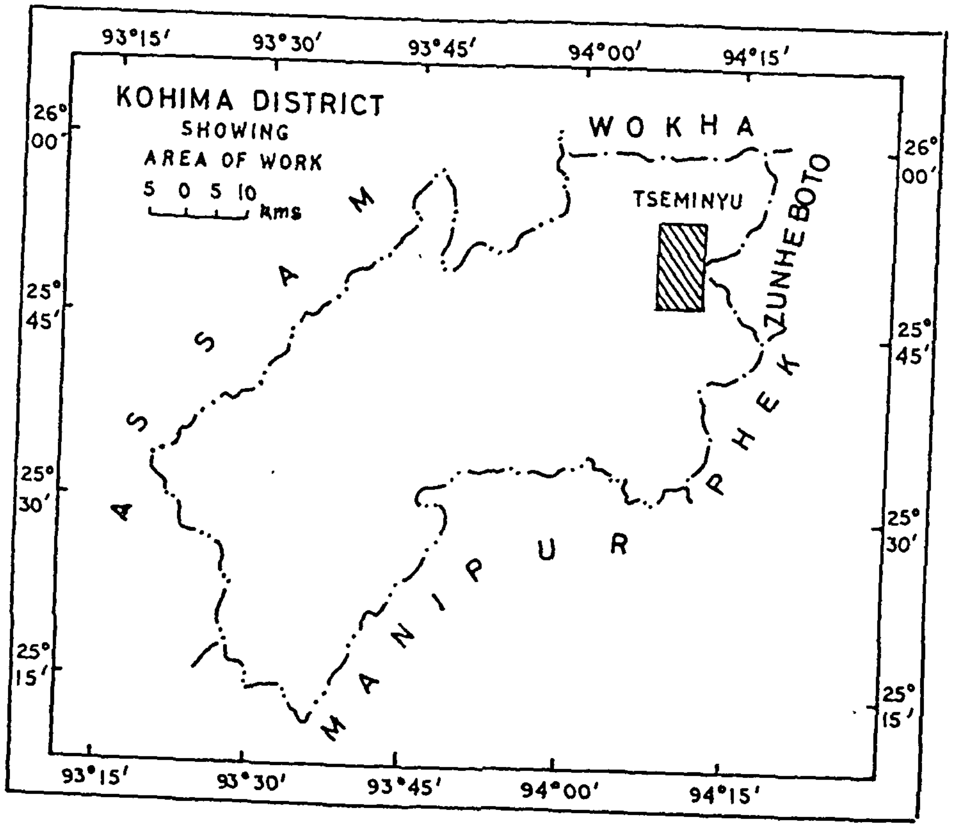

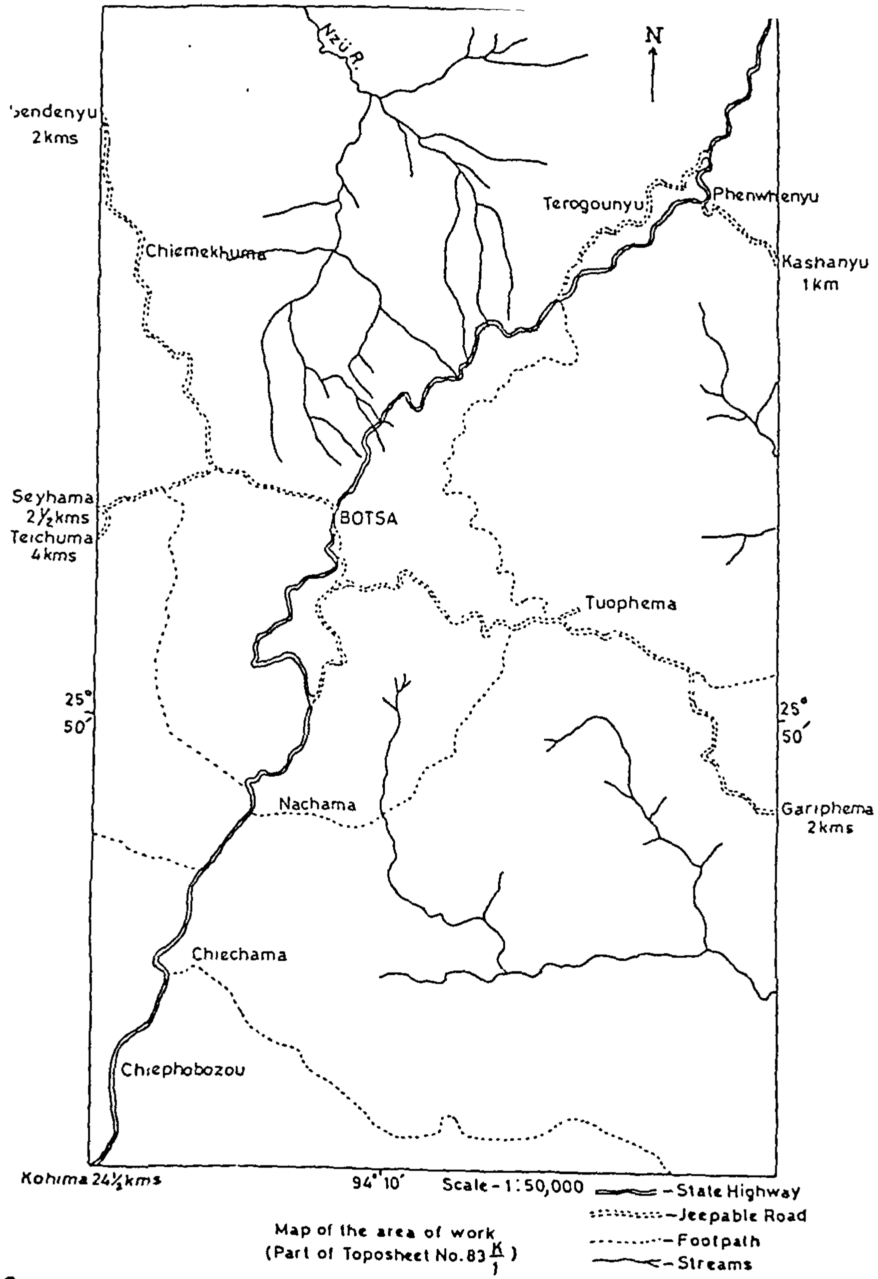

Map of the area of work
(Part of Toposheet No. 83 $\frac{K}{1}$)

FIG: 1·2

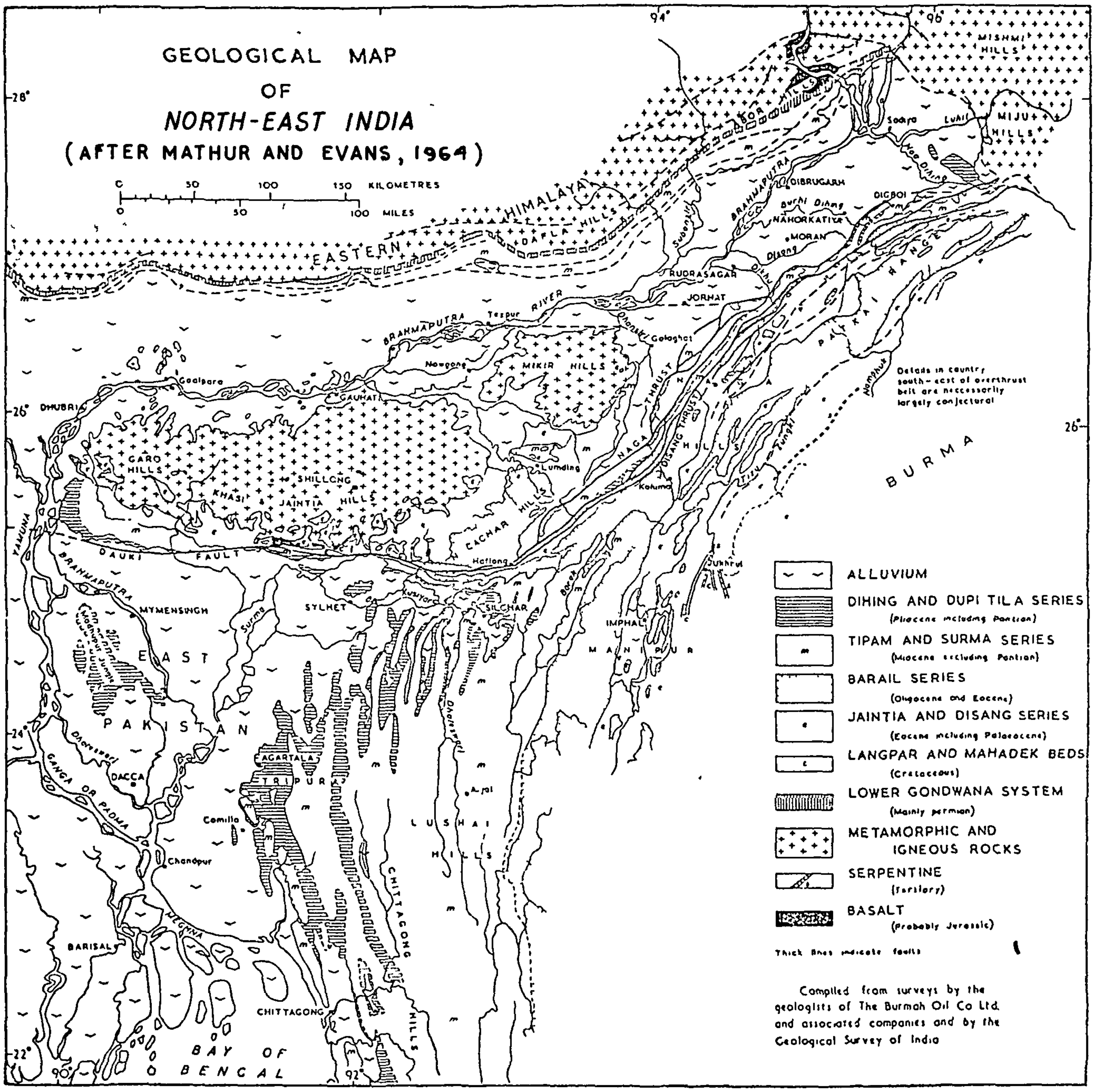
GEOLOGICAL MAP
OF
NORTH-EAST INDIA
(AFTER MATHUR AND EVANS, 1964)
0 50 100 150 KILOMETRES
0 50 100 MILES
ALLUVIUM
DIHING AND DUPI TILA SERIES
(Pliocene including Pontian)
TIPAM AND SURMA SERIES
(Miocene excluding Pontian)
BARAIL SERIES
(Oligocene and Eocene)
JAINTIA AND DISANG SERIES
(Eocene including Palaeocene)
LANGPAR AND MAHADEK BEDS
(Cretaceous)
LOWER GONDWANA SYSTEM
(Mainly permian)
METAMORPHIC AND IGNEOUS ROCKS
SERPENTINE
(Tertiary)
BASALT
(Probably Jurassic)
Thick lines indicate faults
Compiled from surveys by the geologists of The Burmah Oil Co Ltd. and associated companies and by the Geological Survey of India
Details in country south-east of overthrust belt are necessarily largely conjectural
EASTERN HIMALAYA
MISHMI HILLS
MIJU HILLS
DAFLA HILLS
ABOR HILLS
BRAHMAPUTRA RIVER
DIBRUGARH
DIGBOI
NAHORKATIYA
MORAN
RUDRASAGAR
JORHAT
Tezpur
Golaghat
Nowgong
MIKIR HILLS
Goalpara
GAUHATI
DHUBRI
GARO HILLS
KHASI & JAINTIA HILLS
SHILLONG
Lumding
NAGA THRUST
DISANG THRUST
NAGA HILLS
PATKAI RANGE
Kohima
CACHAR HILLS
Haflong
DAUKI FAULT
BURMA
YAMUNA
MYMENSINGH
SYLHET
SILCHAR
IMPHAL
MANIPUR
EAST PAKISTAN
DACCA
AGARTALA
TRIPURA
Comilla
Chandpur
GANGA OR PADMA
MEGHNA
BARISAL
LUSHAI HILLS
CHITTAGONG HILLS
CHITTAGONG
BAY OF BENGAL
28°
26°
24°
22°
90°
92°
94°
96°

FIG: 1·3

Table 1.1

Tertiary succession of Assam
(Mathur and Evans, 1964).

Age (approx)	Series	Stage and local facies		
		Geosynclinal sediments		Shelf sediments
		Surma Valley	Upper Assam and Naga Hills	
Recent and Pleistocene		Alluvium and high level terraces	Alluvium and high level terraces	Alluvium and high level terraces
		--Unconformity--		
Pliocene	Dihing	Not subdivided, 400	Not subdivided, 900	Dhekiajuli Beds, 600
		--Unconformity--		
Mio-Pliocene	Dupi Tila	Upper Dupi Tila, 2800 Lower Dupi Tila, 500	Namsang Beds, 800	Namsang Beds, 600
		--Unconformity--		
Miocene	Tipam	Girujan Clay, 1500	Girujan Clay, 1800	Girujan Clay, 600
		Tipam Sandstone, 1600	Tipam Sandstone, 2300	Tipam Sandstone, 900
	Surma	Boka Bil, 1500	Not subdivided, 900	Not subdivided, 200
		Bhuban, 4000		
		--Unconformity--		
Oligocene	Barail	Renji, 1000 Jenam, 1200 Laisong, 2400	Tikak Parbat, 600 Baragolai, 3300 Naogaon, 2200	Not subdivided, 1200
Eocene	Disang	Over 1500	Probably over 3000	Jaintia Series: Kopili Alternations, 500 Sylhet Limestone, 500 Therria, 100

Note : Figures give maximum thickness in meters.

This was subsequently modified but is still considered the base for all geological purposes. The stratigraphy of Nagaland, established by the Directorate of Geology and Mining, Nagaland (1978), is shown in table 1.2.

Nimi Formation :

This formation is probably a detached part of the pre-Tertiary Burmese continental crust (Directorate of Geology and Mining, Nagaland, 1978) and occupies the eastern fringe of Nagaland. It consists of crystalline limestone, quartzite, phyllite, carbonaceous phyllite, quartz-sericite schists and schistose granites,

Zepuhu Formation :

The Zepuhu Formation, representing the Ophiolite Complex of Nagaland has a linear NE-SW trend. It lies between the Disang Group in the west and the Nimi Formation in the east. This formation is about 90 kms. in length and 5 to 15 kms. in breadth. It consists of amphibolite, dunite, serpentinite, peridotite, pyroxenite, gabbro, diorite, basalt, spillite, andesite, agglomerate, tuff, glaucophane schist, basic schists, etc. These are, in some areas, mixed with such oceanic sediments as chert, tuffaceous chert, graywacke, limestone, phyllite and cherty quartzite.

Disang Group :

The Disangs were first described as a monotonous sequence of splintery shales in Upper Assam by Mallet (1876) who called them the Disang Shales. This was later redesignated the Disang Formation as the lithologic suite was found to be almost uniform and not divisible into further mapable units. The identification

Table 1.2

Stratigraphy of Nagaland
(Directorate of Geology and Mining, Nagaland, 1978).

Age (approx)	Litho formations in "Belt of Schuppen" and intermediate Hills of Nagaland.		Litho formations in Eastern High Hills of Nagaland.
	Tipam	Girujan Clay Tipam Sandstones	Jopi Formation Conglomeratic graywacke and arkose (with plant fossils)
	Surma		
Unconformity			
Upper Eocene to Oligocene (Molassic sediments)	Barail	Tikak Baragolai Naogaon	Lower Barails Fine to medium grained sandstones (with plant fossils)
Upper Cretaceous to Eocene (Flysch sediments)			Disangs Shale/Slate/Phyllite with calcareous lenses in basal sections and invertebrate and plant fossils in upper sections with brine springs.
			Fault/Thrust
Upper Cretaceous to Lower Eocene (Ophiolite Complex)			Zepuhu Formation 1. Chert, quartzites, limestones, graywacke, tuffs, basic volcanics, basic schists, blue schists with minor ultramafites and other suites noted under 2. 2. Gabbro, diorite, quartz-diorite and ultramafites with minor lenses/bodies of rock types noted under 1.
			Fault/Thrust
Pre-Mesozoic (?)			Nimi Formation Phyllites, quartz-chlorite-sericite schist, other schists, feldspathic quartzite, orthoquartzite, limestone and cataclastic granite.

of two distint lithologic units, a basal argillaceous and an upper arenaceous strata, in parts of Nagaland by systematic mapping led to the renaming of this suite as the Disang Group consisting of two formations, viz., the Upper and Lower Disang Formations (Sinha et al., 1982).

This group of rocks, spreading over more than half the surface area of Nagaland, extends from the Upper Cretaceous to the Upper Eocene. Categorised as a geosynclinal facies, the Disangs comprise of flysch sediments (Directorate of Geology and Mining, Nagaland, 1978). They occupy the intermediate hill region of Nagaland to the east of the Disang Thrust and are part of a very mountainous region. In this region, towards the east, some of the highest peaks of the state, like Saramati and its range, are located.

The Disangs contain a thickness of about 3000 m, consisting of well bedded, splintery, dark gray shales intercalated with thin, fine grained, well cemented, flaggy sandstones. The sandstones, which are just a few centimeters thick at the base become very prominent near the top, gradually passing upwards and laterally into the Barails.

The Disang shales show fine laminations and at a number of places they show curved or concentric surfaces. Carbonaceous shales intercalated with massive shales and occasionally fine sandstones also occur in certain areas, especially at the junction of the Disang beds and fault planes. Iron pyrites are common. In most places the Disang beds are squeezed and crumbled to a very high degree.

The Disangs are penetrated by a number of thin quartz veins and serpentinized intrusions at places. Towards the east, a marked degree of metamorphism is noted, with the development of hard, glossy, dark grayish to blue slates. Further east they grade into phyllite, generally talcose and chloritic, and even into schists. Concentrations of ferrugenous concretionary structures and distinct nodules are common, especially in open areas where red ferrugenous soil is seen. Brine and sulphur springs too are common. The Disangs also include black slate, quartzite, limestone and coloured slates (Oldham, 1883; Goswami, 1960) along the eastern parts of Nagaland and Manipur. They abut against an igneous body further south-east which may be a projection of the parent rock of the Arakan-Yoma.

Barail Group :

The Barail Series of Evans was later redesignated the Barail Group. The Barails, named after the Barail Range in North Cachar of Assam, lies conformably over the Disangs. This group consists of molassic sediments (Directorate of Geology and Mining, Nagaland, 1978). Ranging in age from Upper Eocene to Oligocene, the Barails are scattered in patches, in Nagaland. They are exposed in southern Kohima, the eastern parts of Nagaland and all along the western margin of the state. They are essentially arenaceous and are 4000 to 6000 m thick.

The Laisong Formation consists of very hard, gray, thin bedded sandstones alternating with hard, sandy shales. Occasional massive sandstones with intercalations of carbonaceous shales and thin streaks of coal are also encountered.

The Jenam Formation is made up of massive sandstones with intercalations of shale, sandy shale, and calcareous and iron stained shales.

The Barails exposed in southern Kohima belong to the Renji Formation. They extend towards the south-west of Nagaland and beyond into Assam and south, into Manipur. They are massive, hard, ferrugenous and very thick bedded sandstones, intercalated with minor shales. They form a thick forested range with high peaks such as Japfü (3015m).

The Naogaon Formation is exposed in the eastern parts of Nagaland where they form high ranges and cover extensive areas. Towards the south they branch out into strips, one such branch extending into northern Manipur. Sandstones of this formation are hard, gray, fine to medium grained and thin bedded. Some shales and carbonaceous shales are intercalated with these sandstones. Concretionary structures are noted in some areas. The sandstones are thick and massive with occasional thin shale partings towards the southern border of Nagaland. The Naogaon sandstones are indistinguishable from those of the Laisong of Lower Assam.

Towards the west of Nagaland the Laisong, Jenam and Renji are confined to the Belt of Schuppen and are exposed intermittently as isolated inliers, being split up by a system of strike faults. They run along the western border covering Chumukedima and Cholimsen and represent a transitional facies between Lower and Upper Assam.

The Barails show a number of sedimentary structures such as ripple marks, load casts, flute casts, current bedding, etc. These rocks are essentially marine to estuarine but are poor in fossils. Rock types include sandstone, shale, carbonaceous shale and coal. Coal is restricted to a very few places such as the Borjan coal field, Tiru-Valley coal belt, Jhanji-Desai-Valley coal belt and the Tuensang coal belt.

Surma Group :

This group of rocks lying unconformably above the Barails is named after the Surma Valley in Assam. It consists of molassic sediments of Lower Miocene age. The Surma Group, ranging in thickness from 2900 to above 4000 m, comprises of alternations of sandstones, shaly sandstones, mudstones, sandy shales and thin beds of conglomerate. The rocks are exposed in the Belt of Schuppen in the form of a number of long, narrow strips running along almost the entire length of Nagaland on the western margin which gradually thin towards the north. The Surmas have been divided into the Bhuban and the Boka Bil Formations, the former characterised by the presence of conglomerates. The Boka Bils pass vertically and laterally into the overlying Tipams.

Tipam Group :

The Surma Group is conformably overlain by the molassic Tipam Group which ranges in thickness from 3000 to 4000 m. The Tipams are composed of massive sandstones with subordinate clays and shales of Mio-Pliocene age. The sandstones are generally coarse grained, occasionally gritty and ferrugenous. They are commonly green in colour due to the presence of chlorite but are found to be weathering to different shades of brown. Shale and sandy shale partings are few. Mottled clay is occasionally seen with beds of grit and conglomerate.

The sandstones contain calcareous cementing material and occasionally very thin bands of impure limestone. Local patches of ferrugenous matter and streaks of lignite are common. The Tipams are exposed along the western fringe of Nagaland, in the Belt of Schuppen, as long, narrow strips due to strike faulting.

The Girujan Clay Formation that overlies the Tipam Sandstones is essentially argillaceous. It consists of mottled clays, sandy clays and sandstones in subordinate amounts. The Girujan Clays, with a thickness of about 1800 m, are exposed in the western parts of Nagaland where they are confined to the Belt of Schuppen. The formation also contains bluish gray, mottled clays with minor sandstones.

Namsang Beds :

The Namsang Beds belonging to the Dupi Tila Group lie unconformably over the Girujan Clays. These beds have been assigned a Mio-Pliocene age.They consist of sandstones, pebbles of lignite, conglomerate, grit, mottled clay and lenticular seams of lignite which are poorly consolidated. They attain a thickness of about 800 m and are confined to the Belt of Schuppen.

Dihing Group :

The Namsang Beds are unconformably overlain by the Dihing Group of Plio-Pleistocene age. This group consists of an unconsolidated mass of boulders and pebbles interspersed with clay and soft sand. The boulders and pebbles are undoubtedly products of the Barails. These rocks occur as a few patches in the Belt of Schuppen.

Alluvium and High-level Terraces :

Nagaland is extensively covered by alluvium and high-level terraces. The high-level terraces consist of boulder beds, coarse sands, gravels and unassorted clays at various levels above the present rivers. The older alluvium occupies the north-eastern tract of the Naga-Patkai ranges while the newer alluvium covers extensive areas along the western border of Nagaland.

1.3. MAJOR STRUCTURAL FEATURES :

Nagaland comprises of a NE-SW trending anticline with several structural highs separated by structural lows. From a structural and tectonic point of view it appears to be a very complicated area.

Nagaland is divided into three major structural units, viz., the "Belt of Schuppen" running along the entire north-western margin of Nagaland, the "Patkai Synclinorium" occupying the intermediate hill ranges to the south-east of the Belt of Schuppen, and the "Kohima Synclinorium" which lies to the south-west of the Patkai Synclinorium (Goswami, 1960; Mathur and Evans, 1964; Directorate of Geology and Mining, Nagaland, 1978). All these major structural units show a NE-SW trend.

Belt of Schuppen :

The Belt of Schuppen (Fig. 1.4), running along the entire north-western margin of Nagaland, consists of eight NE-SW trending overthrusts. The thrusts are found to override one another forming a very complex pattern.

At the western margin of the Belt of Schuppen, an **en-echelon** fault system know as the "Naga Thrust" is exposed intermittently, juxtaposing parts of the Tipams and Barails against the sub-recent to recent alluvial deposits. The Naga Thrust is made up of a succession of six different thrusts. The uppermost member of the Belt of Schuppen is the "Disang Thrust" which occupies the south-eastern part. This thrust is persistent throughout.

Patkai Synclinorium :

This structural unit lies south-east of the Belt of Schuppen (Fig. 1.5). It covers an extensive area in the middle of the intermediate hill ranges of Nagaland. The Barails make up the rock types of this elevated synclinorium which is broken up by strike faults. The older Disangs are exposed on either side of this synclinorium. The Disang Thrust separates it from the Belt of Schuppen on its north-western flank.

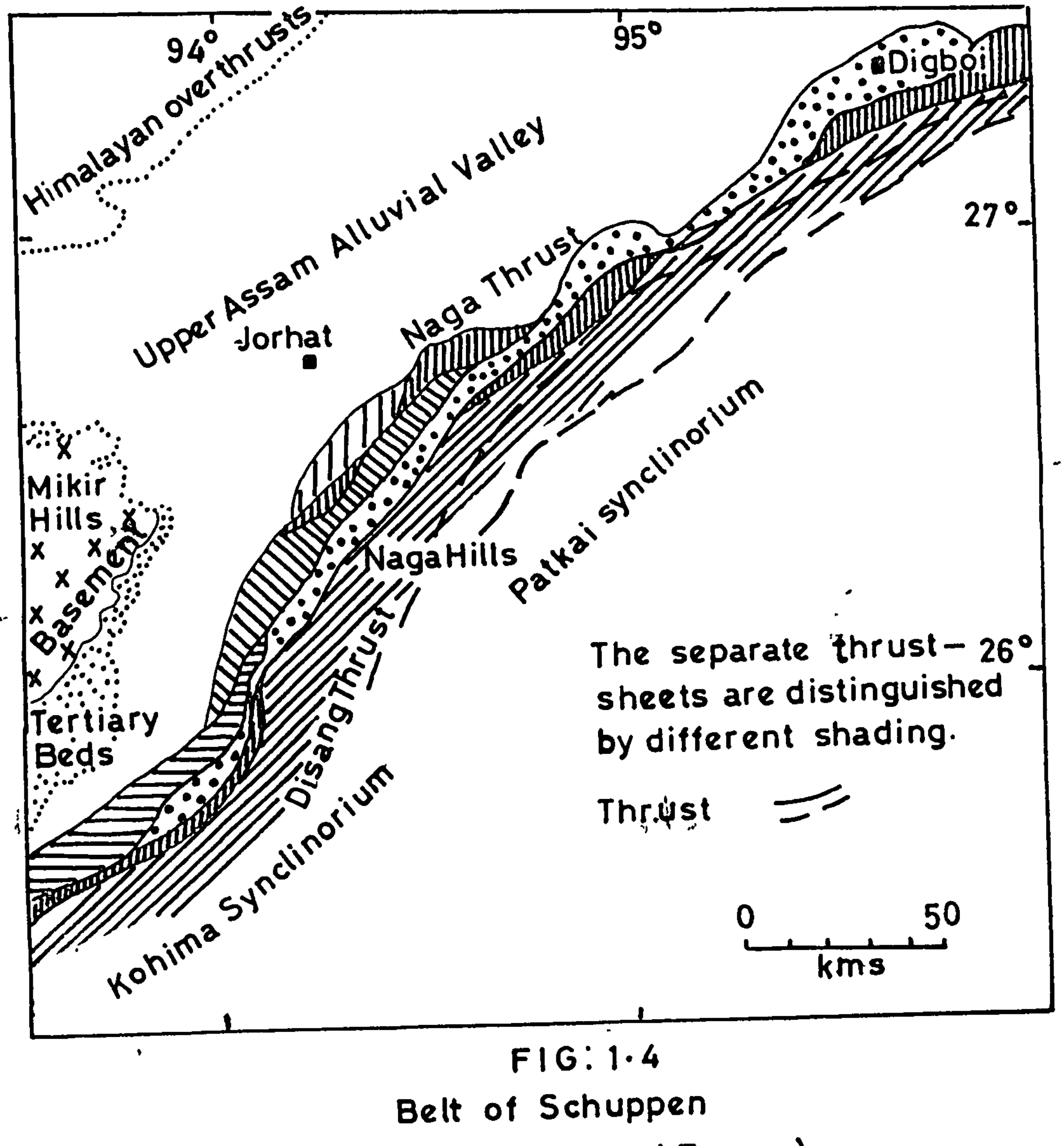

FIG: 1·4
Belt of Schuppen
(After Mathur and Evans,)
1964

Tectonic map of North-East India
(After Mathur and Evans, 1964)

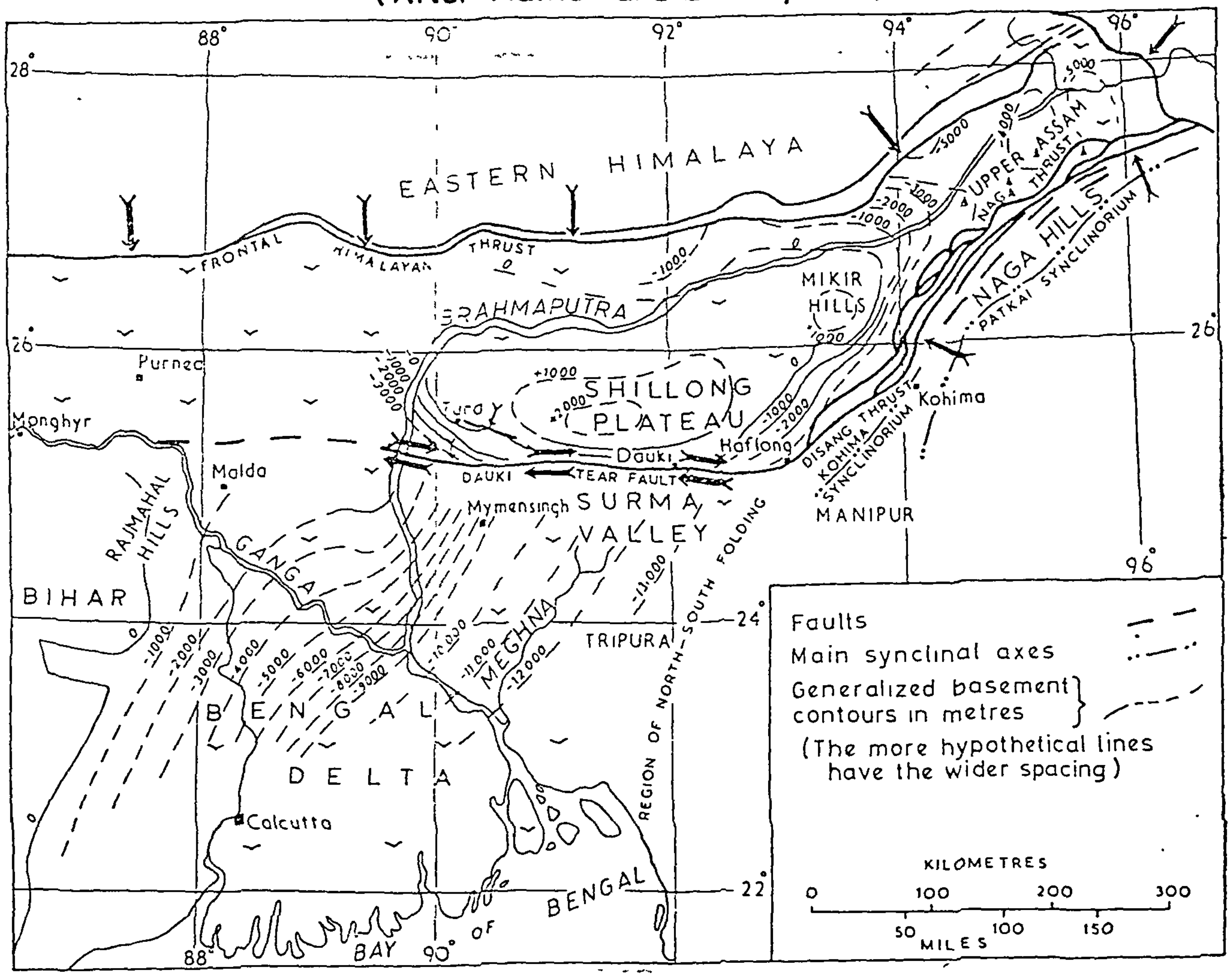

FIG: 1·5

Kohima Synclinorium :

The Kohima Synclinorium (Fig. 1.5) lies south-south-west of the Patkai Synclinorium and to the south-west of Kohima. It consists of broad synclines and narrow, sharp crested anticlines with faults trending approximately north-south. The synclinorium is flanked on all sides by the Disangs . Towards the Surma Valley progressively higher groups of the Tertiary succession such as the Barails, Surmas, Tipams, etc. are encountered in this structural unit. It is bounded on the north-west by the Disang Thrust and in the south it merges into the eastern Surma Valley.

Three generations of folds are recorded in the lithounits which probably correspond to the first, second and third phases of the Himalayan orogenies respectively (Directorate of Geology and Mining, Nagaland, 1978). Each generation is punctuated by an interval of comparative quiescence.

The first set of folds, formed due to orthotectonic movements during the Upper Cretaceous-Eocene period, are isoclinal with low plunges on either side and have north-south of NNE-SSW axial trends. Superimposition of later folds have resulted in the reversal of plunge. Recumbent folds reported from some places between Pfutsero and Chizami are, in all probability, related to the Alpine-Himalayan orogeny.

The second generation folds have NE-SW axial trends and steeply inclined axial surfaces. They show low plunges. The folds are open or moderately tight. In combination with the first generation folds they control the topographic morphometry of the hills and valleys of Nagaland. These folds probably correspond to the second phase of the Alpine-Himalayan orogeny.

The third set of folds have east-west to ESE-WNW axial trends. They are broad and open with their axial planes dipping steeply and show moderate plunges. Crenulation cleavages developed in basic schists and phyllites are due to these folds. These folds might be linked to the Pleistocene movements of the Himalayas. The older Nimi Formation may point to still older folds, atleast pre-Tertiary.

Two sets of distinctive faults have been reported (Directorate of Geology and Mining, Nagaland, 1978). The earlier set, trending NE-SW, shows a conformity with the regional trend of the early folds. The later set has a WNW-ESE trend. The two sets of faults interfere with each other resulting in the formation of large tectonic blocks (Fig. 1.5).

The lithotectonic framework suggests convergence of a plate whereby the Indian plate underthrusted below the Burmese plate (Shan Massif) eastward forming the Indo-Burma ranges along with the Ophiolite Complex of Nagaland (Directorate of Geology and Mining, Nagaland, 1978).

1.4. AIMS AND METHODS OF STUDY :

No detailed geological work has been done on the area of investigation so far, except for some preliminary mapping by the Geological Survey of India in recent years. As regards sedimentological work of the area, this is the first attempt. The proposed investigation aims at preparing a geological map of the area of work and dealing with the following aspects of the clastic rocks.

(i) Petrography and clay mineralogy
(ii) Grain size
(iii) Heavy minerals
(iv) Geochemistry
(v) Provenance, mode of transport, depositional environments and cementation.

Topographical map no. 83 K/1 of the Survey of India, on a scale 1:50,000 (2cms=1km), is used for geological mapping. An altimeter, Brunton compass, measuring tape, geological hammer and chisel, hand lens, etc. are used in the field.

1.5 PREVIOUS LITERATURE :

Literature on the geology of Nagaland is scanty and rarer still on the area of work, except for some broad generalisations which hold good for Nagaland, Manipur, Assam etc. as a whole. The geology of this hilly state is yet to be fully explored and work done so far is summarised below.

Mallet, in 1876, gave a comprehensive report on the Nazira coal field. Oldham (1883) studies the geology of Kohima and parts of North Manipur. In 1910 Hayden conducted some geological studies of a few coal fields of Nagaland. Two years later Pascoe (1912) made a traverse from Dimapur to Saramati and gave a geological account of that line of traverse. Two decades later Evans (1932) gave an excellent account of the Tertiary succession of Assam which includes valuable information on Nagaland as well. Wilson and Metre (1953) also give an account of the geology of Nagaland in their description of Assam and the Arakans. Evans (1959) further contributes to the stratigraphy and tectonics of Nagaland while describing the same of the Assam oil fields.

In his description of the geology of Assam Goswami (1960) mentions the geology of Nagaland. Evans (1964) establishes the tectonic framework of Assam where the tectonics of Nagaland is also dealt with. The stratigraphy, structure and conditions of deposition of the Tertiaries of Upper Assam inculding Nagaland are dealt with by Mathur and Evans (1964). Brunnschweiler (1966) publishes a paper on the regional geology and tectonic history of the Indo-Burma ranges including Nagaland. Krishnan (1968) gives a general description of the geology and tectonic framework of Assam, including Nagaland as well. The report of the Geological Survey of India (1974) includes some geological account of Nagaland. The Directorate of Geology and Mining, Nagaland (1978), also contributes in a general way. Handique and Dutta (1980) and Dutta (1982) have added further to the existing literature on the geology of Nagaland.

CHAPTER 2

GEOLOGY OF THE AREA

2.1. INTRODUCTION :

This chapter deals with the lithology and structure of the area under investigation, besides a general study of the miscellaneous details of communication, physiography, climate, drainage, flora and fauna, and the nature of soil and outcrops.

2.1.1. Communication :

The area under investigation is linked to Wokha in the north and Kohima in the south by the state highway no. 1. The nearest airport and the railhead are located in Dimapur which lies approximately 115 kms. south-west of Botsa. Buses ply regularly between Kohima and Wokha through Botsa, in addition to other modes of transport. Numerous footpaths and trails, through otherwise inaccessible forests, connect the surrounding villages.

2.1.2. Physiography :

The area, as a whole, shows a rugged topography. High hills, narrow valleys, steep cliffs, deep gorges, etc. are common features. The maximum and minimum heights encountered are over 1750 m and below 360 m respectively above mean sea level. Several more or less parallel ranges run NE-SW. Summits of the lofty peaks are thickly wooded, clad with evergreen vegetation. A large portion of the lower hills have become deforested due to jhumming and terrace cultivation. Landslides are common which cause problems at times. The countryside, as a whole, however, commands a majestic landscape.

2.1.3. Climate :

The area lies in the north temperate zone and, owing to its elevation, enjoys a temperate type salubrious climate. Winters are cold but the summers are warm. December and January form the coldest part of the year. Spring-time is warm and humid. The breeze, though invigorating, is interrupted at times by gales. Temperatures range from about 5°C in winter to nearly 30°C in summer. It decreases during the autumn, October and November being the finest part of the year. Botsa and its surroundings get a high amount of rainfall during the monsoon.

2.1.4. Drainage :

The Nzü is the only important river in the area. It originates from the north of Botsa and flows in a northwardly direction before it drains into the Doyang in Wokha district. A number of intermittent streams that feed this river drain the agricultural tracts.

2.1.5. Flora and Fauna :

Thick evergreen forests cover most of the uninhabited areas. Indigenous species include hollock, gamari, oak, alder, chestnut, walnut, etc. besides a variety of shrubs. Bamboos and plantains, and a few varieties of orchids are also found in this area.

Large patches of forests are cleared every year for cultivation of rice and maize. In the older patches, tapioca and corm are cultivated.

The area is rich in its faunistic species. The mammals include tiger and other wild cats, bear, boar, deer, guinea pig, porcupine, mongoose, etc. The reptiles are represented by a great variety of poisonous and non-poisonous snakes and lizards.

Various kinds of insects, bees, snails, frogs, etc. are also common. Numerous species of birds like pigeon, wild fowl, woodpecker, owl, etc. and a large variety of fish are found in the jungles and streams. The area is infested with leeches and mosquitoes during the summer months.

2.1.6. Soil and Outcrops :

The soil cover throughout the area is very thick. Soil exposures commonly show a reddish brown colour. They are dark gray, soft and loamy in areas covered by vegetation. Outcrops are few due to thick soil cover and vegetation which do not permit the tracing of their continuity. Most of the sandstone samples collected are from exposures along road cuttings.

2.2. LITHOLOGY :

Two groups of rocks, namely the Disangs and the Barails, are exposed in the area (Figs. 2.1.1 and 2.1.2). For purpose of detailed study a vertical section for each of the groups is established and sandstones chosen from different horizons. The different sandstone units of the area, in ascending order, are shown in table 2.

Disang Group :

The Disang Group is made up of abundant splinter; shales interbedded with hard, fine grained, flaggy sandstones The shales gradually decrease towards the top while th sandstones attain prominence. There does not exist muc difference in lithological characters of the sandstones.

Some of the sandstone beds are not persistent and i most cases taper into the shales. The sandstones of the area aı poor in fossils. Ferrugenous concretions and quartz veiı

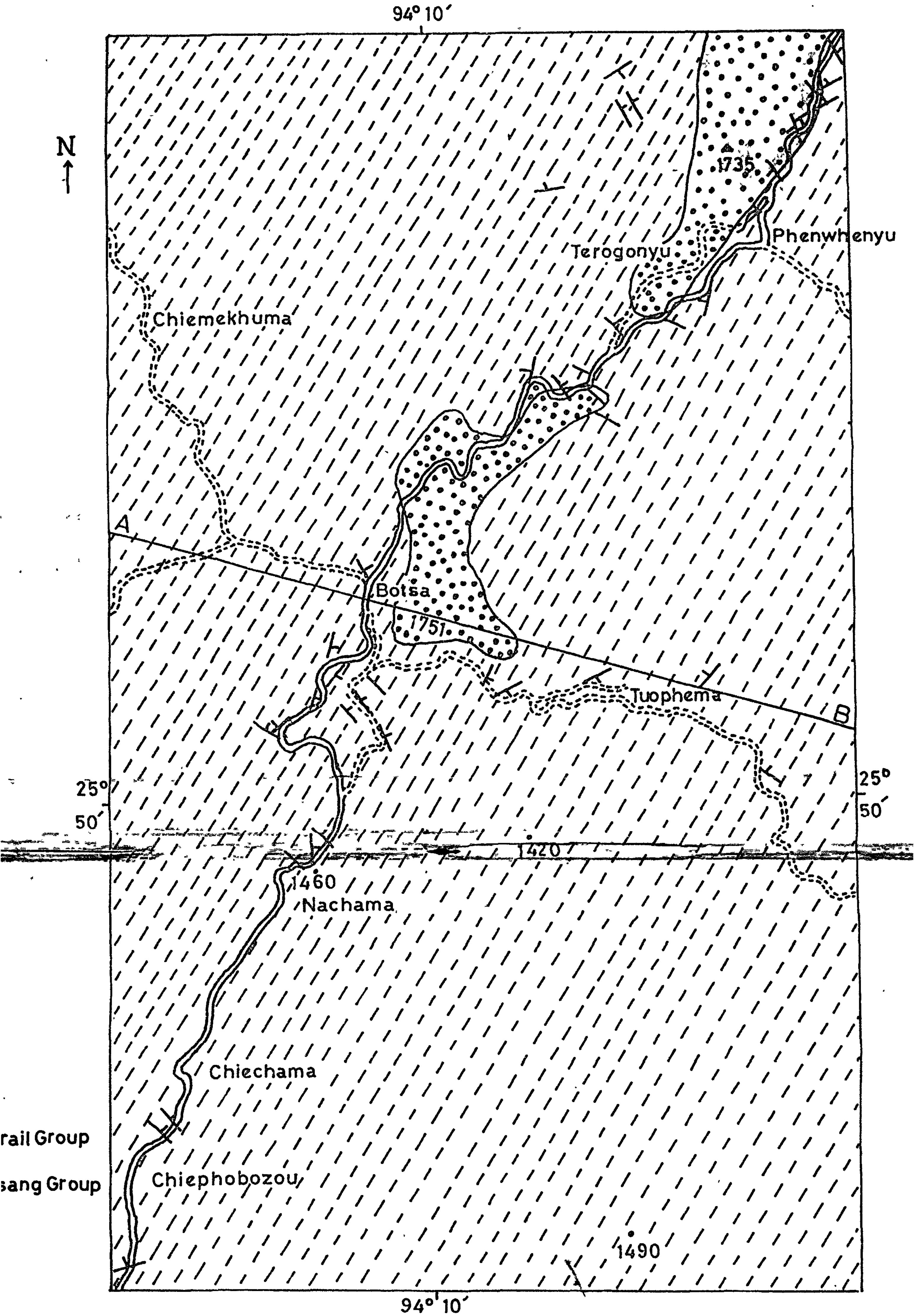

FIG: 2·1·1

Geological map of Botsa and its surroundings.
(Part of toposheet No. 83 $\frac{K}{1}$) Scale - 1 : 50,000

GEOLOGICAL CROSS SECTION ALONG AB

SCALE 1:16,667 (6cms = 1km)

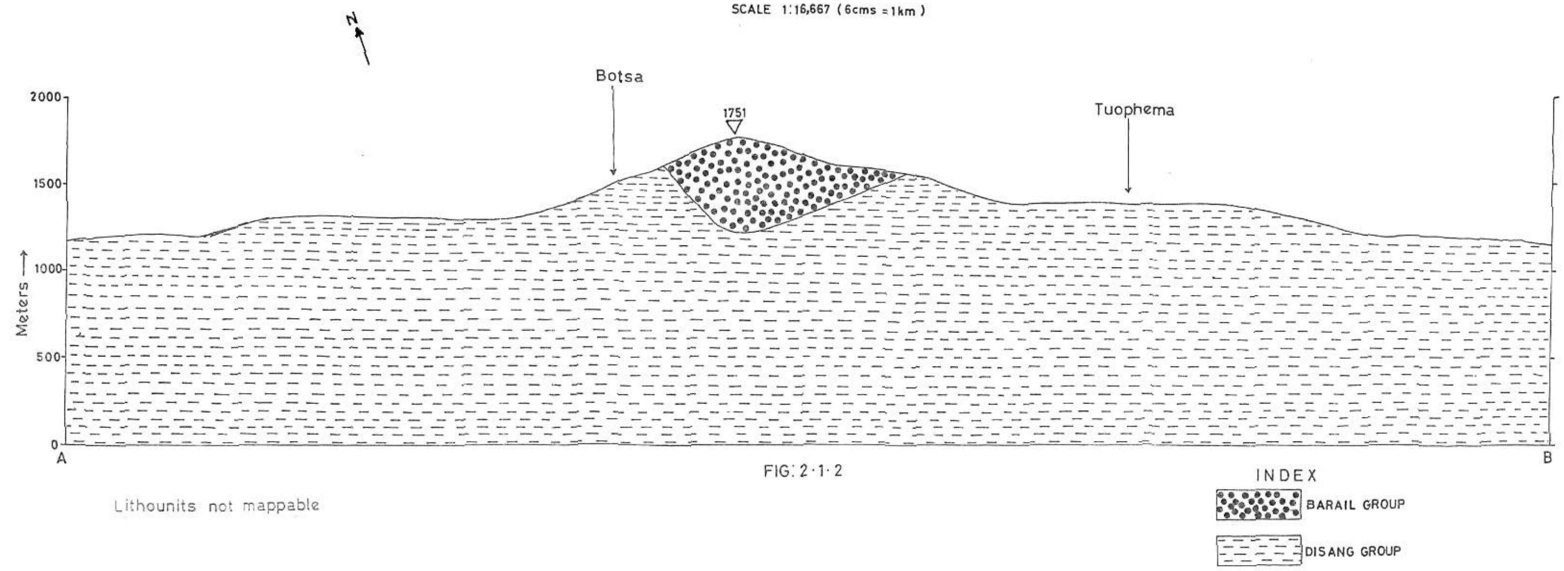

FIG: 2·1·2

Lithounits not mappable

Table 2

Sandstone units of the area around Botsa.

(Vertical Section)

Age	Group	Lithounits
		Light gray, fine grained, tough sandstone (B 1).
		Buff coloured, fine grained, finely laminated sandstone (B 109).
Upper Eocene to Oligocene	Barail	Brownish gray, fine grained, micaceous sandstone (B 22).
		Light gray, fine grained, very hard sandstone (B 83).
		Dark gray, fine grained, laminated sandstone (B 53).
		Dark gray, thin bedded sandstone (D 1).
		Brownish gray, thin bedded, tough sandstone (D 7).
Eocene	Disang	Brownish thin bedded sandstone (D 9).
		Bluish gray, thin bedded, fine grained sandstone (D 13).
		Steel gray, fine grained, tough sandstone (D 24).

———Base not seen———

(Note :- Figures within parentheses indicate sample numbers) penetrating the sandstones are abundant. Depositional structures are not common except for fine laminations. Load casts are exhibited by some of the Disang sandstones. Box-type of weathering is very prominent in the upper horizons. The dips of the lithounits vary from 31° to 80°.

Five samples, D24, D13, D9, D7 and D1, in ascending order (Fig. 2.2), representing different sandstone units of the Disang Group exposed in the area are chosen for detailed study.

Barail Group :

The Barails are made up of fine grained sandstones which are intercalated with very little, thin bedded shales. At the base, thick bedded, massive sandstones are more common which gradually pass upwards into thin bedded ones. There is not much of a difference as regards the lithological characters of the sandstones of this group of the Botsa area.

The sandstones under investigation are poor in their fossil content. Depositional structures, though noted, are by no means abundant. They include laminations, ripple marks and load casts. The lithounits dip from 11° to 41°.

Five representative samples from different levels of the column (Fig. 2.3) are studied in detail. In ascending order these five samples are numbered B53, B83, B22, B109 and B1.

2.3. STRUCTURE :

The area is bounded by the Kohima Synclinorium in the south and the Patkai Synclinorium in the east. The Disang Thrust, with a NE-SW trend, covers the north-west.

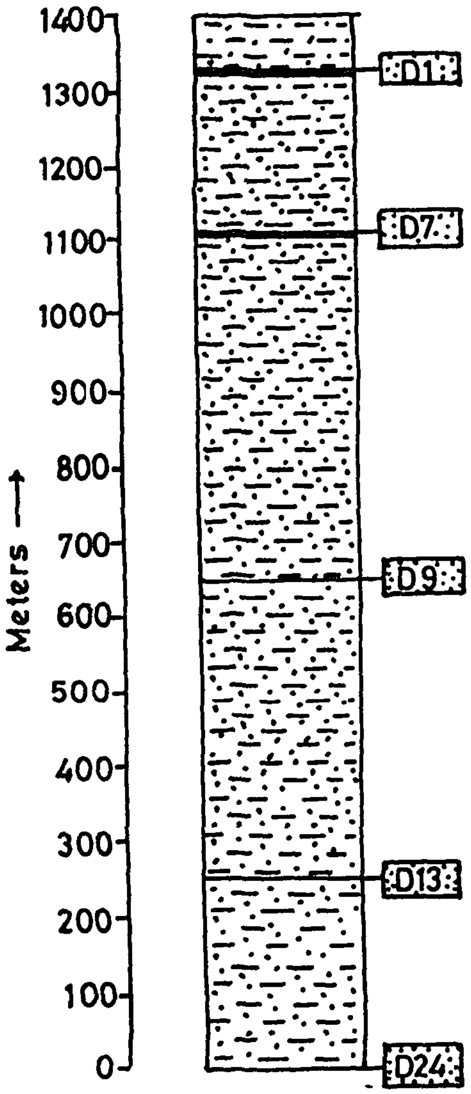

FIG: 2·2
Vertical section of sandstone units of the Disang Group

D1 Dark grey, thin bedded sandstone

D7 Brownish grey, thick bedded, tough sandstone

D9 Brownish, thin bedded sandstone

D13 Bluish grey, thin bedded, fine grained sandstone

D24 Steel grey, fine grained, tough sandstone

Shales with thin bedded sandstone

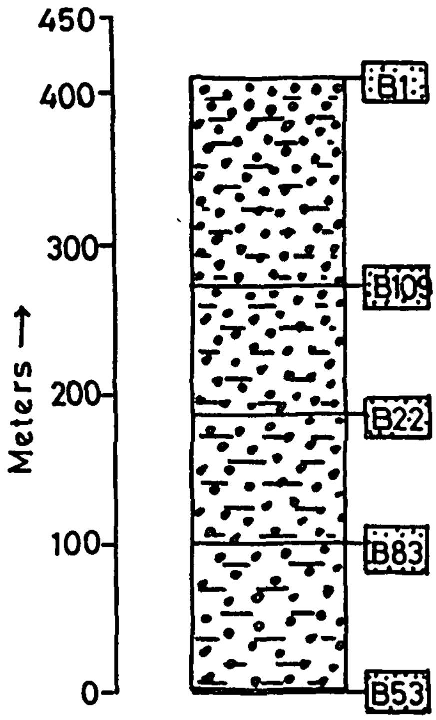

FIG: 2·3

Vertical section of sandstone units of the Barail Group

B1 Light grey, fine grained, tough sandstone

B109 Buff coloured, fine grained, finely laminated sandstone

B22 Brownish grey, fine grained, micaceous sandstone

B83 Light grey, fine grained, very hard sandstone

B53 Dark grey, fine grained, laminated sandstone

Sandstones with very minor shales

The major structural feature of the area is reflected in the distribution of the Barail outcrops. The Barails occur as outliers within the Disangs. This is probably due to the intersection of the three axes of the folds generated during three phases of deformation (Sahu and Venkataswamy, 1990). Besides the above, at places, small scale folds, faults, joints, etc. are also encountered.

CHAPTER 3

METHODOLOGY

3.1. PETROGRAPHY :

The sandstones, being friable, are impregnated with canàda balsam at about 110°C for 2 days prior to the preparation of the thin sections.

The volumetric composition of the different petrographic constituents is determined from the thin sections using a Swift's 'Point Counter' and a mechanical stage (Chayes, 1949). A micrometer eyepiece is used to measure lengths and breadths of quartz grains in each slide. Following Doty and Hubert (1962) mineralogical classifications of the sandstones are made after recalculation, omitting the accessory minerals, cement and matrix. The classification of Kukal (1968) using quartz, feldspar+unstable grains and matrix is also followed for rock nomenclature. Quartz, feldspar and rock fragments are recalculated and plotted in ternary diagrams following Pettijohn (1975) for naming the rocks. Here, the amount of matrix is important. Rocks with less than 15 percent matrix are arenites while those with more than 15 percent are wackes. Different types of quartz are determined and genetic groups estimated (Krynine, 1950; Doty and Hubert, 1962; Folk, 1968). Ratios of polycrystalline quartz and feldspar+rock fragments are plotted against those of total quartz and feldspar+rock fragments to determine the paleoclimate (Suttner and Dutta, 1986). Quartz, feldspar and the lithic fragments are recalculated to 100 percent and plotted in ternary diagrams to determine the paleoclimate (Suttner and Dutta, 1986) and provenance of the sediments (Dickinson *et al.*, 1983). The maturity index of the sandstones is determined using the quartz-feldspar ratio (Pettijohn, 1975) and the quartz-feldspar-rock fragments ratio (Suttner and Dutta, 1986). Length-breadth ratios of quartz are determined for provenance studies (Bokman, 1952).

3.2. CLAY MINERALOGY :

The separation of clay from selected sandstone samples is carried out by washing the crushed samples through a 62-micron stainless steel sieve. The fractions of silt and clay which pass through the sieve are transferred to 1000 ml graduated cylinders. Distilled water is added to bring up the levels to 1000 ml and the samples are stirred for about 10 minutes and then allowed to stand overnight, after checking for flocculation. The pipette analysis for the separation of the clay fractions is done following the procedure given by Krumbein and Pettijohn (1938) and Carver (1971). After drying at room temperature, the separated clay-sized fractions are x-rayed.

A Philips APD-15 X-ray Diffractometer with CuKα radiation is used for the determination of the clay minerals. A graphite monochromater instead of filter, and a silicon standard are used for the analyses. As the clay samples do not contain montmorillonite they are not treated with glycol. They are x-rayed at 20°C and the minerals are identified from the peaks of the diffractograms.

3.3. SIZE ANALYSIS :

Sieve and pipette methods of analysis are carried out for determination of the grain size distribution. Calcite and ferrous iron cements that are occasionally present are first removed by treating the samples with dil.HCl. After complete disaggregation, the materials finer than 4.0 Ø (0.062 mm) are removed by wet sieving. The coarser materials are dried completely and then, using a Ro-tap Automatic Sieve Shaker for about 20 minutes, sieved through a series of nested screens (ASTM sieves) at quarter phi class intervals (Krumbein and Pettijohn, 1938). The weight of each sieve fraction is then taken. The pipette method (Krumbein and Pettijohn, 1938) is used to analyse the materials finer than 4.0 Ø.

Cumulative curves are then drawn from the data on log probability graph paper and statistical parameters, namely graphic mean size (M_z), inclusive graphic standard deviation (δ_i), inclusive graphic skewness (Sk_i) and graphic kurtosis (K_g) are graphically obtained. Sub-populations of the grain size distribution are utilised to establish the mode of transport and deposition of the sediments (Visher, 1969). Interrelationships of the textural parameters in the form of scatter diagrams are used for differentiation of the depositional environments of the sediments (Friedman, 1961; Moiola and Weiser, 1968). CM patterns and FM, LM and AM diagrams are studied to distinguish transportational processes of the sediments (Passega, 1957, 1964; Passega and Byramjee, 1969). C and M, representing the one and fifty percentiles respectively, are converted to millimeters from phi values using a conversion chart (Page, 1955) and then to microns (1 mm = 1000μ). The sandstones are texturally classified by plotting the sand, silt and clay percentages, obtained from the analyses, in ternary diagrams (Folk, 1954).

3.4. HEAVY MINERAL ANALYSIS :

The size grades ranging from 0.250 mm to 0.125 mm of each sample are mixed up thoroughly. Sediments for study are treated with dil.HCl, heated mildly to remove cementing materials, washed with distilled water and dried in an oven at low temperature. The heavy minerals are then separated using bromoform with specific gravity 2.89 (Krumbein and Pettijohn, 1938) and mounted on glass slides with canada balsam.

Percentages of the different heavy minerals present are determined by counting them under the microscope fitted with a mechanical stage. Range tables are then prepared (Evans, Hayman and Majeed, 1934). Non-opaque/opaque ratios are calculated for determination of provenance.

From the heavy mineral assemblage the Z.T.R. maturity index (Hubert, 1962) is determined. Using a calibrated eyepiece, length and breadth of zircon and tourmaline are measured. For finding out the average diameter (D_{av}) of the grains, the formula used is $D_{av} = \sqrt{l+b}$ (Twenhofel and Tyler, 1941)

where l - length of each grain

and b - breadth of each grain.

The mean size or arithmatic mean (M_z) is calculated using the relation $M_z = \frac{\Sigma f.m}{\Sigma f}$

where f - frequency of the size analysis data

and m - mid-point of the class interval.

Elongation quotients of zircon and tourmaline are also calculated. The relationships between length, breadth and elongation ratios to their frequencies are then graphically represented.

To find out if there is any definite relationship among the sets of data obtained for the two groups, i.e., the Disang and the Barail, the coefficient of correlation (r) is determined using the formula.

$$r = \frac{\sum(xy)-n.Mx.My}{\sqrt{\left\{\sum(x^2) -n(Mx)^2\right\}\left\{\sum(y^2)-n(My)^2\right\}}}$$

where, x and y - items to be compared

n - number of items to be compared

and Mx and My - mean values of x and y.

The data on zircon and tourmaline are quantified on the basis of size and elongation quotient by making a quantitative evaluation of the grains for finding out the similarities and dissimilarities existing between the sediments of the Disang and Barail Groups.

Lengths and breadths of zircon and tourmaline grains are plotted against each other to prepare catenae diagrams (Smithson, 1939; Poldervaart, 1955; Venkatarathnam and Rao,1968).

3.5. GEOCHEMISTRY :

Quantitative determination of the major oxides and rare earth elements and semi-quantitative determination of the trace elements in the sandstones under investigation are made for geochemical studies. The samples are crushed and fractions passing through a 150 mesh are taken for analyses of the major oxides, REE and trace elements.

3.5.1. Major oxides :

The finely powdered samples are fused with a fusion mixture. Quantitative analysis for the major oxides is then carried out following the Indian Standards Institution (1963) and Basset et al. (1982). SiO_2 is determined by the method of difference, Al_2O_3/TiO_2 and MnO by colorimetry using an EEL Photoelectric Colorimeter, FeO by titration, Fe_2O_3 by reduction, CaO by permanganimetry, MgO gravimetrically and P_2O_5 by molybdenum-blue method. Na_2O and K_2O are determined using an EEL Flame Photometer.

Ratios of some oxides are calculated. TiO_2/Al_2O_3 ratio is used for determination of paleoclimate (Migdisov, 1960) and provenance (Spears and Sotiriov, 1976). K_2O/Na_2O ratio is useful for determining the type of rock (Kukal, 1968).

Certain relationships of the oxides are used for various purposes. For rock nomenclature (SiO_2+TiO_2), Al_2O_3 and the sum total of the remaining oxides excluding MnO, P_2O_5 and that lost on ignition are recalculated to 100 percent and plotted in triangular diagrams following Kukal (1968).Log values of Fe_2O_3/ K_2O ratios are plotted against those of SiO_2/Al_2O_3 ratios in binary diagrams following Herron (1988), also for rock nomenclature.

Percentages of CaO, Na_2O and K_2O, and that of Fe_2O_3, MgO and TiO_2 are recalculated to 100 percent and plotted in ternary diagrams for provenance determination of the sediments (Condie, 1967). SiO_2 contents are plotted against the combined percentages of Al_2O_3, K_2O and Na_2O in binary diagrams for determination of paleoclimate following Suttner and Dutta (1986).

For determination of the tectonic setting of the sandstones, (Fe_2O_3+MgO), Na_2O and K_2O are recalculated and plotted in triangular diagrams following Blatt et al. (1980). Following Roser and Korsch (1986), SiO_2 content is plotted against K_2O/Na_2O ratio and SiO_2/Al_2O_3 ratio is plotted against K_2O/Na_2O ratio for the same purpose.

Percentage values (P) of Si, Al and FeT (total iron) are calculated from SiO_2, Al_2O_3 and (FeO+Fe_2O_3) percentages respectively, using the formula

$$P = \frac{a.x}{m}$$

where a - atomic weight of the element

m - molecular weight of the oxide

and x - known weight percentage of the oxide.

Si, Al and FeT values are recalculated to 100 percent and plotted in ternary diagrams following Moore and Dennen (1970) for rock nomenclature.

3.5.2. Rare earth elements :

1.0 g of the finely divided sample is treated with $HF-HNO_3-H_2SO_4$ on a water-bath two or three times to get a soluble residue. The digested solution is then evaporated to dryness. After cooling, a few drops of conc.HNO_3 are added to obtain a completely clear solution. This solution is diluted to 100 ml by adding distilled water. The REE abundances, in parts per million, are then determined using a Labtam model 8410 ICP Atomic Emission Spectrometer.

In order to smoothen out natural odd-even effects of REE concentrations, the REE abundances are divided by the corresponding chondrite abundances (Evensen _et al_., 1978). The normalised data are plotted following Coryell _et al_. (1963). Values of Ce* and Eu* are determined by interpolation between La and Pr, and Sm and Gd respectively.

3.5.3. Trace elements :

The trace elements are analysed using a Hilger and Watts large quartz-glass Automatic Spectrograph. The ground samples and specpure graphite powder are mixed thoroughly in 1:1 ratios. 20 mg of the mixtures are loaded in specpure graphite electrodes that are 8 mm deep with 1.5 mm bores and arced for 3 minutes. The same time is then chosen for arcing standard powders to provide similar exposures on pairs of 4"x10" spectroscopic plates. After completion of burning, the plates are developed by putting them, for about 2½ minutes at 18°C, in an Illford, I.D.2 Developer mixed with water in 1:1 ratios. After developing, the plates are immersed into a fixing solution for 4 to 5 minutes, then rinsed in distilled water and dried at room temperature.

The semi-quantitative determination is carried out by visually comparing line intensities in the Jarrel-Ash Console Spectrum Comparator with a series of spectrograms taken from standard mixtures.

Cr/V ratios are calculated for determination of conditions of ventilation in the depositional environment while Ni/Co ratios are calculated for determination of Eh conditions in the depositional basin and provenance of the sandstones (Dykpiv, 1979).

B, Rb and Ga, in parts per million, are recalculated to 100 percent and plotted in ternary diagrams following Degens *et al*.(1957) to determine the depositional environments of the sediments. Bivariate plots of B Vs Ga and B Vs Rb after Degens *et al*. (1957) are also used for the same purpose.

PART II

CHAPTER 4

PETROGRAPHY AND CLAY MINERALOGY

4.1. PETROGRAPHY

4.1.1. INTRODUCTION :

The mineral composition of a sedimentary rock is one of its most important characteristics. The mineralogy, coupled with texture, bears a direct relationship with provenance, transportational processes, depositional environments and diagenesis of the sediments (Suttner, 1974; Pettijohn, 1975). Petrographic studies throw light on climatic conditions and relief of the source area (Mack, 1984) besides revealing the nature of cementation and the effects of pressure solution in changing clastic grains. Detrital grains reveal the nature of the petrographic province and tectonic conditions of deposition (Pettijohn, 1975; Velbel, 1985). They also give information on mixing of materials from various sources and the changes that take place in a suite from a given source due to progressive denudation. The geological history of the rocks, the paleogeography and paleoclimate of the source area, etc. (Suttner and Dutta, 1986) are also interpreted from petrographic studies.

This chapter deals with the study of twenty five thin sections of the Disang sandstones exposed in the area of investigation. The methodology adopted for petrographic studies is described in chapter 3.

4.1.2. FRAMEWORK CONSTITUTION :

The Disang sandstones exhibit remarkable variation in grain size and principal framework constituents (Fig. 4.1.1). The gross mineralogical composition is shown in table 4.1.1.

Quartz :

The different types of quartz are estimated by making point-counts (more than 300) in each section. The basic types of quartz, on a genetic basis, include non-undulatory, undulatory, polycrystalline and reworked (Table 4.1.2). The non-undulatory quartz grains (Fig. 4.1.1) are identified by their complete extinction on a slight rotation of the microscope stage (less than one degree according to Blatt and Christie, 1963). In the Disang sandstones this variety of quartz comprises of 80.58 to 95.01% of the total quartz content which ranges from 38.52 to 44.61%. Undulatory quartz (Fig. 4.1.2) showing typical undulose extinction forms 2.07 to 10.04%. Polycrystalline quartz (Fig. 4.1.1) with composite grains consisting of 2 to 3 units, rarely more, ranges from 1.88 to 5.93% of the total quartz content. Recycled quartz (Fig. 4.1.3) and volcanic quartz grains showing cherty resorption (Fig. 4.1.4) are also observed in a few sections. Some of the quartz grains are coated with iron oxide (Fig. 4.1.2) and a few contain inclusions of zircon and tourmaline (Fig. 4.1.1). Quartz veins penetrating the sandstones appear to be common (Fig. 4.1.8). The length-breadth ratios of the quartz grains range from 1.00 to 6.30 averaging 2.30 (Table 4.1.2). These ratios indicate that the sources of the sediments include both igneous and metamorphic, the latter dominating.

Feldspar :

The feldspars of the Disang sandstones (Fig. 4.1.5), mostly altered, range between 6.69 and 8.53%. The grains are

Fig. 4.1.1

Polymodal Disang sandstone under crossed nicols

A - Non-undulatory quartz
B - Polycrystalline quartz
C - Metaquartzite showing sutured contact
D - Inclusions in quartz
E - Matrx (cherty and fibrous)
F - Metamorphic rock fragment

Fig. 4.1.2

Disang sandstone under crossed nicols

A - Undulose quartz
B - vein quartz
C - Ferrugenous coating around quartz
D - Ferrugenous replacement of matrix

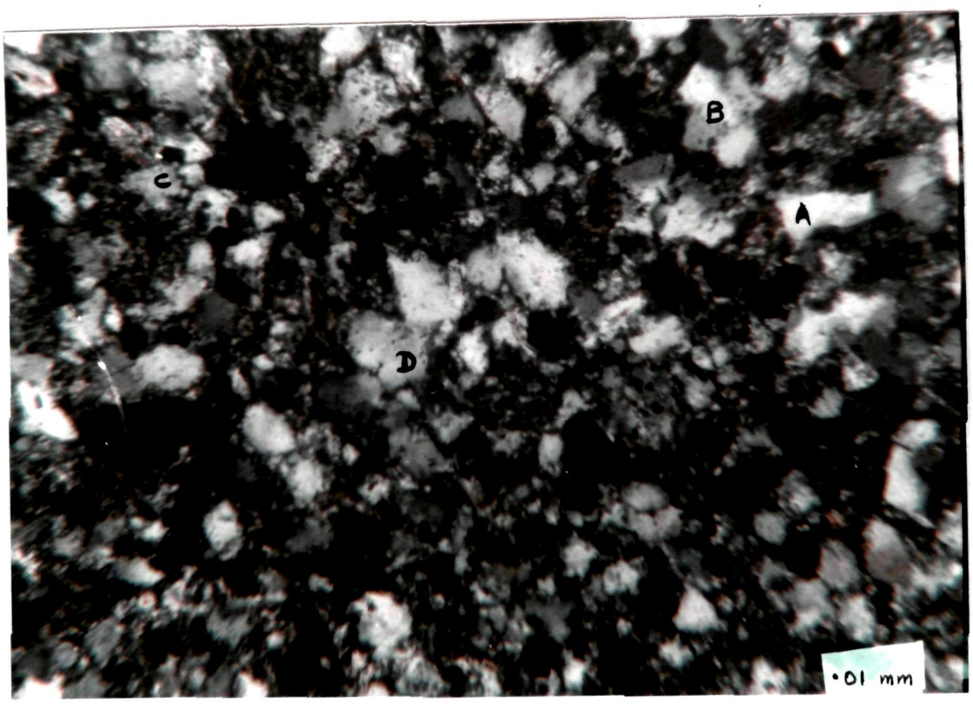
B
A
C
D
·01 mm

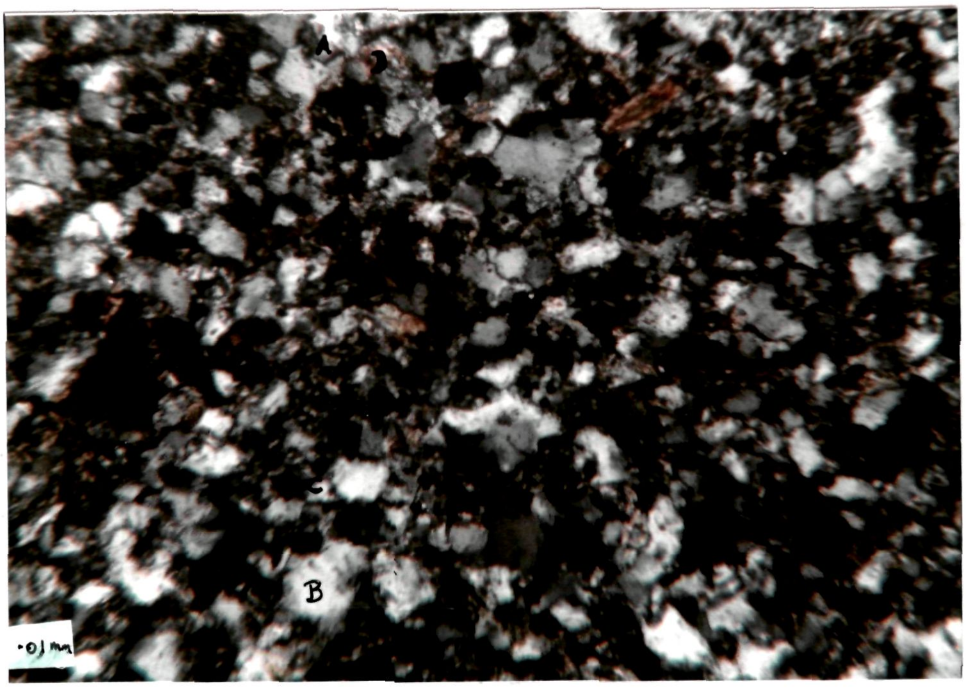
A
C
B
·01 mm

Fig. 4.1.3

Disang sandstone under ordinary light

A - Reworked quartz
B - Chert
C - Ferrugenous replacement of biotite

Fig. 4.1.4

Disang sandstone under crossed nicols

A - Cherty resorption of quartz
B - Authigenic overgrowth of quartz
C - Silica cement

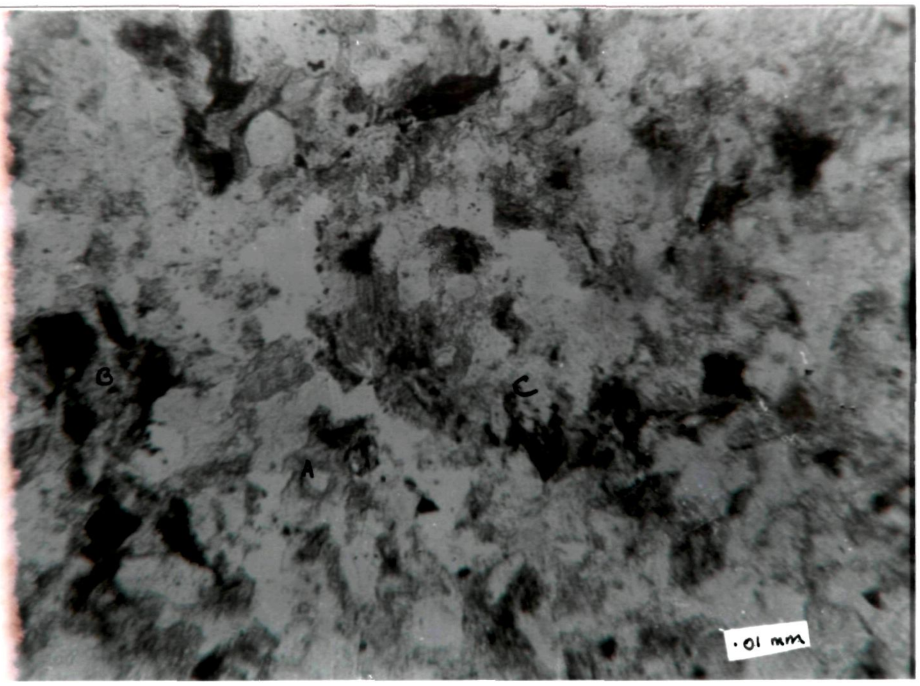
B
C
A
·01 mm

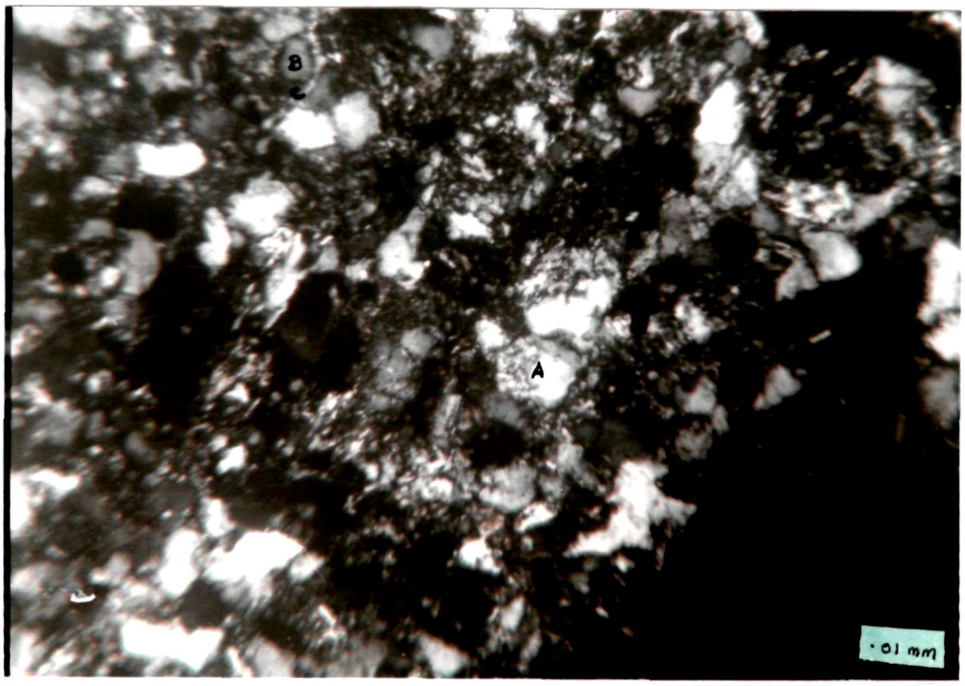
B
C
A
·01 mm

Fig. 4.1.5

Calcareous Disang sandstone under crossed nicols.
A - Plagioclase

Fig. 4.1.6

Calcareous Disang sandstone under ordinary light

A - Kink-bending of muscovite
B - Zircon
C - Biotite

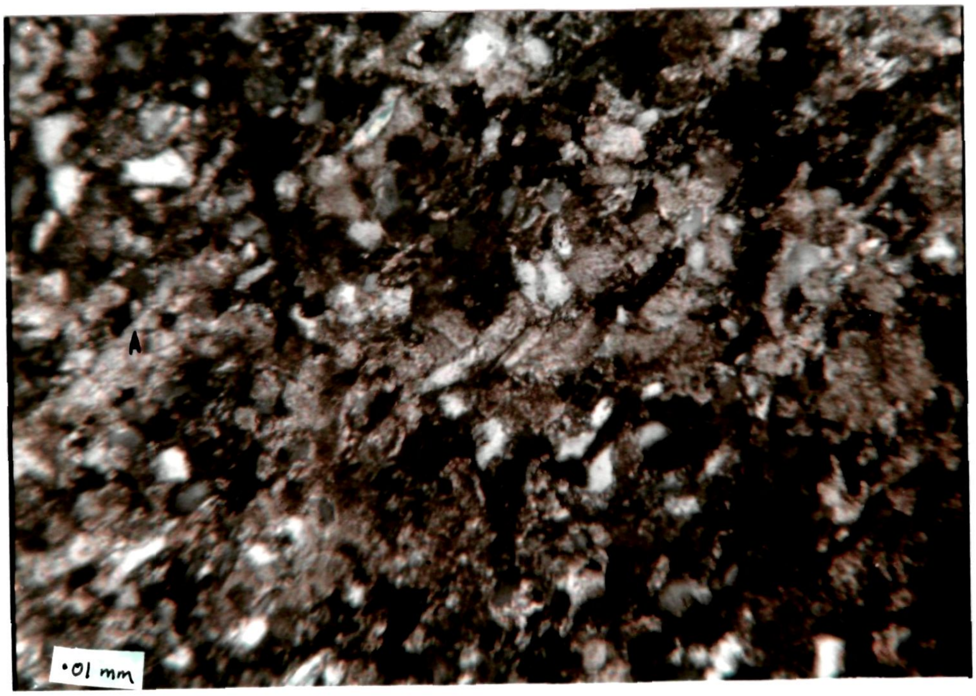
A
·01 mm

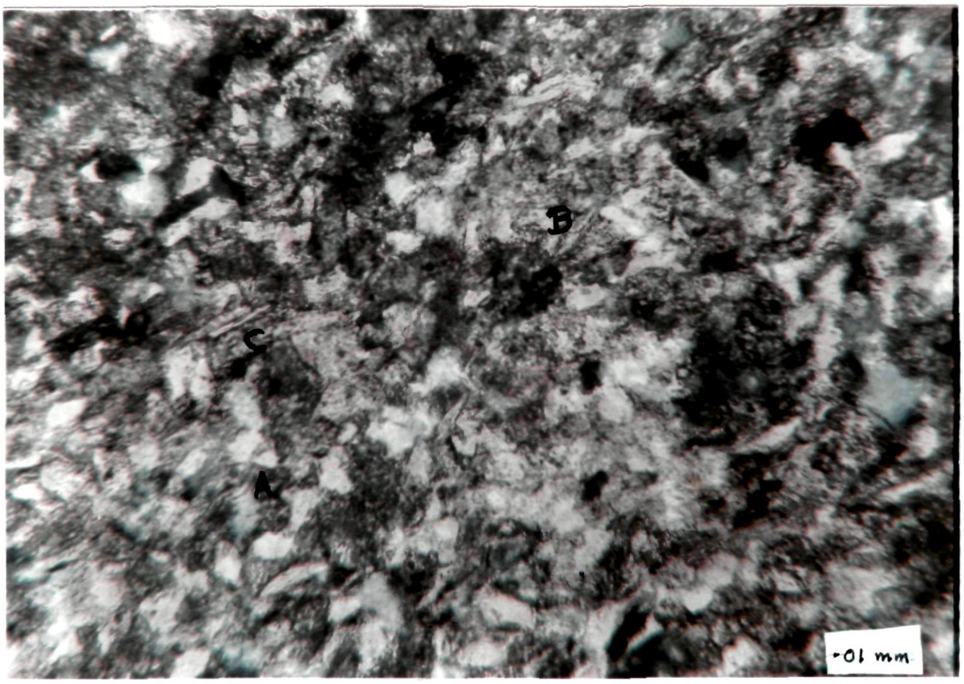
B
C
A
·01 mm

Table 4.1.1

Mineralogical composition of the sandstones of the Disang Group.

Sample No.	Quartz	Feldspar	Mica	Rock fragments: Igneous	Rock fragments: Meta-morphic	Rock fragments: Sedi-mentary	Rock fragments: Total	Other grains	Matrix	Cement
D 1.	40.16	7.45	2.36	6.58	13.54	0.21	20.33	1.47	26.20	2.03
D 4.	40.94	7.19	2.43	5.18	11.72	0.12	17.02	2.77	26.01	3.64
D 5.	40.46	6.98	3.37	5.65	11.11	0.19	16.95	2.91	25.51	3.82
D 6.	41.33	7.27	3.71	5.30	9.97	0.33	15.60	1.07	27.11	3.91
D 7.	42.07	8.53	3.24	2.26	10.43	0.37	13.06	2.13	27.18	3.79
D 8.	40.56	7.16	2.53	4.92	11.56	0.18	16.66	1.01	28.05	4.03
D 9.	41.50	6.86	2.07	3.84	11.01	0.33	15.18	1.21	29.17	4.01
D 10.	38.52	7.75	3.18	3.71	13.19	0.25	17.15	1.43	28.01	3.96
D 13.	42.28	7.98	2.27	5.74	9.23	0.19	15.16	2.06	27.07	3.18
D 14.	40.87	7.24	2.28	4.92	12.58	0.11	17.61	1.43	26.47	4.10
D 16.	42.91	6.95	2.53	5.49	10.39	0.12	16.00	1.77	27.31	2.53
D 18.	43.85	8.17	2.22	4.49	10.44	0.18	15.21	1.57	25.11	3.87
D 19.	41.79	7.07	2.27	6.25	9.86	0.17	16.28	3.15	26.18	3.26
D 20.	43.13	7.44	2.44	7.53	9.33	0.19	17.05	1.11	25.24	3.59
D 22.	42.85	7.07	2.87	6.00	10.17	0.21	16.38	1.27	26.23	3.33
D 23.	41.97	7.83	2.25	5.24	12.53	0.24	18.01	1.78	24.17	3.99
D 24.	40.84	7.03	2.81	7.23	12.17	0.18	19.58	1.29	25.27	3.18
D 25.	40.35	6.91	3.65	4.02	13.23	0.20	17.45	2.12	25.54	3.98
D 26.	40.37	7.32	2.50	5.71	12.45	0.13	18.29	1.94	26.07	3.51
D 28.	39.40	7.55	2.87	6.61	12.15	0.19	18.95	2.06	25.15	4.02
D 30.	42.58	7.83	2.30	4.60	12.24	0.22	17.06	1.32	24.93	3.98
D 31.	39.33	6.69	3.07	5.43	13.66	0.23	19.32	2.15	26.27	3.17
D 32.	42.66	7.00	2.12	5.29	12.54	0.29	18.12	1.27	25.17	3.66
D 35.	38.57	7.13	2.89	5.40	13.89	0.18	19.47	2.13	26.63	3.18
D 36.	44.61	7.37	2.38	3.77	12.21	0.17	16.15	1.40	25.12	2.97
Average:	41.36	7.35	2.66	5.25	11.66	0.21	17.12	1.75	26.21	3.55

Table 4.1.2

Genetic quartz types and length-breadth ratios of quartz of the Disang sandstones.

Sample No.	Non-undulatory	Undulatory	Polycry-stalline	Re-worked	L/B - <2		L/B - > 2		Average of 50 grains
					Minimum	Maximum	Minimum	Maximum	
D 1.	87.07	7.90	5.03	-	1.11	1.94	2.02	2.62	1.93
D 4.	90.67	6.70	2.63	-	1.61	1.92	2.00	3.05	2.24
D 5.	90.19	6.06	3.75	-	1.14	1.79	2.09	2.28	1.73
D 6.	93.67	3.82	2.51	-	-	-	2.24	3.65	2.88
D 7.	90.10	3.97	5.93	-	1.20	1.80	2.00	3.45	2.46
D 8.	95.01	3.01	1.98	-	1.42	1.71	2.10	4.00	2.53
D 9.	92.14	2.07	5.79	-	-	-	2.21	6.30	4.52
D 10.	84.93	9.56	5.51	-	1.13	1.89	2.01	3.18	2.18
D 13.	86.22	9.42	4.36	-	1.01	1.76	2.16	3.28	2.35
D 14.	89.95	7.34	2.71	-	-	-	2.00	4.33	3.24
D 16.	88.66	8.74	2.60	-	1.07	1.98	2.00	3.58	2.14
D 18.	87.23	7.62	5.15	-	1.10	1.91	2.00	3.81	2.31
D 19.	88.58	8.80	2.62	-	1.00	1.66	2.11	2.16	1.39
D 20.	86.64	8.08	5.28	-	1.43	1.90	2.06	2.81	2.06
D 22.	91.18	6.94	1.88	-	1.50	1.70	2.08	3.83	2.40
D 23.	86.66	9.79	3.55	-	-	-	2.00	4.35	2.64
D 24.	89.90	6.32	3.78	-	1.59	1.95	2.00	3.45	2.20
D 25.	85.21	9.63	5.16	-	1.17	1.91	2.00	2.60	1.91
D 26.	87.44	9.75	2.81	-	1.74	1.98	2.00	3.07	2.13
D 28.	85.21	8.85	4.98	0.96	1.43	1.87	2.01	2.45	1.93
D 30.	88.18	4.74	6.95	0.13	1.08	1.96	2.08	2.86	2.00
D 31.	86.39	8.18	4.86	0.57	1.31	1.98	2.00	2.87	2.05
D 32.	92.57	4.70	2.73	-	1.38	1.93	2.05	2.72	2.10
D 35.	86.10	10.04	3.86	-	1.07	1.99	2.37	2.56	1.68
D 36.	93.08	3.65	2.31	0.96	-	-	2.16	3.00	2.46
Average :	88.92	7.03	3.95	0.10					

sub-angular to sub-rounded, a number of them being coated with thin films of iron oxide. The feldspars include plagioclase and untwinned varieties. The alteration of the feldspar detritals to matrix is due to diagenesis of the sediments.

Mica :

The Disang sandstones commonly contain flakes of detrital muscovite and biotite (Fig. 4.1.6). The mica constituents range between 2.07 and 3.65%. In some of the thin sections the mica flakes show sutured ends which are due to alteration to the clayey matrix which is common. Their boundaries are also found replaced by hematite (Fig. 4.1.3). Some of the grains show kink-bending while others are found squeezed between quartz detritals (Fig. 4.1.6).

Other minerals :

The other mineral grains, including zircon, tourmaline, rutile, kyanite, garnet, epidote and opaques, range from 1.01 to 3.15%. These minerals, all of a higher density than the common minerals, are studied in detail as heavy minerals in chapter 6.

Rock fragments :

The rock fragments found in the Disang sandstones include volcanic (Fig. 4.1.7), metamorphic (Fig. 4.1.1) and cherty varieties (Fig. 4.1.3) and as a group range from 13.06 to 20.33%. The igneous rock fragments range from 2.26 to 7.53%, the metamorphic types from 9.23 to 13.89% and reworked fragments range from 0.11 to 0.37% of the total mineralogical composition.

Matrix and cement :

The matrix of the Disang sandstones is made up of chert and clay (Fig. 4.1.1), probably illite and chlorite as confirmed

Fig. 4.1.7

Ferrugenous Disang sandstone under crossed nicols

A - Pyrite
B - Tourmaline
C - Ferrugenous alteration of volcanic rock fragments

Fig. 4.1.8

Disang sandstone under crossed nicols showing quartz vein.

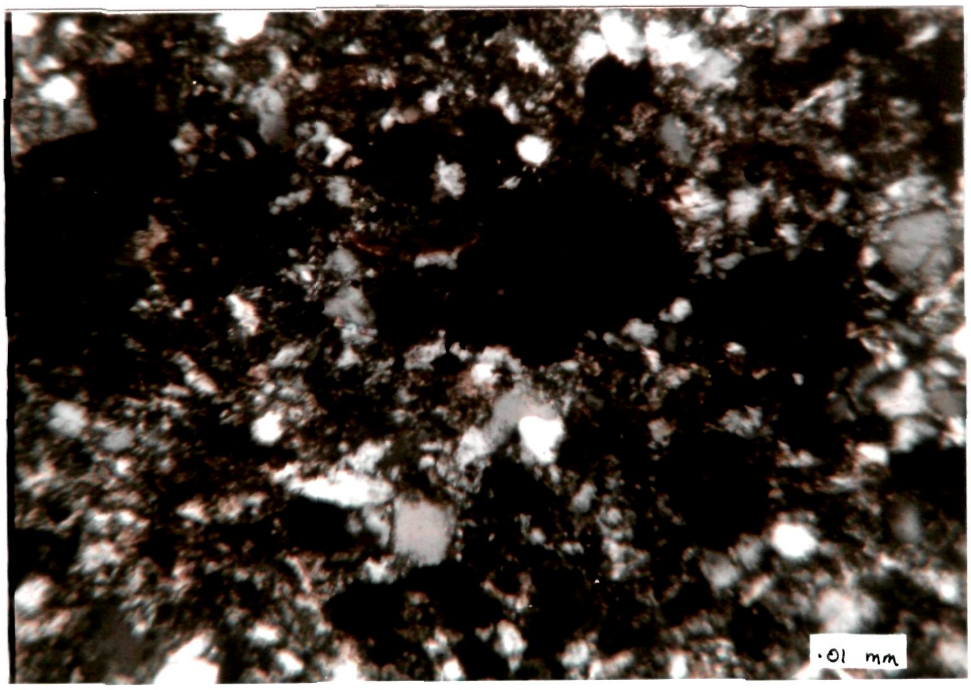
.01 mm

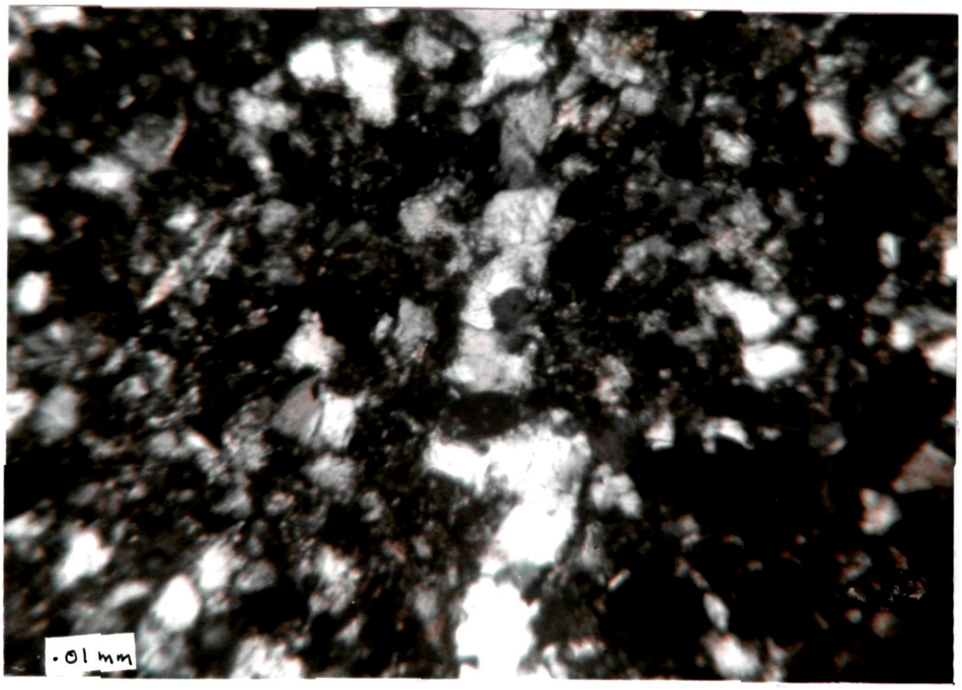
.01 mm

by x-ray diffraction which is discussed later in the chapter under the subheading 'Clay mineralogy'. The clayey matrix, which ranges between 24.17 and 29.17%, usually occurs as fibrous laths in the pore spaces. Iron oxides (Fig. 4.1.7) and silica (Fig. 4.1.4) are the cementing materials besides calcium carbonate, which is noted in a few sections (Fig. 4.1.5). Pyrite (Fig. 4.1.7) appears to be common in some of the sandstones. The allogenic clayey matrix is occasionally seen to be replaced by ferrugenous materials (Fig. 4.1.2). Cement, as a whole, ranges from 2.03 to 4.10%.

The vertical distribution of the various constituents of the Disang sandstones is shown in figure 4.1.9. The distribution pattern is found to be irregular.

4.1.3. RELATIONSHIPS OF SOME FRAMEWORK CONSTITUENTS :

In the past three decades or so, a number of classifications for sandstones has been proposed. However, no single classification has been accepted as satisfactory by petrographers. In the present investigation three classificatory schemes have been followed.

The classification of Doty and Hubert (1962) is followed where recalculated values of quartz, feldspar and mica+micaceous rock fragments are plotted in a ternary diagram (Fig. 4.1.10, Table 4.1.3). By this method the Disang sandstones are classified as quartzose graywackes and feldspathic graywackes, the former dominating. The method of kukal (1968), using recalculated percentages of quartz, feldspar+unstable grains and matrix plotted in a ternary diagram (Fig. 4.1.11, Table 4.1. 3), indicate that the rocks are graywackes and subgraywackes. The quartz, feldspar and rock fragments plots in a ternary diagram (Fig. 4.1.12, Table 4.1.3) following Pettijohn (1975) indicate that the Disang sandstones are lithic graywackes.

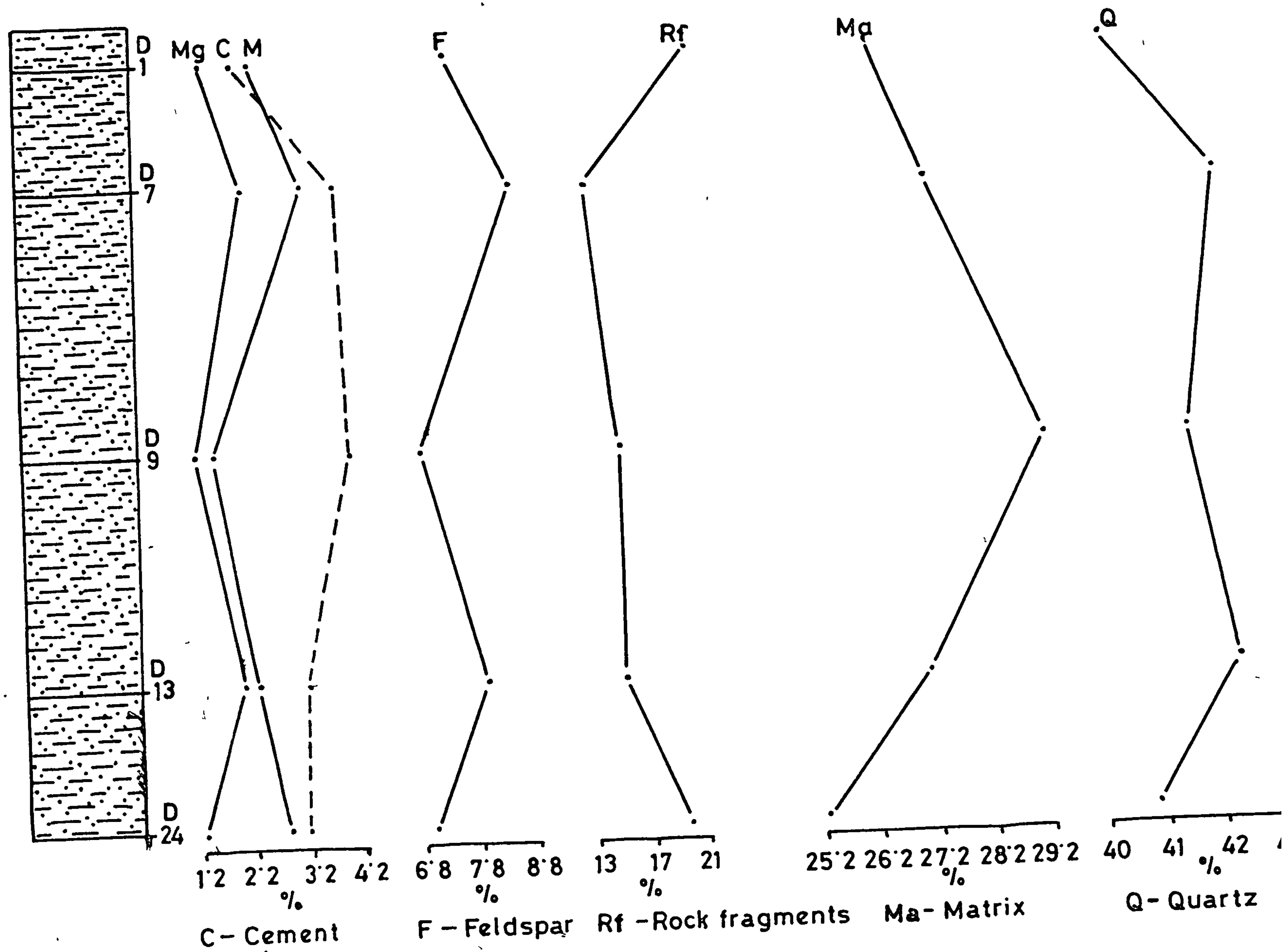

FIG: 4·1·9

VERTICAL VARIATION OF MINERAL CONSTITUENTS OF THE DISANG SANDSTONES

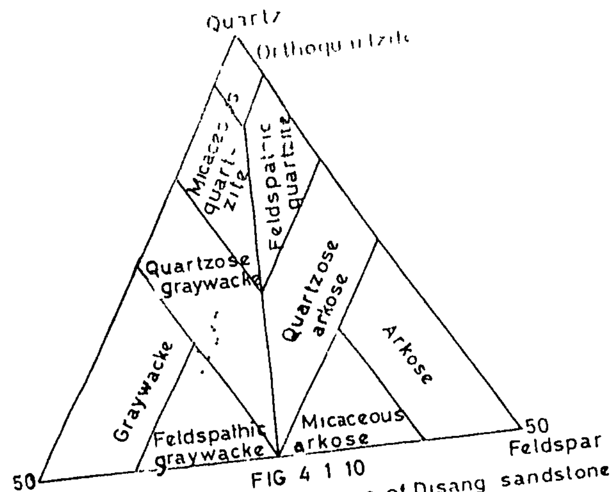

FIG 4 1 10
Mineralogical classification of Disang sandstones
(After Doty & Hubert,1962)

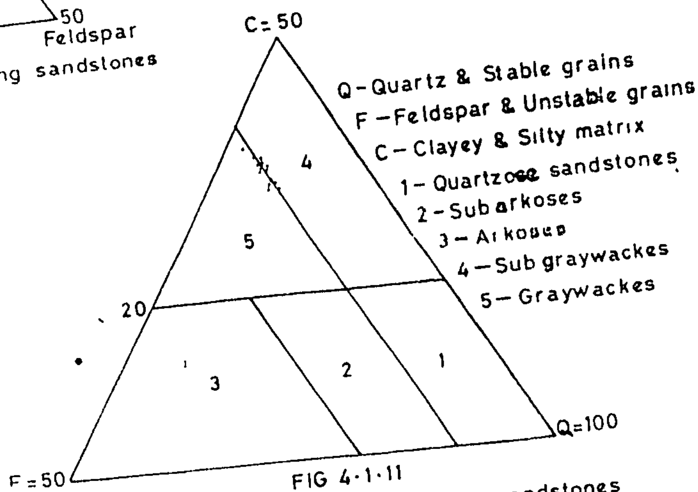

FIG 4·1·11
Mineralogical classification of Disang sandstones
(After Kukal,1968)

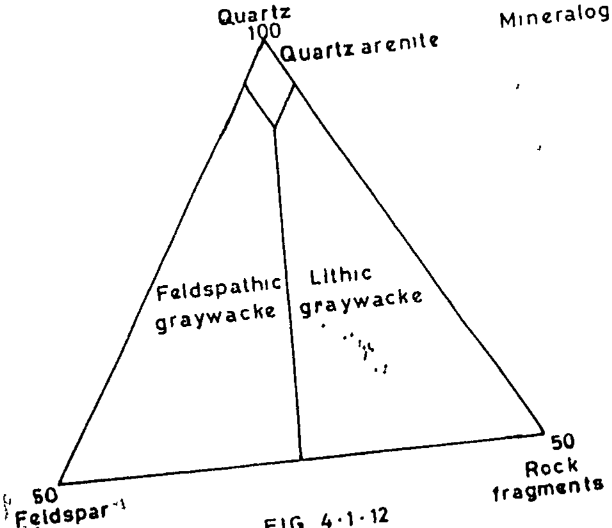

FIG 4·1·12
Mineralogical classification of Disang sandstones
(After Pettijohn,1975)

Table 4.1.3

Mineralogical classification of the Disang sandstones.

Sample No.	Q	F	R	Rock type	Q	F	M	Rock type	Q	F	C	Rock type
D 1.	59.11	10.96	29.92	Lithic graywacke	63.23	11.73	25.04	Feldspathic graywacke	54.41	10.09	35.50	Graywacke
D 4.	62.84	11.04	26.12	Lithic graywacke	65.73	11.54	22.72	Quartzose graywacke	55.22	9.70	35.08	Subgraywacke
D 5.	62.83	10.84	26.34	Lithic graywacke	65.34	11.27	23.38	Quartzose graywacke	55.46	9.57	34.97	Subgraywacke
D 6.	64.38	11.32	24.30	Lithic graywacke	66.36	11.67	21.96	Quartzose graywacke	54.59	9.60	35.81	Subgraywacke
D 7.	66.08	13.40	20.51	Lithic graywacke	65.46	13.27	21.27	Quartzose graywacke	54.09	10.97	34.94	Graywacke
D 8	63.00	11.12	25.88	Lithic graywacke	65.62	11.58	22.79	Quartzose graywacke	53.53	9.45	37.02	Subgraywacke
D 9.	65.31	10.80	23.89	Lithic graywacke	67.54	11.16	21.29	Quartzose graywacke	53.53	8.85	37.62	Subgraywacke
D 10.	60.74	12.22	27.04	Lithic graywacke	61.49	12.37	26.13	Feldspathic graywacke	51.86	10.43	37.71	Graywacke
D 13.	64.63	12.20	23.17	Lithic graywacke	68.46	12.92	18.62	Quartzose graywacke	54.67	10.32	35.01	Graywacke
D 14.	62.19	11.02	26.79	Lithic graywacke	64.90	11.50	23.60	Quartzose graywacke	54.80	9.71	35.49	Subgraywacke
D 16.	65.15	10.55	24.29	Lithic graywacke	68.35	11.07	20.58	Quartzose graywacke	55.60	9.01	35.39	Subgraywacke
D 18.	65.22	12.12	22.62	Lithic graywacke	67.79	12.63	19.57	Quartzose graywacke	56.85	10.59	32.56	Graywacke
D 19.	64.15	10.85	24.99	Lithic graywacke	68.52	11.59	19.89	Quartzose graywacke	55.69	9.42	34.89	Subgraywacke
D 20.	63.78	11.00	25.21	Lithic graywacke	69.18	11.93	18.88	Quartzose graywacke	56.89	9.81	33.29	Subgraywacke
D 22.	64.63	10.66	24.70	Lithic graywacke	68.06	11.23	20.71	Quartzose graywacke	56.27	9.28	34.45	Subgraywacke
D 23.	61.89	11.55	26.56	Lithic graywacke	64.99	12.12	22.89	Quartzose graywacke	56.74	10.58	32.86	Graywacke
D 24.	60.55	10.42	29.03	Lithic graywacke	64.98	11.18	23.84	Quartzose graywacke	55.84	9.61	34.55	Subgraywacke
D 25.	62.35	10.68	26.97	Lithic graywacke	62.91	10.77	26.32	Feldspathic graywacke	55.42	9.49	35.08	Subgraywacke
D 26.	61.18	11.09	27.72	Lithic graywacke	64.45	11.68	23.87	Quartzose graywacke	54.73	9.92	35.34	Subgraywacke
D 28.	59.79	11.46	28.75	Lithic graywacke	63.58	12.18	24.24	Quartzose graywacke	54.65	10.47	34.88	Graywacke
D 30.	63.11	11.60	25.28	Lithic graywake	65.56	12.05	22.39	Quartzose graywacke	56.52	10.39	33.09	Graywacke
D 31.	60.19	10.24	29.57	Lithic graywacke	62.68	10.66	26.66	Feldspathic graywacke	54.40	9.25	36.34	Subgraywacke
D 32.	62.94	10.33	26.73	Lithic graywacke	66.32	10.88	22.79	Quartzose graywacke	57.01	9.35	33.64	Subgraywacke
D 35.	59.18	10.94	29.87	Lithic graywacke	61.73	11.41	26.86	Feldspathic graywacke	53.32	9.86	36.82	Subgraywack
D 36.	65.48	10.82	23.70	Lithic graywacke	67.01	11.07	21.92	Quartzose graywacke	57.86	9.56	32.58	Subgraywacke
Average:	62.83	11.17	26.00		65.61	11.66	22.73		55.20	9.81	34.99	

Q - Quartz, F- Feldspar, R - Rock fragments, M- Mica+micaceous rock fragments, C - Matrix

For paleoclimatic studies ratios of polycrystalline quartz and feldspar+rock fragments, and that of total quartz and feldspar+rock fragments are plotted against each other (Fig. 4.1. 13, Table 4.1.4) following Suttner and Dutta (1986). The plots indicate semi-arid to semi-humid conditions. Semi-humid paleoclimatic conditions is also suggested by triangular plots of Suttner and Dutta (1986) using quartz, feldspar and lithic fragments (Fig. 4.1.14, Table 4.1.3). The same plots (Fig. 4.1. 14, Table 4.1.3) following Dickinson et al. (1983) indicate that the source is a recycled orogen.

4.1.4. RATIOS OF SOME FRAMEWORK CONSTITUENTS :

The quartz-feldspar ratio (Pettijohn, 1975) and the quartz-feldspar-rock fragments ratio (Suttner and Dutta, 1986) give some idea about the mineralogical maturity of sandstones. The quartz-feldspar ratios of the Disang sandstones range between 4.93 and 6.17, and average 5.64 (Table 4.1.4). The average quartz-feldspar-rock fragments ratio (Table 4.1.3) is 62.83-11.17 -26.00. These ratios reflect the immature nature of the sandstones of the Disang Group.

4.2. CLAY MINERALOGY

4.2.1. INTRODUCTION :

The clay minerals form one of the most important constituents of sediments. They are stable secondary products formed by the decomposition of other aluminosilicates (Pettijohn, 1975, Mason and Moore, 1982). The formation of a clay mineral is dependant on the chemical character of the parent material and the physico-chemical environment in which alteration of the mineral takes place (Krumbein and Sloss, 1963; Pettijohn, 1975, Mason and Moore,1982). Macro and microclimatic factors also bear a direct relationship to the formation of a particular type of

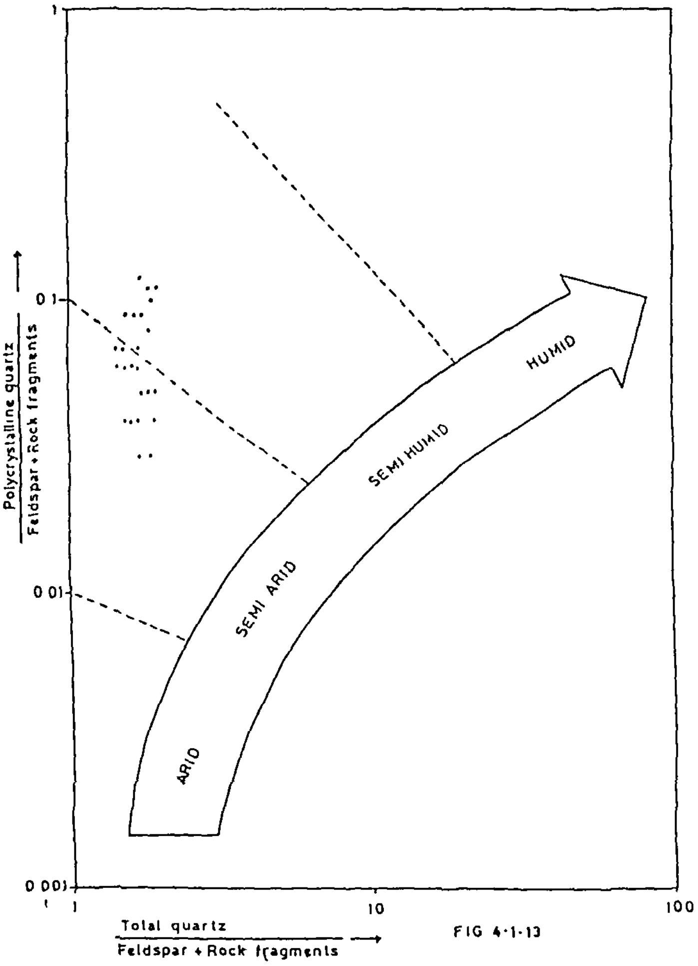

FIG 4·1·13

Bivariant log-log plots of the ratios of Polycrystalline quartz to Feldspar + Rock fragments and Total quartz to Feldspar + Rock fragments of the sandstones of the Disang Group

(After Suttner and Dutta, 1986)

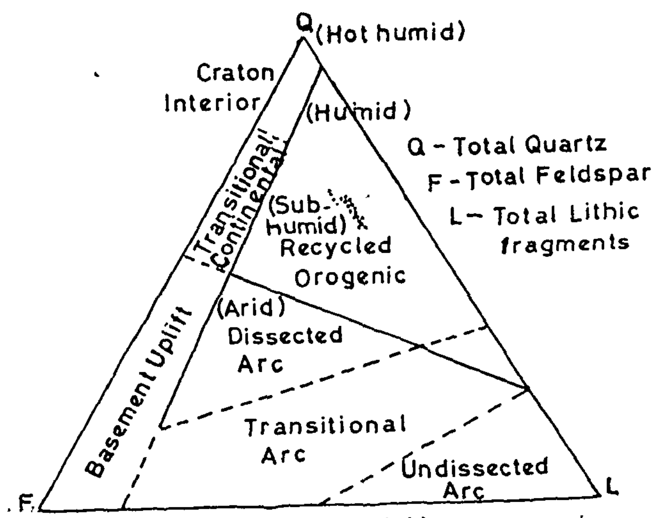

FIG. 4·1·14

QFL Provenance-discrimination diagram of Disang sandstones

(After Dickinson et al., 1983)

Table 4.1.4

Ratios of some framework constituents of the Disang sandstones.

Sample No.	Polycrystalline quartz / Feldspar + rock fragments	Total quartz / Feldspar + rock fragments	Quartz / Feldspar
D 1.	0.07	1.45	5.39
D 4.	0.04	1.69	5.69
D 5.	0.06	1.69	5.80
D 6.	0.05	1.81	5.68
D 7.	0.12	1.95	4.93
D 8.	0.03	1.70	5.66
D 9.	0.11	1.88	6.05
D 10.	0.09	1.55	4.97
D 13.	0.08	1.83	5.30
D 14.	0.04	1.64	5.64
D 16.	0.05	1.87	6.17
D 18.	0.10	1.88	5.37
D 19.	0.05	1.79	5.91
D 20.	0.09	1.76	5.80
D 22.	0.03	1.83	6.06
D 23.	0.06	1.62	5.36
D 24.	0.06	1.53	5.81
D 25.	0.09	1.66	5.84
D 26.	0.04	1.58	5.51
D 28.	0.07	1.49	5.22
D 30.	0.12	1.71	5.44
D 31.	0.07	1.51	5.88
D 32.	0.07	1.70	6.09
D 35.	0.06	1.45	5.41
D 36.	0.04	1.90	6.05
Average :	0.07	1.70	5.64

clay mineral, so also organic decomposition and type of concentration of inorganic ions in the genetic environment (Lewis, 1984). Other factors like temperature, the alkalinity or acidity of associated fluids, oxidising or reducing conditions, character and amount of dissolved salts and the presence or absence of organic material also appear to be involved (Krumbein and Sloss, 1963). Clay minerals are mainly detrital in origin and tend to reflect the character of their source areas (Weaver, 1958). Clay minerals, being very susceptible to change, readjust to the new environment and are thus used to ascertain the nature of ancient environments. Depths of burial, aging of sediments, due to differing atmospheric and biospheric conditions in the past (Weaver, 1967), etc. give rise to certain clay minerals (Pettijohn, 1975).

Therefore, to probe deeper into the study of the Disang sandstones, eight samples are chosen for clay mineral studies. They are analysed by the x-ray diffraction method which is discussed in chapter 3.

4.2.2. MINERALOGY :

Illite and chlorite are the only clay minerals detected in the Disang sandstones (Fig. 4.2). They are present in small amounts and their relative proportions are shown in table 4.2. The distribution of illite and chlorite in the different lithounits is more or less even.

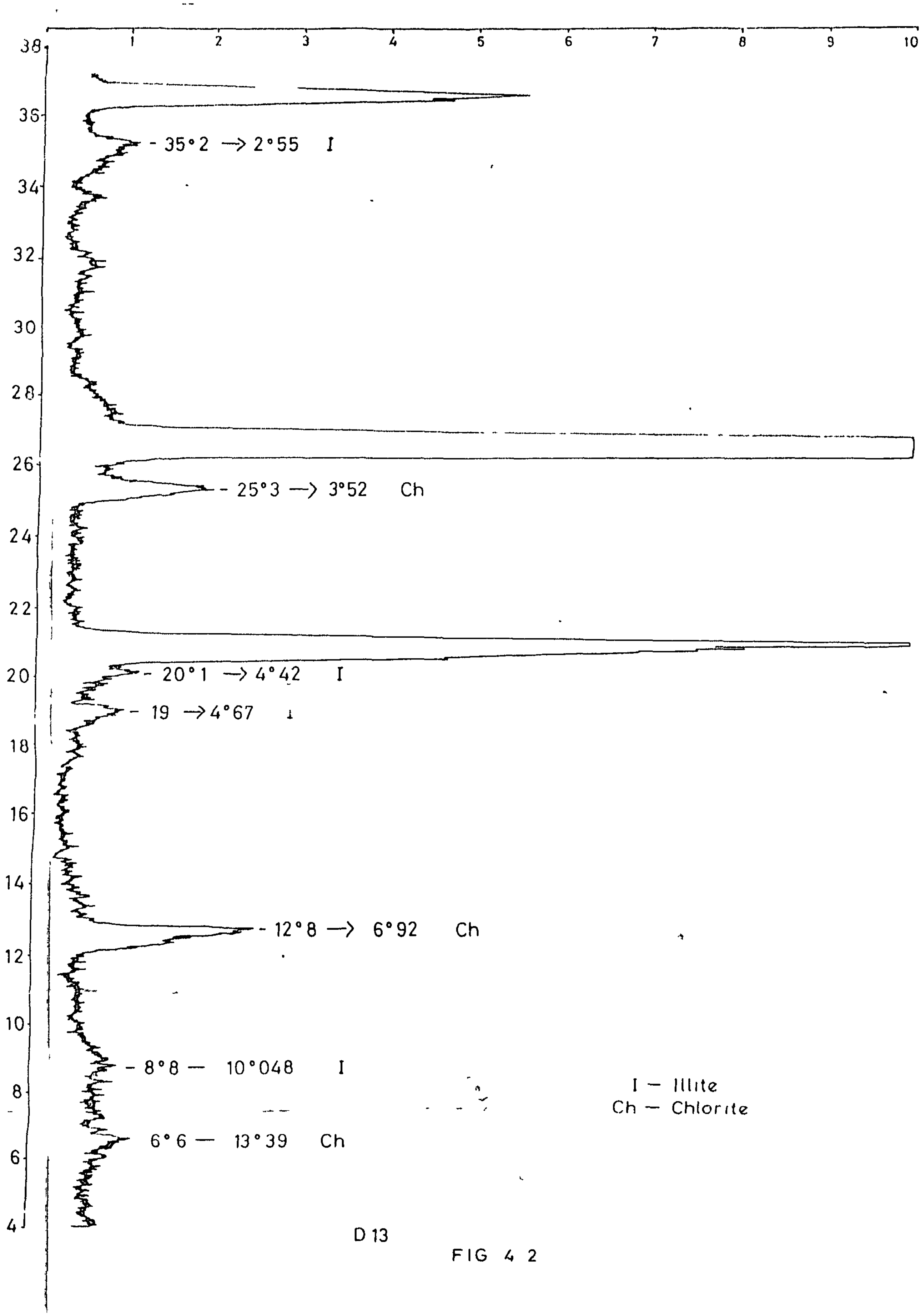

1 2 3 4 5 6 7 8 9 10
38 36 34 32 30 28 26 24 22 20 18 16 14 12 10 8 6 4
35°2 → 2°55 I
25°3 → 3°52 Ch
20°1 → 4°42 I
19 → 4°67 I
12°8 → 6°92 Ch
8°8 — 10°048 I
6°6 — 13°39 Ch
I — Illite
Ch — Chlorite

D 13

FIG 4 2

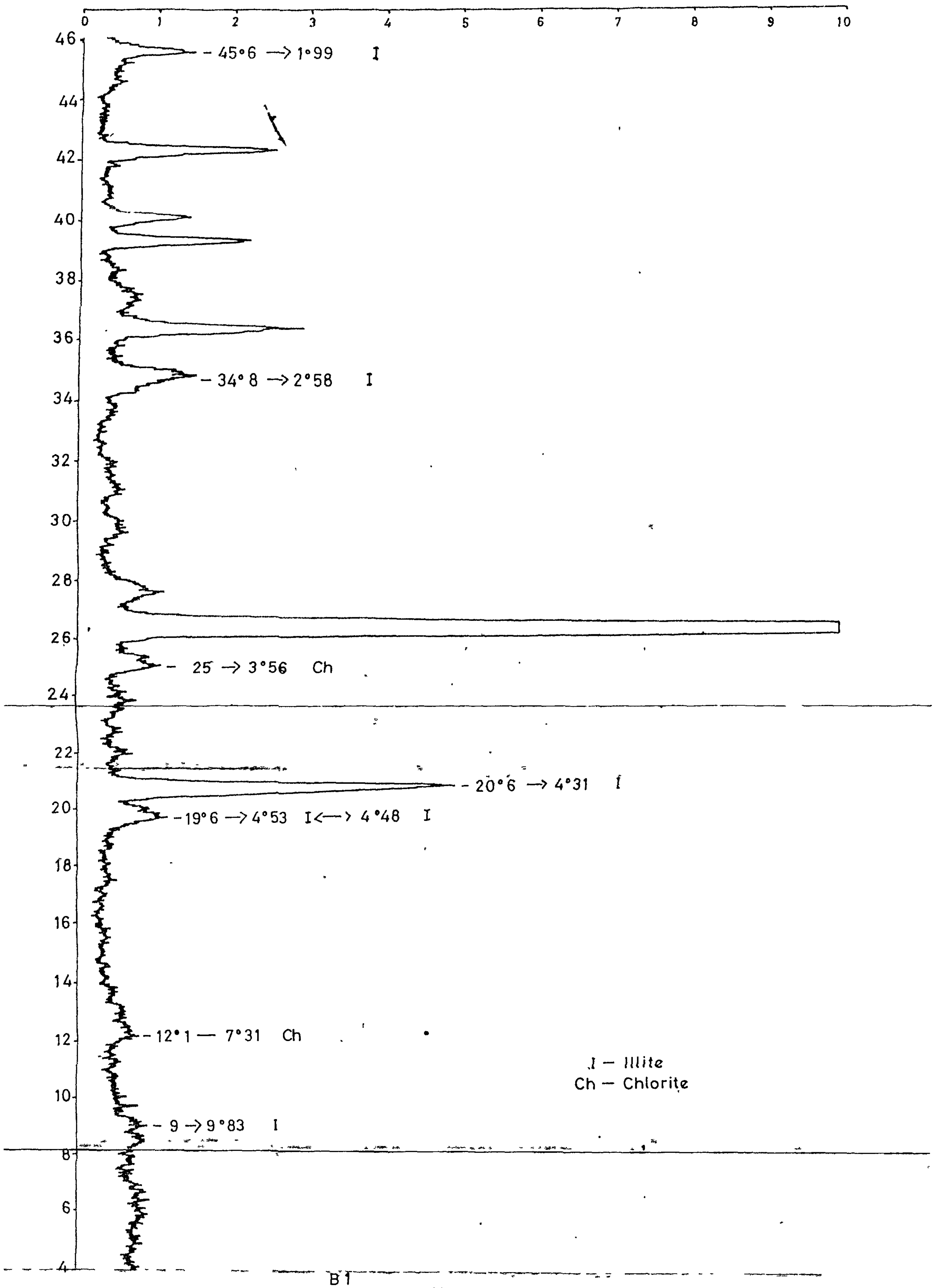

0 1 2 3 4 5 6 7 8 9 10
46 44 42 40 38 36 34 32 30 28 26 24 22 20 18 16 14 12 10 8 6 4
- 45°6 → 1°99 I
- 34°8 → 2°58 I
- 25 → 3°56 Ch
- 20°6 → 4°31 I
-19°6 → 4°53 I ←→ 4°48 I
-12°1 — 7°31 Ch
- 9 → 9°83 I
I — Illite
Ch — Chlorite
B1

FIG. 8·2

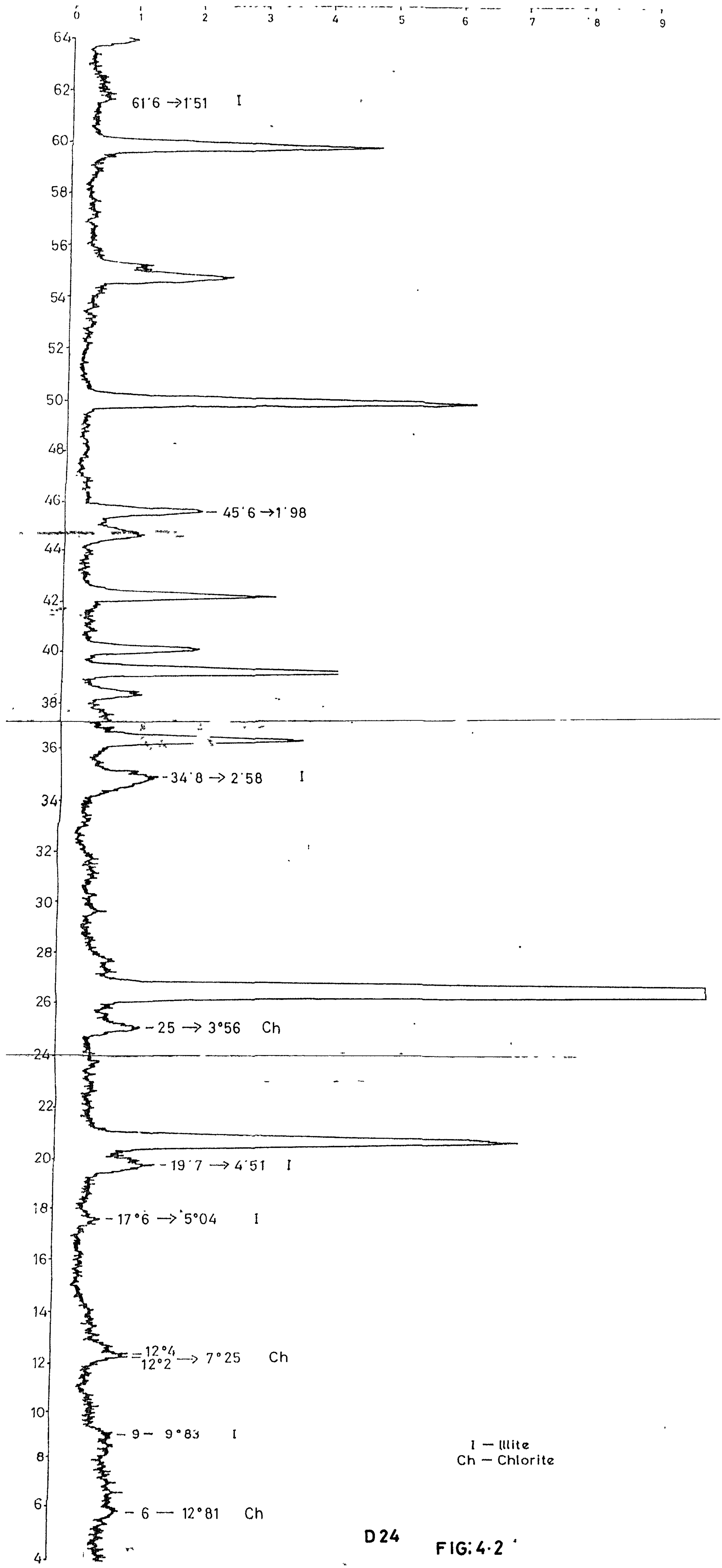

61'6 → 1'51 I
45'6 → 1'98
34'8 → 2'58 I
25 → 3°56 Ch
19'7 → 4'51 I
17°6 → 5°04 I
12°4
12°2 → 7°25 Ch
9 — 9°83 I
6 — 12°81 Ch
I — Illite
Ch — Chlorite
D 24

FIG. 4·2

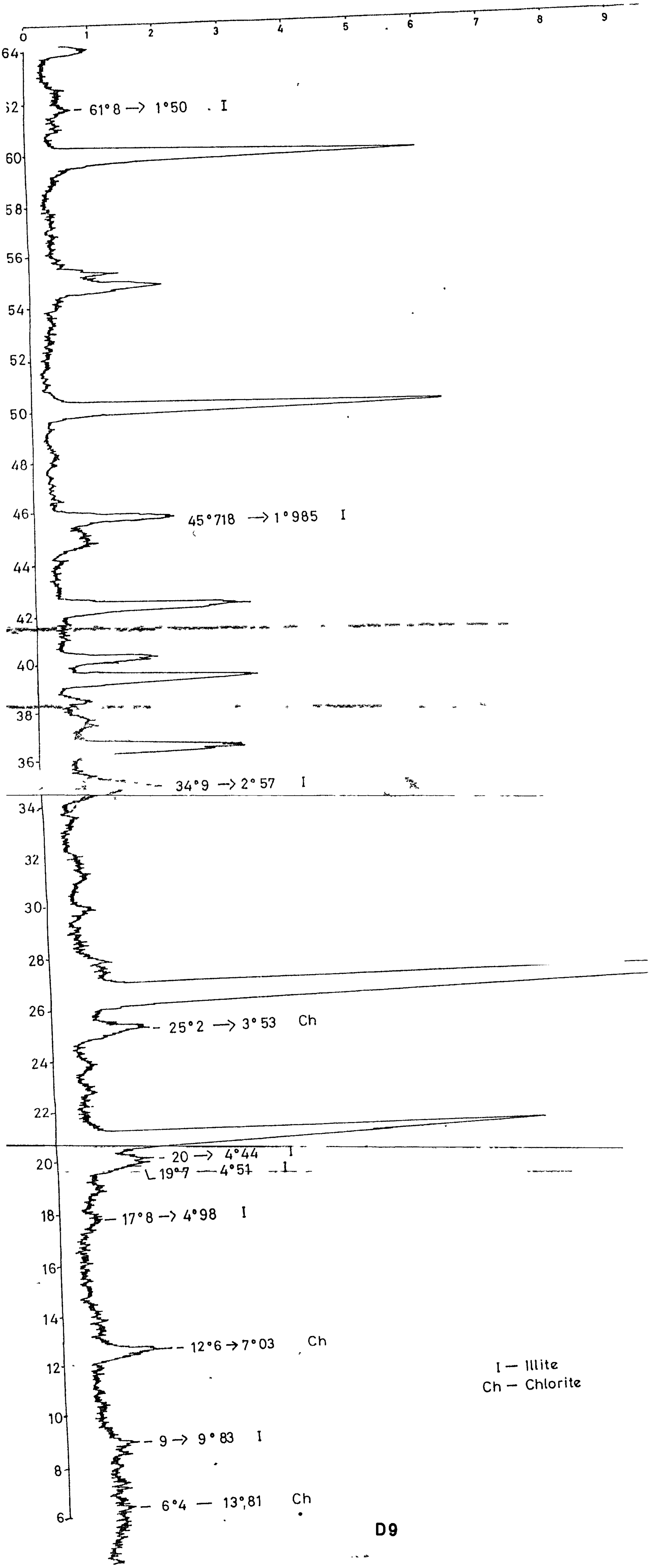

0 1 2 3 4 5 6 7 8 9
64 62 60 58 56 54 52 50 48 46 44 42 40 38 36
34 32 30 28 26 24 22
20 18 16 14 12 10 8 6
61°8 → 1°50 I
45°718 → 1°985 I
34°9 → 2°57 I
25°2 → 3°53 Ch
20 → 4°44 I
19°7 — 4°51 I
17°8 → 4°98 I
12°6 → 7°03 Ch
9 → 9°83 I
6°4 — 13°,81 Ch
I — Illite
Ch — Chlorite

D9

Table 4.2

Clay minerals in the sandstones of the Disang Group.

Sample No.	Constituents detected						
	Major	Minor	Good amount	Considerable amount	Small amount	Trace	Trace likely
D 1.	-	-	-	-	Illite	Chlorite	-
D 7.	-	-	-	-	Illite Chlorite	-	-
D 9.	-	-	-	-	Chlorite Illite	-	-
D 13.	-	-	-	-	Chlorite Illite	-	-
D 23.	-	-	-	-	Illite Chlorite	-	-
D 24.	-	-	-	-	Chlorite Illite	-	-
D 30.	-	-	-	-	Illite Chlorite	-	-
D 36.	-	-	Chlorite	-	Illite	-	-

CHAPTER 5

SIZE ANALYSIS

5.1. INTRODUCTION :

Grain size is a very important property of clastic sediments as it bears a fundamental relationship with the physical forces involved in transportation and deposition of sediments. Studies by Passega (1957, 1964), Friedman (1967) and others have demonstrated that there is a certain correlation of grain size with depositional environments of sediments and that it is possible to decipher the nature of the depositional processes by studying the grain size statistical parameters. Pettijohn, Potter and Siever (1973) have opined that the relation between size distribution of sandstones to their environments of deposition is limited because results have not been consistent. According to Reineck and Singh (1980), as grain size distribution is a product of hydrodynamic factors of an environment, the same kind of hydrodynamic factors may be active in different environments and similar grain size distributions may result. Keeping this in mind the author has carried out grain size analysis of twenty two samples of the Disang sandstones from the area under study (Table 5.1).

5.2. CUMULATIVE CURVES AND TEXTURAL PARAMETERS :

The cumulative curves of the Disang sandstones are characteristically bimodal and polymodal (Fig. 5.1). The grain size curves consist of two populations, namely, saltation and suspension (Fig. 5.2, Table 5.2). The saltation population shows good to excellent sorting and constitutes 23 to 60% of the total population, averaging 34%. The position of truncation points is variable. The fine truncation points between the saltation and

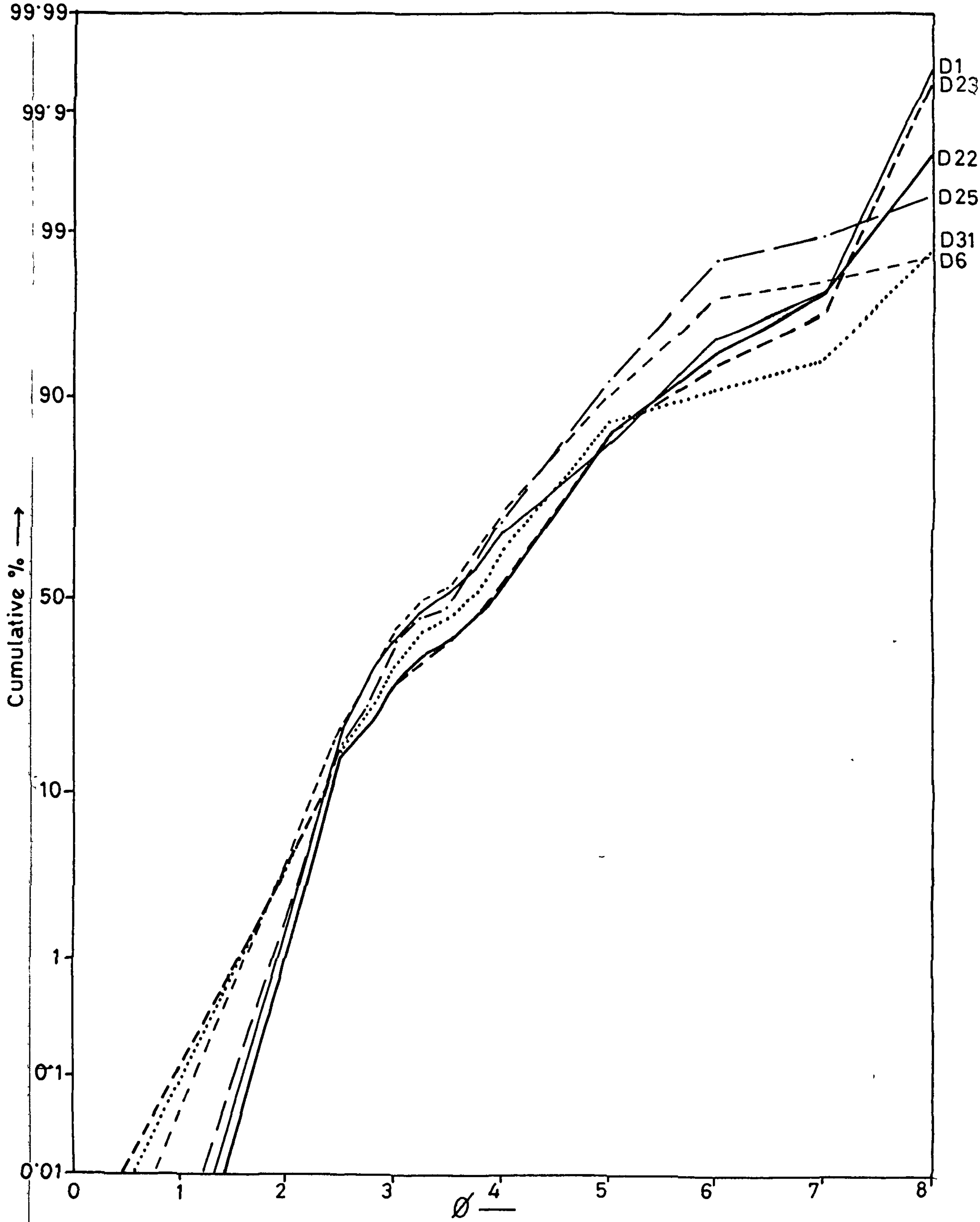

FIG. 5·1
Cumulative curves of Disang sandstones

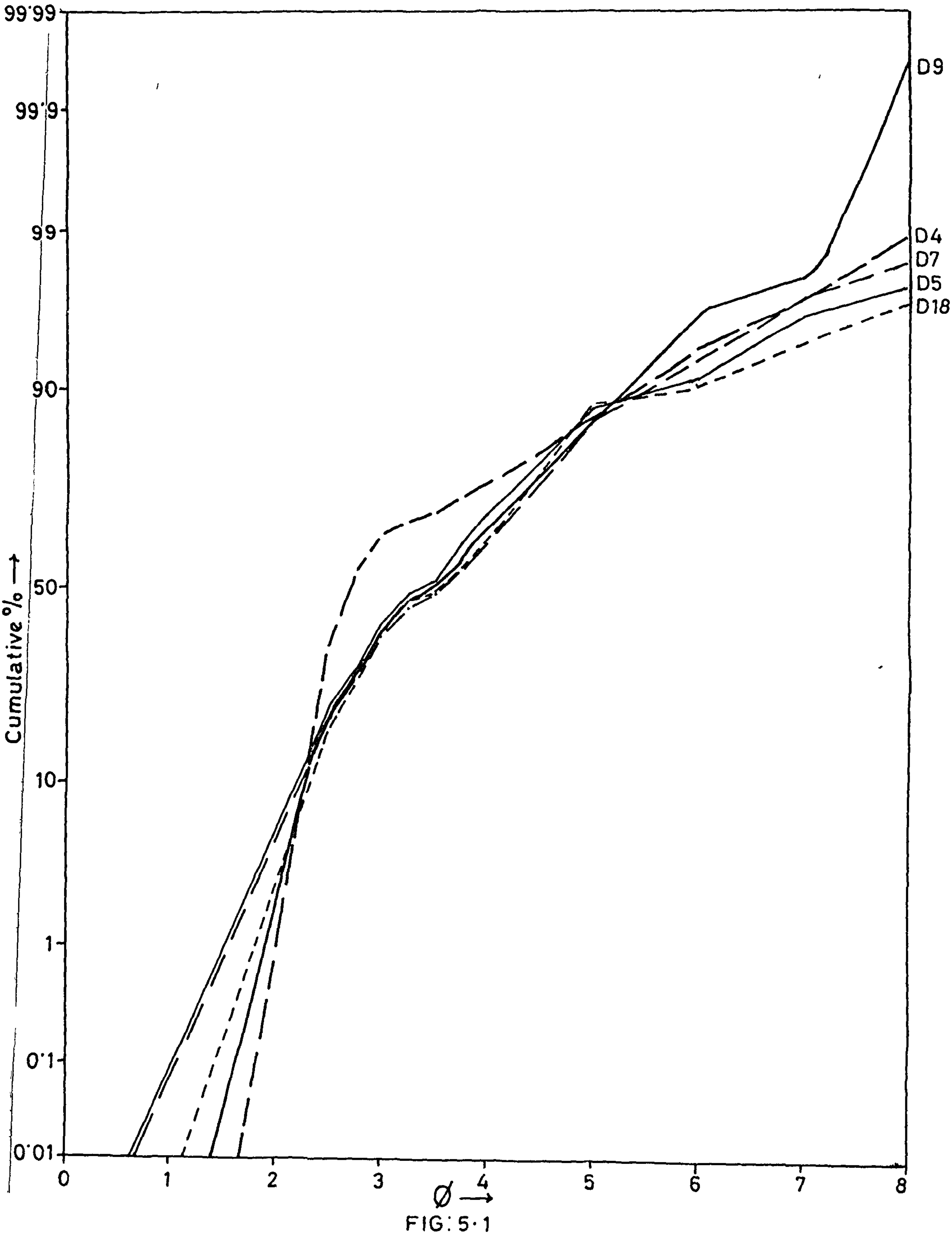

FIG: 5·1
Cumulative curves of Disang sandstones

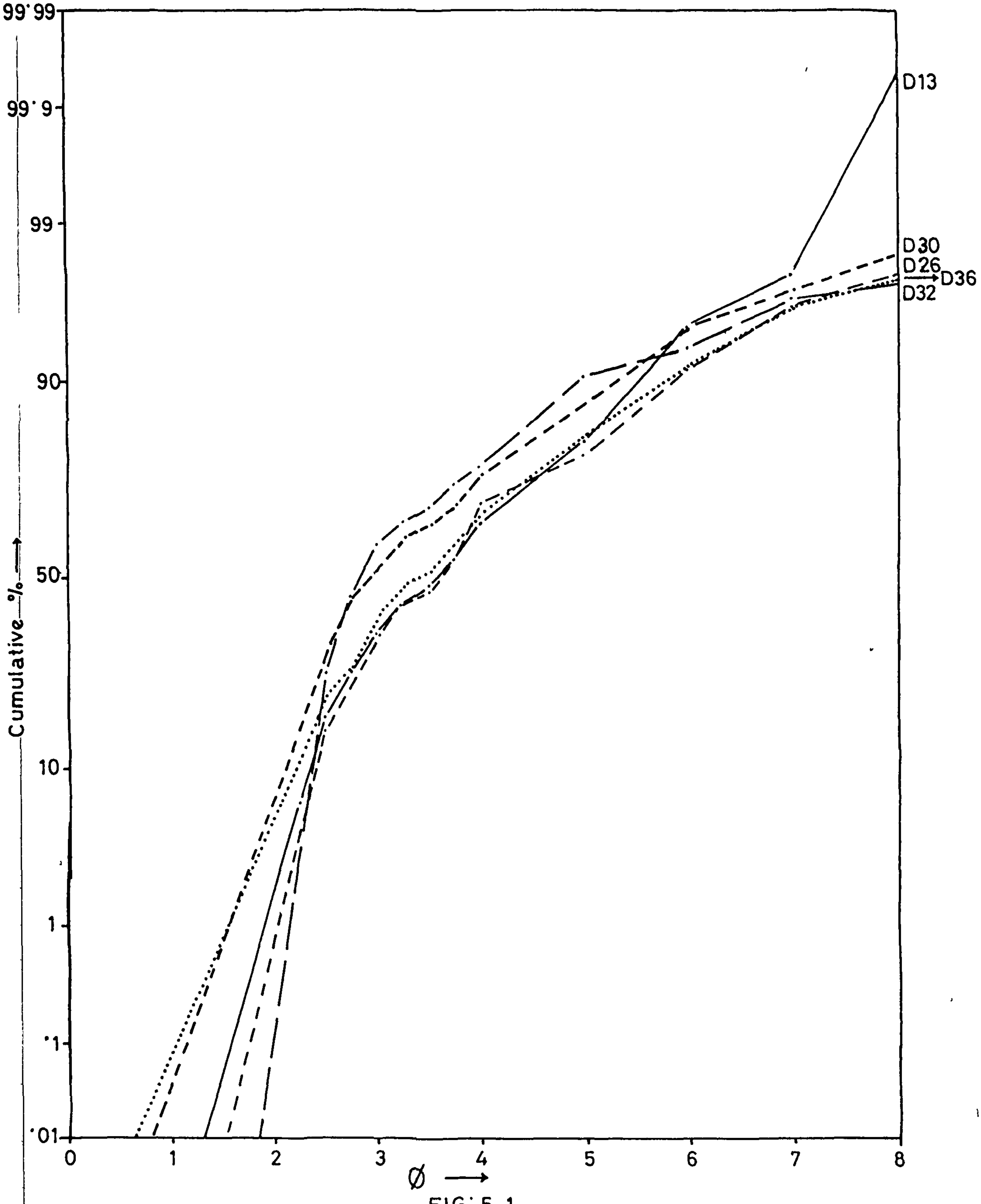

FIG: 5·1
Cumulative curves of Disang sandstones

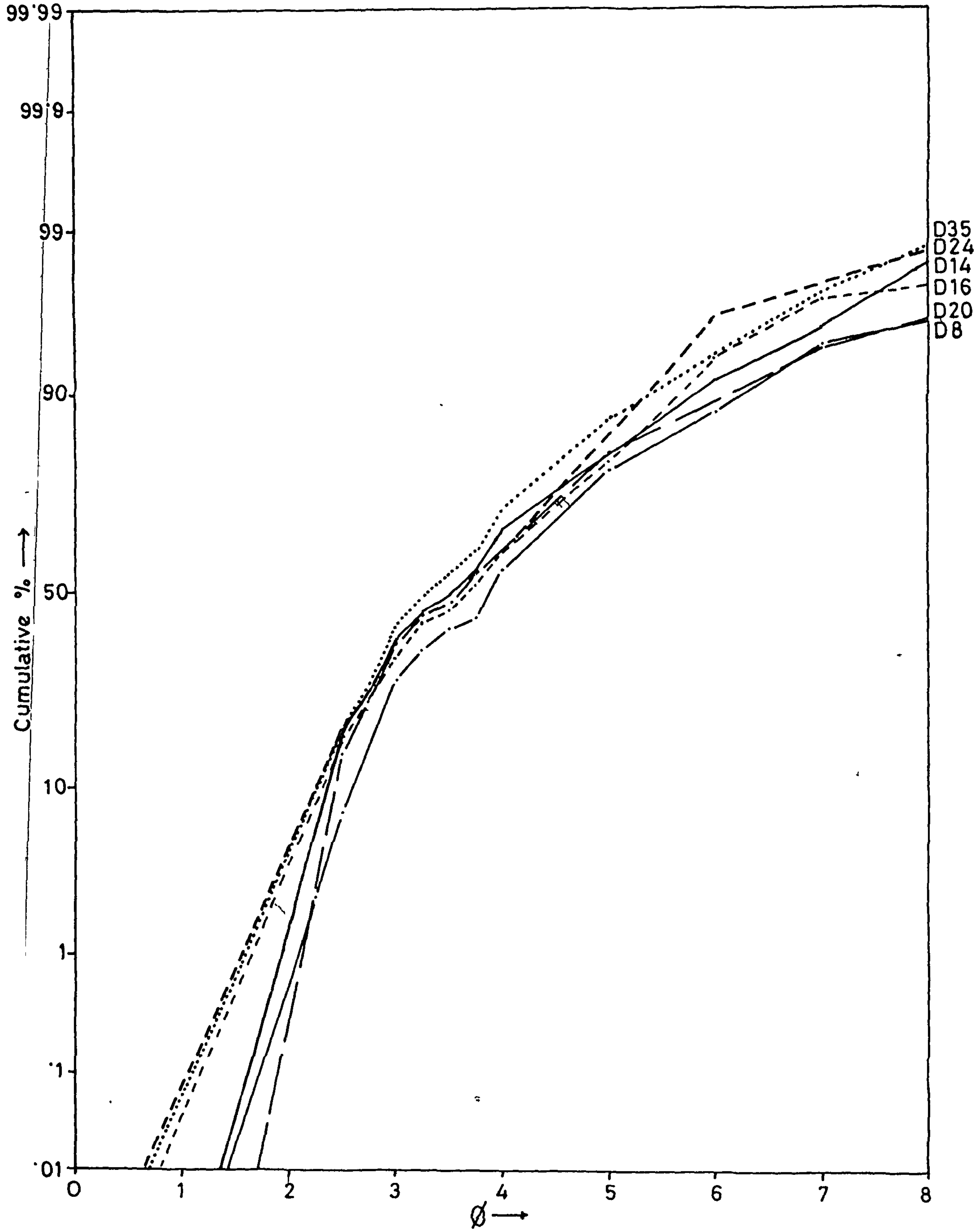

FIG: 5·1
Cumulative curves of Disang sandstones

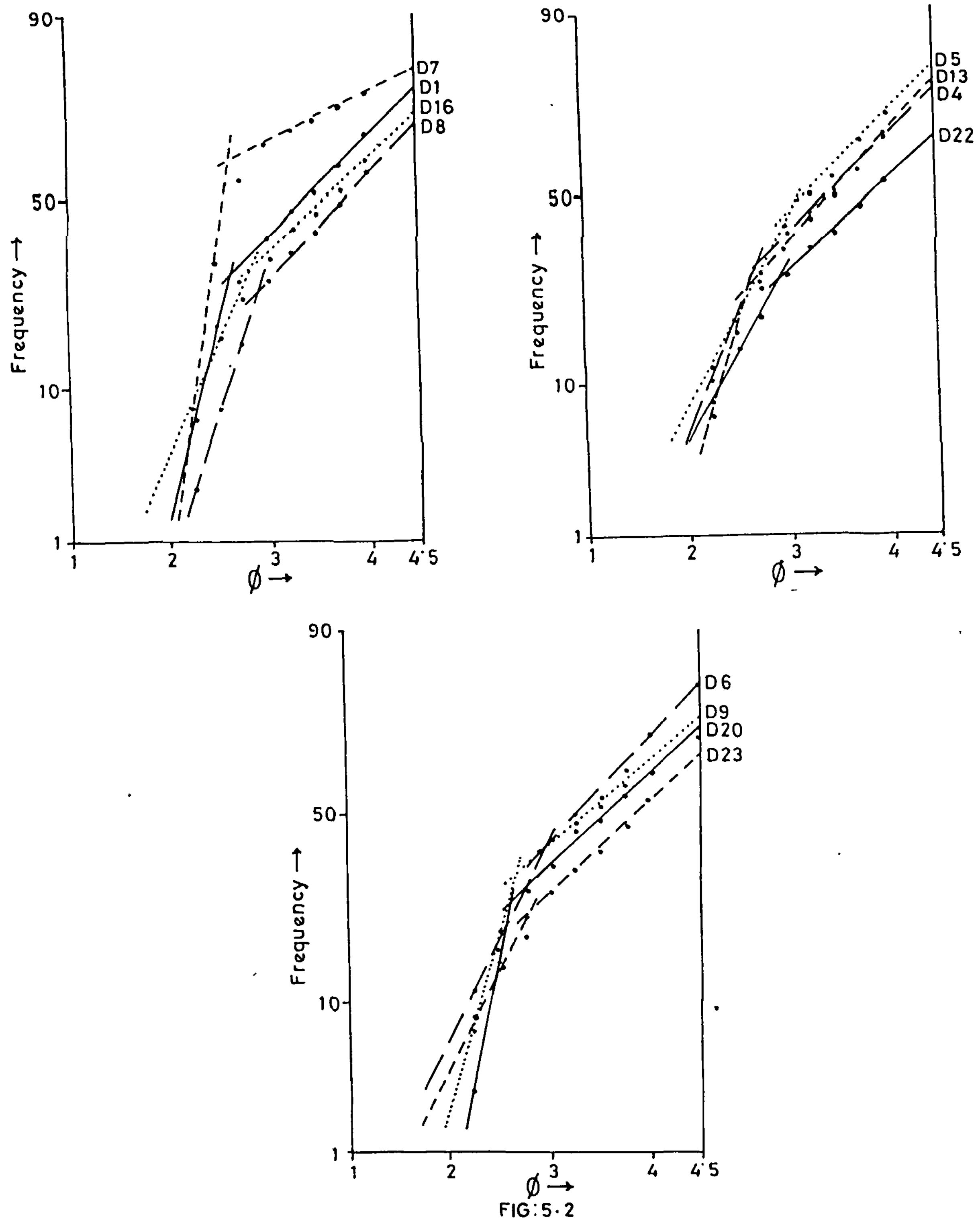

FIG: 5·2
Relation of Sediment transport to
Grainsize distribution in Disang sandstones
(After Visher, 1969)

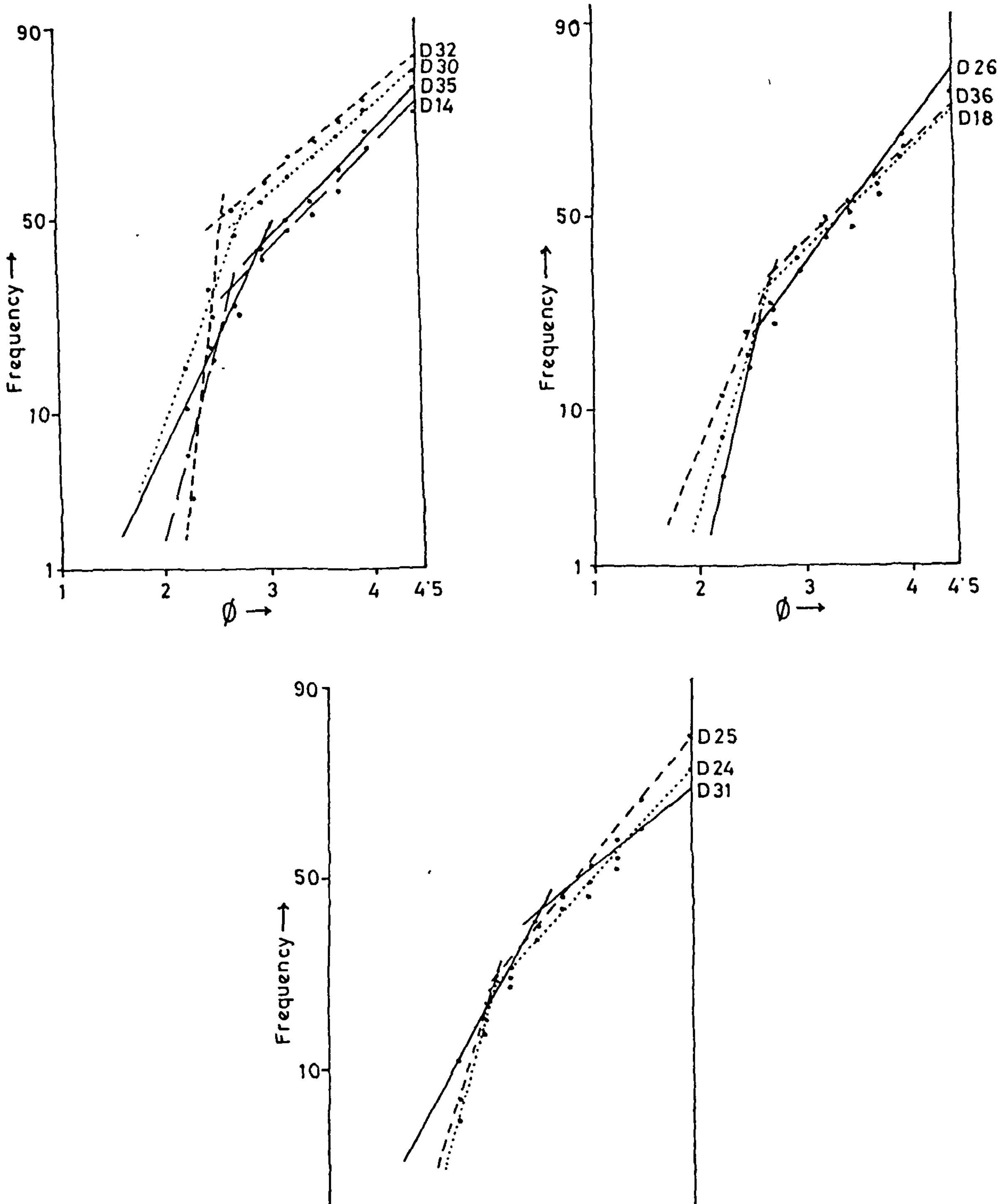

FIG: 5·2
Relation of Sediment transport to
Grainsize distribution in Disang sandstones.
(After Visher, 1969)

Table 5.1

Cumulative weight percentage of the Disang sandstones.

Sample No.	Phi scale												
	2.25	2.50	2.75	3.00	3.25	3.50	3.75	4.00	5.00	6.00	7.00	8.00	9.00
D 1.	6.65	19.36	29.02	38.91	46.11	51.76	58.78	66.91	84.41	95.29	97.44	99.96	99.99
D 4.	10.24	19.74	27.25	37.38	45.02	48.97	55.82	63.96	86.81	93.97	96.90	98.85	99.96
D 5.	11.31	20.94	28.83	39.98	48.55	52.62	62.48	69.59	88.71	91.63	96.10	97.63	99.96
D 6.	10.83	20.91	29.05	41.74	49.19	53.84	61.89	71.24	90.46	97.19	97.85	98.50	99.96
D 7.	7.61	33.40	54.26	64.12	67.27	69.34	72.42	75.64	86.99	93.36	96.95	98.34	99.96
D 8.	2.55	7.71	16.04	28.77	35.26	40.28	47.46	56.88	78.73	88.36	94.78	95.99	99.94
D 9.	6.60	19.69	29.52	40.22	46.41	50.74	57.33	64.95	85.82	95.89	97.76	99.96	99.98
D 13.	6.56	17.37	25.95	34.97	42.63	47.79	55.23	64.58	82.17	95.00	97.60	99.95	99.99
D 14.	6.13	17.75	26.23	38.34	45.88	50.02	57.20	67.10	81.97	91.77	95.62	98.25	99.95
D 16.	8.81	17.10	24.19	33.60	41.92	45.44	52.80	60.51	80.95	93.70	97.08	97.69	99.95
D 18.	7.26	17.69	26.39	37.25	46.07	49.84	56.68	63.01	88.23	90.29	94.21	96.69	99.90
D 20.	2.92	14.81	23.90	35.56	44.18	47.60	54.94	61.94	82.58	89.63	94.19	96.09	99.99
D 22.	7.92	14.74	20.18	29.18	35.15	38.65	45.78	52.72	85.48	94.19	97.33	99.75	99.96
D 23.	7.91	14.51	19.75	28.74	34.05	38.25	45.32	53.30	85.55	93.09	96.44	99.95	99.98
D 24.	10.40	19.89	26.44	37.05	44.04	47.35	54.13	62.40	85.40	96.35	97.72	98.63	99.96
D 25.	6.79	16.74	24.81	36.36	44.39	48.00	59.90	69.65	91.87	98.37	98.91	99.45	99.98
D 26.	4.31	15.17	22.96	34.19	43.01	45.67	54.85	69.02	79.41	91.31	96.10	97.69	99.95
D 30.	16.18	31.69	44.12	52.83	60.87	64.22	69.22	75.21	87.87	95.20	97.40	98.31	99.97
D 31.	5.09	14.92	22.95	33.01	40.71	44.14	51.37	62.60	87.04	90.63	93.28	98.44	99.95
D 32.	3.35	26.01	45.24	59.33	65.07	68.50	73.34	77.32	91.07	93.30	96.49	97.29	99.95
D 35.	10.23	19.68	27.76	40.40	48.97	53.09	61.86	70.72	87.11	93.93	97.35	98.74	99.97
D 36.	11.27	21.44	26.76	39.70	46.83	51.00	58.28	65.86	82.10	91.28	95.87	97.09	99.95

Table 5.2

Populations of the sandstones of the Disang Group.

Sample No.	Saltation			Suspension			
	Per-cent	Sorting	F.T. Point	Per-cent	Sorting	Mixing A&B	F.T. Point
D 1.	30	Excellent	2.63	70	Poor	Much	>4.5
D 4.	32	Good	2.74	68	Poor	Much	>4.5
D 5.	45	Good	3.10	55	Poor	Average	>4.5
D 6.	41	Good	3.00	59	Poor	Little	>4.5
D 7.	60	Excellent	2.67	40	Poor	Much	>4.5
D 8.	27	Excellent	3.03	73	Poor	Little	>4.5
D 9.	33	Excellent	2.68	67	Poor	Much	>4.5
D 13.	25	Excellent	2.65	75	Poor	Much	>4.5
D 14.	31	Excellent	2.70	69	Poor	Much	>4.5
D 16.	32	Good	2.85	68	Poor	Much	>4.5
D 18.	31	Excellent	2.72	69	Poor	Much	>4.5
D 20.	27	Excellent	2.61	73	Poor	Much	>4.5
D 22.	28	Good	2.95	72	Poor	Average	>4.5
D 23.	24	Good	2.75	76	Poor	Much	>4.5
D 24.	40	Good	3.05	60	Poor	Little	>4.5
D 25.	26	Excellent	2.62	74	Fair	Much	>4.5
D 26.	23	Excellent	2.60	77	Fair	Much	>4.5
D 30.	49	Good	2.83	51	Poor	Average	>4.5
D 31.	23	Excellent	2.60	77	Poor	Much	>4.5
D 32.	48	Excellent	2.62	52	Poor	Much	>4.5
D 35.	42	Good	3.02	58	Poor	Much	>4.5
D 36.	34	Good	2.78	66	Poor	Much	>4.5
Average :	34		2.78	66			>4.5

suspension populations lie between 2.60 and 3.10 Ø, averaging 2.78 Ø. The suspension population with poor to fair sorting ranges from 40 to 73% of the total distribution, the average being 66%. There appears to be much mixing between the two populations.

Percentile values are calculated (Table 5.3) from which the statistical parameters, namely, mean size, standard deviation, skewness and kurtosis are obtained. The mean grain size (M_z) of the Disang sandstones ranges from 2.491 to 4.010 Ø (0.1780 to 0.0621 mm), averaging 3.580 Ø (0.0836 mm), standard deviation (σ_i) from 0.997 to 1.437 Ø, averaging 1.263 Ø, skewness (Sk_i) from -0.007 to 0.726 Ø, averaging 0.285 Ø and kurtosis (k_g) ranges from 0.837 to 1.257 Ø, averaging 1.036 Ø (Table 5.4).

The sandstones of the Disang Group are made up of fine sands. They are generally poor to moderately sorted and range from near symmetrical to fine in skewness. The sediments are leptokurtic to platykurtic, mesokurtic ones being dominant.

The vertical distribution of mean size, standard deviation, skewness and kurtosis are shown in figure 5.3. It is found that the distribution of the different parameters is erratic.

5.3. DISCRIMINANT FUNCTIONS :

Sahu (1964) utilised the following relations to differentiate the processes of transportation and environments of deposition.

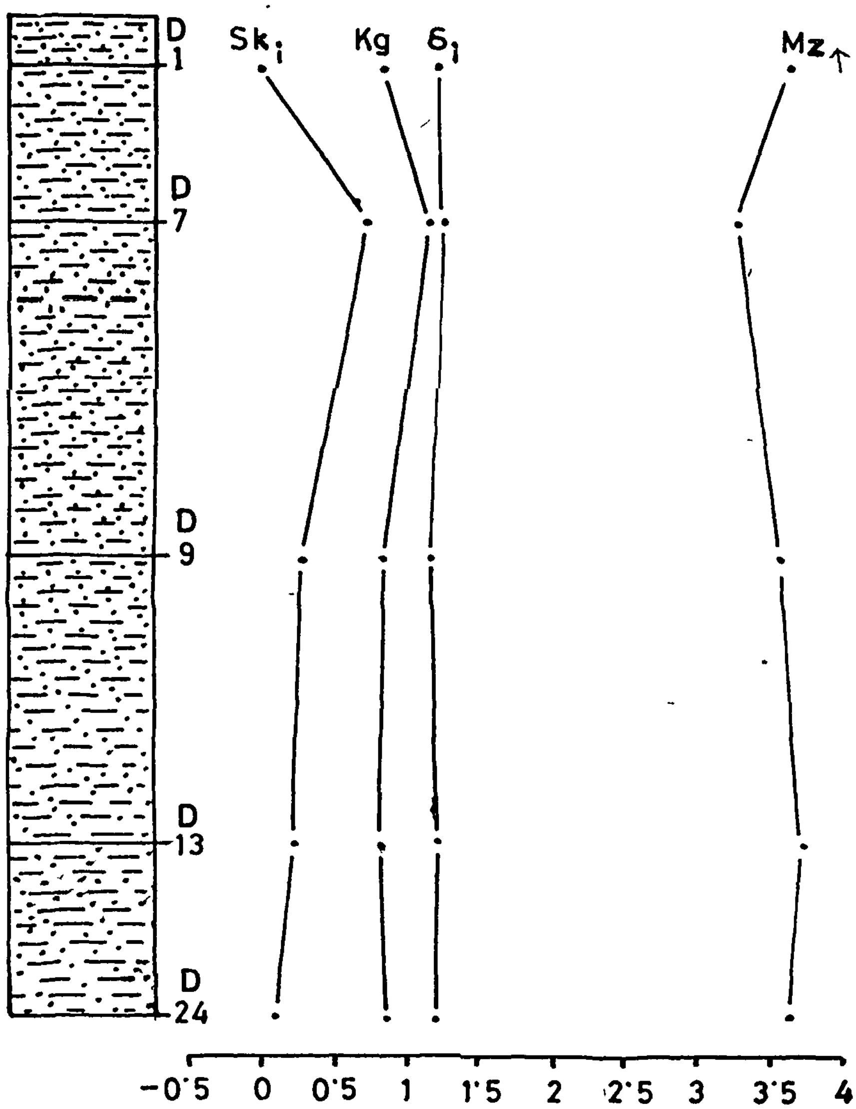

FIG: 5·3

VERTICAL VARIATION OF TEXTURAL PARAMETERS OF DISANG SANDSTONES

Table 5.3

Percentile values, CM values (in microns) and values finer than 125(F), 31(L) and 4(A)μ of the sandstones of the Disang Group.

Sample No.	P_1	P_5	P_{16}	P_{25}	P_{50}	P_{75}	P_{84}	P_{95}	$C=P_1$	$M=P_{50}$	F	L	A
D 1.	1.92	2.20	2.46	2.65	3.44	4.46	5.00	5.97	2643	921	61.08	15.58	0.03
D 4.	1.62	1.98	2.41	2.67	3.55	4.44	4.85	6.30	3253	854	62.18	13.15	1.11
D 5.	1.55	1.95	2.37	2.60	3.30	4.25	4.69	6.70	3415	1015	59.98	11.25	2.33
D 6.	1.59	2.00	2.40	2.63	3.28	4.18	4.60	5.58	3322	1029	58.22	9.50	1.46
D 7.	2.02	2.19	2.33	2.43	2.70	3.95	4.75	6.42	2466	1539	35.84	12.97	1.62
D 8.	2.05	2.40	2.74	2.93	3.80	4.80	5.49	7.25	2415	718	71.17	21.21	3.95
D 9.	1.90	2.20	2.45	2.65	3.41	4.44	4.90	5.88	2679	941	59.75	14.15	0.01
D 13.	1.90	2.20	2.46	2.72	3.58	4.58	5.11	6.00	2679	836	65.02	17.82	0.04
D 14.	1.93	2.20	2.48	2.70	3.50	4.53	5.17	6.78	2624	884	61.61	17.98	1.70
D 16.	1.68	2.06	2.48	2.75	3.66	4.69	5.20	6.34	3121	791	66.35	19.00	2.26
D 18.	1.84	2.15	2.48	2.72	3.50	4.40	4.78	7.28	2793	884	62.65	11.67	3.21
D 20.	2.11	2.32	2.53	2.77	3.58	4.60	5.20	7.40	2316	836	64.43	17.41	3.93
D 22.	1.61	2.06	2.56	2.90	3.90	4.62	4.94	6.23	3276	670	70.78	14.48	0.21
D 23.	1.60	2.05	2.60	2.90	3.89	4.61	4.94	6.50	3299	675	71.22	14.41	0.01
D 24.	1.57	1.90	2.41	2.69	3.60	4.52	4.92	5.80	3368	825	62.91	14.56	1.33
D 25.	1.86	2.18	2.49	2.76	3.52	4.20	4.55	5.36	2755	872	63.62	8.11	0.53
D 26.	2.05	2.27	2.51	2.80	3.62	4.54	5.30	6.70	2415	813	65.76	20.54	2.26
D 30.	1.55	1.88	2.22	2.40	2.90	4.00	4.65	6.00	3415	1340	47.14	12.10	1.66
D 31.	1.96	2.23	2.54	2.82	3.70	4.45	4.85	7.23	2570	769	66.94	12.91	1.51
D 32.	2.15	2.29	2.43	2.49	2.83	3.86	4.40	6.44	2253	1406	40.62	8.88	2.66
D 35.	1.58	2.01	2.53	2.67	3.32	4.22	4.76	6.25	3345	1001	59.57	12.86	1.23
D 36.	1.55	1.97	2.37	2.68	3.44	4.56	5.14	6.78	3415	921	60.25	17.85	2.86
Average :	1.80	2.12	2.47	2.70	3.46	4.40	4.92	6.42	2902	934	60.78	14.47	1.63

Table 5.4

Statistical measures and verbal classification of the sandstones of the Disang Group.

Sample No.	Mean size		Standard Deviation		Skewness		Kurtosis	
D 1.	3.633	VFS	1.206	MS	-0.007	NS	0.854	Pk
D 4.	3.603	VFS	1.264	MS	0.167	FS	1.000	Mk
D 5.	3.453	VFS	1.300	MS	0.315	VFS	1.180	Lk
D 6.	3.427	VFS	1.092	MS	0.582	VFS	0.946	Mk
D 7.	3.260	VFS	1.246	MS	0.726	VFS	1.140	Lk
D 8.	4.010	Si	1.422	PS	0.325	VFS	1.063	Mk
D 9.	3.587	VFS	1.170	MS	0.279	FS	0.842	Pk
D 13.	3.717	VFS	1.238	MS	0.214	FS	0.837	Pk
D 14.	3.717	VFS	1.366	MS	0.337	VFS	1.026	Mk
D 16.	3.780	VFS	1.328	MS	0.192	FS	0.904	Mk
D 18.	3.587	VFS	1.348	MS	0.293	FS	1.251	Lk
D 20.	3.770	VFS	1.437	PS	0.359	VFS	1.138	Lk
D 22.	3.800	VFS	1.227	MS	-0.004	NS	0.994	Mk
D 23.	3.810	VFS	1.259	MS	0.035	NS	1.066	Mk
D 24.	3.643	VFS	1.218	MS	0.090	NS	0.873	Pk
D 25.	3.520	VFS	0.997	MS	0.079	NS	0.905	Mk
D 26.	3.810	VFS	1.369	MS	0.297	FS	1.043	Mk
D 30.	3.257	VFS	1.232	MS	0.472	VFS	1.055	Mk
D 31.	3.697	VFS	1.335	MS	0.204	FS	1.257	Lk
D 32.	2.491	FS	1.121	MS	0.667	VFS	1.241	Lk
D 35.	3.537	VFS	1.200	MS	0.337	VFS	1.121	Lk
D 36.	3.650	VFS	1.421	PS	0.308	VFS	1.048	Mk
Average	3.580		1.263		0.285		1.036	

VFS - very fine sand
FS - fine sand
Si - silt

VFS - very finely skewed
FS - finely skewed
NS - near symmetrical

Pk - platykurtic
Mk - mesokurtic
Lk - leptokurtic

MS - moderately sorted
PS - poorly sorted

1. $Y_{aeolian:beach} = -3.5688\ M_z + 3.7016\ \delta_i^2 - 2.0766\ Sk_i + 3.1135\ K_g.$

2. $Y_{beach:shallow\ marine} = 15.6534\ M_z + 65.7091\ \delta_i^2 - 18.1071\ Sk_i + 18.5043\ K_g.$

3. $Y_{shallow\ marine:fluviatile} = 0.2852\ M_z - 8.7604\ \delta_i^2 - 4.8932\ Sk_i + 0.0482\ K_g.$

4. $Y_{fluviatile:turbidity} = 0.7215\ M_z - 0.4030\ \delta_i^2 + 6.7322\ Sk_i + 5.2927\ K_g.$

According to Sahu, in case of the first relation, values less than -2.741 indicate aeolian deposition while greater values suggest beach deposition. Values obtained in the present case using this relation indicate an aeolian environment. However, as all other findings suggest that the sediments are water laid, the first relation is not considered. In case of the second relation, values less than 65.350 indicate beach deposition while greater values suggest shallow agitated marine deposition. For the third relation, values lesser than -7.4190 indicate a fluvial (deltaic) environment of deposition, while greater values indicate a shallow marine environment. In the case of the fourth relation, values lesser than 9.8433 indicate turbidity currents whereas greater values indicate fluvial processes.

The values obtained in the present study using the second, third and fourth relations of Sahu suggest shallow agitated marine and fluvial (deltaic) environments, and fluvial and turbidity processes for the Disang sandstones (Table 5.5).

Table 5.5

Environments of deposition of the sandstones of the Disang Group as obtained by discriminant function analyses.

Sample No.	1st relation	2nd relation	3rd relation
D 1.	Shallow agitated marine	Fluvial	Turbidity
D 4.	Shallow agitated marine	Fluvial	Turbidity
D 5.	Shallow agitated marine	Fluvial	Fluvial
D 6.	Shallow agitated marine	Fluvial	Fluvial
D 7.	Shallow agitated marine	Fluvial	Fluvial
D 8.	Shallow agitated marine	Fluvial	Fluvial
D 9.	Shallow agitated marine	Fluvial	Turbidity
D 13.	Shallow agitated marine	Fluvial	Turbidity
D 14.	Shallow agitated marine	Fluvial	Turbidity
D 16.	Shallow agitated marine	Fluvial	Turbidity
D 18.	Shallow agitated marine	Fluvial	Fluvial
D 20.	Shallow agitated marine	Fluvial	Fluvial
D 22.	Shallow agitated marine	Fluvial	Turbidity
D 23.	Shallow agitated marine	Fluvial	Turbidity
D 24.	Shallow agitated marine	Fluvial	Turbidity
D 25.	Shallow agitated marine	Fluvial	Turbidity
D 26.	Shallow agitated marine	Fluvial	Turbidity
D 30.	Shallow agitated marine	Fluvial	Fluvial
D 31.	Shallow agitated marine	Fluvial	Fluvial
D 32.	Shallow agitated marine	Fluvial	Fluvial
D 35.	Shallow agitated marine	Fluvial	Fluvial
D 36.	Shallow agitated marine	Fluvial	Turbidity

Note : The first, second and third relations of the table correspond to the second, third and fourth relations of Sahu (1964) respectively.

5.4. SCATTER PLOTS OF TEXTURAL PARAMETERS :

Bivariate plots of textural parameters are commonly used to study the relationships between these values and to discriminate sedimentary environments. Significant trends have been obtained by different workers by plotting size parameters against each other.

In the present work a similar attempt is made to investigate the presence of any definite trend and also to determine the environments of deposition of the sandstones.

Mean size Vs standard deviation :

It has been recognised by various authors that the sorting coefficient (standard deviation) is strongly dependant upon the mean size (Krumbein and Aberdeen, 1937; Inman, 1949; Emery and Stevenson, 1950; Griffiths, 1951).

Mean size plotted against standard deviation throws some light on the depositional environment (Inman, 1949). Following Friedman (1961) mean size and standard deviation are plotted against each other using a quarter phi scale (Fig. 5.4.1) to differentiate river from inland dune and mixed environments. These two variables are also plotted against each other following Moiola and Weiser (1968) to discriminate between coastal dune and river environments (Fig. 5.4.2) and beach and river environments (Fig. 5.4.3). The points fall in the area of river environment.

Plots of these two parameters after Folk and Ward (1957) result in the formation of only one limb of the V-shaped pattern (Fig. 5.4.4). It is observed that with decrease in mean size the value of standard deviation increases. Thus, the mean size influences the sorting coefficient. This indicates poorer

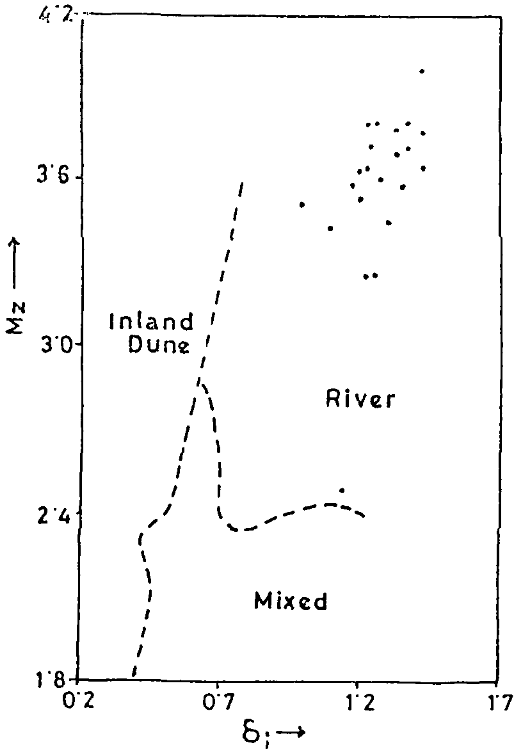

FIG: 5·4·1
Combination plots of Meansize Vs. Standard deviation of the Disang sandstones (After Friedman, 1961)

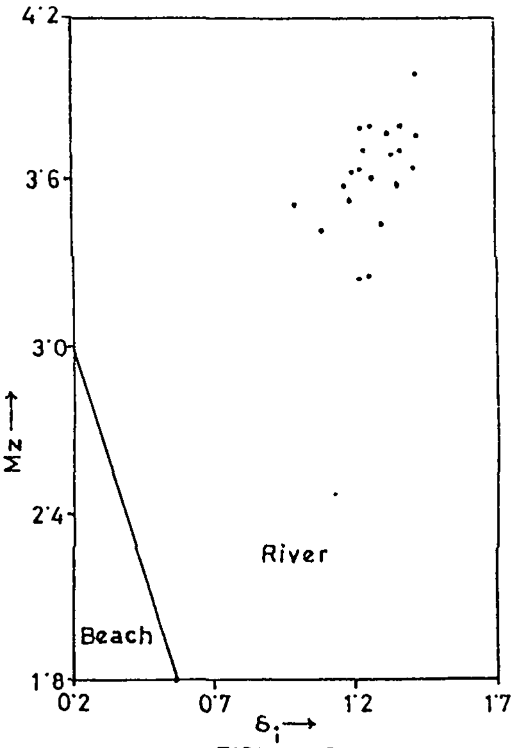

FIG: 5·4·3
Combination plots of Meansize Vs. Standard deviation of Disang sandstones (After Moiola & Weiser, 1968)

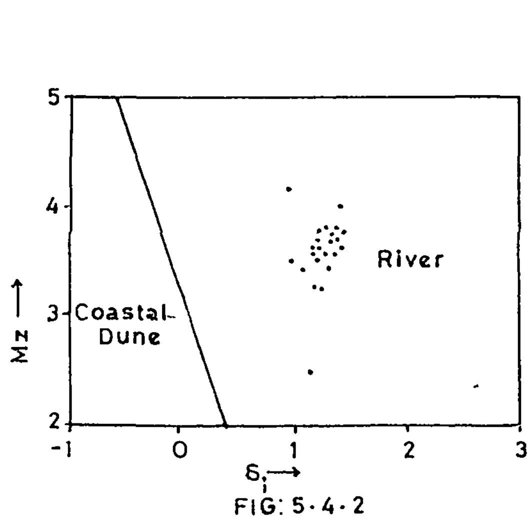

FIG: 5·4·2
Combination plots of Meansize Vs. Standard deviation of Disang sandstones (After Moiola & Weiser, 1968)

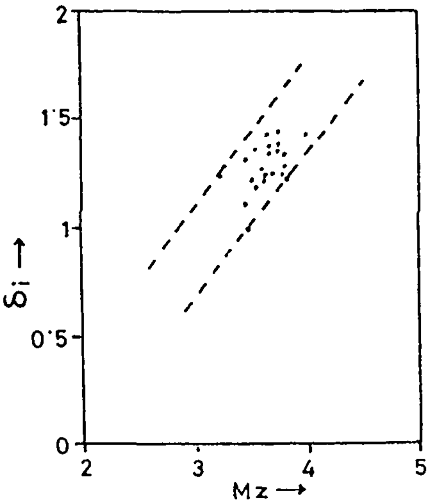

FIG: 5·4·4
Combination plots of Standard deviation Vs. Mean size of Disang sandstones (After Folk & Ward, 1957)

sorting with increase in fineness of the sediments.

Skewness Vs standard deviation :

Friedman (1961) showed that plots of standard deviation Vs skewness give a good separation between beach and river sands with only 10.5% of the samples deviating from their environmentally designated fields. In the present case, on plotting these two parameters against each other following Friedman (1961) and Moiola and Weiser (1968), a river environment of deposition is indicated (Figs. 5.5.1 and 5.5.2).

Sorting and skewness bear a mathematical relationship with each other as both parameters are functions of mean size (Folk and Ward, 1957). Bivariate plots of these two variables following Folk and Ward (1957) form a circle (Fig. 5.5.3) to the right of the normal line of skewness, except for two points which represent the negatively skewed sediments. The rest are near symmetrical to finely skewed. The scattering of the positively skewed sediments indicates some variation in proportions of sand and silt modes.

Mean size Vs skewness :

On plotting the two parameters against each other following Friedman (1961), a river environment of deposition is indicated (Fig. 5.6.1).

It is noted that the finer the sediments the more skewed they tend to become (Hough, 1942). Inman (1949) also studied the relationship between mean size and skewness and supports this view. Pettijohn (1975), however, opines that the fine grained sediments show a somewhat different relation. Skewness is a function of grain size in bimodal sediments in which the

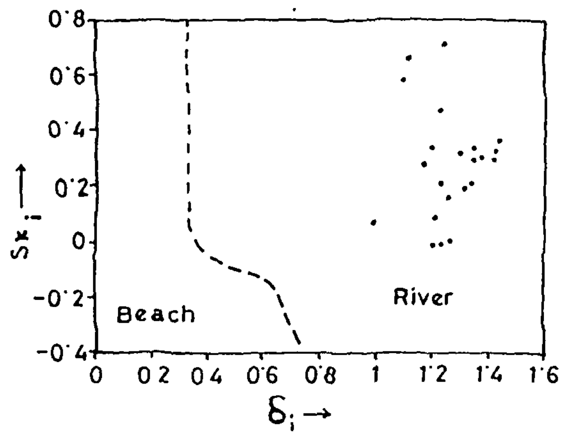

FIG: 5·5·1
Combination plots of Skewness Vs. Standard deviation of the Disang sandstones.
(After Friedman, 1961)

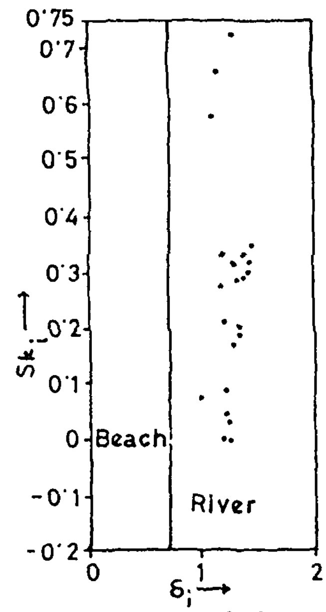

FIG: 5·5·2
Combination plots of Skewness Vs. Standard deviation of Disang sandstones (After Moiola & Weiser, 1968)

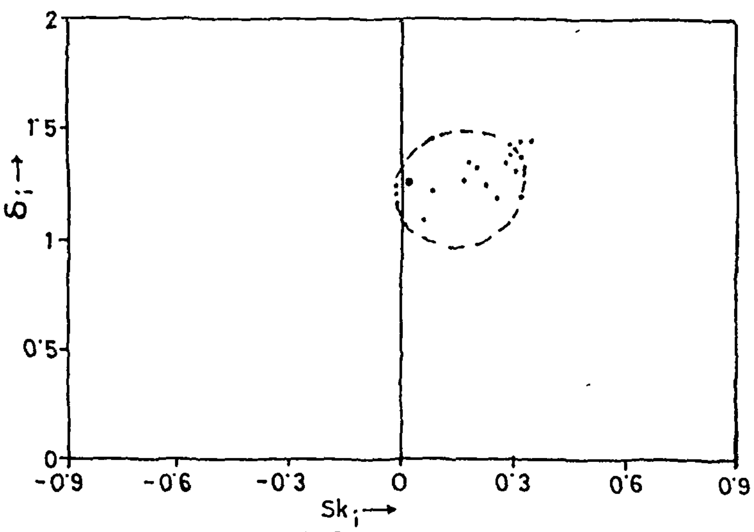

FIG: 5·5·3
Combination plots of Standard deviation Vs. Skewness of Disang sandstones
(After Folk & Ward, 1957)

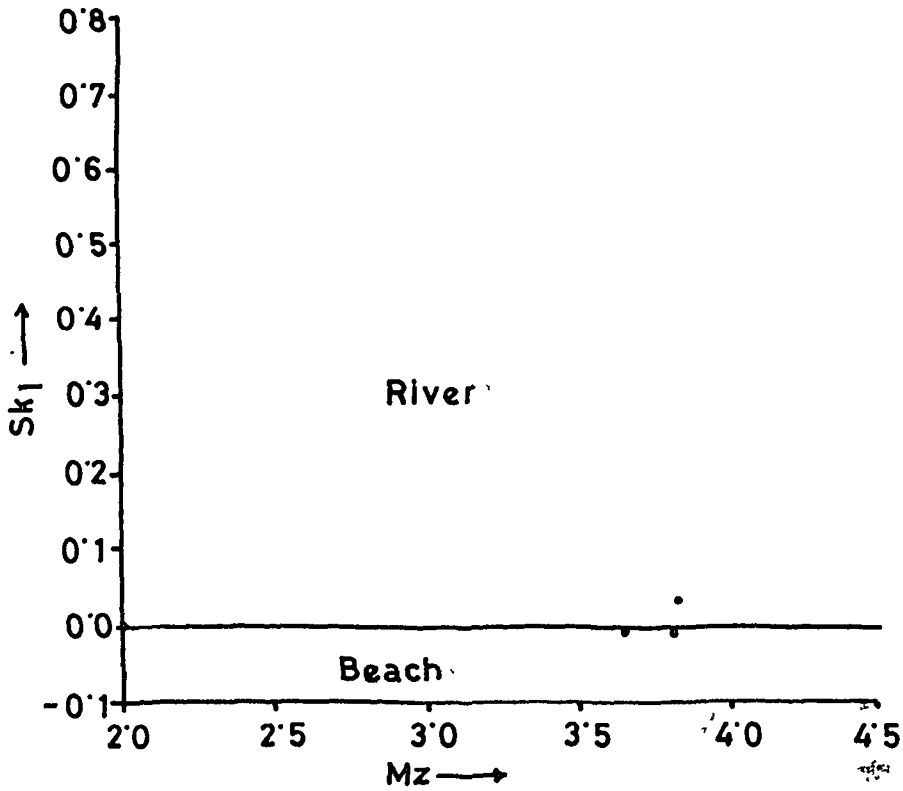

FIG: 5·6·1

Bivariate plots of Mean size Vs. Skewness of the Disang sandstones (After Friedman, 1961)

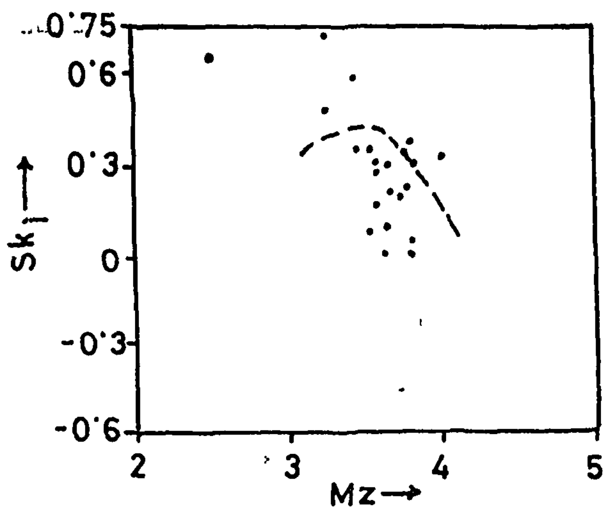

FIG: 5·6·2

Combination plots of Skewness Vs. Mean size of Disang sandstones (After Folk & Ward, 1957) negative skewness is due to the dominance of a finer mode while the positive skewness is due to a coarser mode (Folk and Ward, 1957). The present mean size-skewness plots (Fig. 5.6.2) show a mixture of sand and silt modes. As seen in the figure, skewness values tend to fall with decreasing mean size.

Skewness Vs kurtosis :

Scatter plots of skewness and kurtosis following Friedman (1961) for the Disang sediments under study are shown in figure 5.7.1. Friedman suggests that the "0-0" skewness line is an environmental boundary between river and beach sediments. From the plots it is observed that the Disang sediments were deposited mainly in a river environment. This interrelationship can be analysed after Thomas et al. (1972) where 4 zones are delineated and designated A, B, C and D on the basis of skewness and kurtosis values (Fig. 5.7.2). Basically the zones relate to the intermixing of two or more populations with modification of the characteristic grain size symmetry and peakedness of the populations involved.The zones A to D are related to hydraulic energy that controls the sorting process. The diagram suggests that the sediments of the Disang Group were subjected to fairly high hydraulic energy processes.

Scatter plots between skewness and kurtosis following Folk and Ward (1957) show a somewhat wide dispersal, more to the right of the normal line of skewness (Fig. 5.7.3). The scattering is due to a more or less wide separation between modes and ineffective sorting.

Mean size Vs kurtosis :

Plots between these two parameters following Folk and Ward (1957) tend to take a sinusoidal trend (Fig. 5.8).There is a tendency for the sediments to become normal with increase in grain size but with further increase the sediments become

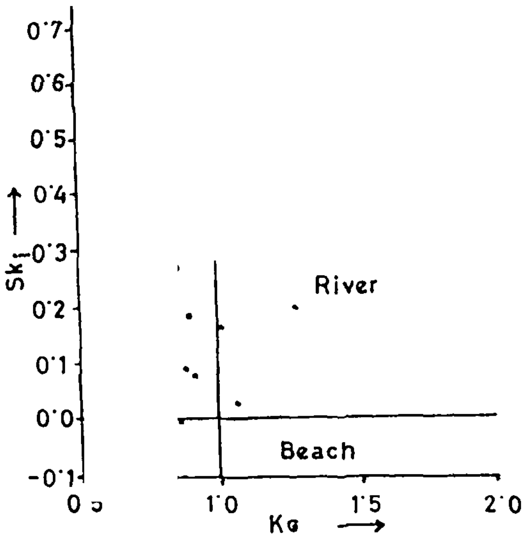

FIG: 5·7·1

Bivariate plots between Skewness and Kurtosis of the Disang sandstones (After Friedman,1961)

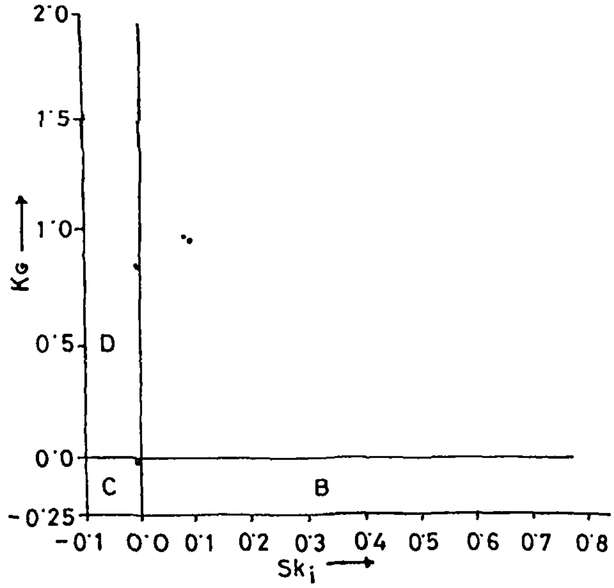

FIG: 5·7·2

Bivariate plots between Skewness and Kurtosis of the Disang sandstones (After Thomas *et al.*,1972)

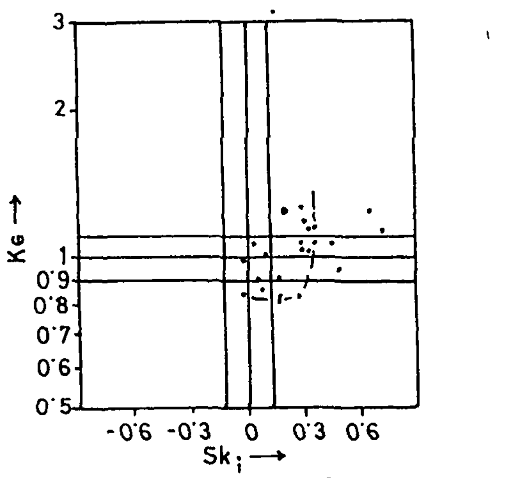

FIG: 5·7·3

Scatter plots of Kurtosis Vs. Skewness of Disang sandstones (After Folk & Ward,1957)

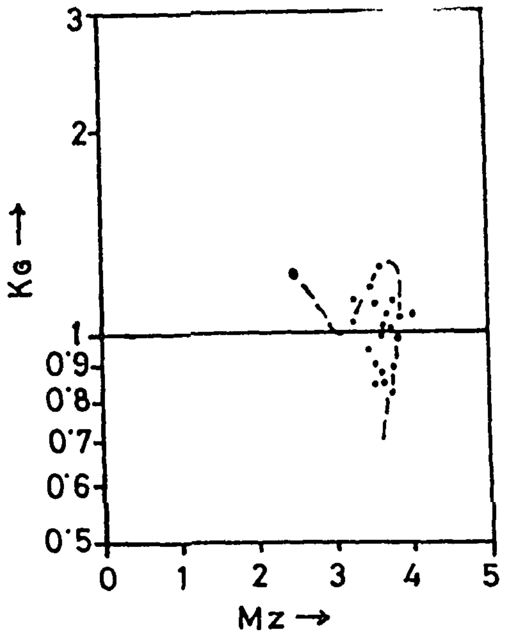

FIG: 5·8

Scatter plots Kurtosis Vs. Mean size of Disang sand-stones

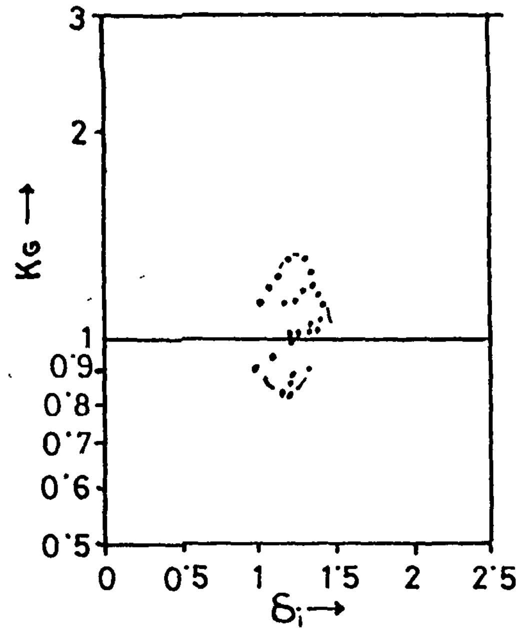

FIG: 5·9

Scatter plots of Kurtosis Vs Standard deviation of Disang sandstones

(After Folk & Ward, 1957)

leptokurtic and then platykurtic.

Standard deviation Vs kurtosis :

Scatter plots between these two parameters following Folk and Ward (1957) form an inverted V (Fig. 5.9). The bimodality of the grain size distribution causes a scattering around the normal. The values of kurtosis in the present case suggest poor to moderate sorting of the two modes (Folk and Ward, 1957).

5.5 CM PATTERN :

Passega (1957, 1964) suggested the use of CM patterns for environmental analysis. C is the one percentile diameter in microns, an approximation of the maximum grain size and M, the fifty percentile diameter in microns, is the median. The position of points in a CM digaram depends upon the mode of deposition of sediments. Deposits of various environments give characteristic patterns.

Passega (1957) states the significance of C and M in the interpretation of the depositional agencies. M, the median grain size is the size such that 50 percent of the sample is coarser than this size, which is an approximation of the maximum grain size present in the population. He states that the loads of coarse and fine sediments in hydrodynamic equilibrium are largely independent of each other. The coarse fraction of a sediment is almost invariably more representative of the depositional agent than the fine fraction.

Advantage is taken of these observations in representing texture in the CM diagram. The only parameter of the overall texture used in the CM diagram is the median which expresses the average coarseness of the sediments. C, the one percentile, is the parameter which measures the competency of the depositing agent to transport. The one percentile value is selected for a parameter as an approximation of the maximum grain size because some coarser grains may have been introduced by extraneous agents.

On the CM diagram the limit of the area in which points can fall is restricted by line C=M. It is designated as the limit of the diagram. Points situated on this line represent samples in which the median approximately equals the coarsest grain size.

C comprises of grains between 2253 and 2415 μ while M ranges from 670 to 1539 μ (Table 5.3). C is plotted against M (Figs. 5.10.1 and 5.10.2) following Passega (1957, 1964), Passega and Byramjee (1969) and Reineck and Singh (1980). The patterns suggest that the sediments are an admixture of fine sand, silt and clay which were transported in uniform suspension and saltation and that turbidity currents were responsible for their deposition.

F, L and A, representing weight percentages finer than 125, 31 and 4 μ respectively (Passega and Byramjee, 1969), have minimum and maximum values of 35.84 and 71.22, 8.11 and 21.21, and 0.01 and 3.95 respectively (Table 5.3). The FM, LM and AM patterns, as deduced from plots (Fig. 5.11) are characteristically convex upwards. According to Passega and Byramjee (1969) this signifies transportation of these fine sediments in uniform suspension.

5.6 TEXTURAL CLASSIFICATION :

The Disang sandstones contain fine sand, silt and some clay. Sand ranges from 45.32 to 73.34%, averaging 57.59%, silt from 23.15 to 51.55%, averaging 38.91% and clay ranges from 1.07 to 6.67% with an average of 3.46% (Table 5.6). The percentages of sand, silt and clay, plotted in a triangular diagram (Fig. 5.12) following Folk (1954), indicate that most of the samples are silty sandstones.

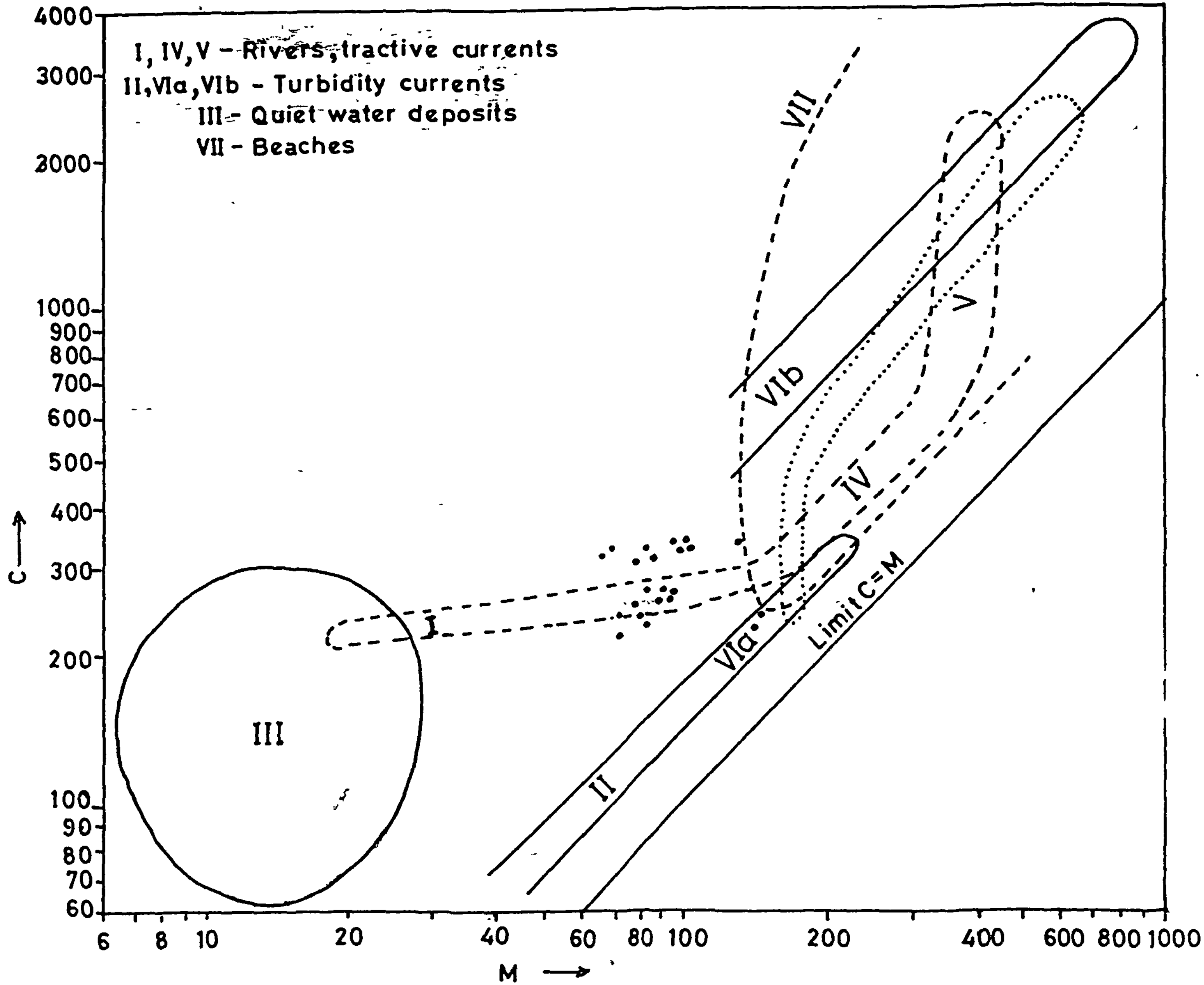

FIG: 5·10·1

CM Pattern of Disang sandstones

(After Passega, 1957)

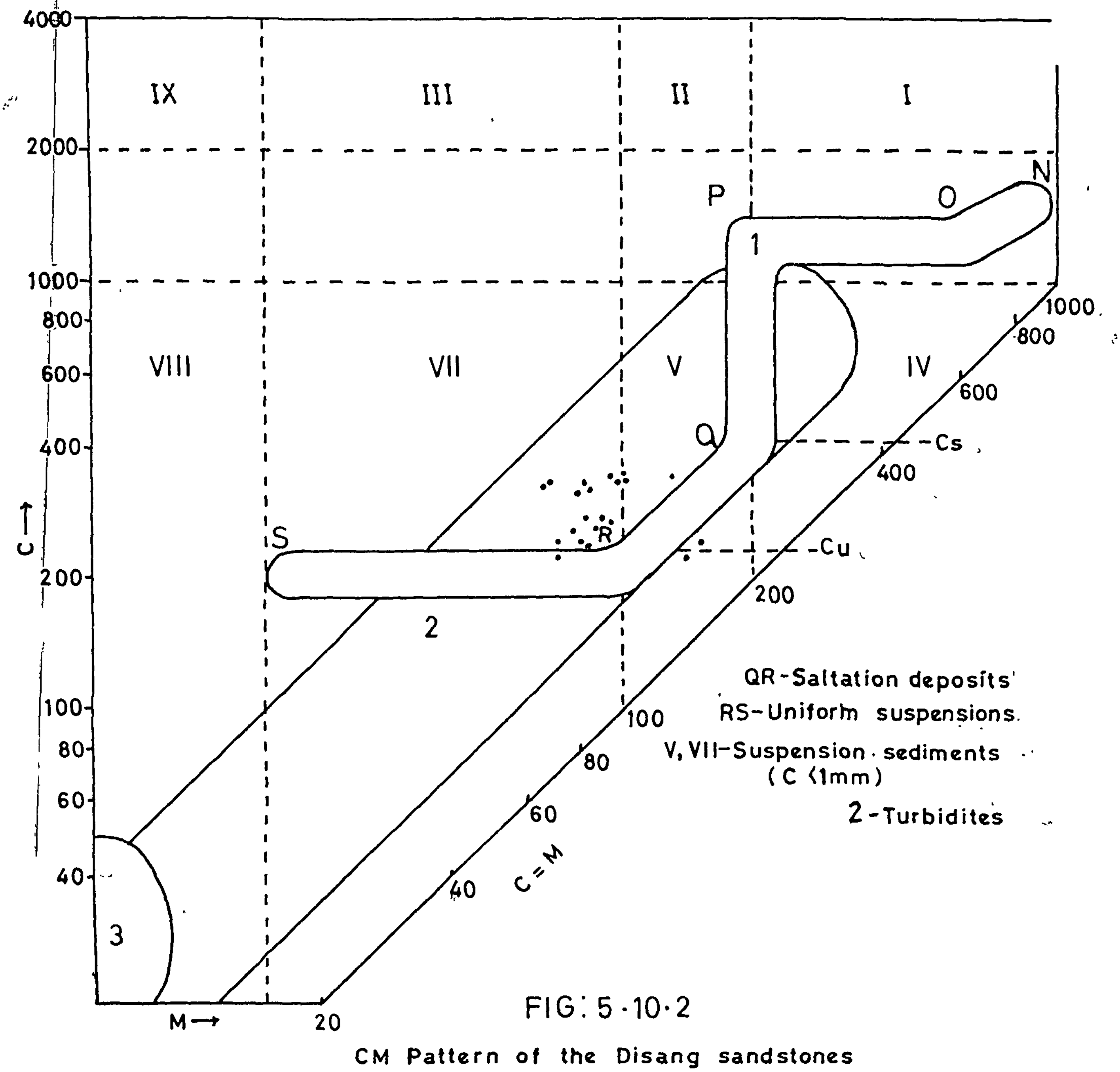

FIG: 5·10·2

CM Pattern of the Disang sandstones
(After Passega 1957, 1964; Passega and Byramjee, 1969; Reineck and Singh, 1980)

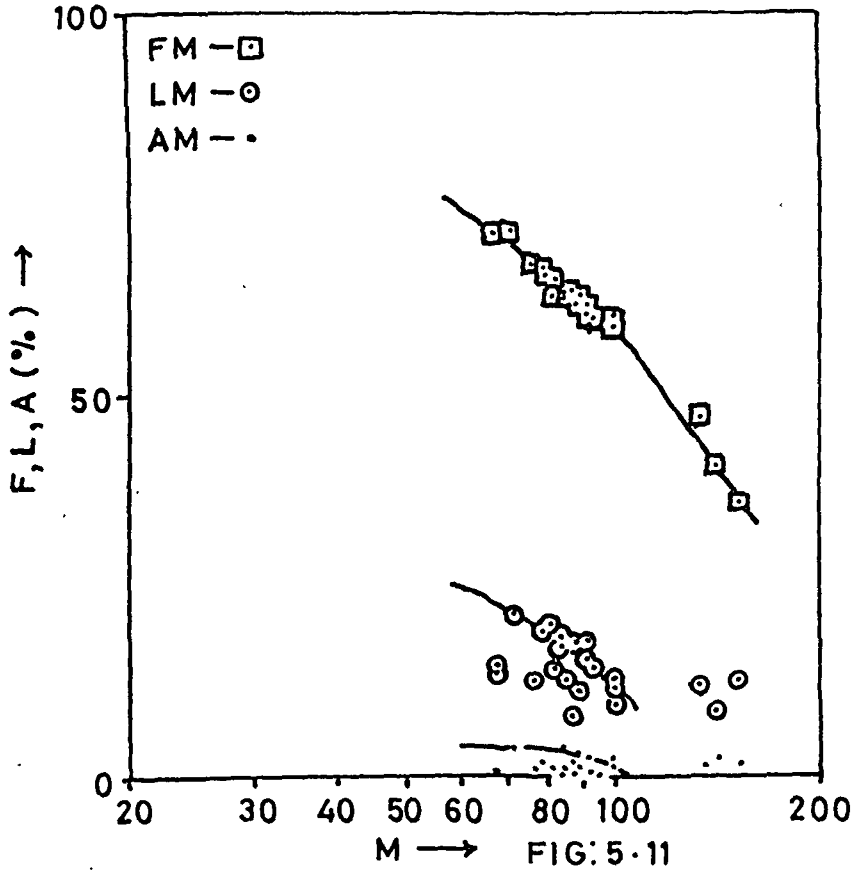

FIG: 5·11

FM, LM, & AM diagrams of Disang Sandstones

(After Passega & Byramjee, 1969)

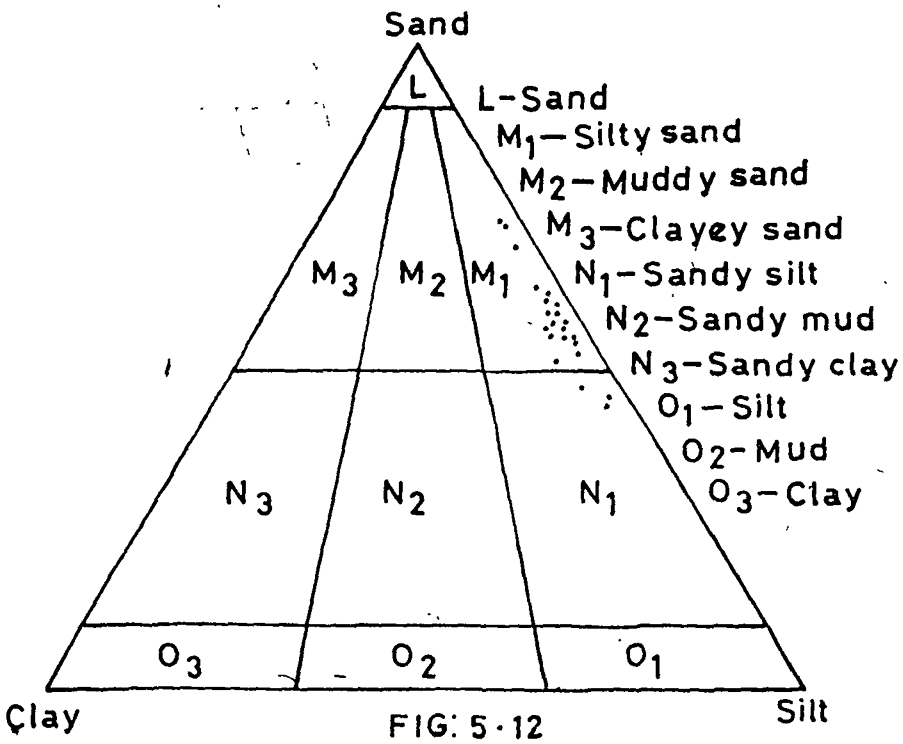

FIG: 5·12

Textural Classification of Disang sandstones

Table 5.6

Textural classification of the Disang sandstones.

Sample No.	Textural components (Percentage)			Textural classification
	Sand	Silt	Clay	
D 1.	58.78	38.66	2.55	Silty sandstone
D 4.	55.82	41.08	3.06	Silty sandstone
D 5.	62.48	33.62	3.86	Silty sandstone
D 6.	61.89	35.96	2.11	Silty sandstone
D 7.	72.42	24.53	3.01	Silty sandstone
D 8.	47.46	47.32	5.16	Sandy siltstone
D 9.	57.33	40.43	2.21	Silty sandstone
D 13.	55.23	42.37	2.39	Silty sandstone
D 14.	57.20	38.42	4.33	Silty sandstone
D 16.	52.80	44.28	2.87	Silty sandstone
D 18.	56.68	37.53	5.69	Silty sandstone
D 20.	54.94	39.25	5.80	Silty sandstone
D 22.	45.78	51.55	2.63	Sandy siltstone
D 23.	45.32	51.12	3.52	Sandy siltstone
D 24.	54.13	43.59	2.24	Silty sandstone
D 25.	59.90	39.01	1.07	Silty sandstone
D 26.	54.85	41.25	3.85	Silty sandstone
D 30.	69.22	27.82	2.93	Silty sandstone
D 31.	51.37	41.91	6.67	Silty sandstone
D 32.	73.34	23.15	3.46	Silty sandstone
D 35.	61.86	35.49	2.62	Silty sandstone
D 36.	58.28	37.59	4.08	Silty sandstone
Average	57.59	38.91	3.46	

5.7 SEDIMENTARY STRUCTURES :

The Disang sandstones exposed in the area are poor in sedimentary structures. The only structures noted are some fine parallel laminations, load casts, concretions and box-type of weathering.

The laminations range from 0.5 to 2.0 mm in thickness. They run parallel to the general bedding (Fig. 5.13.1). The load casts occur as irregular, bulbous features (Fig. 5.13.2). Their distribution is very scanty. Concretions are very common, especially in the upper horizons. They are mostly ferrugenous and shaly matter enclosing coarser sediments (Fig. 5.13.3). Box-type of weathering is very common in the upper horizons. Here, weathering has taken place in the rock units along bedding and joint planes. The joint planes run perpendicular to the bedding (Fig. 5.13.4).

Fig. 5.13.1

Laminated Disang sandstone

Fig. 5.13.2

Load casts in the Disang sandstones

Fig. 5.13.3

Concretions in the Disang sediments

Fig. 5.13.4

Box-type of weathering of the Disangs

Panoramic view of Disang country

CHAPTER 6

HEAVY MINERAL ANALYSIS

6.1. INTRODUCTION :

More than a hundred species of high density minerals constituting less than 0.1% of terrigenous sediments are identified. Pettijohn (1975) has defined these minerals as those of pre-existing rocks that have survived mechanical and chemical action, and intrastratal solution. Their durability and high specific gravity enable them to be transported with larger grains of lesser density. Due to differences in specific gravity, heavy minerals show considerable variation in physical and chemical stability. This variation in their distribution helps in establishing the erosional and tectonic history of basins (Van Andel, 1959). Heavy mineral studies further help in an understanding of the lithology of the source rocks, their differential stability and resistance to long continued abrasion and hydrodynamic conditions of the depositional basin.

Relatively immature sandstones contain the greatest diversity of heavy minerals and for this purpose heavy mineral studies are very helpful in provenance interpretation (Owen, 1987).

Length and breadth of detrital grains reflect the energy of the depositional environment. The value of elongation quotient of detrital grains, therefore, corresponds to a particular environmental setting (Bhattacharyya, 1984). Keeping this in view the data on zircon and tourmaline have been quantified on the basis of size data and elongation quotient for making a quantitative evaluation of the grains. Altogether twelve samples are taken for detailed analysis.

6.2. HEAVY MINERAL COMPOSITION :

The heavy mineral suite of the Disang sandstones comprises of opaques, kyanite, tourmaline, zircon, epidote, garnet and rutile in order to decreasing abundances (Table 6.1).

Opaques :

The opaques (Fig. 6.1) are, by far, the most dominant group ranging from 84.60 to 94.75% of the total heavy mineral distribution and averaging 91.23% with a frequency range of 8 to 8^{+}. The opaques include hematite and pyrite in varying proportions. Hematite occurs as dark brownish grains. Pyrite shows the development of cubic faces.

Kyanite :

Kyanite (Fig. 6.1) makes up 1.27 to 4.76% of the heavy mineral assemblage, averaging 2.63%. The frequency ranges between 2 and 4. The grains are angular to subangular. Kyanite occurs as long prismatic grains and bears a light blue colour. The mineral is weakly pleochroic. It shows moderate relief. Birefringence is moderate and extinction is oblique. Cross fractures are seen in some of the grains.

Tourmaline :

Tourmaline (Fig. 6.1) ranges from 1.04 to 3.51% and averages 1.95% with a frequency varying from 2 to 3. Tourmaline grains, mostly subhedral, are subangular to subrounded. The grains bear pale brown, pale green and blue shades and show distinct pleochroism from pale brown to dark brown and pale green to dark green colours. The mineral shows moderate to high relief and moderate birefringence. Some of the grains bear inclusions.

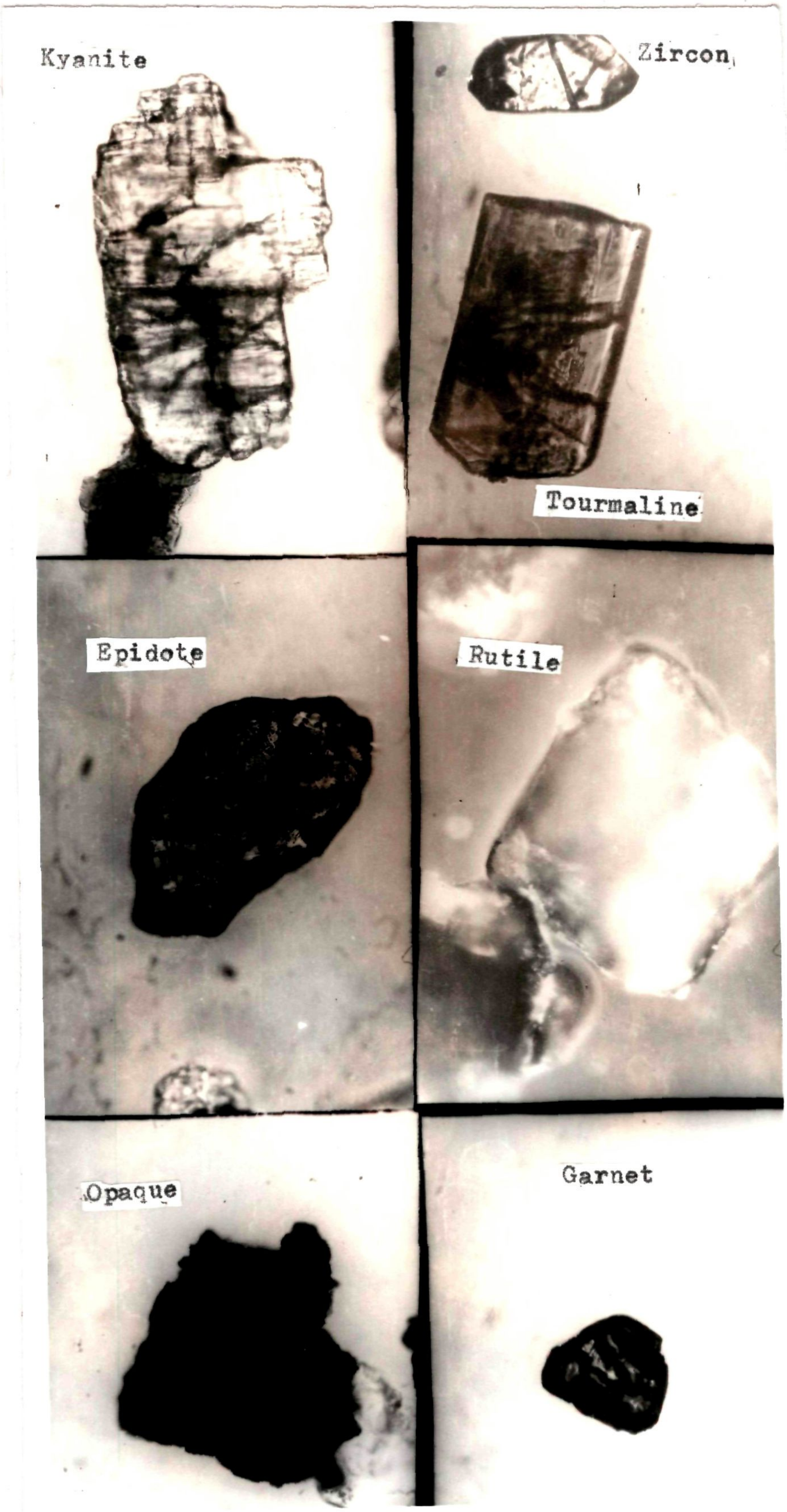

Fig.6.1

Table 6.1

Heavy mineral composition and frequency of the Disang sandstones.

Sample No.	Opaques	Zircon	Tourmaline	Rutile	Kyanite	Garnet	Epidote
D 1.	94.52	1.38	1.15	0.20	1.40	0.50	0.85
	(8^+)	(2)	(2)	(1*)	(2)	(1)	(1)
D 4.	94.43	1.39	1.04	0.31	1.27	0.59	0.97
	(8^+)	(2)	(2)	(1*)	(2)	(1)	(1)
D 6.	94.74	1.04	1.42	0.16	1.38	0.34	0.92
	(8^+)	(2)	(2)	(1*)	(2)	(1*)	(1)
D 7.	94.79	1.01	1.13	0.33	1.42	0.33	0.99
	(8^+)	(2)	(2)	(1*)	(2)	(1*)	(1)
D 8.	93.86	1.46	1.29	0.26	1.43	0.49	1.21
	(8^+)	(2)	(2)	(1*)	(2)	(1*)	(2)
D 9.	91.22	1.89	1.91	0.35	2.32	0.43	1.88
	(8^+)	(2)	(2)	(1*)	(3)	(1*)	(2)
D 13.	86.99	2.71	2.89	0.43	3.81	0.29	2.88
	(8)	(3)	(3)	(1*)	(3)	(1*)	(3)
D 14.	92.72	1.68	1.35	0.42	1.95	0.41	1.47
	(8^+)	(2)	(2)	(1*)	(2)	(1*)	(2)
D 20.	88.58	2.63	2.82	0.03	4.11	0.20	1.63
	(8)	(3)	(3)	(1*)	(4)	(1*)	(2)
D 24.	91.22	1.70	1.84	0.50	3.27	0.43	1.04
	(8^+)	(2)	(2)	(1)	(3)	(1*)	(2)
D 30.	84.60	3.75	3.51	0.17	4.76	0.31	2.90
	(8)	(3)	(3)	(1*)	(4)	(1*)	(3)
D 32.	87.15	2.55	3.02	0.51	4.43	0.46	1.88
	(8)	(3)	(3)	(1)	(4)	(1*)	(2)
Average :	91.23	1.93	1.95	0.31	2.63	0.40	1.55

Note : Figures within parentheses indicate frequencies.

The prismatic grains show parallel extinction.

Zircon :

Zircon (Fig. 6.1) ranges from 1.01 to 3.75%, averaging 1.93% with a frequency from 2 to 3. The mineral occurs as short, prismatic, subhedral grains with or without pyramidal faces. They are mostly subangular to subrounded and have thick dark outlines. The majority of the grains are colourless but some of them are pale pink to straw yellow and pale brown. The coloured grains show weak pleochroism. The grains show strong birefringence. The prismatic grains show parallel extinction. Inclusions of opaques and non-opaque minerals are seen in some of the grains.

Epidote :

Epidote (Fig. 6.1) makes up 0.85 to 2.90% of the heavy mineral assemblage with an average of 1.55%. The frequency ranges from 1 to 3. The mineral occurs as subangular to subrounded grains which are of pale green and pale yellow shades. Some of the grains are colourless. The coloured grains show distinct pleochroism from pale yellow and pale green to pistachio green. Irregular fractures are noticed in some of the grains. The mineral shows strong birefringence.

Garnet :

Garnet (Fig. 6.1) is present in very small amounts in the Disang sandstones and ranges from 0.20 to 0.59%, averaging 0.40%, the frequency being 1. The grains are subangular to subrounded. They are pale brown to almost colourless with high relief. Some of the grains are fractured while others have pitted surfaces.

Rutile :

Rutile (Fig. 6.1), averaging 0.31%, ranges from 0.03 to 0.51% with a frequency of 1*. It is found in the smallest amounts. The grains are euhedral to subhedral and more or less subangular. Colours range from yellow to blood red. Most of the grains have thick dark outlines. Some of the grains are fractured. The prismatic grains show straight extinction.

The non-opaques/opaques ratios range from 0.05 to 0.18, averaging 0.10 (Table 6.2). The ratios indicate a mixed source for the sediments.

The vertical distribution of the heavy minerals, which is found to be irregular, is shown in figure 6.2. The frequency distribution is shown in figure 6.3.

6.3. Z.T.R. MATURITY INDEX :

The maturity of the sandstones is reflected in the Z.T.R. maturity index (Hubert, 1962). The maturity index for the Disang sediments varies from 46.01 to 49.81, averaging 47.97 (Table 6.2). The maturity index of the samples in the vertical section is shown in figure 6.3. It is noted that the index gradually increases from bottom to top.

6.4. QUANTIFICATION AND CORRELATION OF ZIRCON AND TOURMALINE DATA :

Calculations for finding out the average diameters and the value of mean size of zircon and tourmaline of the Disang Group are made according to procedures explained in chapter 3. Mean sizes of zircon and tourmaline are 0.08 and 0.07 respectively and are shown in tables 6.3.1 and 6.3.2 respectively.

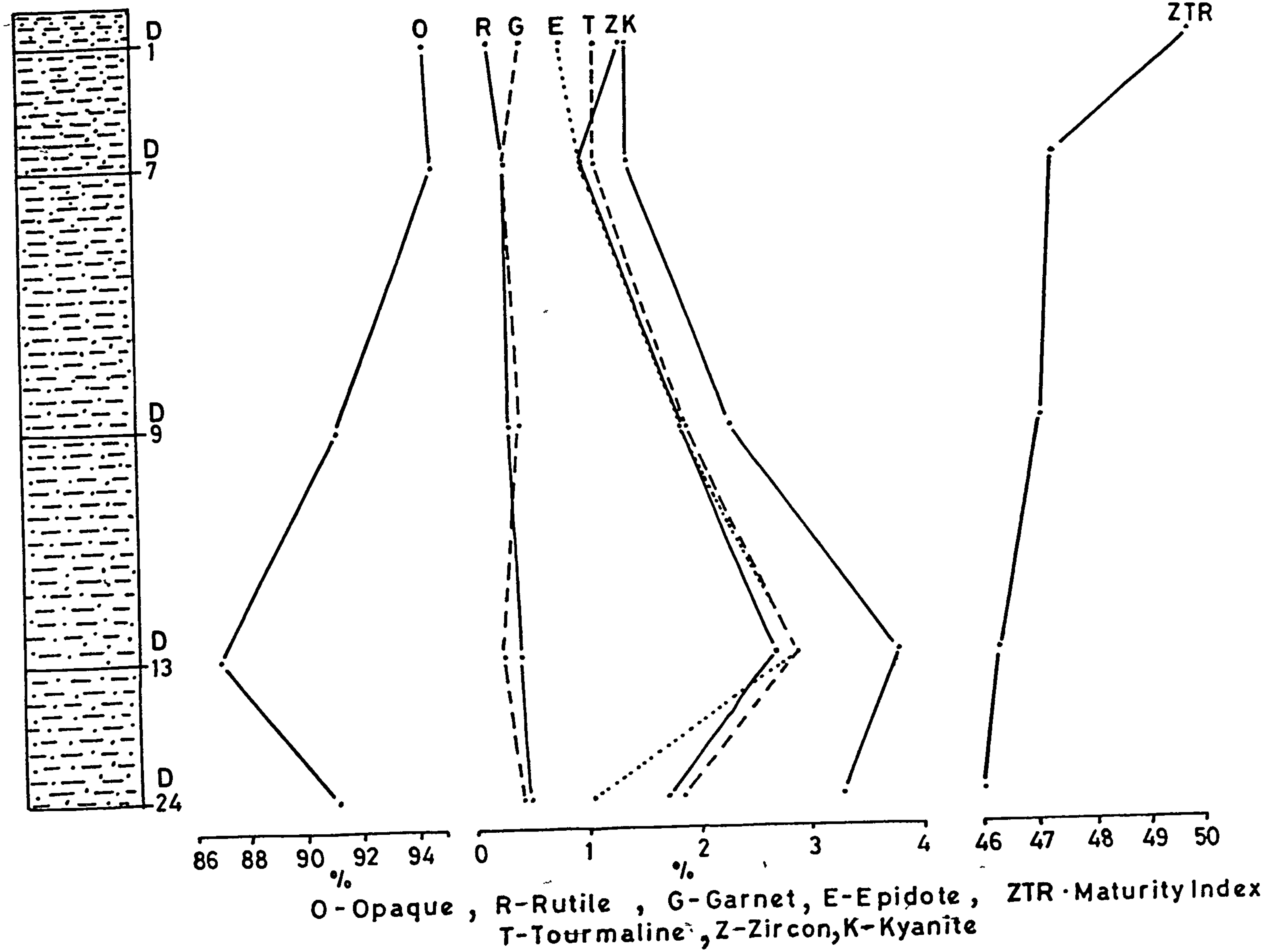

FIG: 6·2

VERTICAL VARIATION OF HEAVY MINERALS AND ZTR MATURITY INDEX OF THE DISANG SANDSTONES

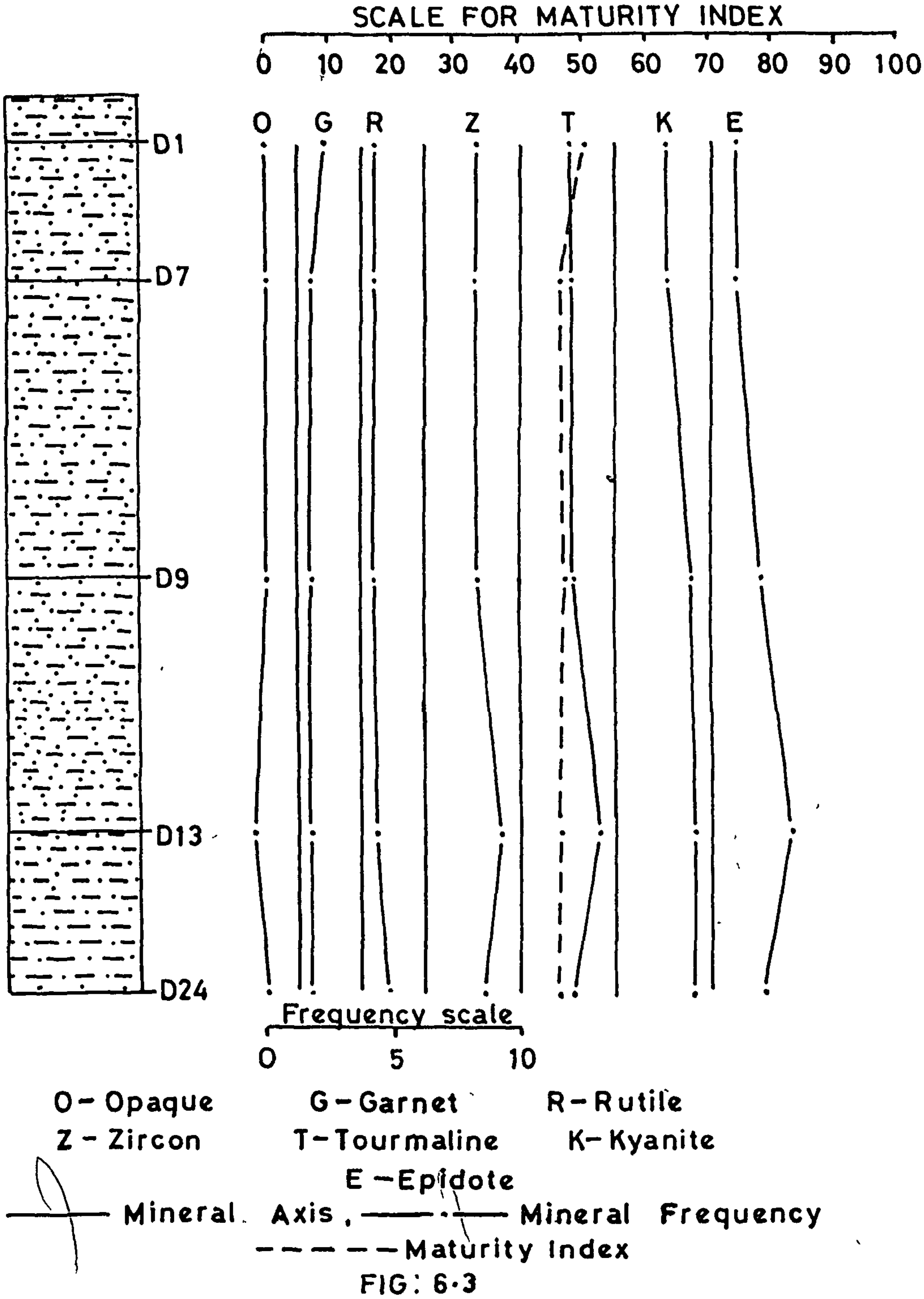

FIG: 6·3

FREQUENCY DISTRIBUTION OF HEAVY MINERALS AND Z.T.R. MATURITY INDEX OF THE SANDSTONES OF THE DISANG GROUP

Table 6.2

Z.T.R. maturity index and non-opaque/opaque ratios of the Disang sandstones.

Sample No.	Recalculated percentages of zircon, tourmaline and rutile			Z.T.R. index	Non-opaque / opaque
	Zircon	Tourmaline	Rutile		
D 1.	25.18	20.98	3.65	49.81	0.06
D 4.	24.96	18.67	5.39	49.02	0.06
D 6.	19.77	27.00	3.04	49.81	0.06
D 7.	19.38	21.69	6.33	47.40	0.05
D 8.	23.78	21.01	4.23	49.02	0.07
D 9.	21.53	21.75	3.99	47.27	0.10
D 13.	20.83	22.21	3.31	46.35	0.15
D 14.	23.08	18.54	5.77	47.39	0.08
D 20.	23.03	24.69	0.26	47.98	0.13
D 24.	19.36	20.96	5.69	46.01	0.10
D 30.	24.35	22.79	1.10	48.24	0.18
D 32.	19.84	23.50	3.97	47.31	0.15
Average :	22.09	21.98	3.89	47.97	0.10

Table 6.3.1

Mean size (M_z) of zircon of the Disang sandstones.

Class interval (Diameter in mm)	Class mid-point (m)	Frequency (f)	f x m	M_z
0.010 - 0.030	0.020	4	0.08	
0.030 - 0.050	0.040	7	0.28	
0.050 - 0.070	0.060	12	0.72	
0.070 - 0.090	0.080	8	0.64	
0.090 - 0.110	0.100	10	1.00	0.080
0.110 - 0.130	0.120	5	0.60	
0.130 - 0.150	0.140	5	0.70	
0.150 - 0.170	0.160	1	0.16	

$\Sigma f = 52 \quad \Sigma f \times m = 4.18$

$$M_z = \frac{\Sigma f \times m}{\Sigma f} = \frac{4.18}{52} = 0.080$$

Table 6.3.2

Mean size (M_z) of tourmaline of the Disang sandstones.

Class interval (Diameter in mm)	Class mid-point (m)	Frequency (f)	f x m	M_z
0.030 - 0.050	0.040	12	0.48	
0.050 - 0.070	0.060	11	0.66	
0.070 - 0.090	0.080	7	0.56	0.072
0.090 - 0.110	0.100	10	1.00	
0.110 - 0.130	0.120	4	0.48	

$\Sigma f = 44 \quad \Sigma f \times m = 3.18$

$$M_z = \frac{3.18}{44} = 0.072$$

It is important to find out whether there is any definite relationship among the sets of size data of zircon and tourmaline of the Disang and Barail Groups. This has been done by statistically correlating the data by means of a "Coefficient of correlation". This measure, in fact, does not carry the sense of geological correlation as it implies no time relationship nor any other casual relation; it merely expresses similarity or mathematical dependance of any set of data upon another (Krumbein and Pettijohn, 1938). The coefficient of correlation and determination from it whether there exists or not any definite relationship among the zircon and tourmaline size data between the Disang and Barail Groups is discussed in chapter 10.

6.5. LENGTH AND BREADTH FREQUENCIES AND ELONGATION RATIO FREQUENCIES OF ZIRCON AND TOURMALINE :

The minimum and maximum length frequencies of 4 and 25% of zircon of the Disang Group correspond to class intervals 0.010 to 0.030 mm and 0.070 to 0.090 mm respectively. The maxima and minima of the length frequency curve lie at 0.080 and 0.020 mm respectively (Fig. 6.4.1, Table 6.4). The minimum and maximum breadth frequencies of 2 and 25% of zircon represent class intervals of 0.130 to 0.150 mm and 0.030 to 0.070 mm respectively. The maxima and minima of the frequency curve lie at 0.040 and 0.060 mm, and 0.140 mm respectively (Fig. 6.4.2, Table 6.4). The elongation ratio frequency of zircon ranges from 1.20 to 2.10 with 4% (minimum) of the grains lying between class interval of 2.00 and 2.10 and a maximum of 19% between class interval of 1.80 and 1.90 (Fig. 6.4.3, Table 6.4). The maxima and minima lie at 1.85 and 2.05 respectively.

The lowest length frequency of 9% for tourmaline falls within the class interval of 0.090 to 0.110 mm while the maximum length frequency of 20% falls within 0.070 and 0.090 mm, and 0.130 and 0.150 mm. The maxima and minima of the length frequency

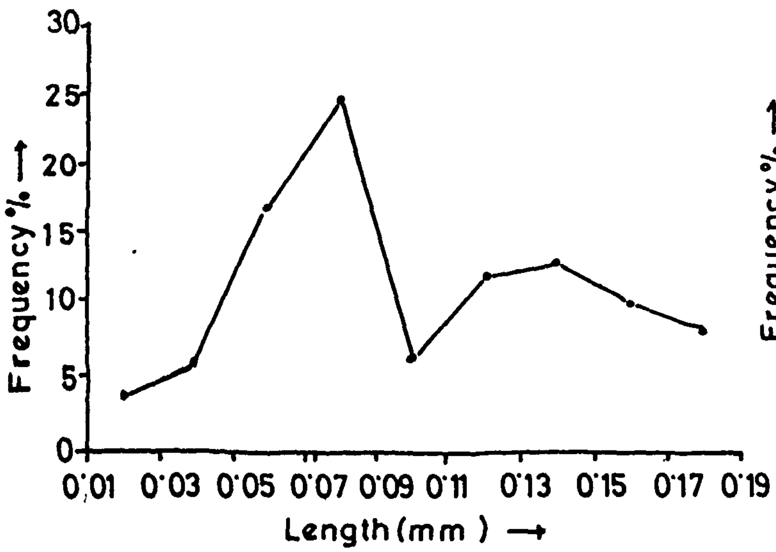

FIG: 6·4·1

Relationship between Length and Frequency of Zircon of the sandstones of Disang Group.

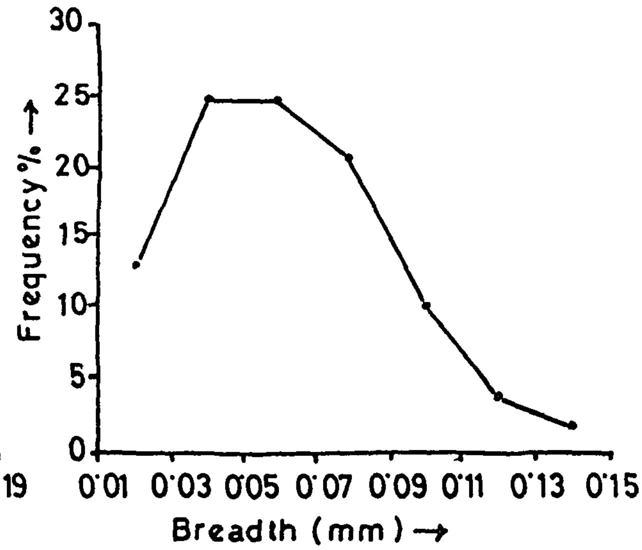

FIG: 6·4·2

Relationship between Breadth and Frequency of Zircon of the sandstones of Disang Group.

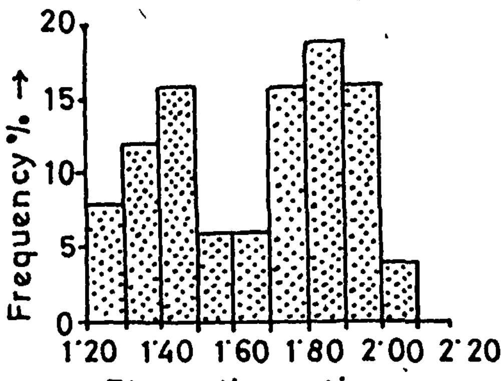

Elongation ratio - frequency histogram of Zircon of the sandstones of Disang Group

FIG: 6·4·3

Table 6.4

Length, breadth and elongation ratio frequencies of zircon of the Disang sandstones.

Class interval	Length		Breadth		Class interval	Elongation ratio	
	No. of grains	Frequency (%)	No. of grains	Frequency (%)		No. of grains	Frequency (%)
0.010-0.030	2	4	7	13	1.20-1.30	4	8
0.030-0.050	3	6	13	25	1.30-1.40	6	12
0.050-0.070	9	17	13	25	1.40-1.50	8	16
0.070-0.090	13	25	11	21	1.50-1.60	3	6
0.090-0.110	3	6	5	10	1.60-1.70	3	6
0.110-0.130	6	12	2	4	1.70-1.80	8	16
0.130-0.150	7	13	1	2	1.80-1.90	10	19
0.150-0.170	5	10	-	-	1.90-2.00	8	16
0.170-0.190	4	8	-	-	2.00-2.10	2	4

Table 6.5

Length, breadth and elongation ratio frequencies of the Disang sandstones.

Class interval	Length		Breadth		Class interval	Elongation ratio	
	No. of grains	Frequency (%)	No. of grains	Frequency (%)		No. of grains	Frequency (%)
0.010-0.030	-	-	8	18	1.20-1.30	2	5
0.030-0.050	6	14	11	25	1.30-1.40	4	9
0.050-0.070	8	18	14	32	1.40-1.50	4	9
0.070-0.090	9	20	8	18	1.50-1.60	4	9
0.090-0.110	4	9	3	7	1.60-1.70	2	5
0.110-0.130	8	18	-	-	1.70-1.80	5	11
0.130-0.150	9	20	-	-	1.80-1.90	7	16
					1.90-2.00	6	14
					2.00-2.10	-	-
					2.10-2.20	1	2
					2.20-2.30	1	2
					2.30-2.40	7	16
					2.40-2.50	1	2

curve occur at 0.080 and 0.140 mm, and 0.100 mm respectively (Fig. 6.5.1, Table 6.5). The lowest breadth frequency of 7% lies between class interval of 0.090 and 0.110 mm and the highest of 32% between 0.050 and 0.070 mm class interval. The maxima of the breadth frequency curve occurs at 0.060 mm while the minima occurs at 0.100 mm (Fig. 6.5.2, Table 6.5). The minimum elongation ratio frequency of 2% lies between class intervals of 2.10 and 2.20, and 2.20 and 2.30, and maximum of 16% lies between class intervals of 1.80 and 1.90, and 2.30 and 2.40. The maxima of the elongation frequency curve occurs at 1.85 and 2.35 while the minima occurs at 2.15 and 2.25 (Fig. 6.5.3, Table 6.5).

6.6. CATENAE OF ZIRCON AND TOURMALINE :

The base of the catena diagram obtained for zircon (Fig. 6.6) lies away from the 1:1 line but well below the 1:5 line. The maximum concentration of points are located within 1:1 and 1:2 lines. The catena diagram of tourmaline shows a similar pattern (Fig. 6.7). Zircon shows a wavy outline towards the 1:5 line. Both zircon and tourmaline are characteristically fan shaped with scattering of the points away from the points of origin of the coordinates.

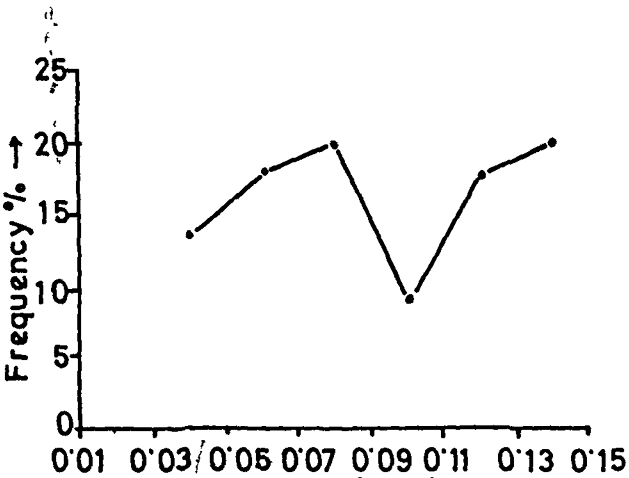

FIG: 6·5·1

Relationship between Length and Frequency of Tourmaline of the sandstones of Disang Group

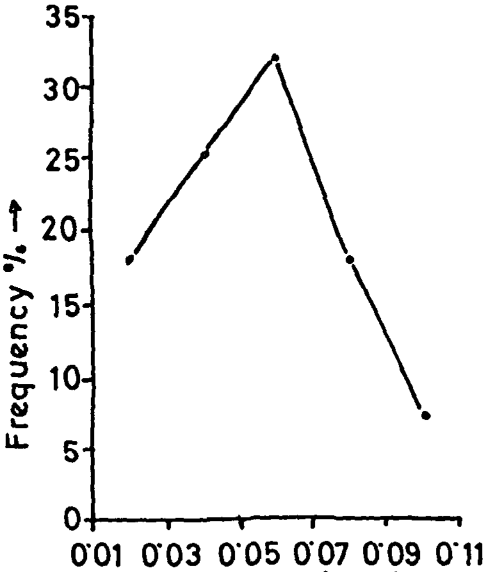

FIG: 6·5·2

Relationship between Breadth and Frequency of Tourmaline of the sandstones of Disang Group.

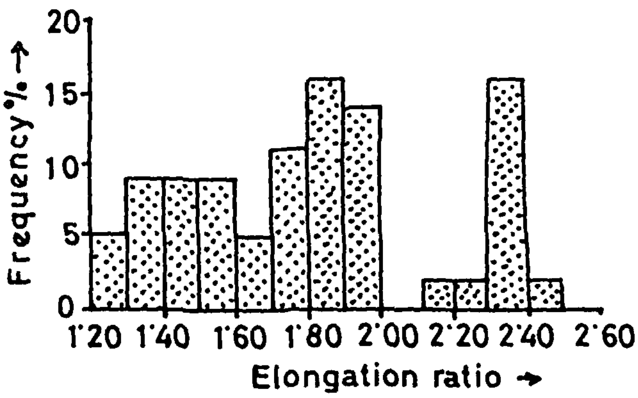

FIG: 6·5·3

Elongation ratio-frequency histogram of Tourmaline of the sandstones of *Disang Group*

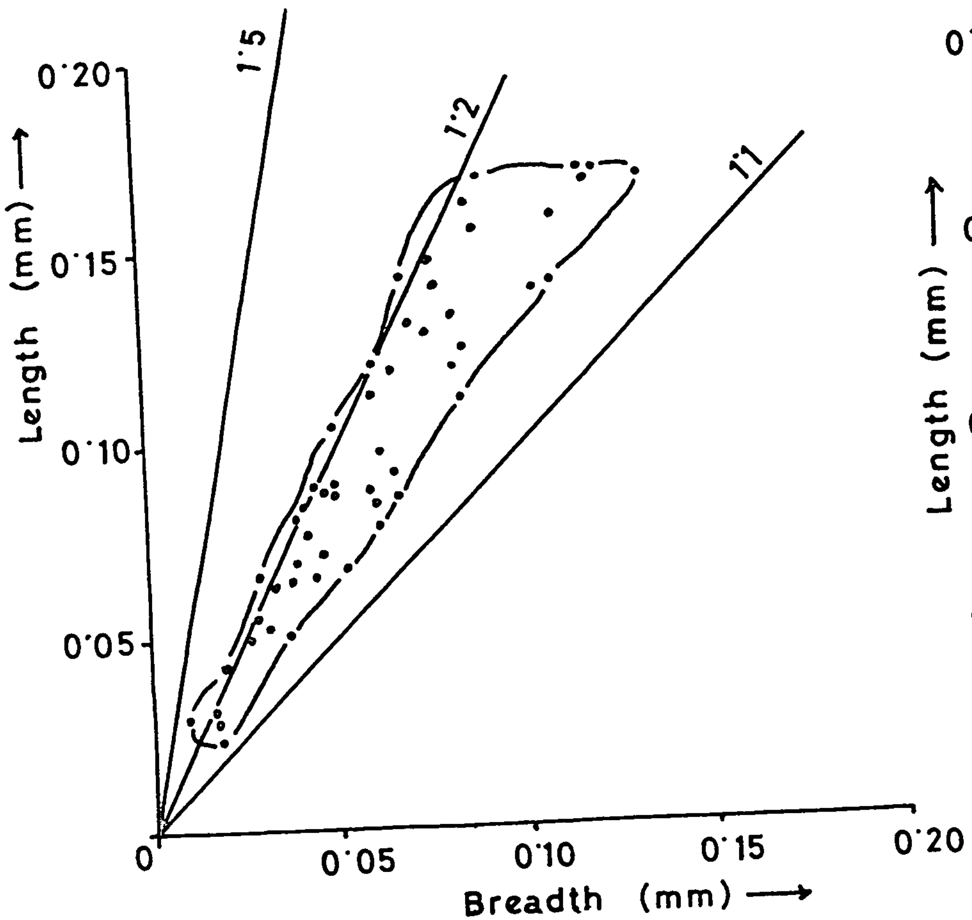

FIG: 6·6

Relationship between Length and Breadth of Zircon of the sandstones of the Disang Group.

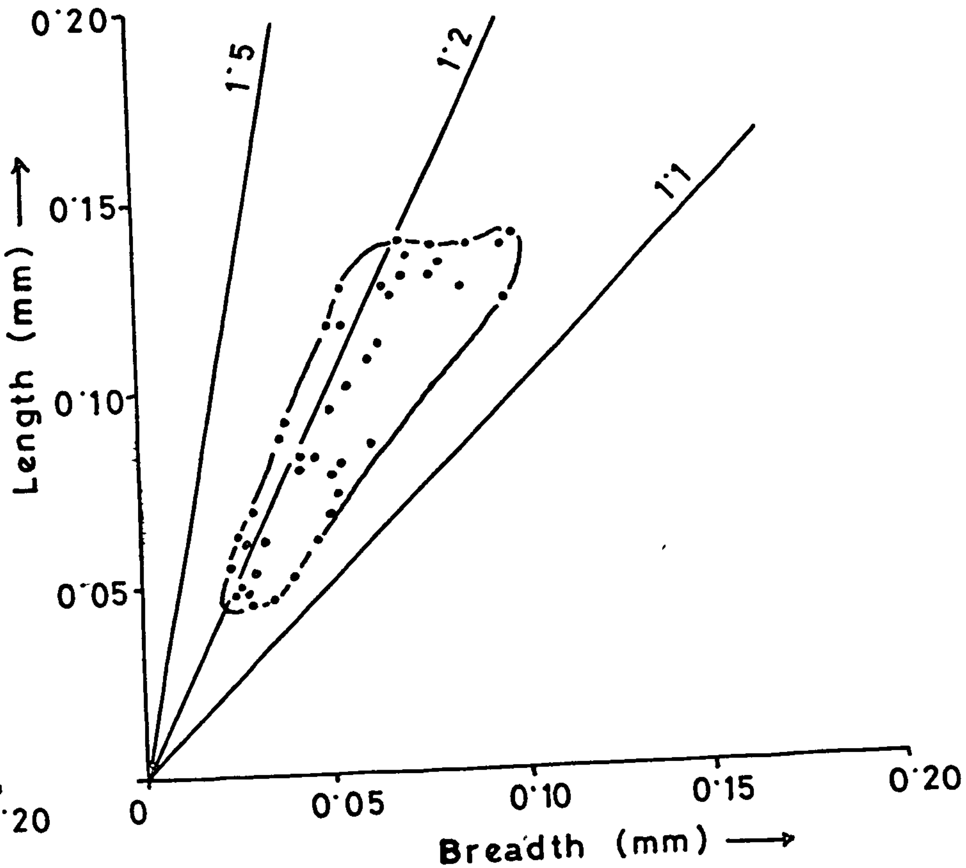

FIG: 6·7

Relationship between Length and Breadth of Tourmaline of the sandstones of the Disang Group.

CHAPTER 7

GEOCHEMISTRY

7.1. INTRODUCTION :

Sediments are products of large scale chemical and mechanical fractionation processes by which the constituents are separated into more or less chemically homogenous end products. The petrographic composition of a sandstone is therefore inferable from its chemical composition (Roser and Korsch, 1986). Petrographic studies are not often accurate because of probable obliteration of framework grains due to various factors including destruction by post depositional modification. Another reason may be due to inherent difficulties in correct identification of the grains. Therefore geochemical studies supplement for these deficiencies in identifying provenances and tectonic settings of the sandstones and give an idea of the redistribution of elements during and after deposition (Bhatia, 1983).

The geochemical composition of terrigenous sedimentary rocks is a function of the complex interaction of variables such as provenance, weathering, transportation and diagenesis. The relationship among the framework grains of the sandstones, provenance type and tectonic setting of sedimentary basins is shown by Crook (1974), Schwab (1975) and Dickinson and Suczek (1979). The chemical composition of sedimentary rocks therefore aids in an understanding of their evolution and the geochemical processes involved (Pettijohn, 1975; McLennan and Taylor, 1991). Excellent chemical indicators for petrographic composition of sandstones are TiO_2, Al_2O_3, Fe_2O_3, Na_2O and K_2O (Kukal, 1968).

Geochemical studies are important in dealing with altered clastic sedimentaries and useful in discriminating sediment compositions into broadly defined tectonic or sedimentary environments (Argast and Donnelly, 1987). Variations in major element composition can be used to make specific inferences about the original detrital constituents though post depositional processes may have altered the rock. The bulk chemical composition throws light in paleoclimatic studies and gives an idea of the chemical maturity of rocks (Potter, 1978b; Suttner and Dutta, 1986).

Several factors control the presence of trace elements in sandstones and these include pressure and temperature, the physical and chemical properties of the elements and the chemical environment (Taylor, 1965). The presence of certain trace elements in sedimentary rocks is indicative of the mode of formation and environment of deposition of the sediments (Majumder _et_ _al_., 1980).

The rare earth elements comprise of the lanthanides - lanthanum (La, Z=57) to lutetium (Lu, Z=71), including yttrium (Y, Z=39). Geochemically yttrium resembles dysprosium (Dy, Z=66) and holmium (Ho, Z=67) and is typically included with the heavy rare earths (HREE) - gadolinium (Gd, Z=64) to lutetium. These HREE are commonly known as the yttrium earths. The light rare earth elements (LREE) - lanthanum to samarium (Sm, Z=62), are known as the cerium earths (Fairbridge, 1972). The most characteristic feature of the rare earths including yttrium is the presence of a trivalent state. Among the trivalent REE cerium (Ce, Z=58) and europium (Eu, Z=63) behave differently under specific conditions and are regarded as environment-sensitive. Under reducing conditions europium may exist in the divalent state whereas Ce^{3+} may be oxidised to Ce^{4+}. However, apart from these anomalies the REE behave as an unusually coherent group of elements. The significance of REE in evaluating the evolution of sedimentary rocks is based on the fact that no internal fractionation takes place within the REE during metamorphism or in sedimentary processes except for oxidation of cerium to the quadrivalent state (Wildeman and Haskin, 1973).

Therefore, to ascertain the provenance and depositional conditions, and for rock nomenclature, twenty samples of the Disang sandstones are quantitatively analysed for the major oxides and five for the rare earths. Ten samples are semi-quantitatively analysed for trace elements. The laboratory methods employed are discussed in chapter 3.

7.2 MAJOR OXIDES :

The major oxides include SiO_2, TiO_2, Al_2O_3, Fe_2O_3, FeO, MnO, CaO, MgO, Na_2O, K_2O and P_2O_5 (Table 7.2.1). In percentage they range from 63.40 to 79.26, 0.73 to 1.48, 7.16 to 15.44, 0.66 to 4.65, 2.25 to 6.30, $<$0.01 to 0.05, 0.35 to 3.94, 0.66 to 3.37, 0.18 to 0.55, 0.58 to 1.61 and $<$0.05 to 0.16 respectively. The average percentages are 71.39, 1.02, 9.83, 2.49, 4.11, 0.02, 2.23, 2.16, 0.39, 1.08 and 0.06 respectively. Values of Si, Al and FeT (total iron) are calculated from their oxides and are shown in table 7.2.2. The vertical distribution of the oxides in the different lithounits in ascending order is shown in figure 7.2.1. In most cases they show an irregular distribution.

7.2.1. RATIOS OF SOME OXIDES :

The ratios of some oxides are shown in table 7.2.3. In the Disang sandstones the TiO_2/Al_2O_3 ratios range from 0.07 to 0.20 and average 0.11. The ratios suggest acidic and basic sources for the sediments and sub-humid climatic conditions (Spears and Sotiriov, 1976). The K_2O/Na_2O ratios ranging between

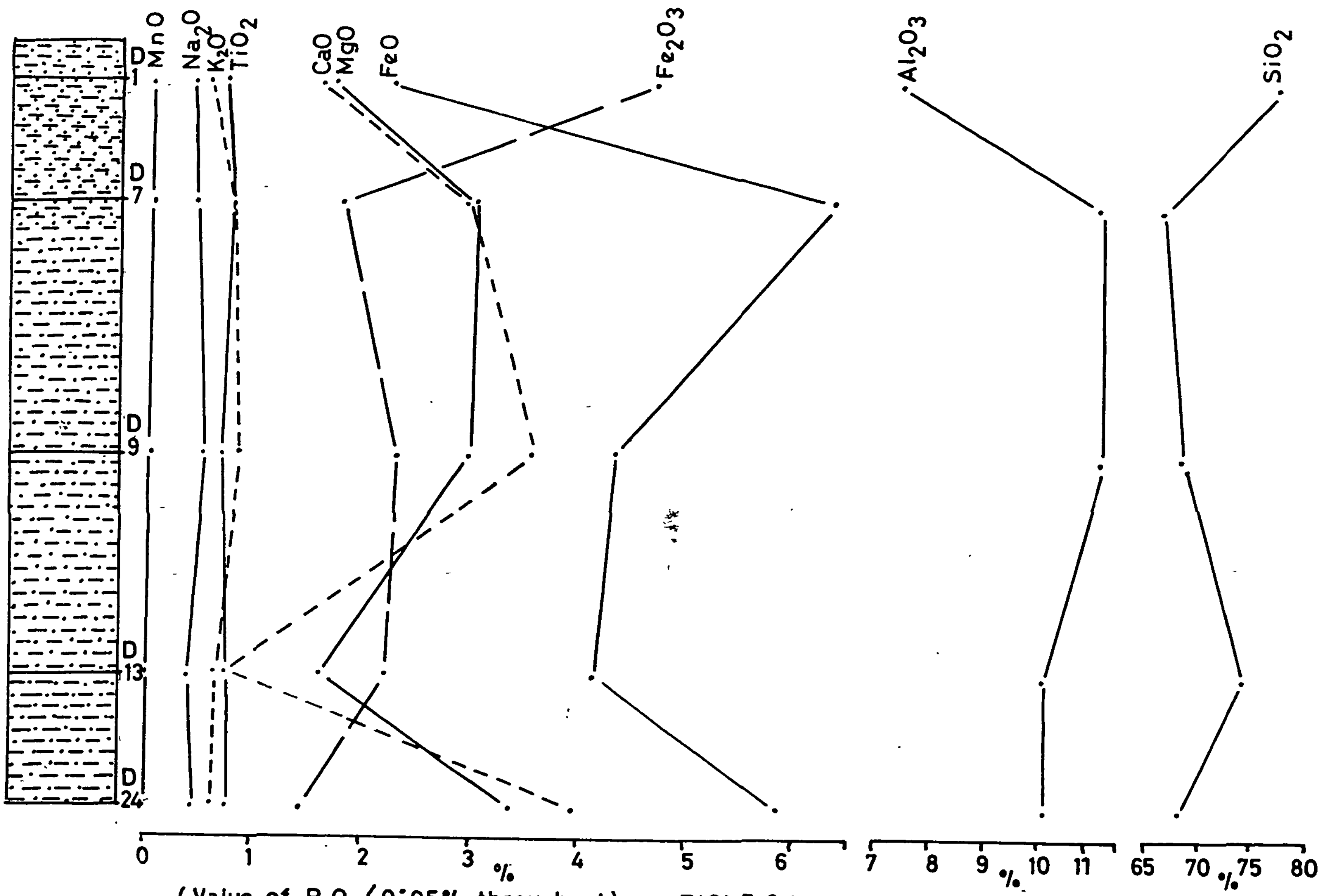

(Value of P_2O_5 < 0·05% throughout) FIG: 7·2·1

VERTICAL VARIATION OF MAJOR OXIDES OF THE DISANG SANDSTONES

Table 7.2.1

Major oxide composition (percentage) of the sandstones of the Disang Group.

Sample No.	SiO_2	TiO_2	Al_2O_3	Fe_2O_3	FeO	MnO	CaO	MgO	Na_2O	K_2O	P_2O_5	L.O.I.
D 1.	76.43	0.73	7.34	4.65	2.25	0.03	1.60	1.73	0.44	0.58	<0.05	4.17
D 4.	72.45	1.03	8.93	2.75	3.19	0.02	1.89	2.01	0.45	1.30	0.06	5.92
D 5.	73.01	0.98	9.86	2.35	2.91	0.01	1.93	2.45	0.43	1.20	<0.05	4.82
D 7.	66.22	0.80	11.03	1.77	6.30	0.05	2.94	3.03	0.47	0.80	<0.05	6.54
D 8.	69.13	0.79	9.35	2.33	4.25	0.04	3.52	2.83	0.42	1.17	<0.05	6.12
D 9.	68.00	0.73	11.11	2.32	4.32	0.04	3.54	2.96	0.55	0.87	<0.05	5.51
D 10.	71.35	1.13	9.50	2.96	3.87	0.02	1.58	1.97	0.40	1.26	0.06	5.90
D 13.	74.40	0.75	10.03	2.23	4.14	0.02	0.75	1.60	0.42	0.65	<0.05	4.96
D 16.	68.51	1.32	9.98	2.71	4.96	0.05	3.89	2.72	0.31	1.29	0.08	4.18
D 18.	70.56	0.91	9.69	1.90	3.03	<0.01	3.52	3.13	0.53	1.61	<0.05	5.06
D 20.	63.40	1.16	15.44	2.87	6.30	0.04	1.41	1.96	0.55	1.50	0.12	5.25
D 22.	73.55	1.34	8.24	1.42	3.29	0.04	2.88	1.87	0.38	0.94	0.07	5.98
D 23.	76.92	0.75	9.65	3.33	2.26	<0.01	0.44	0.66	0.27	1.09	0.12	4.50
D 24.	68.70	0.77	10.09	1.45	5.85	<0.01	3.94	3.37	0.44	0.61	<0.05	4.72
D 26.	69.30	1.41	7.16	2.68	5.13	0.03	3.56	3.15	0.41	1.33	0.07	5.77
D 28.	67.13	1.39	10.01	3.17	4.51	0.04	3.27	2.95	0.49	1.43	<0.05	5.46
D 30.	79.26	1.10	7.85	2.73	2.80	<0.01	0.48	0.68	0.18	0.97	0.07	3.87
D 32.	75.22	1.48	11.63	0.66	3.26	<0.01	0.35	0.86	0.20	1.26	0.06	5.01
D 35.	74.01	0.82	8.30	1.56	4.17	<0.01	2.67	2.15	0.38	0.92	0.05	4.92
D 36.	69.74	1.03	11.40	4.06	5.40	0.02	0.43	1.24	0.22	1.00	0.16	5.30
Average:	71.39	1.02	9.83	2.49	4.11	0.03	2.23	2.16	0.39	1.08	0.07	5.20

Table 7.2.2

Weight percentages and ratios of Si, Al and FeT (total iron) of the sandstones of the Disang Group.

Sample No.	Si	Al	FeT	Si :	FeT :	Al
D 1.	35.729	1.942	4.993	83.74	11.70	4.55
D 4.	33.834	4.724	4.401	78.76	10.24	11.00
D 5.	34.096	5.216	3.904	78.90	9.03	12.07
D 7.	30.956	2.919	5.839	77.95	14.70	7.35
D 8.	32.284	4.946	4.931	76.57	11.69	11.73
D 9.	31.788	2.940	4.805	80.41	12.15	7.44
D 10.	33.320	5.025	5.076	76.74	11.69	11.57
D 13.	34.780	2.654	4.609	82.72	10.96	6.31
D 16.	31.994	5.279	5.748	74.37	13.36	12.27
D 18.	32.951	5.126	3.682	78.91	8.82	12.27
D 20.	29.638	4.086	6.635	73.44	16.44	10.12
D 22.	34.348	4.359	3.548	81.29	8.40	10.31
D 23.	35.958	2.554	4.045	84.49	9.50	6.00
D 24.	32.115	2.670	5.282	80.15	13.19	6.66
D 26.	32.363	3.788	5.859	77.04	13.95	9.02
D 28.	31.350	5.295	2.720	74.00	13.50	12.50
D 30.	37.052	2.077	4.001	85.91	9.28	4.82
D 32.	35.163	3.077	2.836	85.60	6.90	7.49
D 35.	34.563	4.391	4.330	79.85	10.00	10.14
D 36.	32.602	3.017	6.845	76.78	16.12	7.10
Average :	33.344	3.804	4.854	79.38	11.58	9.04

Table 7.2.3

Major oxide composition (volatile-free) and some ratios of the Disang sandstones.

Sample No.	SiO_2	TiO_2	Al_2O_3	Fe_2O_3	FeO	CaO	MgO	Na_2O	K_2O	A	B	C	D
D 1.	80.26	0.77	7.71	4.88	2.36	1.68	1.82	0.46	0.61	10.41	0.10	8.02	1.31
D 4.	77.07	1.10	9.50	2.92	3.39	2.01	2.14	0.48	1.38	8.11	0.11	2.12	2.89
D 5.	76.76	1.03	10.37	2.47	3.06	2.03	2.58	0.45	1.26	7.40	0.10	1.96	2.79
D 7.	70.85	0.86	11.80	1.89	6.74	3.15	3.24	0.50	0.85	6.00	0.07	2.21	1.70
D 8.	73.71	0.84	9.67	2.48	4.53	3.75	3.02	0.45	1.25	7.39	0.08	1.99	2.78
D 9.	71.96	0.77	11.76	2.46	4.57	3.75	3.13	0.58	0.92	6.12	0.07	2.67	1.58
D 10.	75.89	1.20	10.10	3.15	4.12	1.68	2.10	0.43	1.34	7.51	0.12	2.35	3.15
D 13.	78.28	0.79	10.55	2.35	4.36	0.79	1.68	0.44	0.68	7.42	0.07	3.43	1.54
D 16.	71.60	1.38	10.43	2.83	5.18	4.07	2.84	0.32	1.35	6.86	0.13	2.10	4.16
D 18.	74.37	0.96	10.21	2.00	3.19	3.71	3.30	0.56	1.70	7.28	0.09	1.18	3.04
D 20.	66.91	1.22	16.30	3.03	6.65	1.49	2.07	0.58	1.58	4.11	0.07	1.91	2.72
D 22.	78.32	1.43	8.77	1.51	3.50	3.07	1.99	0.40	1.00	8.92	0.16	1.51	2.47
D 23.	80.54	0.79	10.10	3.49	2.37	0.46	0.69	0.28	1.14	7.97	0.08	3.06	4.03
D 24.	72.10	0.81	10.59	1.52	6.14	4.14	3.54	0.46	0.64	6.81	0.08	2.38	1.38
D 26.	73.62	1.50	7.61	2.85	5.45	3.78	3.35	0.44	1.41	9.68	0.20	2.02	3.24
D 28.	71.07	1.47	10.60	3.36	4.78	3.46	3.12	0.52	1.51	6.71	0.14	2.22	2.92
D 30.	82.45	1.14	8.17	2.84	2.91	0.50	0.71	0.19	1.01	10.10	0.14	2.81	5.38
D 32.	79.19	1.56	12.24	0.69	3.43	0.37	0.91	0.21	1.33	6.47	0.13	0.52	6.30
D 35.	77.92	0.86	8.74	1.64	4.39	2.81	2.26	0.40	0.97	8.92	0.10	1.70	2.42
D 36.	73.64	1.09	12.04	4.29	5.70	0.45	1.31	0.23	1.05	6.12	0.09	4.06	4.54
Average:	75.32	1.08	10.36	2.63	4.34	2.33	2.29	0.41	1.15	7.51	0.11	2.51	3.02

A - SiO_2/Al_2O_3

B - TiO_2/Al_2O_3

C - Fe_2O_3/K_2O

D - K_2O/Na_2O

1.31 and 6.30, and averaging 3.02 are indicative of exogeosynclinal sediments (Middleton, 1960). The rocks of this environment are typically subgraywackes.

7.2.2. RELATIONSHIPS OF SOME OXIDES :

For rock nomenclature values of (SiO_2+TiO_2), Al_2O_3 and the remaining oxides minus MnO and P_2O_5 (Table 7.2.3) are recalculated and plotted (Fig. 7.2.2) in a ternary diagram following Kukal (1968). According to this scheme of classification the Disang sandstones may be termed graywackes and subgraywackes. Log values of Fe_2O_3/K_2O ratios plotted against those of SiO_2/Al_2O_3 ratios (Fig. 7.2.3, Table 7.2.4) following Herron (1988) indicate that the rocks are mostly litharenites and graywackes.

Ternary plots of recalculated percentages of CaO, Na_2O and K_2O (Fig. 7.2.4, Table 7.2.4), and Fe_2O_3, MgO and TiO_2 (Fig. 7.2.5, Table 7.2.4) following Condie (1967) suggest basaltic and granitic sources, the latter dominating. SiO_2 contents of the analyses are plotted against the total contents of Al_2O_3, K_2O and Na_2O (Fig. 7.2.6) in a binary diagram following Suttner and Dutta (1986). Points indicate semi-arid to semi-humid paleoclimatic conditions.

The percentages of (Fe_2O_3+MgO), Na_2O and K_2O are recalculated and used as end members of a ternary diagram (Fig. 7.2.7, Table 7.2.4) following Blatt <u>et</u> <u>al</u>. (1980) the plots of which indicate an exogeosynclinal environment for the Disang sandstones. Binary plots of SiO_2 contents Vs K_2O/Na_2O ratios (Fig. 7.2.8, Table 7.2.3) and that of SiO_2/Al_2O_3 Vs K_2O/Na_2O ratios (Fig. 7.2.9, Table 7.2.3) following Roser and Korsch (1986) suggest a passive continental margin.

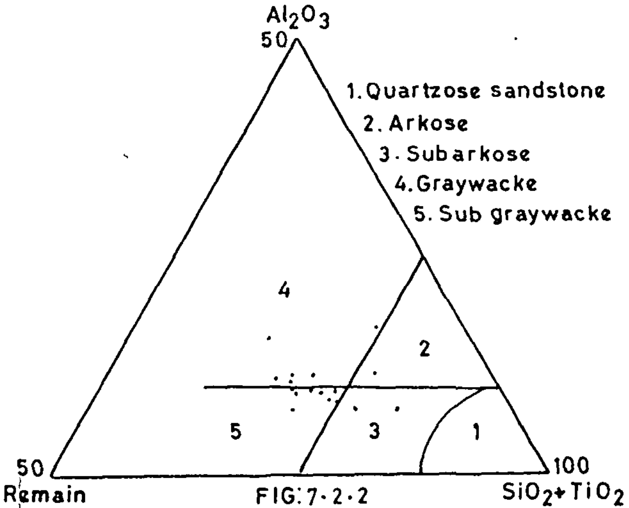

FIG: 7·2·2

Chemical composition of Disang sandstones expressed in the $SiO_2(+TiO_2)-Al_2O_3$-Remaining oxides triangle (After Kukal, 1968)

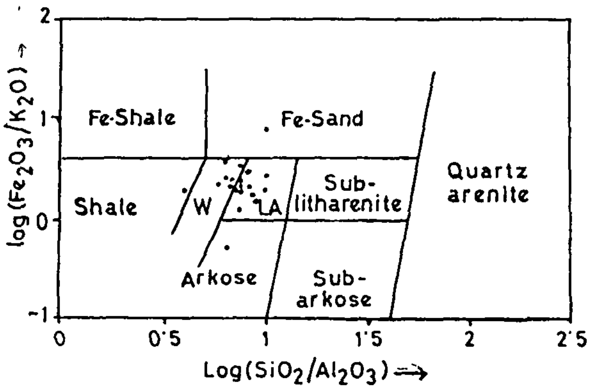

FIG: 7·2·3

W - Wacke LA - Litharenite

Geochemical classification of the sandstones of the Disang Group (After Herron, 1988)

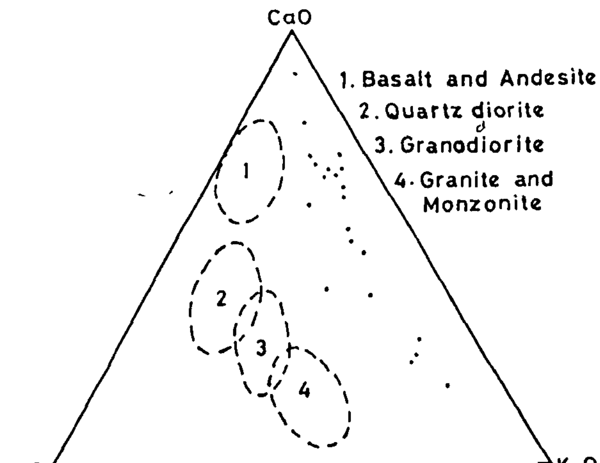

FIG: 7·2·4

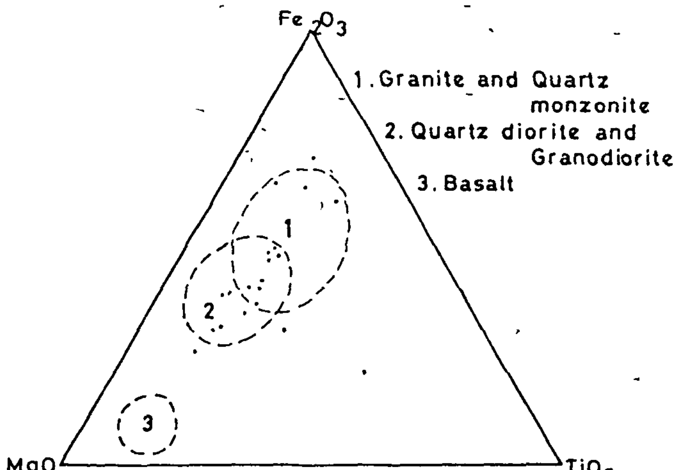

FIG: 7·2·5

Chemical composition of Disang sandstones in relation to Provenance (After Condie, 1967)

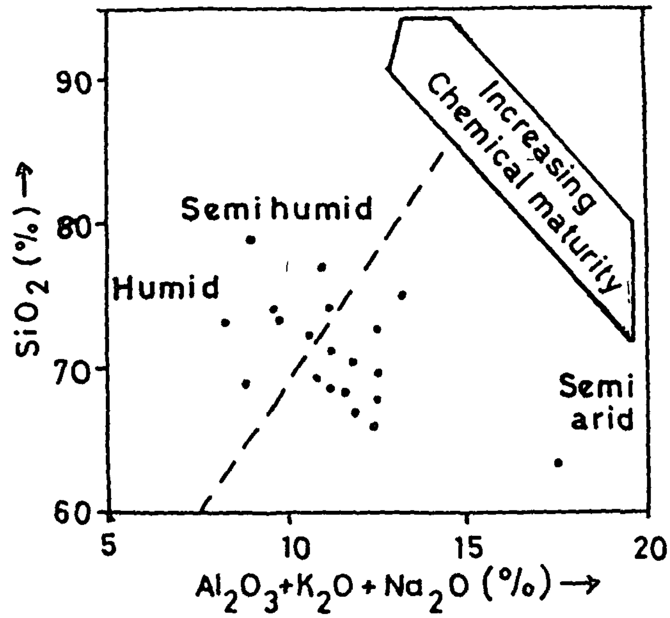

FIG: 7·2·6

Bivariate plots between SiO_2 and Total Al_2O_3 Na_2O and K_2O percentages of the Disang sandstones.

(After Suttner and Dutta, 1986)

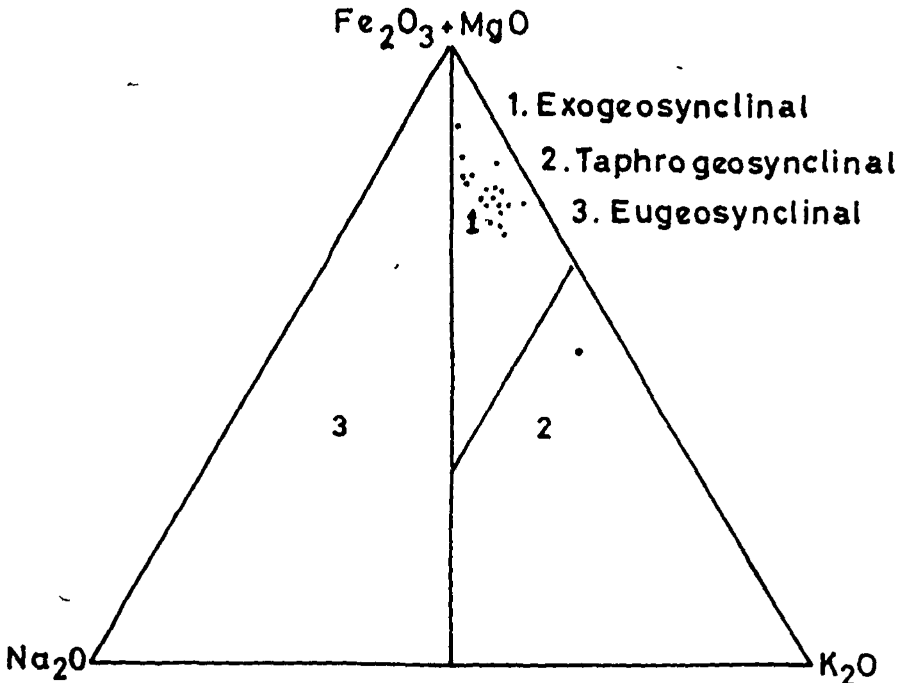

FIG: 7·2·7

Chemical composition of Disang sandstones in relation to Tectonic setting

(After Blatt *et al.*, 1980)

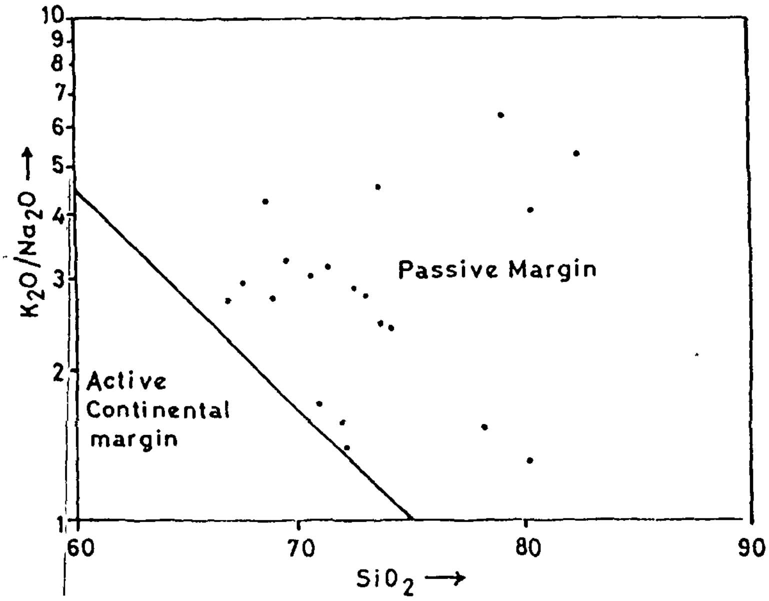

FIG: 7·2·8

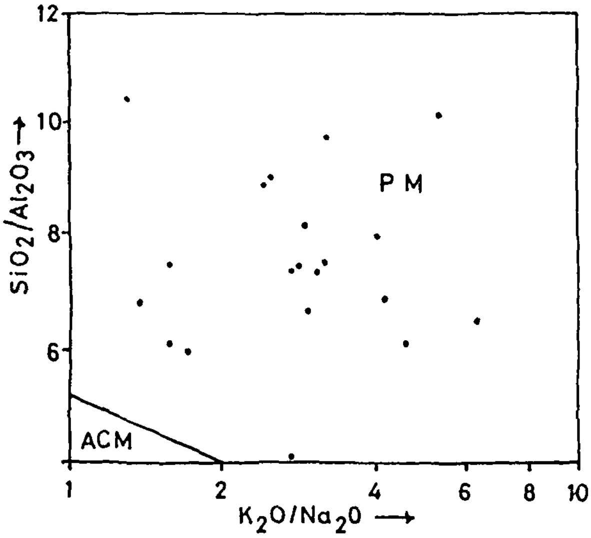

FIG: 7·2·9

Tectonic discrimination diagram for Disang sandstones
(After Roser & Korsch, 1986)

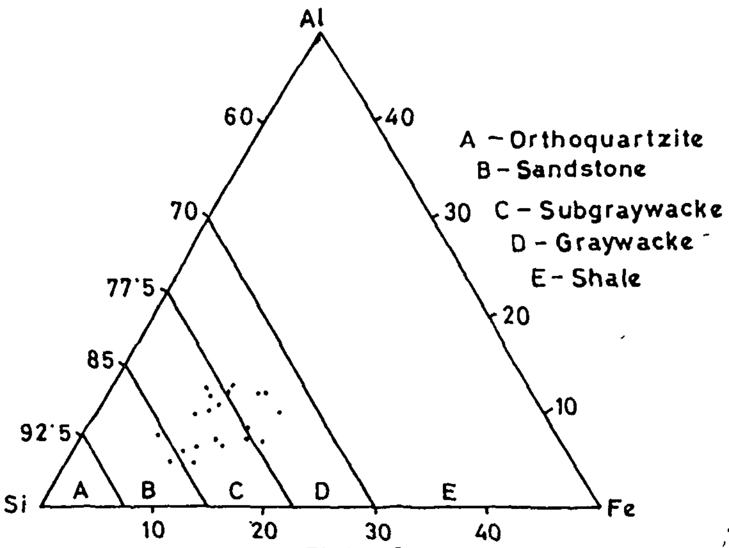

FIG: 7·2·10
Ternary plots of Si–Fe–Al of Disang sandstones
(After Moore & Dennen, 1970)

Table 7.2.4

Log values of some ratios and ratios among some major oxides of the Disang sandstones.

Sample No.	log (Fe_2O_3/K_2O)	log (SiO_2/Al_2O_3)	CaO	: Na_2O :	K_2O	Fe_2O_3 :	MgO :	TiO_2	$Fe_2O_3 + MgO$:	Na_2O :	K_2O
D 1.	0.90	1.02	61.07	16.79	22.14	65.40	24.33	10.27	86.22	5.94	7.84
D 4.	0.33	0.91	51.92	12.36	35.71	47.50	34.71	17.79	73.12	6.91	19.97
D 5.	0.29	0.87	54.21	12.08	33.71	40.66	42.39	16.95	74.65	6.69	18.66
D 7.	0.34	0.78	69.83	11.16	19.00	31.61	54.11	14.28	79.08	7.74	13.18
D 8.	0.30	0.87	68.88	8.22	22.90	39.16	47.56	13.28	76.44	6.22	17.33
D 9.	0.43	0.79	71.37	11.09	17.54	38.67	49.33	12.17	78.80	8.21	12.98
D 10.	0.37	0.88	48.76	12.34	38.89	48.84	32.51	18.65	74.81	6.07	19.12
D 13.	0.54	0.87	41.21	23.08	35.71	48.69	34.93	16.37	78.16	8.94	13.26
D 16.	0.32	0.84	70.86	5.65	23.50	40.15	40.30	19.55	77.24	4.41	18.35
D 18.	0.07	0.86	62.19	9.36	28.44	31.99	52.69	15.32	70.15	7.39	22.45
D 20.	0.28	0.61	39.61	15.89	43.35	47.91	32.72	19.36	70.20	7.99	21.80
D 22.	0.18	0.95	68.57	9.05	22.38	30.67	40.39	28.94	71.37	8.24	20.39
D 23.	0.49	0.90	24.44	15.00	60.55	70.25	13.92	15.82	74.58	5.05	20.37
D 24.	0.38	0.83	78.96	8.82	12.22	25.94	60.29	13.77	82.11	7.49	10.39
D 26.	0.31	0.99	67.17	7.73	25.09	37.02	43.51	19.47	77.01	5.42	17.57
D 28.	0.35	0.83	63.00	9.44	27.55	42.21	39.28	18.31	76.12	6.09	17.79
D 30.	0.45	1.00	29.45	11.04	59.51	60.53	15.08	24.39	74.78	3.95	21.27
D 32.	0.28	0.81	19.34	11.05	69.61	22.00	28.67	49.33	51.01	6.71	42.28
D 35.	0.23	0.95	67.25	9.57	23.17	34.44	47.46	18.10	74.05	7.58	18.36
D 36.	0.61	0.79	26.06	13.33	60.60	64.14	19.59	16.27	81.29	3.37	15.34
Average :	0.37	0.87	54.21	11.65	34.14	43.39	37.69	18.92	75.06	6.52	18.42

7.2.3. RELATIONSHIP OF SOME MAJOR ELEMENTS :

The values of Si, Al and FeT are recalculated to 100 percent and used as end members in a binary diagram (Fig. 7.2.10, Table 7.2.2) following Moore and Dennen (1970). The plots suggest that the rocks under investigation are mostly graywackes and subgraywackes.

7.3. RARE EARTH ELEMENTS :

The Disang sandstones are analysed for Ce, Pr, Nd, Pm, Sm, Eu, Gd, Tb, Dy, Ho, Er, Tm, Yb, Lu and Y (Table 7.3.1). These elements range from 16 to 27, 32 to 57, 4.30 to 7.70, 16 to 28, 3.36 to 5.20, 0.56 to 0.98, 1.86 to 3.56, 0.26 to 0.49, 1.43 to 2.20, 0.18 to 0.34, 0.46 to 0.83, 0.05 to 0.09, 0.29 to 0.48, <0.04 to 0.06 and 3.15 to 6.00 ppm respectively. In average they are 18.80, 39.40, 5.10, 20.40, 4.02, 0.71, 2.50, 0.36, 1.62, 0.25, 0.58, 0.06, 0.37, 0.05 and 4.73 ppm respectively. Their distribution in the different lithounits in the vertical section is shown in figure 7.3.1.

The patterns developed from the chondrite normalised REE values (Table 7.3.2) of the Disang sandstones are shown in figure 7.3.2. The REE distributions exhibit a steep LREE enriched-HREE depleted pattern (ΣLREE/ΣHREE - 10.18 to 20.21) which are similar to those of other young sedimentary rocks. These sandstones show a Eu-depleted pattern (Eu/Eu* - 0.56 to 0.77), higher ΣREE content (77.45 to 131.85 ppm) and strong negative Ce anomaly (Ce/Ce* - 0.80 to 0.87).

7.4. TRACE ELEMENTS :

The trace elements analysed include B, Mo, Ni, Co, V, Cr, Rb, Ga, Cd, Zn, and Zr (Table 7.4). In parts per million

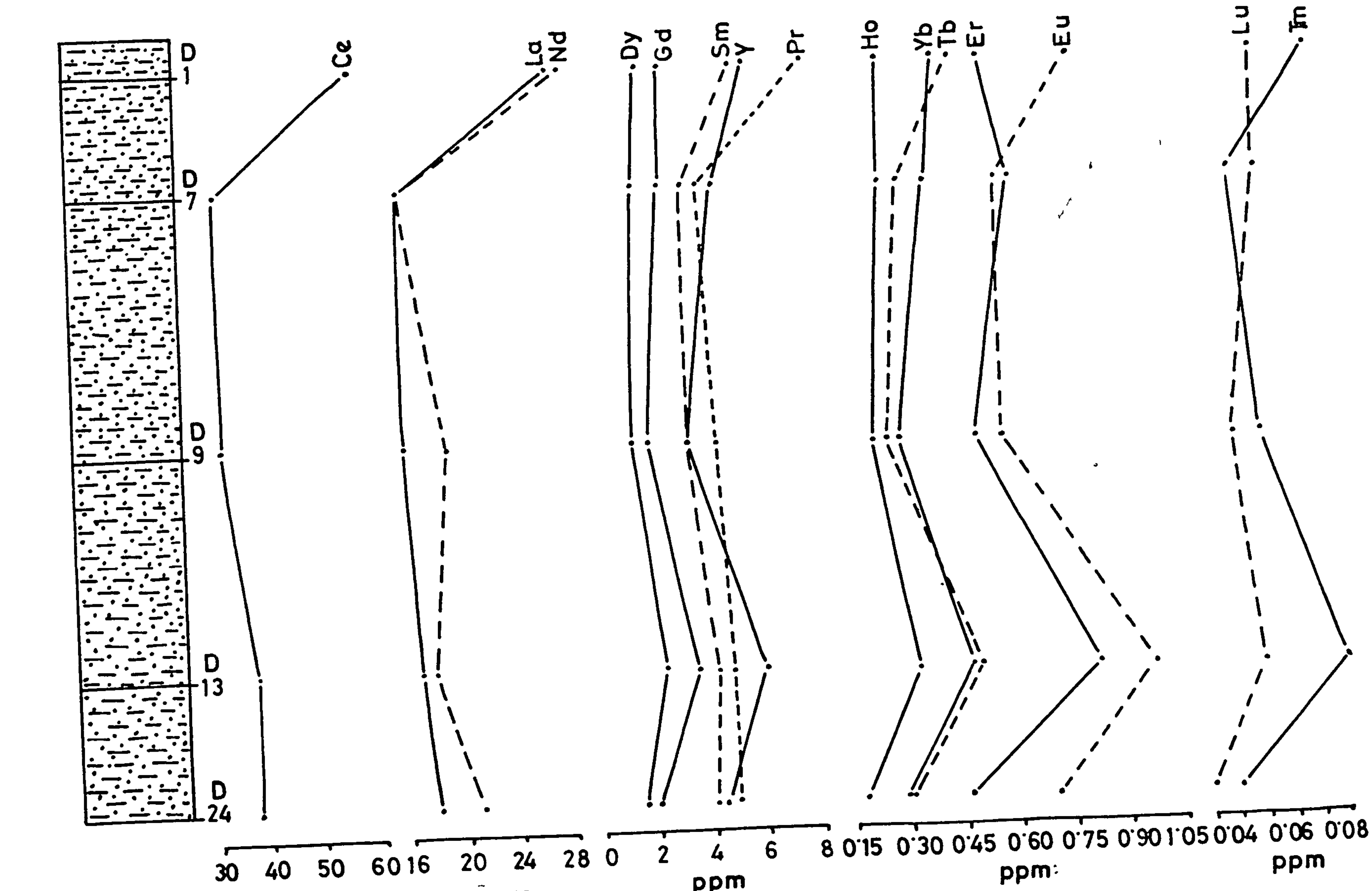

FIG: 7·3·1

VERTICAL VARIATION OF RARE EARTH ELEMENTS OF THE DISANG SANDSTONES

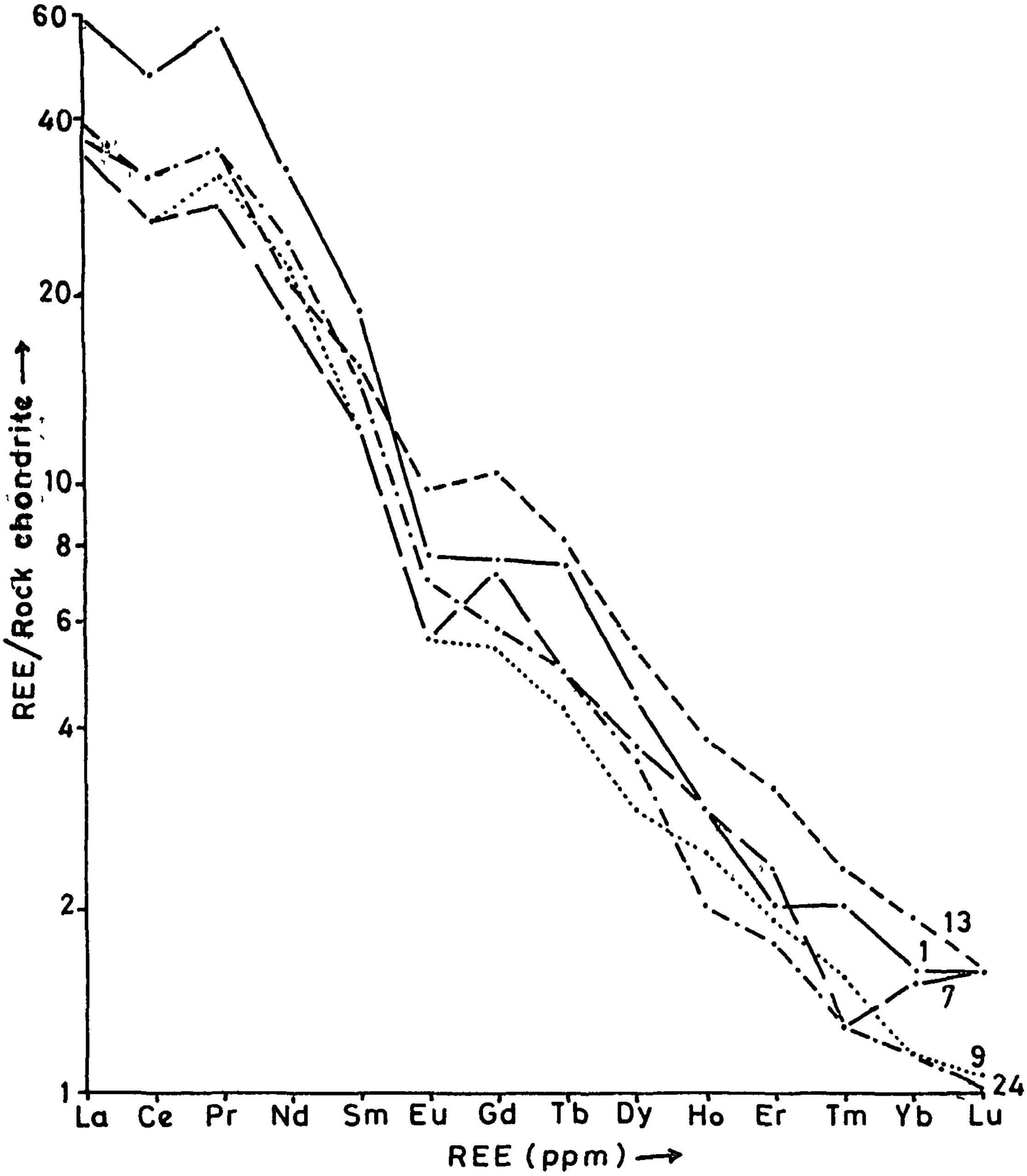

FIG: 7·3·2

Chondrite normalised REE pattern of the sandstones of the Disang Group.

(After Evensen *et al.*, 1978)

Table 7.3.1

Rare earth element composition and values of total LREE and HREE of the Disang sandstones.

Element	D 1	D 7	D 9	D 13	D 24	Average
La	27.00	16.00	16.00	17.00	18.00	18.80
Ce	57.00	32.00	32.00	38.00	38.00	39.40
Pr	7.70	3.90	4.30	4.80	4.80	5.10
Nd	28.00	16.00	19.00	18.00	21.00	20.40
Sm	5.20	3.36	3.36	4.20	4.00	4.02
Eu	0.77	0.56	0.56	0.98	0.70	0.71
Gd	2.60	2.48	1.86	3.56	2.00	2.50
Tb	0.45	0.30	0.26	0.49	0.30	0.36
Dy	1.80	1.50	1.17	2.20	1.43	1.62
Ho	0.26	0.26	0.22	0.34	0.18	0.25
Er	0.53	0.60	0.50	0.83	0.46	0.58
Tm	0.08	0.05	0.06	0.09	0.05	0.06
Yb	0.40	0.38	0.29	0.48	0.29	0.37
Lu	0.06	0.06	0.04	0.06	$<$0.04	0.05
Y	5.70	4.40	3.15	6.00	4.40	4.73
Total:	137.55	81.85	82.77	97.03	95.65	
La/Yb	67.50	42.11	55.17	35.42	62.07	
ΣLREE	124.90	71.26	74.66	82.00	85.80	
ΣHREE	6.18	5.63	4.40	8.05	4.75	

Table 7.3.2

Chondrite normalised REE values of the Disang sandstones.

Element	D 1	D 7	D 9	D 13	D 24	Average
La	58.696	34.783	34.783	36.957	39.130	40.870
Ce	47.500	26.667	26.667	31.667	31.667	32.834
Pr	56.204	28.467	31.387	35.036	35.036	37.226
Nd	32.941	18.824	22.353	21.176	24.706	24.000
Sm	19.259	12.444	12.444	15.556	14.815	14.904
Eu	7.778	5.657	5.657	9.899	7.071	7.212
Gd	7.647	7.294	5.471	10.471	5.882	7.353
Tb	7.500	5.000	4.333	8.167	5.000	6.000
Dy	4.500	3.750	2.925	5.500	3.575	4.050
Ho	2.921	2.921	2.472	3.820	2.022	2.831
Er	2.038	2.308	1.923	3.192	1.769	1.838
Tm	2.051	1.282	1.538	2.308	1.282	1.692
Yb	1.600	1.520	1.160	1.920	1.160	1.472
Lu	1.579	1.579	1.053	1.579	1.026	1.363
Eu/Eu*	0.56	0.62	0.71	0.77	0.77	0.69
Ce/Ce*	0.81	0.84	0.80	0.87	0.86	0.84

Table 7.4

Trace element composition and some ratios of the Disang sandstones.

Sample No.	B	Mo	Ni	Co	V	Cr	Rb	Ga	Cd	Zn	Zr	Cr/V	Ni/Co
D 1.	<20	<10	40	<20	<10	<10	<20	<10	20	90	150	1.00	2.05
D 7.	<20	<10	80	20	20	20	<20	<10	40	100	40	1.00	4.00
D 9.	<20	<10	80	35	<10	<10	<20	<10	35	110	20	1.00	2.29
D 13.	<20	<10	70	20	<10	<10	<20	<10	25	80	15	1.00	3.50
D 20.	<20	<10	100	60	25	40	<20	10	50	150	80	1.60	1.67
D 23.	<20	<10	60	40	<10	<10	<20	<10	40	80	60	1.00	1.50
D 24.	<20	<10	85	35	<10	<10	<20	<10	30	90	35	1.00	2.43
D 30.	<20	<10	40	40	10	10	<20	<10	40	90	100	1.00	1.00
D 32.	<20	<10	70	30	10	10	<20	<10	25	95	50	1.00	2.33
D 36.	<20	<10	125	40	15	15	<20	<10	20	120	50	1.00	3.12
Average	<20	<10	75	33.95	12.75	14.25	<20	<10	32.50	100.50	60	1.06	2.39

Ni ranges from 40 to 125, Co from <20 to 60, V from <10 to 25, Cr from <10 to 40, Cd from 20 to 50, Zn from 80 to 150 and Zr from 15 to 150. B and Rb are <20 ppm while Ga and Mo are <10 ppm in the Disang sandstones. In average B, Mo, Ni, Co, V, Cr, Rb, Ga, Cd, Zn and Zr are <20, <10, 75, 34, 13, 14, <20, <10, 33, 100 and 60 ppm respectively. The vertical distribution of these elements in the different lithounits is shown in figure 7.4.1. in ascending order. Their distribution does not show any definite pattern.

7.4.1. RATIOS OF SOME TRACE ELEMENTS

Some ratios have significance in certain geological interpretations and these include Cr/V and Ni/Co. Cr/V ratios ranging from 1.00 to 1.60 and averaging 1.06 (Table 7.4) indicate good ventilation in the depositional environment (Dykpiv, 1979). Ni/Co ratios range from 1.00 to 4.00 and average 2.39 (Table 7.4). The values suggest decreasing Eh conditions in the depositional basin (Dykpiv, 1979).

7.4.2. RELATIONSHIPS OF SOME TRACE ELEMENTS :

The percentages of B, Rb and Ga, recalculated and plotted in a ternary diagram (Fig. 7.4.2, Table 7.4) following Degens _et al_. (1957) indicate a marine environment of deposition. Binary plots of ppm B Vs ppm Ga (Fig. 7.4.3) and ppm B Vs ppm Rb (Fig. 7.4.4), also after Degens _et al_. (1957), indicate fresh and mixed environments of deposition respectively for the Disang sandstones.

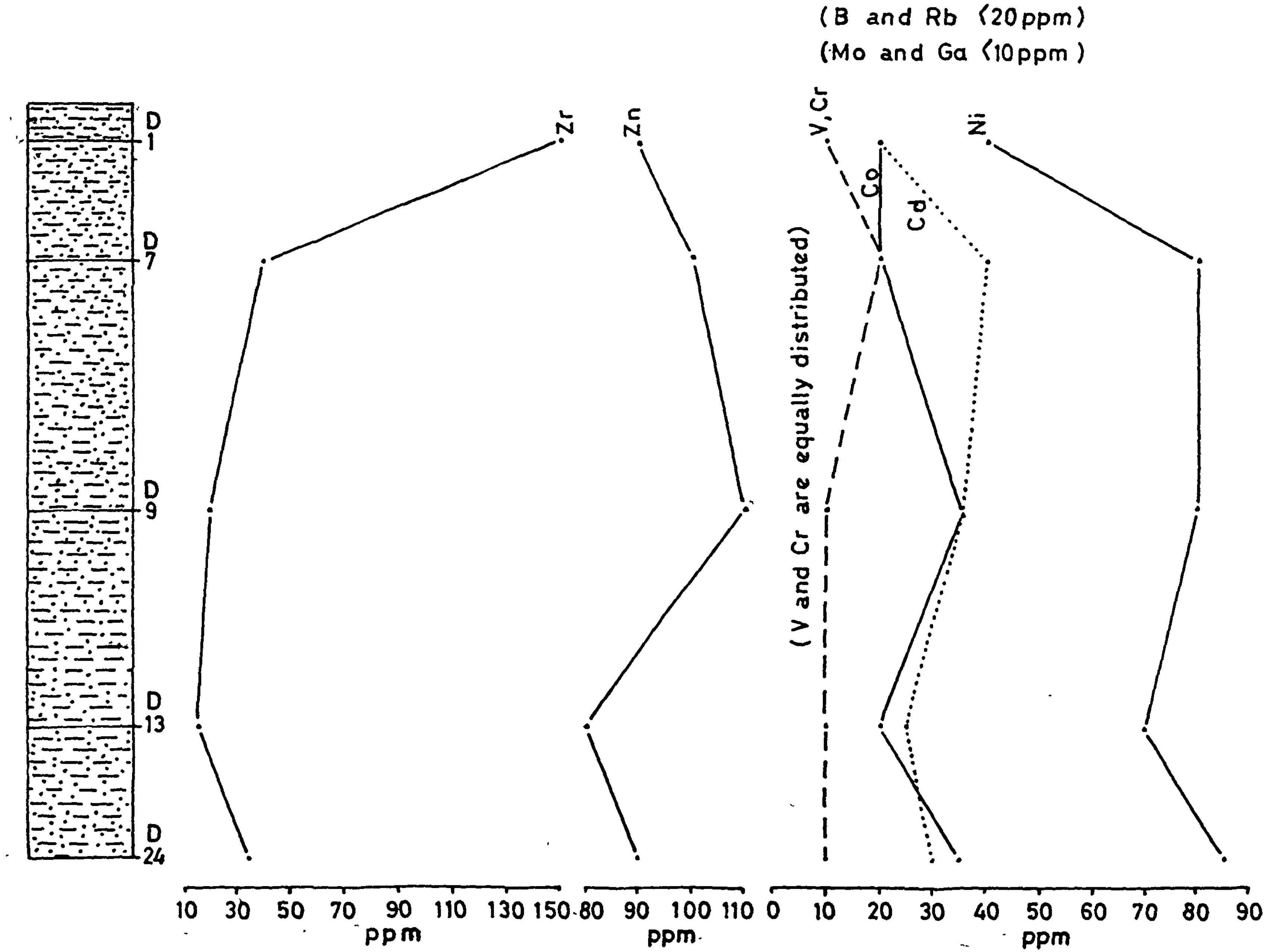

FIG: 7·4·1
VERTICAL VARIATION OF TRACE ELEMENTS OF THE DISANG SANDSTONES

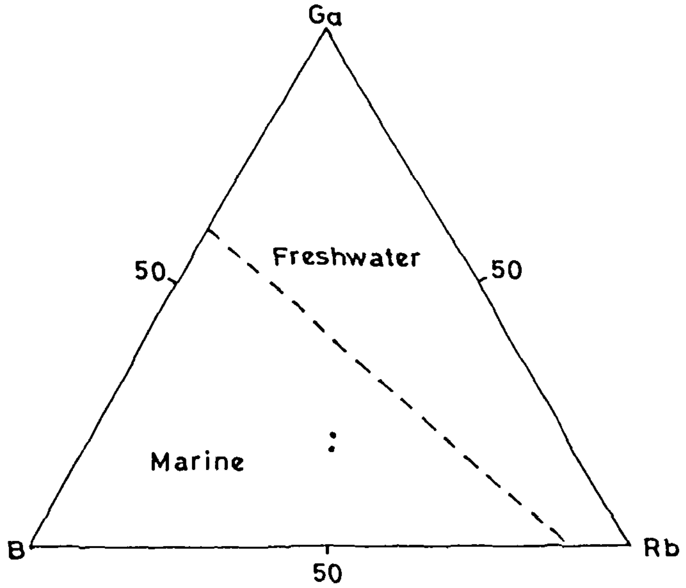

FIG: 7·4·2

Relationship among Ga, B and Rb in Disang sandstones

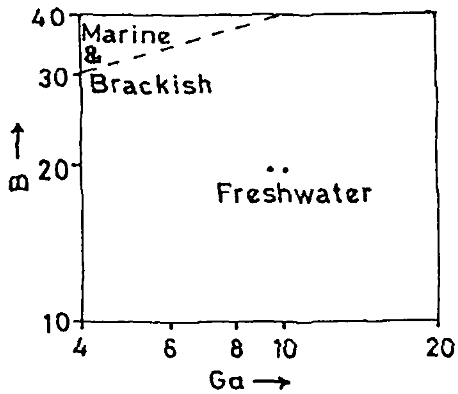

FIG: 7·4·3

Relationship between B and Ga (ppm) in Disang sandstones

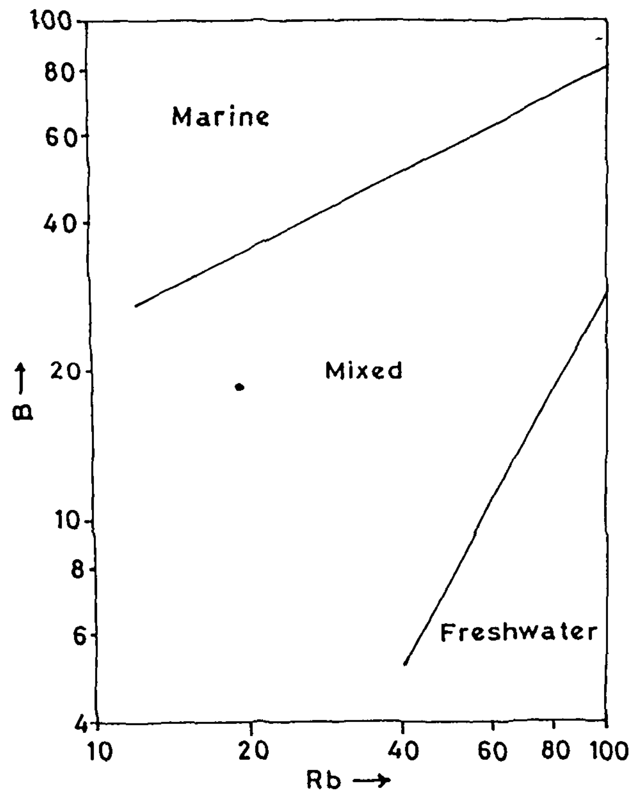

FIG: 7·4·4

Relationship between B & Rb (ppm) in Disang sandstones

PART III

CHAPTER 8

PETROGRAPHY AND CLAY MINERALOGY

8.1. PETROGRAPHY

8.1.1. INTRODUCTION :

The importance of petrographic studies in geology has already been mentioned in chapter 4. An attempt is made in this chapter to determine, from a study of twenty five thin sections, the provenance, paleoclimate, maturity and tectonic setting of the Barail sandstones, and to classify them. The methods of study are described in chapter 3.

8.1.2. FRAMEWORK CONSTITUTION :

The sandstones of the Barail Group, like those of the Disangs, show marked variation in grain size and principal framework constituents in thin sections (Fig. 8.1.1). The mineralogical composition is shown in table 8.1.1.

Quartz :

This is the major constituent of the Barail sandstones and ranges from 50.06 to 60.83%. More than 300 point-counts are made in each section to estimate the different genetic types of quartz which include non-undulatory, undulatory, polycrystalline and reworked categories (Table 8.1.2). The non-undulatory quartz grains (Fig. 8.1.1), constituting 58.09 to 91.23%, become totally extinct on slight rotation of the stage. Undulatory

Fig. 8.1.1

Ferrugenous Barail sandstone under crossed nicols

1

A - Partial alteration of plagioclase
B - Embayed quartz
C - Clayey matrix
D - Non-undulose quartz
E - Ferrugenous replacement of rock fragment.

Fig. 8.1.2

Polymodal Barail sandstone under crossed nicols

2

A - Reworked quartz
B - Metamorphic rock fragment
C - Metaquartzite showing sutured contact
D - Undulose quartz
E - Inclusions in quartz

Fig. 8.1.3

Barail sandstones under crossed nicols

A - Resorped quartz
B - Chert
C - Polycrystalline quartz
D - Ferrugeneous coating over quartz
E - Silica cemented quartz grains
F - Cherty matrix

2

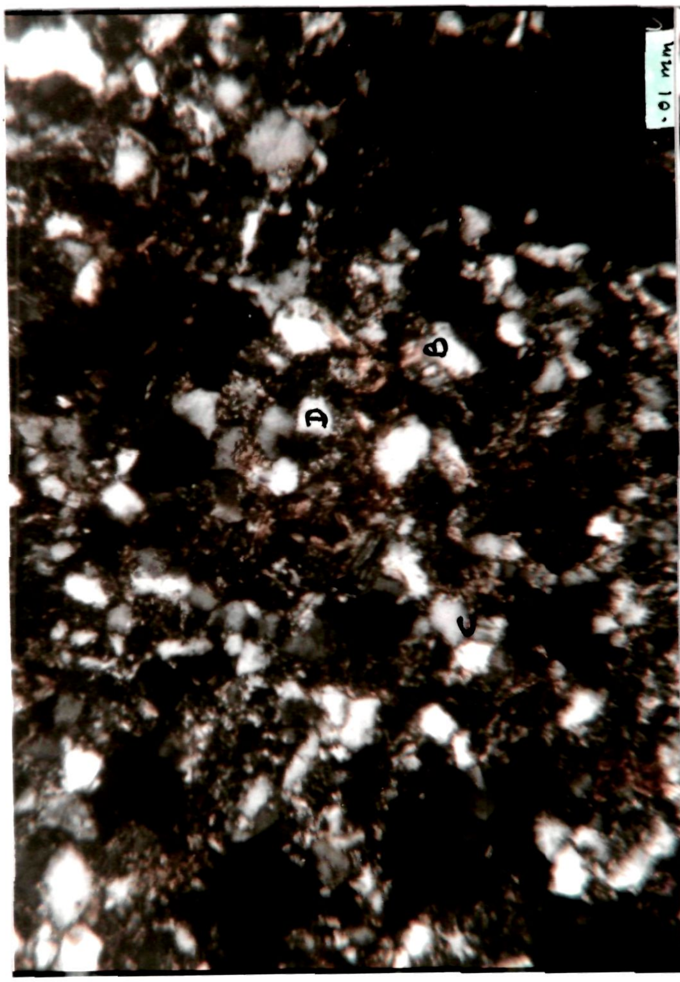

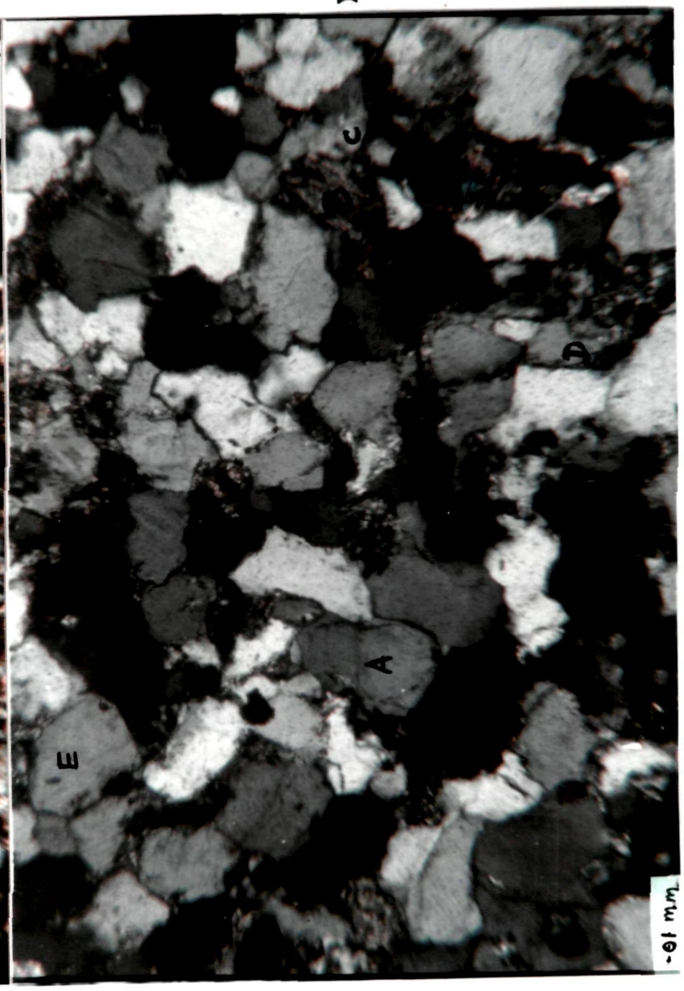

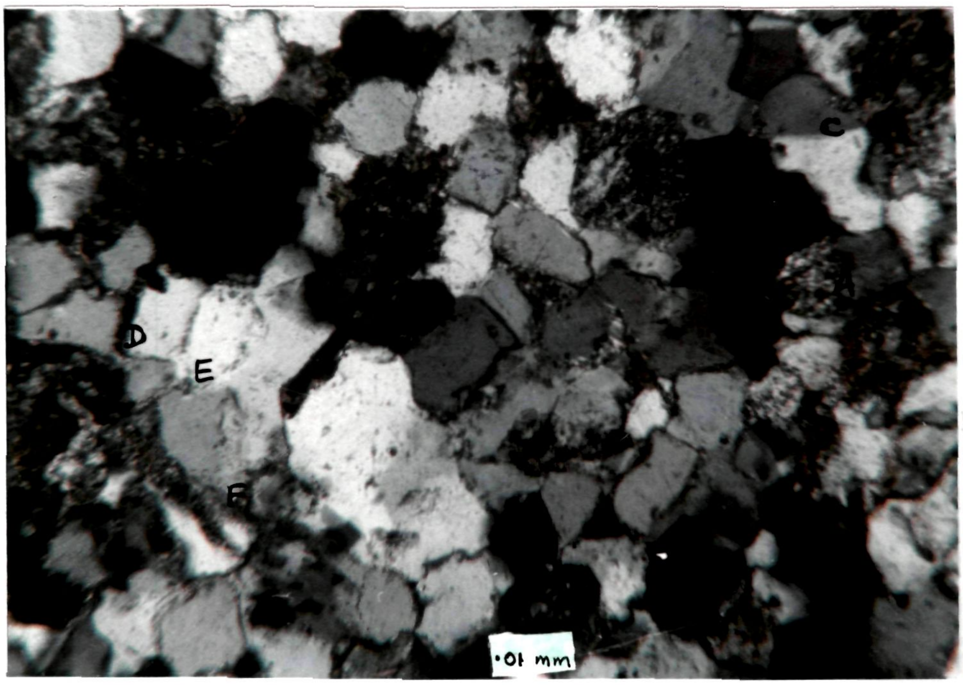

Fig. 8.1.4

1 Barail sandstone under crossed nicols
showing quartz vein

Fig. 8.1.5

Barail sandstone under crossed nicols

2 A - Vein quartz
B - Ferrugeneous grain
C - Matrix
D - Biotite altered to matrix and showing
kink-bending.

Fig. 8.1.6

Barail sandstone under crossed nicols

A - Ferrugenous stain on cherty matrix
B - Undulose quartz
C - Bent muscovite

1

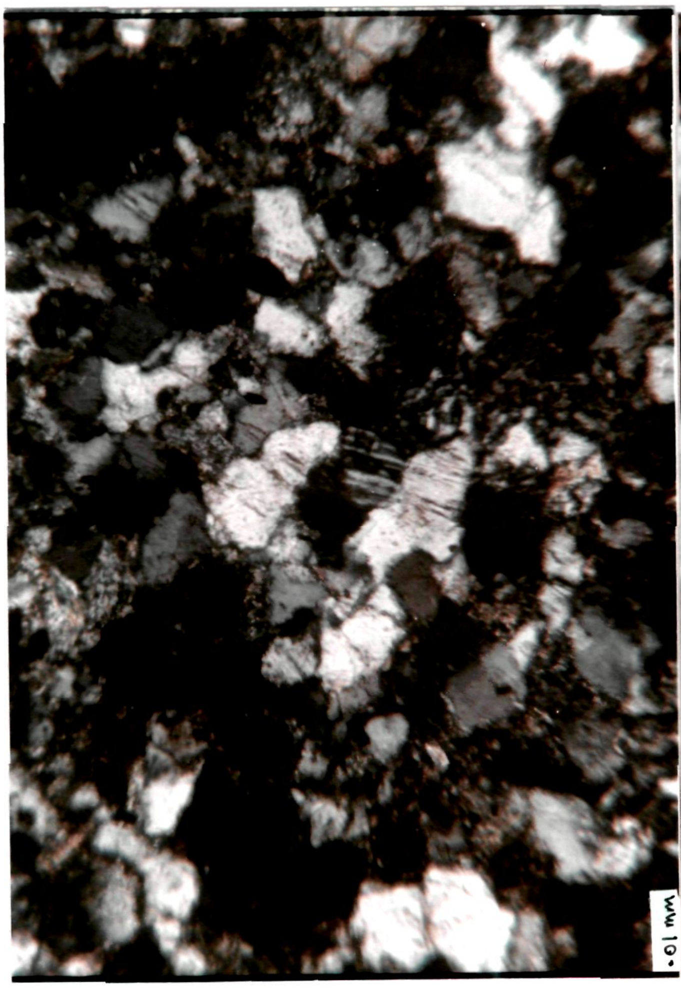

2

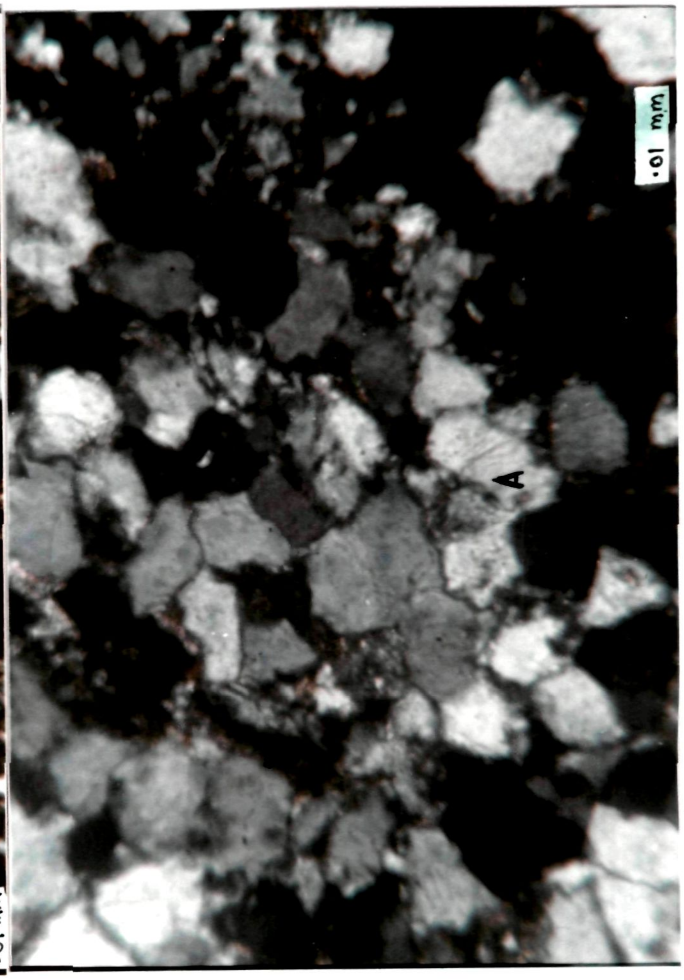

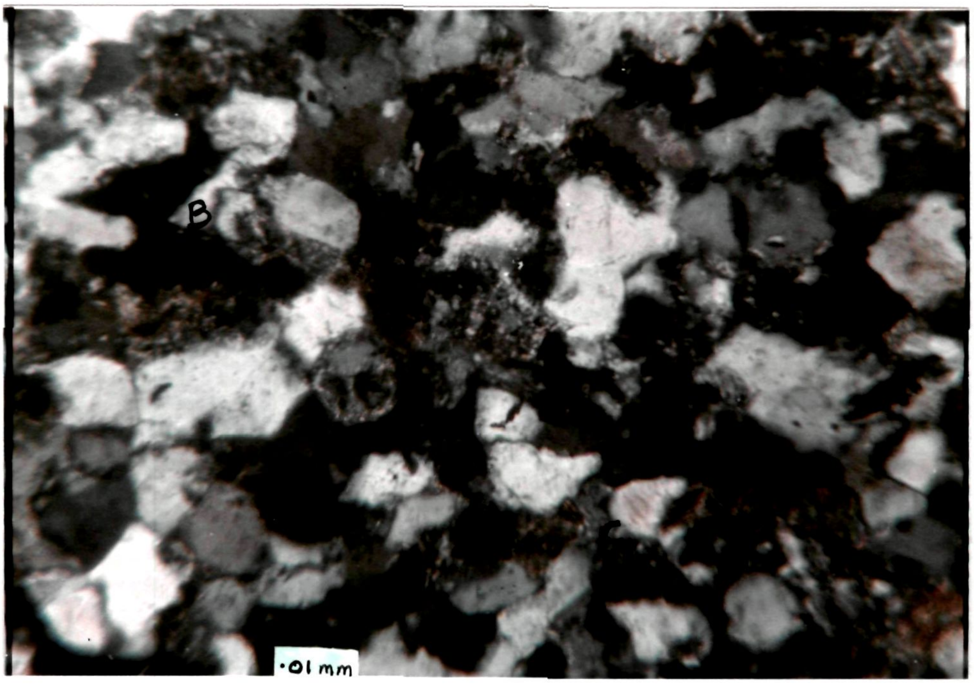

Table 8.1.1

Mineralogical composition of the sandstones of the Barail Group.

Sample No.	Quartz	Feldspar	Mica	Rock fragments: Igneous	Rock fragments: Meta-morphic	Rock fragments: Sedi-mentary	Rock fragments: Total	Other grains	Matrix	Cement
B 1.	57.17	2.06	2.81	8.53	10.04	0.53	19.10	1.84	12.83	4.19
B 7.	58.30	3.55	3.69	8.73	8.13	0.33	17.19	1.81	11.33	4.13
B 22.	54.03	2.86	3.76	7.72	9.41	0.31	17.44	1.92	14.88	5.11
B 25.	57.55	2.24	3.07	8.16	8.98	0.47	17.61	2.59	12.93	4.01
B 30.	51.11	2.54	2.96	10.71	9.33	0.35	20.39	2.22	14.25	6.53
B 32.	57.24	5.01	3.03	6.29	7.19	0.87	14.35	1.51	13.63	5.23
B 39.	53.77	4.05	1.50	10.48	9.25	0.52	20.25	1.03	13.14	6.26
B 45.	59.70	2.52	2.00	9.59	7.15	0.77	17.51	2.95	10.19	5.13
B 49.	50.06	2.33	1.48	11.27	10.23	0.71	22.21	1.97	16.18	5.77
B 53.	55.91	2.37	2.28	10.63	6.11	0.82	17.56	1.08	14.11	6.69
B 54.	59.25	1.23	2.02	10.11	6.83	0.78	17.72	1.03	14.56	4.19
B 55.	54.39	2.51	3.13	9.63	7.18	0.32	17.13	2.32	13.41	7.11
B 57.	50.55	2.17	2.53	10.75	9.25	0.49	20.49	3.08	14.47	6.71
B 61.	54.56	1.12	1.36	9.32	8.19	0.51	18.02	3.68	14.01	7.25
B 69.	60.57	2.22	2.10	8.05	7.11	0.93	16.09	1.15	13.61	4.26
B 83.	54.36	2.89	2.57	8.86	7.89	0.81	17.56	3.01	13.63	5.98
B 92.	60.06	2.11	2.03	10.01	6.58	0.73	17.32	1.06	12.92	4.50
B 96.	59.45	2.30	2.00	7.12	6.39	0.80	14.31	3.11	14.69	4.14
B 99.	55.29	3.01	2.58	7.07	7.12	0.39	14.58	4.72	15.26	4.56
B 101.	59.39	2.55	2.02	8.48	8.13	0.51	17.12	1.10	14.75	3.07
B 105.	52.70	2.93	6.44	7.39	7.22	0.48	15.09	3.21	13.46	6.17
B 106.	58.08	2.49	2.51	7.20	8.13	0.59	15.92	3.13	14.76	3.11
B 109.	58.45	2.36	3.07	6.75	9.25	0.64	16.64	2.11	13.36	4.01
B 111.	58.41	1.79	2.40	10.02	8.15	0.45	18.62	1.03	13.56	4.19
B 113.	60.83	2.06	2.50	7.50	8.28	0.34	16.12	1.85	12.51	4.13
Average:	56.45	2.53	2.63	8.81	8.06	0.58	17.45	2.18	13.70	5.06

Table 8.1.2

Genetic quartz types and length-breadth ratios of quartz of the Barail sandstones.

Sample No.	Non-undulatory	Undulatory	Polycry-stalline	Re-worked	L/B - <2 Minimum	L/B - <2 Maximum	L/B - > 2 Minimum	L/B - > 2 Maximum	Average of 50 grains
B 1.	81.99	1.46	13.41	3.14	1.05	1.91	2.32	2.65	1.74
B 7.	83.29	2.00	11.29	3.42	1.06	1.90	2.25	4.30	2.27
B 22.	85.19	3.09	10.21	1.51	1.11	1.86	2.16	2.87	1.75
B 25.	84.63	0.80	13.79	0.78	1.10	1.88	2.15	5.47	2.40
B 30.	85.87	3.89	10.24	-	1.07	1.80	2.06	6.40	2.49
B 32.	76.56	3.04	18.36	2.04	1.69	1.84	2.08	3.63	2.67
B 39.	84.92	2.83	9.50	2.75	1.31	1.64	2.05	4.73	2.05
B 45.	84.75	4.70	8.70	1.85	1.04	1.84	3.57	5.08	1.83
B 49.	87.14	1.11	10.41	1.34	1.10	1.72	2.38	3.77	2.10
B 53.	78.56	0.93	20.51	-	1.01	1.93	2.00	2.35	1.58
B 54.	88.58	0.99	9.32	1.11	1.11	1.74	2.16	2.91	1.50
B 55.	89.31	1.42	9.27	-	1.18	1.85	2.25	2.76	1.94
B 57.	83.39	4.88	9.79	1.94	1.17	1.96	2.00	3.18	1.98
B 61.	89.40	1.64	8.96	-	1.16	1.72	2.00	3.00	1.79
B 69.	71.41	4.44	24.15	-	1.65	1.95	2.00	3.20	2.39
B 83.	85.06	5.05	7.69	2.20	1.03	1.98	2.10	2.98	1.89
B 92.	58.09	14.89	27.02	-	1.20	1.98	2.04	2.36	1.82
B 96.	88.77	4.14	7.09	-	1.06	1.91	2.02	3.00	1.66
B 99.	91.23	2.23	6.54	-	1.21	1.86	2.32	6.36	2.35
B 101.	84.98	2.39	12.63	-	-	-	2.40	4.75	3.58
B 105.	85.27	4.47	10.26	-	1.41	1.87	2.05	5.16	2.64
B 106.	87.17	1.32	11.51	-	1.00	1.83	2.00	7.50	2.31
B 109.	89.33	0.89	7.89	1.89	1.07	1.92	2.00	4.00	1.94
B 111.	90.75	1.16	8.09	-	1.95	1.97	2.25	4.11	2.76
B 113.	83.72	3.20	13.08	-	1.71	1.97	2.33	4.21	2.73
Average :	83.97	3.08	11.99	0.96					

quartz (Fig. 8.1.2) showing undulose extinction constitutes 6.54 to 27.02%. Polycrystalline quartz (Fig. 8.1.3) constituting 0.80 to 14.89% are made up of composite grains of 2 to 3 units although grains showing more than 3 units are not uncommon. Recycled quartz with overgrowths are noted in a few sections while inclusions of zircon and tourmaline (Fig. 8.1.2) are common. Some of the grains are stained with iron oxides (Fig. 8. 1.3) and cherty resorption of quartz is noted in certain sections (Fig. 8.1.3). Quartz veins penetrating the sandstones are common. The quartz grains have length-breadth ratios ranging from 1.50 to 3.58 and averaging 2.17 (Table 8.1.2). The ratios suggest a mixed source for the sediments.

Feldspar :

The feldspars are mainly sodic plagioclases (Fig. 8.1. 1) with some untwinned varieties. They range from 1.12 to 5.01%. Some of the feldspar grains are found to be altered. They are mostly sub-angular, some being coated with iron oxides.

Mica :

Flakes of detrital muscovite and biotite are fairly common (Figs. 8.1.5 and 8.1.6) and as a group the micas range from 1.36 to 6.44%. Some of them are altered at the boundaries to a clayey matrix. A feature very commonly noted is kink-bending of the grains.

Other minerals :

This category includes minerals such as zircon, tourmaline, rutile, kyanite, epidote, garnet and opaques and as a group ranges from 1.03 to 4.72%. These constituents are studied as heavy minerals in chapter 10.

Rock fragments :

The rock fragments are from diverse sources including igneous, metamorphic and sedimentary (Figs. 8.1.1, 8.1.2 and 8.1.3). As a group they range from 14.31 to 22.21%. The igneous fragments range from 6.29 to 10.75% while the metamorphic types range from 6.11 to 10.23%. Reworked fragments, including chert, form a small group ranging from 0.31 to 0.93% of the total petrographic composition of the Barail sandstones.

Matrix and Cement :

The matrix of the Barail sandstones consist of fibrous laths of a clayey matrix (Fig. 8.1.5) which is probably illite and chlorite as detected by x-ray diffraction which is discussed subsequently in this chapter. The matrix ranges from 10.19 to 16.18%. Silica is the dominant cementing material followed by ferrugenous cements (Figs. 8.1.3 and 8.1.6). The cements range from 3.07 to 7.25%.

The distribution of the various constituents in the vertical section is shown in figure 8.1.7. Their distribution, as seen, is very erratic.

8.1.3. RELATIONSHIPS OF SOME FRAMEWORK CONSTITUENTS :

Three methods of classification of the Barail sandstones are used. Quartz, feldspar and mica+micaceous rock fragments are recalculated to 100 percent and plotted in a ternary diagram (Fig. 8.1.8, Table 8.1.3) following Doty and Hubert (1962). The Barail sandstones, according to this scheme can be termed quartzose graywackes and micaceous quartzites. Following Kukal (1968) recalculated values of quartz,

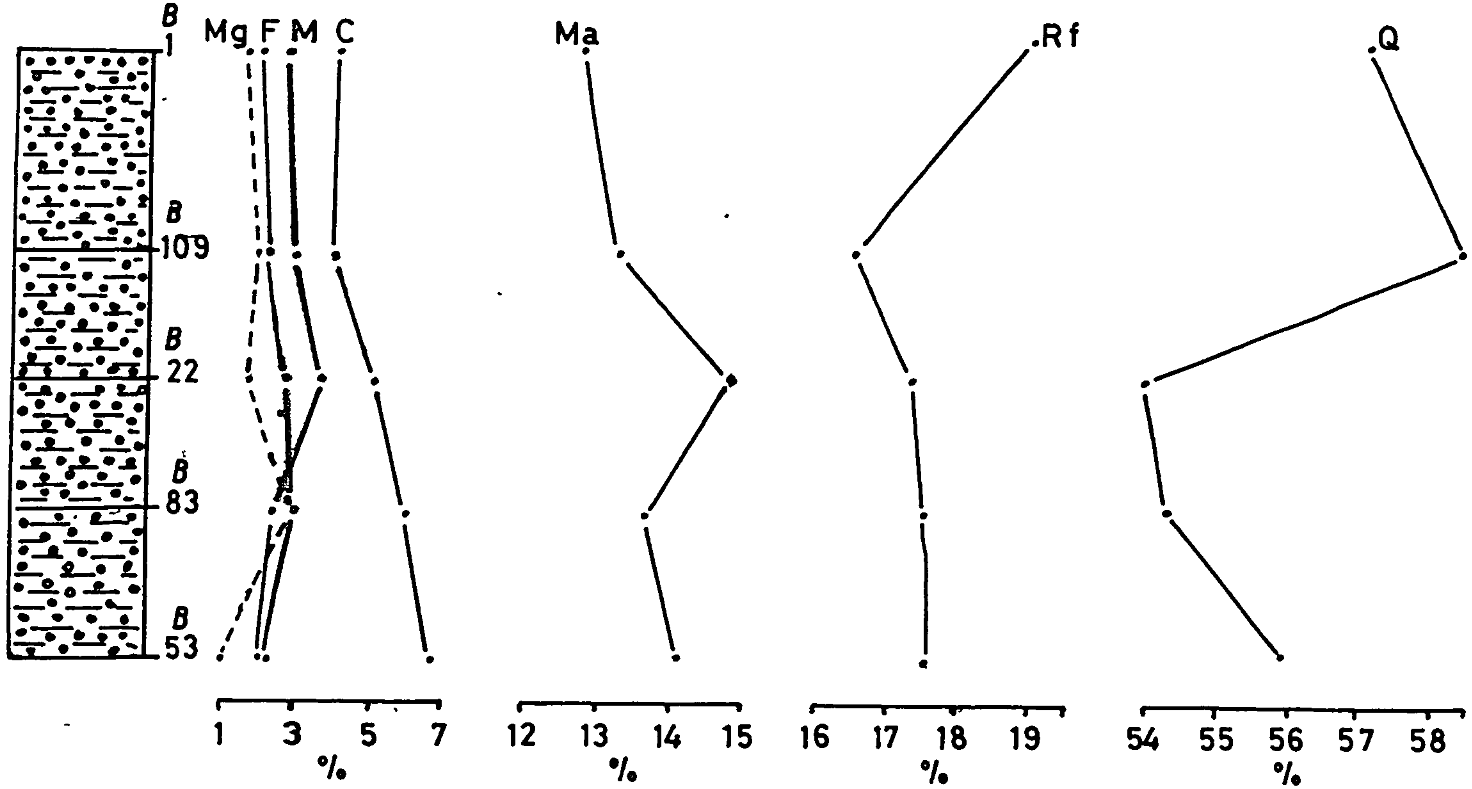

F – Feldspar C – Cement RF – Rock fragments Q – Quartz
M – Mica Ma – Matrix
MG – Miscellaneous grains

FIG: 8·1·7

VERTICAL VARIATION OF MINERAL CONSTITUENTS OF THE BARAIL SANDSTONES

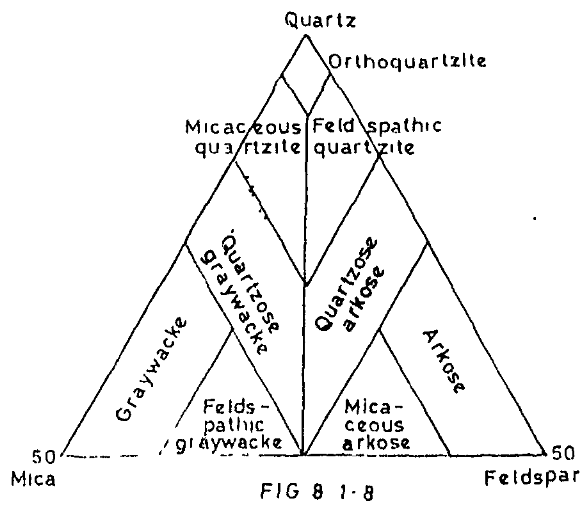

FIG 8 1·8

Mineralogical classification of Barail sandstones

(After Doty & Hubert, 1962)

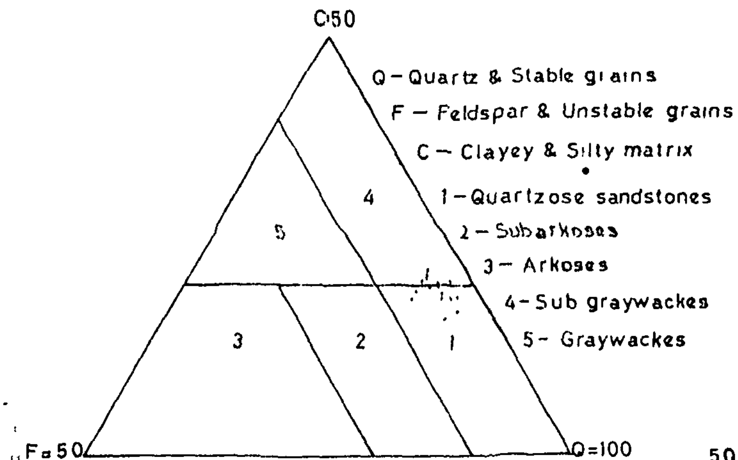

FIG' 8·1·9

Mineralogical classification of Barail sandstones

(After Kukal, 1968)

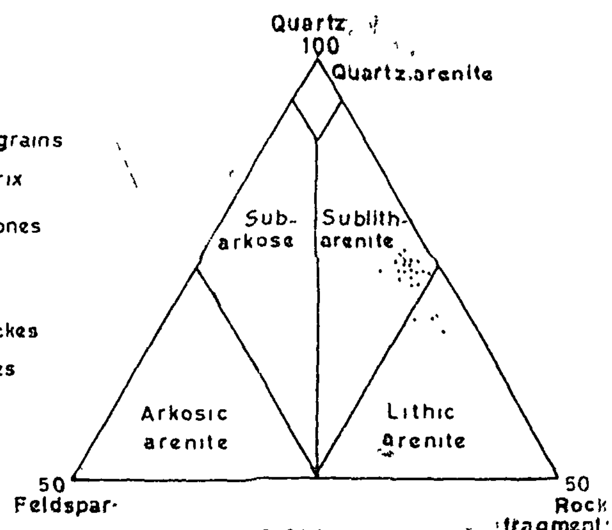

FIG: 8-1-10

Mineralogical classification of Barail sandstone

(After Pettijohn, 1975)

Table 8.1.3

Mineralogical classification of the Barail sandstones.

Sample No.	Q	F	R	Rock type	Q	F	M	Rock type	Q	F	C	Rock type
B 1.	72.79	2.63	24.38	Sublitharenite	79.31	2.86	17.83	Quartzose graywacke	79.34	2.86	17.80	Quartzose sandstone
B 7.	73.76	4.49	21.75	Sublitharenite	79.14	4.82	16.04	Quartzose graywacke	79.67	4.85	15.48	Quartzose sandstone
B 22.	72.69	3.85	23.46	Sublitharenite	77.12	4.08	18.80	Quartzose graywacke	75.28	3.98	20.73	Subgraywacke
B 25.	74.35	2.89	22.75	Sublitharenite	80.11	3.12	16.77	Quartzose graywacke	79.14	3.08	17.78	Quartzose sandstone
B 30.	69.03	3.43	27.54	Lithic arenite	77.51	3.85	18.64	Quartzose graywacke	75.27	3.74	20.99	Subgraywacke
B 32.	74.73	6.54	18.73	Sublitharenite	78.98	6.91	14.10	Micaceous quartzite	75.43	6.60	17.96	Quartzose sandstone
B 39.	68.87	5.19	25.94	Lithic arenite	78.42	5.91	15.68	Quartzose graywacke	75.77	5.71	18.52	Quartzose sandstone
B 45.	74.88	3.16	21.96	Sublitharenite	83.65	3.53	12.82	Micaceous quartzite	82.45	3.48	14.07	Quartzose sandstone
B 49.	67.10	3.12	29.77	Lithic arenite	78.10	6.63	18.27	Quartzose graywacke	73.01	3.40	23.60	Subgraywacke
B 53.	73.72	3.12	23.15	Sublitharenite	83.86	3.55	12.58	Micaceous quartzite	77.23	3.27	19.49	Quartzose sandstone
B 54.	75.77	1.57	22.66	Sublitharenite	85.46	1.77	12.76	Micaceous quartzite	78.96	1.64	19.40	Quartzose sandstone
B 55.	73.47	3.39	23.14	Sublitharenite	80.93	3.73	15.34	Quartzose graywacke	77.36	3.57	19.07	Quartzose sandstone
B 57.	69.05	2.96	27.99	Lithic arenite	78.37	3.36	18.26	Quartzose graywacke	75.23	3.23	21.54	Subgraywacke
B 61.	74.03	1.52	24.45	Sublitharenite	83.64	1.72	14.64	Micaceous quartzite	78.29	1.61	20.10	Subgraywacke
B 69.	76.79	2.81	20.40	Sublitharenite	84.12	3.08	12.71	Micaceous quartzite	79.28	2.91	17.81	Quartzose sandstone
B 83.	72.66	3.86	23.47	Sublitharenite	80.28	4.27	15.45	Quartzose graywacke	76.69	4.08	19.23	Quartzose sandstone
B 92.	75.56	2.65	21.79	Sublitharenite	84.85	2.98	12.16	Micaceous quartzite	79.98	2.81	17.21	Quartzose sandstone
B 96.	78.16	3.02	18.81	Sublitharenite	84.76	3.28	11.96	Micaceous quartzite	77.77	3.01	19.22	Quartzose sandstone
B 99.	75.86	4.13	20.01	Sublitharenite	81.31	4.43	14.26	Micaceous quartzite	75.16	4.09	20.74	Subgraywacke
B 101.	75.12	3.23	21.65	Sublitharenite	82.38	3.54	14.08	Micaceous quartzite	77.44	3.33	19.23	Quartzose sandstone
B 105.	74.52	4.14	21.34	Sublitharenite	76.06	4.23	19.71	Quartzose graywacke	76.28	4.24	19.48	Quartzose sandstone
B 106.	75.93	3.26	20.81	Sublitharenite	81.56	3.50	14.94	Micaceous quartzite	77.10	3.31	19.59	Quartzose sandstone
B 109.	75.47	3.05	21.48	Sublitharenite	79.93	3.23	16.85	Quartzose graywacke	78.81	3.18	18.01	Quartzose sandstone
B 111.	74.11	2.27	23.62	Sublitharenite	82.56	2.53	14.91	Micaceous quartzite	79.19	2.43	18.38	Quartzose sandstone
B 113.	76.99	2.61	20.40	Sublitharenite	82.57	2.80	14.63	Micaceous quartzite	80.68	2.73	16.59	Quartzose sandstone
Average:	76.82	3.32	19.86		81.00	3.63	15.37		77.63	3.49	18.88	

Q - Quartz, F - Feldspar, R - Rock fragments, M - Mica+micaceous rock fragments, C - Matrix feldspar+unstable grains and matrix, plotted in a ternary diagram (Fig. 8.1.9, Table 8.1.3), indicate that the sandstones are quartzose sandstones and subgraywackes. Following Pettijohn (1975), quartz, feldspar and rock fragments, recalculated to 100 percent and plotted in a ternary diagram (Fig. 8.1.10, Table 8. 1.3), indicate that the Barail sandstones are mostly sublitharenites and partly lithic arenites.

The ratios of polycrystalline quartz and feldspar+rock fragments, and total quartz and feldspar+rock fragments are plotted in a binary diagram against each other (Fig. 8.1.11, Table 8.1.4) following Suttner and Dutta (1986) for paleoclimatic studies. Plots indicate a dominantly semi-humid climate. Following Suttner and Dutta (1986) plots of quartz, feldspar and lithic fragments (Fig. 8.1.12, Table 8.1.3) also indicate semi-humid climatic conditions. Plots of the same components (Fig. 8.1.12, Table 8.1.3) following Dickinson et al. (1983) suggest that the Barail sediments are recycled and from an orogenic source.

8.1.4. RATIOS OF SOME FRAMEWORK CONSTITUENTS :

The quartz-feldspar ratio (Pettijohn, 1975) and the quartz-feldspar-rock fragments ratio (Suttner and Dutta, 1986) are used to determine the mineralogical maturity of the Barail sandstones. The quartz-feldspar ratio (Table 8.1.4) ranges from 11.42 to 48.71 and averages 24.85 indicating a moderate maturity. The quartz-feldspar-rock fragments ratio (Table 8.1.3) averages 73.82-3.32-22.86 which also indicates moderate maturity.

8.2. CLAY MINERALOGY

8.2.1. INTRODUCTION :

The importance of clay mineral studies in sedimentology

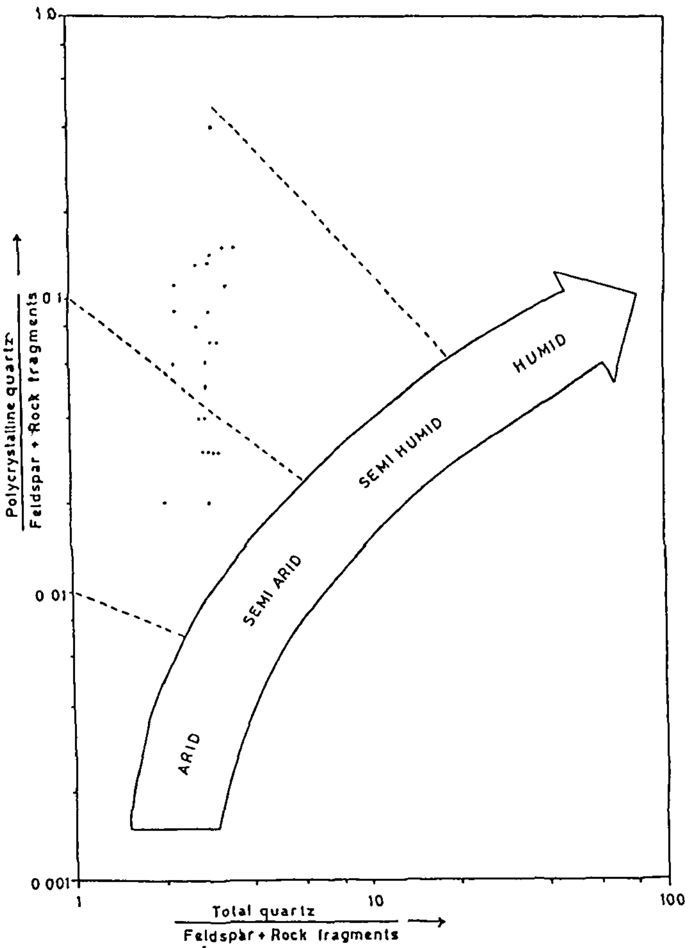

FIG: 8·1·11

Bivariant log-log plots of the ratios of Polycrystalline quartz to Feldspar + Rock fragments and Total quartz to Feldspar + Rock fragments of the sandstones of the Barail Group
(After Suttner and Dutta, 1986)

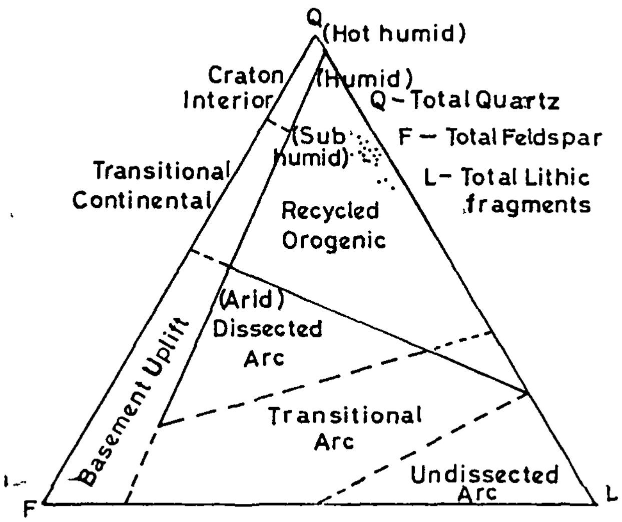

FIG: 8·1·12

QFL Provenance-discrimination diagram of Barail sandstones.
(After Dickinson *et al.*, 1983)

Table 8.1.4

Ratios of some framework constituents of the Barail sandstones.

Sample No.	Polycrystalline quartz / Feldspar + rock fragments	Total quartz / Feldspar + rock fragments	Quartz / Feldspar
B 1.	0.04	2.70	27.75
B 7.	0.06	2.81	16.42
B 22.	0.08	2.66	18.89
B 25.	0.02	2.90	25.69
B 30.	0.09	2.23	20.12
B 32.	0.09	2.96	11.42
B 39.	0.06	2.21	13.28
B 45.	0.14	2.98	23.69
B 49.	0.02	2.04	21.48
B 53.	0.03	2.81	23.59
B 54.	0.03	3.13	48.17
B 55.	0.04	2.77	21.67
B 57.	0.11	2.23	23.29
B 61.	0.05	2.85	48.71
B 69.	0.15	3.31	27.28
B 83.	0.13	2.66	18.81
B 92.	0.46	3.09	28.46
B 96.	0.15	3.58	25.85
B 99.	0.07	3.14	18.37
B 101.	0.07	3.02	23.29
B 105.	0.13	2.92	17.99
B 106.	0.04	3.15	23.32
B 109.	0.03	3.08	24.77
B 111.	0.03	2.86	32.63
B 113.	0.11	3.35	29.53
Average :	0.09	2.86	24.85

is well documented. Clay minerals throw light on the provenance of sediments and the diagenetic changes they go through. A discussion on these aspects is provided for in chapter 4. The clay minerals present in the Barail sandstones are detected by semi-quantitative analysis of eight representative samples. The laboratory techniques of analysis are described in chapter 3.

8.2.2. MINERALOGY :

The Barail sandstones contain only two clay minerals - illite and chlorite (Fig. 8.2, Table 8.2). These minerals are found in small amounts and more or less evenly distributed in the different lithounits.

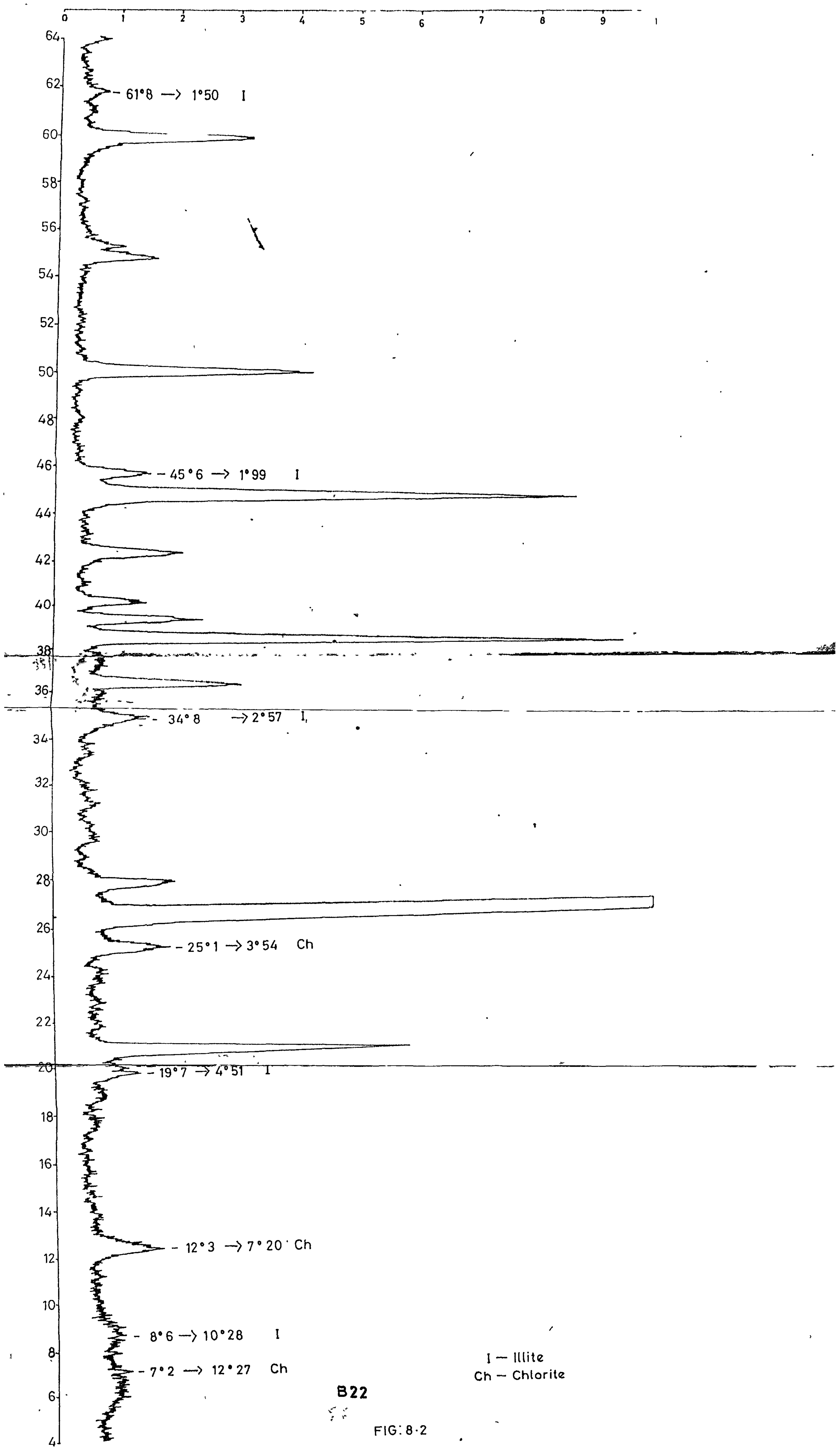

61°8 —> 1°50 I
45°6 —> 1°99 I
34°8 —> 2°57 I
25°1 —> 3°54 Ch
19°7 —> 4°51 I
12°3 —> 7°20 Ch
8°6 —> 10°28 I
7°2 —> 12°27 Ch
I — Illite
Ch — Chlorite
B22

FIG: 8·2

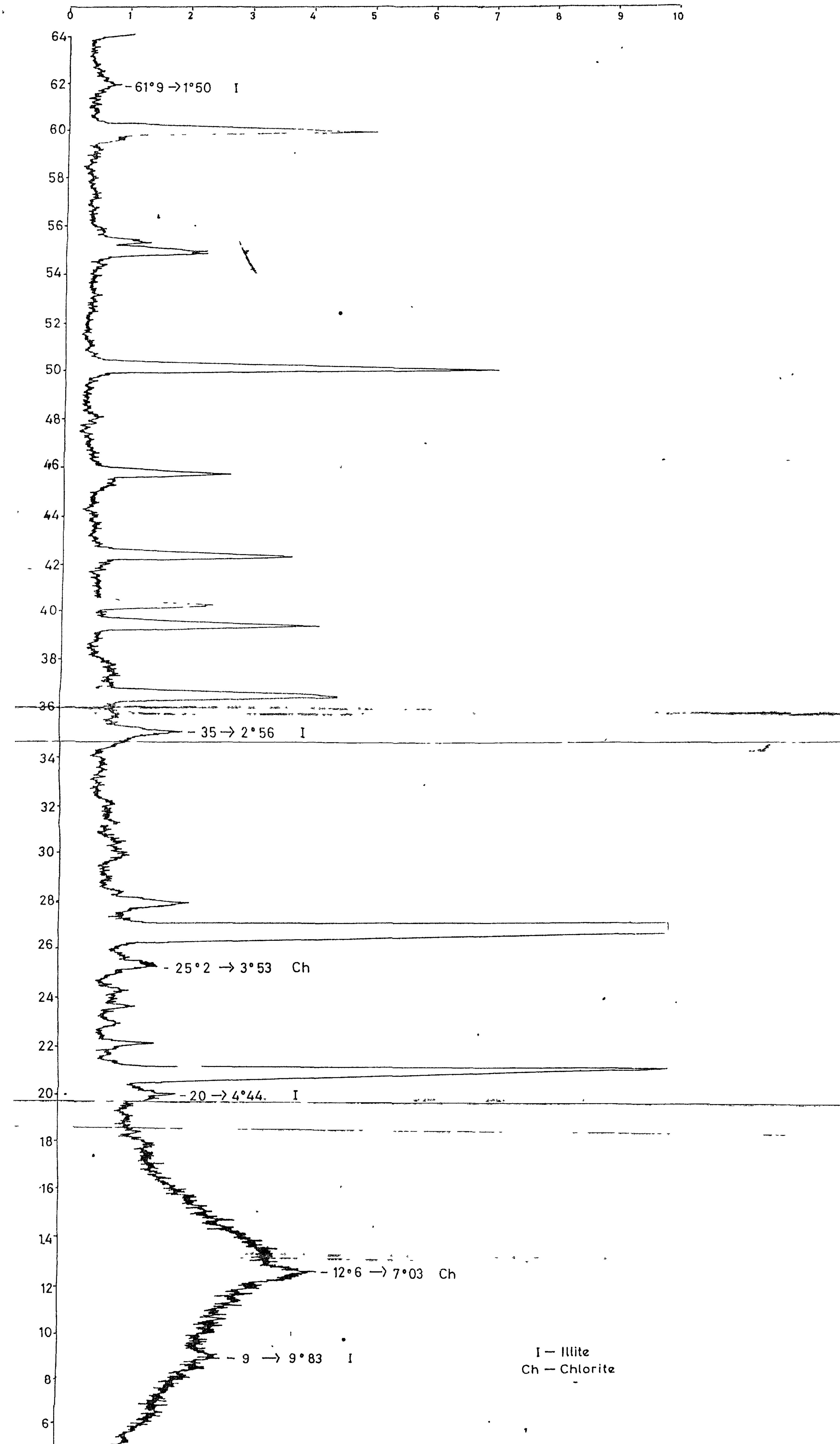

0 1 2 3 4 5 6 7 8 9 10
64 62 60 58 56 54 52 50 48 46 44 42 40 38 36 34 32 30 28 26 24 22 20 18 16 14 12 10 8 6 4
- 61°9 → 1°50 I
- 35 → 2°56 I
- 25°2 → 3°53 Ch
- 20 → 4°44. I
- 12°6 → 7°03 Ch
- 9 → 9°83 I
I — Illite
Ch — Chlorite

B 109
FIG. 8·2

Table 8.2

Clay minerals in the sandstones of the Barail Group.

Sample No.	Constituents detected						
	Major	Minor	Good amount	Considerable amount	Small amount	Trace	Trace likely
B 1.	-	-	-	-	Chlorite Illite	-	-
B 22.	-	-	-	-	Chlorite Illite	-	-
B 34.	-	-	-	Chlorite	Illite	-	-
B 53.	-	-	-	-	Chlorite Illite	-	-
B 65.	-	-	-	-	Chlorite Illite	-	-
B 83.	-	-	-	-	Chlorite Illite	-	-
B 92.	-	-	-	-	Illite	Chlorite	-
B 109.	-	-	-	-	Chlorite Illite	-	-

CHAPTER 9

SIZE ANALYSIS

9.1. INTRODUCTION :

An important property of clastic rocks is their grain size which bear a fundamental relationship with the physical forces of transportation and deposition of sediments. There is a certain correlation of grain size with the depositional environments of sediments and it is possible to decipher the nature of the depositional processes by studying the statistical parameters of grain size. A discussion of the above is made in chapter 5 and the methodology adopted is described in chapter 3. Twenty sandstone samples of the Barail Group are analysed for grain size studies (Table 9.1).

A differentiation of the depositional environments of the sediments of the Barail Group is made from interrelationships between the textural parameters (Friedman, 1961; Sahu, 1964; Moiola and Weiser, 1968). The modes of transportation of the sediments and their deposition are established following Visher (1969). A study of CM patterns and FM, LM and AM diagrams is made to distinguish the transportational processes of the sediments (Passega, 1957, 1964; Passega and Byramjee, 1969).

9.2. CUMULATIVE CURVES AND TEXTURAL PARAMETERS :

The Barail sandstones are characterised by both bimodal and polymodal cumulative curves (Fig. 9.1). The grain size curves show two populations - saltation and suspension (Fig. 9.2, Table 9.2). The saltation population, constituting 18 to 80% of the total population distribution with an average of 40%, shows good

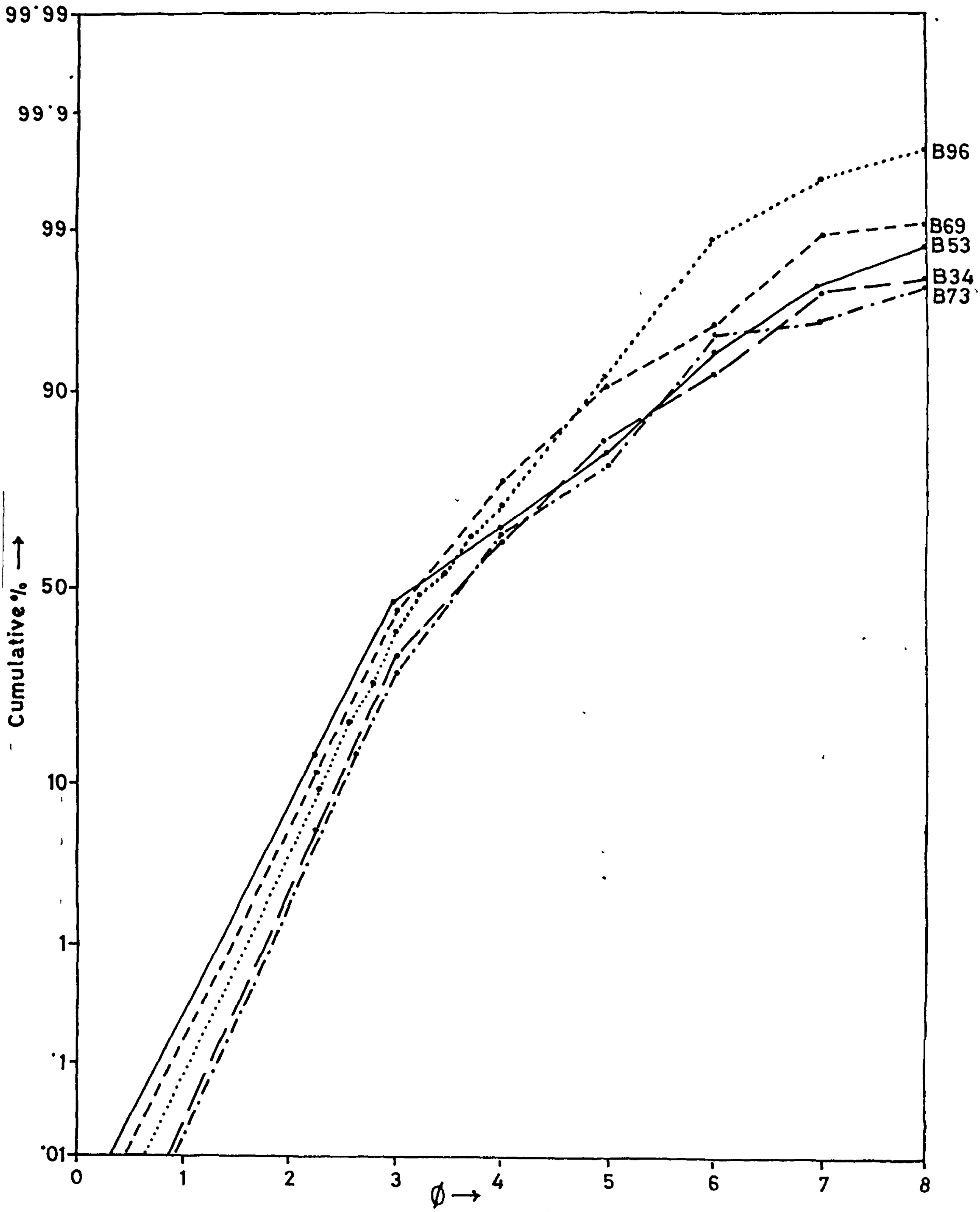

FIG. 9·1

Cumulative curves of Barail Sandstones

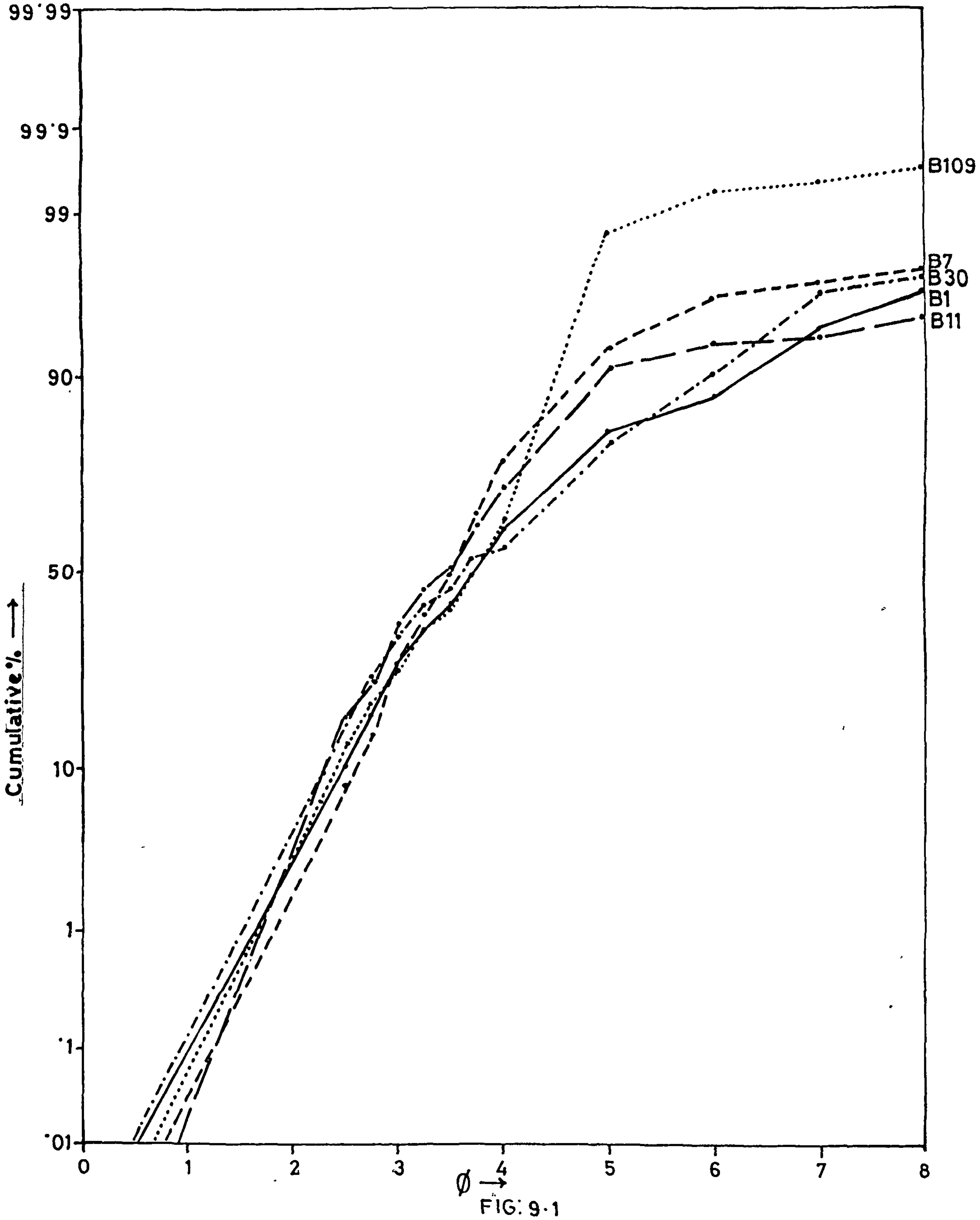

FIG. 9·1

Cumulative curves of Barail Sandstones

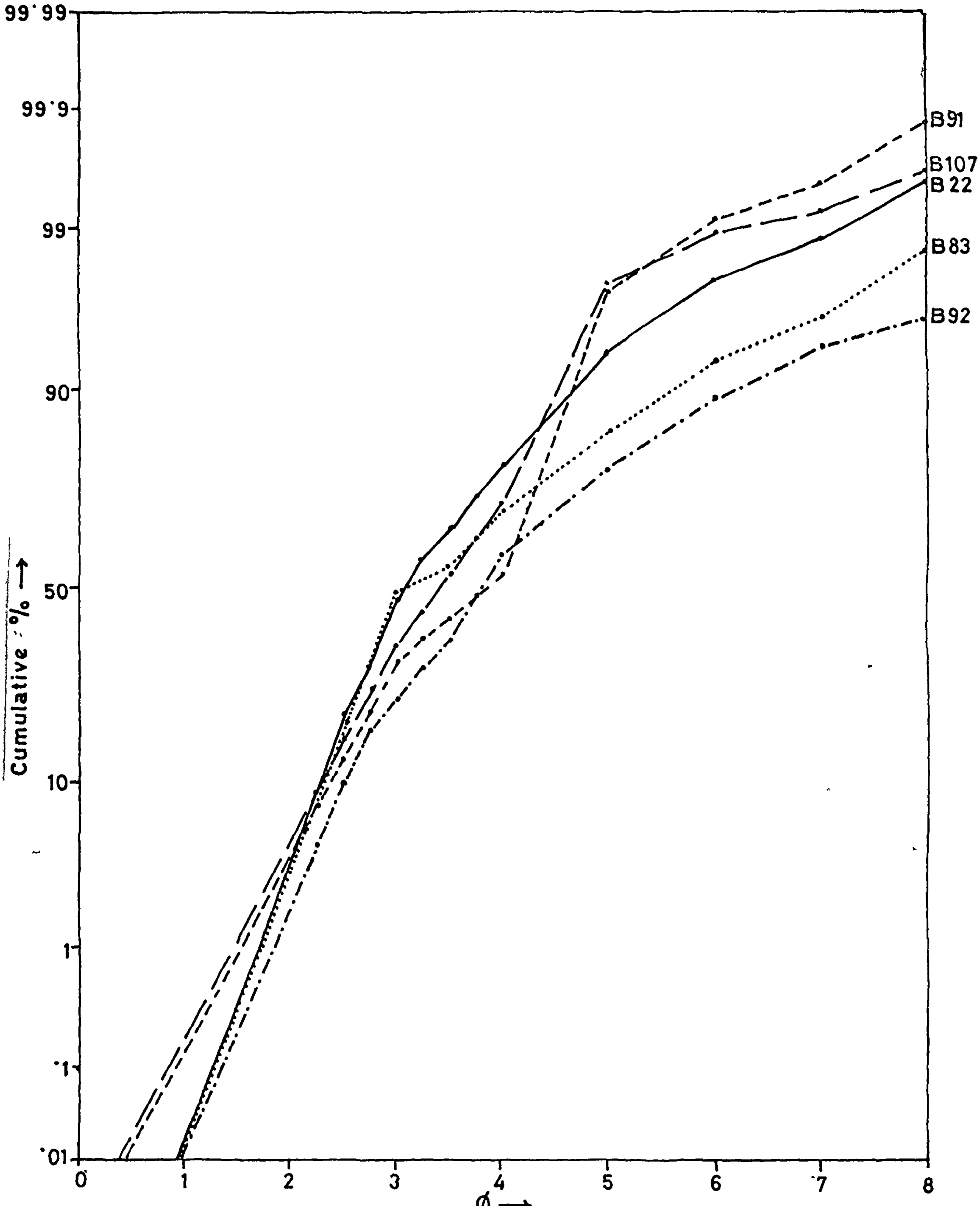

FIG: 9·1

Cumulative curves of Barall sandstones

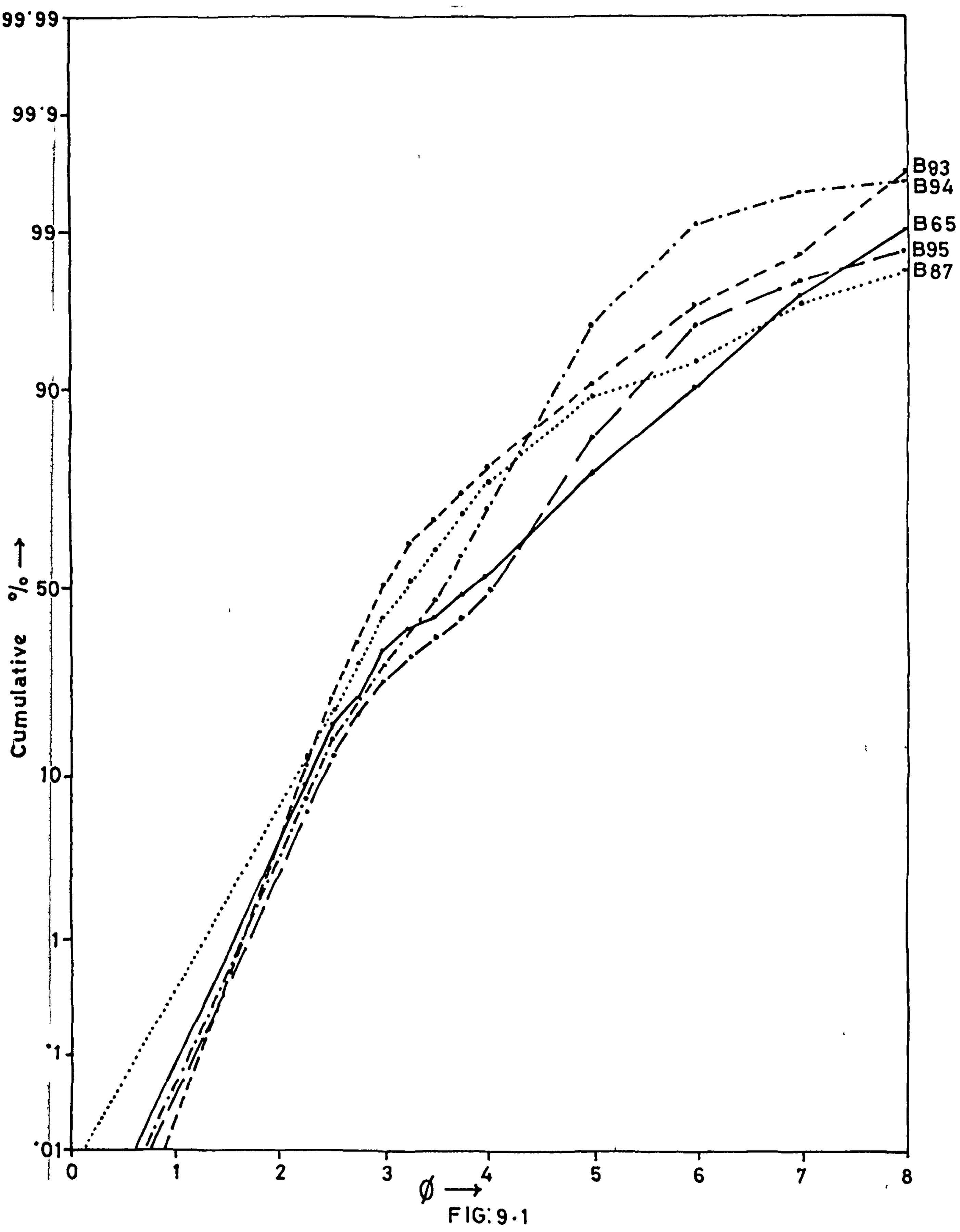

FIG. 9·1

Cumulative curves of Barail sandstones

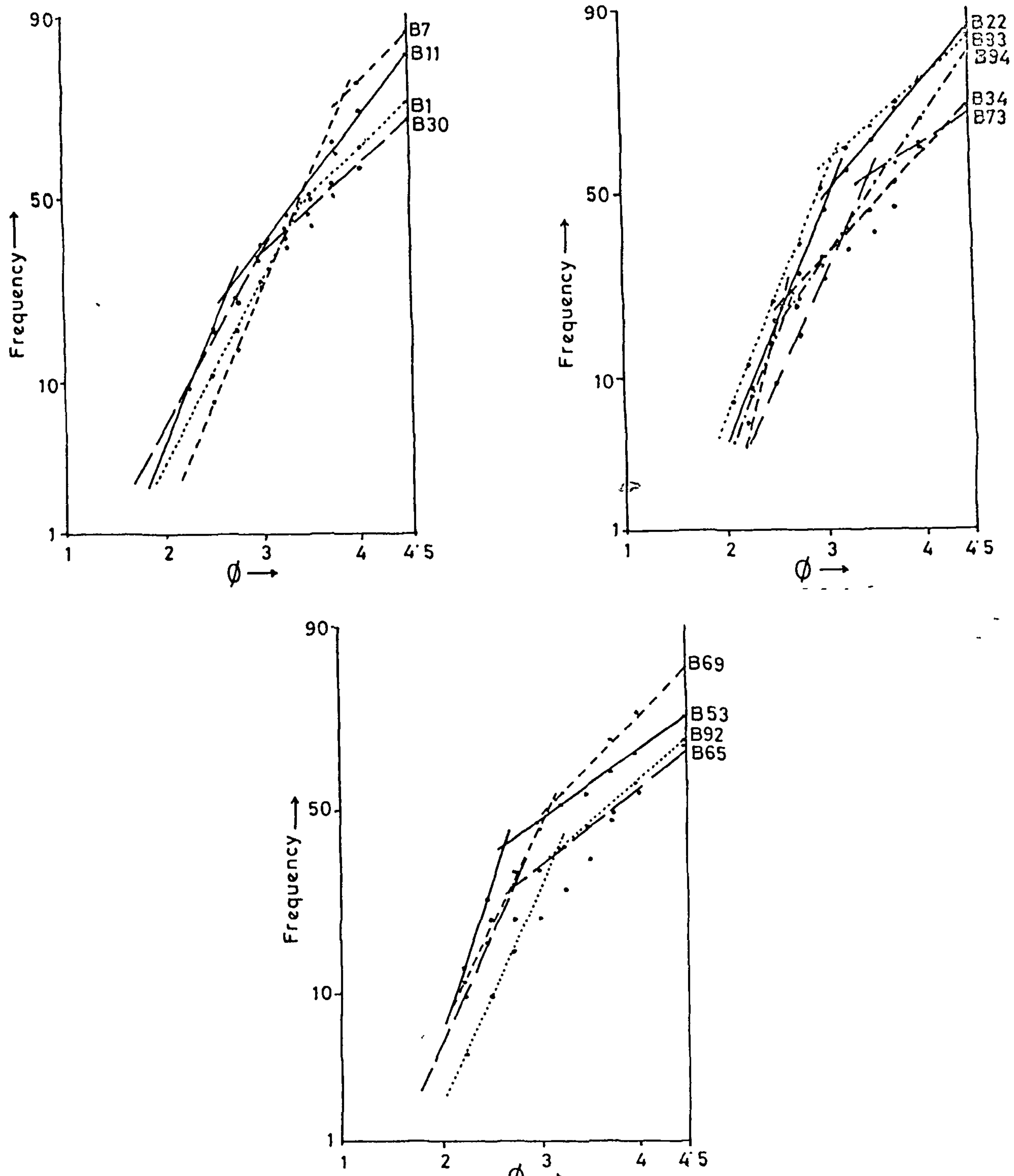

FIG: 9 .2
Relation of Sediment transport to
Grainsize distribution in Barail sandstones
(After Visher, 1969)

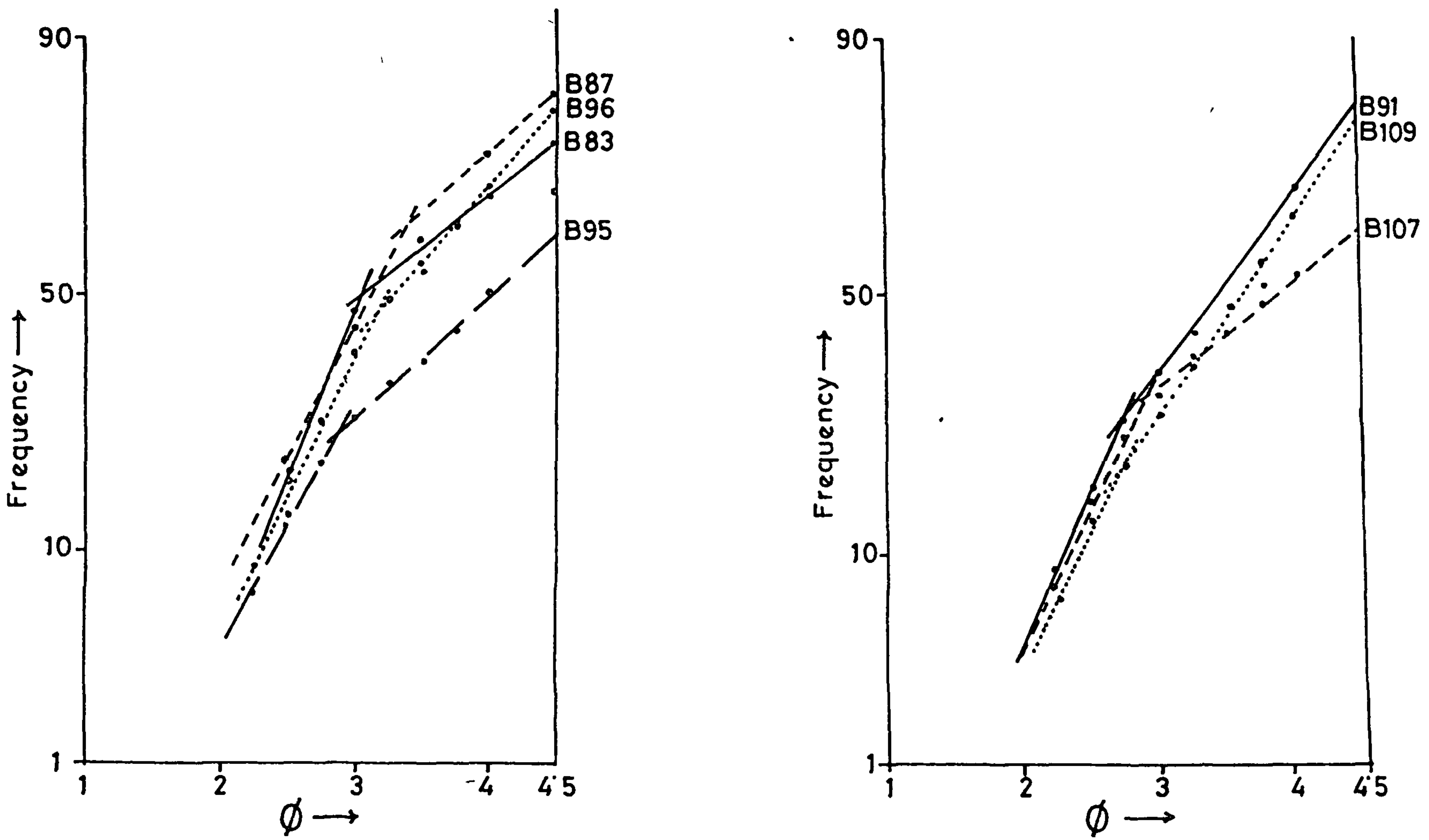

FIG: 9·2
Relation of Sediment transport to
Grainsize distribution in Barail sandstones
(After Visher, 1969)

Table 9.1

Cumulative weight percentage of the Barail sandstones.

Sample No.	Phi scale												
	2.25	2.50	2.75	3.00	3.25	3.50	3.75	4.00	5.00	6.00	7.00	8.00	9.00
B 1.	-	10.23	17.19	27.15	34.75	41.30	49.85	63.08	83.10	88.73	94.93	96.90	99.98
B 7.	-	7.92	14.07	26.95	38.04	49.29	65.33	78.45	93.14	96.58	97.10	97.60	99.96
B 11.	9.33	17.94	23.35	36.11	44.93	50.75	62.56	73.33	91.64	93.94	94.52	95.38	99.96
B 22.	8.94	19.10	28.96	46.14	57.33	64.28	72.11	77.92	93.23	97.52	98.66	99.53	99.96
B 30.	9.28	17.23	24.07	33.22	40.21	45.23	54.19	58.38	81.40	91.03	96.73	97.45	99.98
B 34.	5.51	15.05	21.79	32.25	39.76	44.46	53.51	62.83	83.26	91.94	97.14	97.80	99.96
B 53.	13.36	26.49	32.59	46.33	51.64	54.88	60.79	66.10	81.41	93.73	97.37	98.58	99.96
B 65.	9.45	17.80	22.51	33.54	39.45	42.48	48.81	54.79	77.78	90.48	97.05	99.09	99.96
B 69.	11.28	22.11	29.19	43.98	54.37	54.14	69.01	75.68	90.51	95.25	98.81	99.05	99.97
B 73.	-	9.43	16.59	28.40	34.37	38.94	46.03	64.30	78.90	94.91	95.66	97.36	99.96
B 83.	-	18.52	-	47.01	-	55.00	-	69.64	84.62	92.97	95.82	98.48	99.97
B 87.	-	20.33	-	42.75	-	60.12	-	76.00	89.81	93.08	96.89	98.16	99.97
B 91.	8.94	17.21	27.60	35.28	43.28	48.03	56.80	70.91	97.28	99.14	99.53	99.87	99.98
B 92.	4.62	9.77	16.07	22.44	29.56	35.53	46.50	58.47	77.55	88.74	93.61	95.55	99.95
B 93.	11.74	23.28	35.71	51.50	61.97	67.30	73.24	78.30	90.81	96.69	98.52	99.66	99.95
B 94.	7.75	15.27	22.61	30.87	39.78	46.66	58.24	70.07	95.48	99.12	99.51	99.61	99.97
B 95.	6.63	13.15	19.62	26.11	31.76	36.16	41.89	49.55	83.68	95.72	97.60	98.63	99.96
B 96.	8.94	17.78	25.88	37.54	48.34	55.53	63.70	69.98	90.75	98.69	99.53	99.75	99.97
B 107.	7.68	15.16	21.78	30.32	37.23	41.33	47.45	53.97	97.44	98.93	99.28	99.63	99.97
B 109.	6.62	13.00	19.30	27.67	35.08	41.40	50.25	64.69	97.60	99.33	99.46	99.59	99.96

Table 9.2

Populations of the sandstones of the Barail Group.

Sample No.	Saltation			Suspension			
	Per-Cent	Sorting	F.T. Point	Per-cent	Sorting	Mixing A&B	F.T. Point
B 1.	47	Good	3.45	53	Poor	Much	>4.5
B 7.	80	Good	3.90	20	Poor	Much	>4.5
B 11.	25	Good	2.65	75	Fair	Much	>4.5
B 22.	53	Good	3.15	47	Fair	Little	>4.5
B 30.	35	Good	3.05	65	Poor	Little	>4.5
B 34.	23	Excellent	2.60	77	Poor	Much	>4.5
B 53.	40	Excellent	2.67	60	Poor	Much	>4.5
B 65.	29	Good	2.76	71	Poor	Much	>4.5
B 69.	51	Good	3.10	49	Poor	Average	>4.5
B 73.	54	Good	3.46	46	Poor	Much	>4.5
B 83.	50	Good	3.05	50	Poor	Much	>4.5
B 87.	62	Good	3.36	38	Poor	Much	>4.5
B 91.	27	Good	2.73	73	Fair	Average	>4.5
B 92.	38	Good	3.18	62	Poor	Much	>4.5
B 93.	59	Good	3.12	41	Poor	Little	>4.5
B 94.	18	Good	2.56	82	Fair	Little	>4.5
B 95.	23	Good	2.85	77	Poor	Little	>4.5
B 96.	44	Good	3.12	66	Poor	Little	>4.5
B 107.	30	Good	2.86	70	Poor	Much	>4.5
B 109.	20	Good	2.75	80	Fair	Average	>4.5
Average :	40		3.02	60			>4.5

sorting. This population is truncated on the finer side between limits of 2.56 and 3.90 Ø, and averages 3.02 Ø. The suspension population is poorly to fairly sorted and ranges from 20 to 80% with an average of 60%. The curves indicate much mixing between the two populations.

The percentile values are graphically obtained (Table 9.3) from which the statistical parameters are calculated. The Barail sandstones have a mean size (M_z) ranging from 3.233 Ø (0.1066 mm) to 4.013 Ø (0.0621 mm) and averaging 3.600 Ø (0.0825 mm), standard deviation (δ_i) from 0.815 to 1.496 Ø, the average of which is 1.151 Ø, skewness (Sk_i) from -0.323 to 0.481 Ø, averaging 0.201 Ø and kurtosis (K_g) ranging from 0.777 to 1.700 Ø with an average of 1.075 Ø (Table 9.4).

These sandstones are made up of very fine sands and are poorly to moderately sorted. They are coarse to finely skewed and dominantly leptokurtic but with a range from mesokurtic to platykurtic. The vertical distribution of mean size, standard deviation, skewness and kurtosis values is shown in figure 9.3 where an irregular pattern is seen.

9.3. DISCRIMINANT FUNCTION :

Sahu (1964) successfully used certain relations, such as discussed in chapter 5, to discriminate among aeolian, beach, shallow marine and fluviatile environments of deposition and between transporting processes such as fluvial and turbidity. Utilising these discriminant functions shallow agitated marine and fluvial environments of deposition are indicated for the Barail sandstones, the transporting processes for which are turbidity and fluvial (Table 9.5).

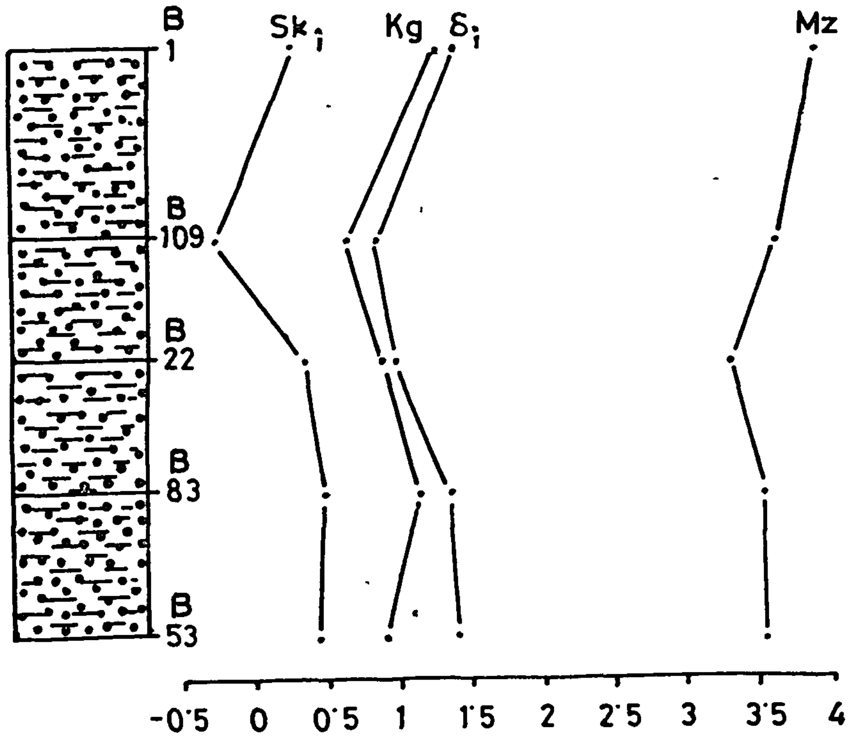

FIG: 9·3

VERTICAL VARIATION OF TEXTURAL PARAMETERS OF THE BARAIL SANDSTONES

Table 9.3

Percentile values, CM values (in microns) and values finer than 125(F), 31(L) and 4(A)μ of the sandstones of the Barail Group.

Sample No.	P_1	P_5	P_{16}	P_{25}	P_{50}	P_{75}	P_{84}	P_{95}	$C=P_1$	$M=P_{50}$	F	L	A
B 1.	1.65	2.18	2.69	2.94	3.68	4.50	5.10	7.00	3186	780	72.83	16.88	3.08
B 7.	1.92	2.36	2.80	3.00	3.38	3.90	4.28	5.40	2643	960	73.01	6.82	2.36
B 11.	1.50	2.00	2.52	2.74	3.32	4.09	4.42	7.60	3536	1001	63.85	8.32	4.58
B 22.	1.71	2.05	2.43	2.66	3.08	3.86	4.30	5.30	3057	1183	53.82	6.73	0.43
B 30.	1.49	2.02	2.57	2.81	3.69	4.71	5.22	6.55	3560	775	66.76	18.58	2.53
B 34.	1.77	2.21	2.66	2.86	3.50	4.50	5.05	6.50	2932	884	67.71	16.70	2.16
B 53.	1.34	1.84	2.31	2.55	3.14	4.60	5.19	6.29	3950	1134	53.63	18.55	1.38
B 65.	1.56	2.02	2.46	2.82	3.80	4.90	5.39	6.60	3392	718	66.42	22.18	0.87
B 69.	1.46	1.94	2.41	2.64	3.14	4.01	4.46	5.95	3635	1134	55.99	9.46	0.92
B 73.	1.84	2.29	2.72	2.94	3.62	4.75	5.28	6.20	2793	813	71.56	21.06	2.60
B 83.	1.62	2.05	2.44	2.64	3.15	4.33	4.96	6.70	3253	1127	52.96	15.34	1.49
B 87.	1.41	1.85	2.36	2.63	3.20	3.96	4.52	6.50	3763	1088	57.22	10.16	1.81
B 91.	1.47	2.00	2.52	2.79	3.41	4.10	4.31	4.77	3610	941	64.70	2.70	0.11
B 92.	1.85	2.28	2.74	3.10	3.80	4.83	5.50	7.60	2774	718	77.51	22.40	4.40
B 93.	1.62	2.00	2.35	2.53	2.98	3.81	4.37	5.64	3253	1267	48.45	9.14	0.29
B 94.	1.66	2.10	2.54	2.83	3.56	4.12	4.38	4.95	3164	848	69.10	4.49	0.36
B 95.	1.67	2.15	2.61	2.95	4.02	4.64	5.02	5.90	3143	616	73.85	16.28	1.33
B 96.	1.70	2.06	2.48	2.72	3.30	4.20	4.57	5.40	3078	1015	62.43	9.22	0.22
B 107.	1.54	2.09	2.61	2.88	3.88	4.33	4.50	4.84	3439	679	69.65	2.53	0.34
B 109.	1.70	2.14	2.64	2.93	3.75	4.19	4.35	4.70	3078	743	72.29	1.36	0.37
Average :	1.62	2.08	2.54	2.80	3.47	4.32	4.76	6.02	3262	921	64.69	11.94	1.58

Table 9.4

Statistical measures and verbal classification of the sandstones of the Barail Group.

Sample No.	Mean size		Standard deviation		Skewness		Kurtosis	
B 1.	3.873	VFS	1.345	MS	0.237	FS	1.242	Lk
B 7.	3.487	VFS	0.831	MS	0.272	FS	1.384	Lk
B 11.	3.420	VFS	1.323	MS	0.343	VFS	1.700	VLk
B 22.	3.270	VFS	0.959	MS	0.335	VFS	1.110	Lk
B 30.	3.827	VFS	1.349	MS	0.209	FS	0.907	Mk
B 34.	3.737	VFS	1.247	MS	0.348	VFS	1.072	Mk
B 53.	3.547	VFS	1.394	MS	0.420	VFS	0.890	Pk
B 65.	3.883	VFS	1.426	PS	0.154	FS	0.902	Mk
B 69.	3.337	VFS	1.120	MS	0.345	VFS	1.199	Lk
B 73.	3.873	VFS	1.232	MS	0.308	VFS	0.885	Pk
B 83.	3.517	VFS	1.334	MS	0.481	VFS	1.127	Lk
B 87.	3.360	VFS	1.244	MS	0.335	VFS	1.433	Lk
B 91.	3.413	VFS	0.867	MS	-0.006	NS	0.867	Pk
B 92.	4.013	Si	1.496	PS	0.330	VFS	1.260	Lk
B 93.	3.233	VFS	1.056	MS	0.419	VFS	1.165	Lk
B 94.	3.643	VFS	0.892	MS	-0.066	NS	0.905	Mk
B 95.	3.883	VFS	1.171	MS	-0.084	NS	0.909	Mk
B 96.	3.450	VFS	1.028	MS	0.237	FS	0.925	Mk
B 107.	3.663	VFS	0.889	MS	-0.323	CS	0.777	Pk
B 109.	3.580	VFS	0.815	MS	-0.278	CS	0.833	Pk
Average	3.600		1.151		0.201		1.075	

VFS - very fine sand
Si - silt
MS - moderately sorted
PS - poorly sorted

VFS - very finely skewed
FS - finely skewed
NS - near symmetrical
CS - coarsely skewed

Pk - platykurtic
Mk - mesokurtic
Lk - leptokurtic
VLk - very leptokurtic

Table 9.5

Environments of deposition of the sandstones of the Barail Group as obtained by discriminant function analyses.

Sample No.	1st relation	2nd relation	3rd relation
B 1.	Shallow agitated marine	Fluvial	Fluvial
B 7.	Shallow agitated marine	Shallow marine	Fluvial
B 11.	Shallow agitated marine	Fluvial	Fluvial
B 22.	Shallow agitated marine	Fluvial	Fluvial
B 30.	Shallow agitated marine	Fluvial	Turbidity
B 34.	Shallow agitated marine	Fluvial	Fluvial
B 53.	Shallow agitated marine	Fluvial	Turbidity
B 65.	Shallow agitated marine	Fluvial	turbidity
B 69.	Shallow agitated marine	Fluvial	Fluvial
B 73.	Shallow agitated marine	Fluvial	Turbidity
B 83.	Shallow agitated marine	Fluvial	Fluvial
B 87.	Shallow agitated marine	Fluvial	Fluvial
B 91.	Shallow agitated marine	Shallow marine	Turbidity
B 92.	Shallow agitated marine	Fluvial	Fluvial
B 93.	Shallow agitated marine	Fluvial	Fluvial
B 94.	Shallow agitated marine	Shallow marine	Turbidity
B 95.	Shallow agitated marine	Fluvial	Turbidity
B 96.	Shallow agitated marine	Fluvial	Turbidity
B 107.	Shallow agitated marine	Shallow marine	Turbidity
B 109.	Shallow agitated marine	Shallow marine	Turbidity

Note : The first, second and third relations of the table correspond to the second, third and fourth relations of Sahu (1964) respectively.

9.4. SCATTER PLOTS OF TEXTURAL PARAMETERS :

Interrelationships of the different textural parameters are studied to get an idea of the trends shown by them and to determine the environments of deposition of the Barail sandstones.

Mean size Vs standard deviation :

The sorting coefficient is strongly dependent upon the mean size (Krumbein and Aberdeen, 1937; Inman, 1949; Emery and Stevenson, 1950; Griffiths, 1951) and their interrelationship gives some idea of the depositional environments (Inman, 1949). A differentiation of river environment from those of inland dune and mixed environments is made for the Barail sandstones by plotting mean size against standard deviation on a quarter phi scale (Fig. 9.4.1) following Friedman (1961). A distinction is also made between coastal dune and river (Fig. 9.4.2) and beach and river environments (Fig. 9.4.3) following Moiola and Weiser (1968). A river environment of deposition is indicated.

The two parameters are also plotted following Folk and Ward (1957) where, in case of the Barail sandstones, only one limb of the V-shaped pattern is developed (Fig. 9.4.4). The plots indicate that with a decrease in mean size the value of standard deviation increases, indicating poorer sorting with increasing fineness of sediments.

Skewness Vs standard deviation :

These parameters are plotted against each other to effectively differentiate between river and beach environments (Friedman, 1961; Moiola and Weiser, 1968). The points of these sandstones fall in the area of river environment (Figs. 9.5.1 and 9.5.2).

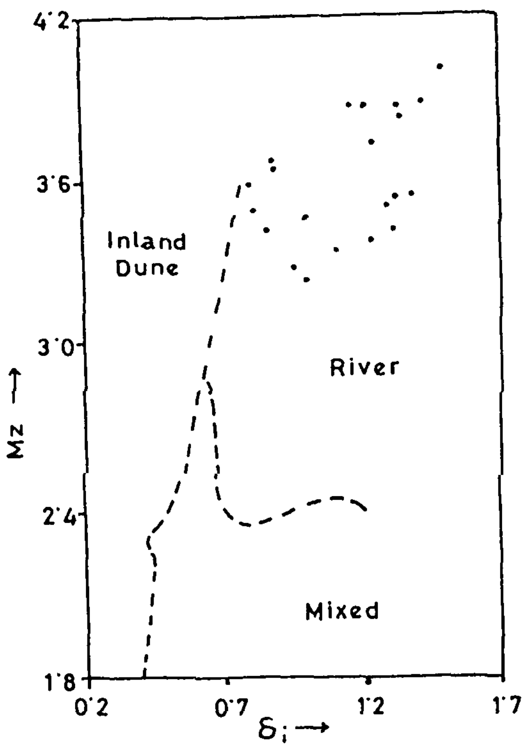

FIG: 9·4·1
Combination plots of Mean size Vs. Standard deviation of Barail sandstones
(After Friedman, 1961)

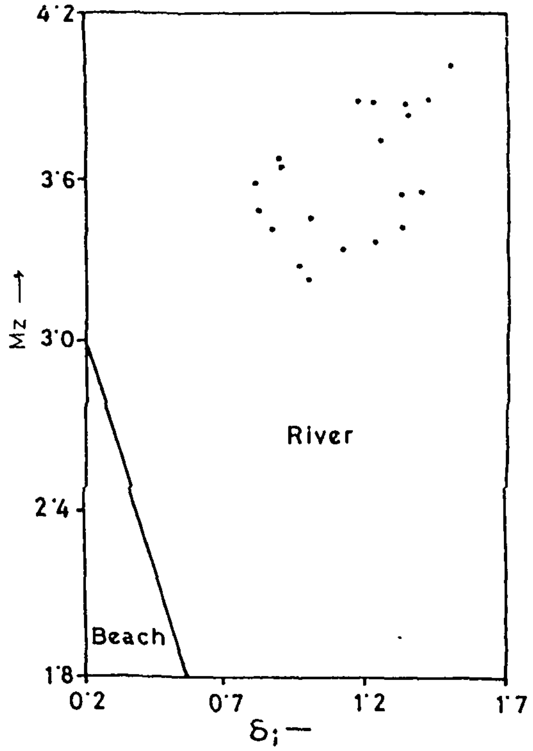

FIG: 9·4·3
Combination plots of Mean size Vs. Standard deviation of Barail sandstones
(After Moiola & Weiser, 1968)

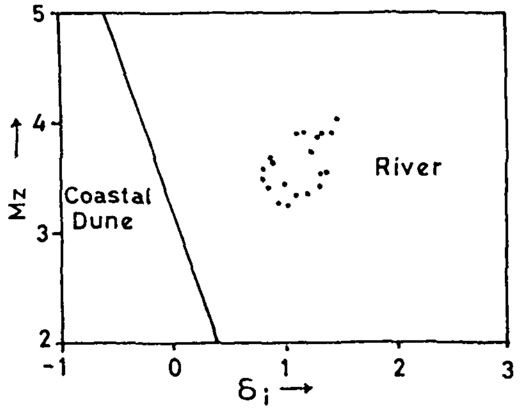

FIG: 9·4·2
Combination plots of Mean size Vs. Standard deviation of Barail sandstones
(After Moiola & Weiser, 1968)

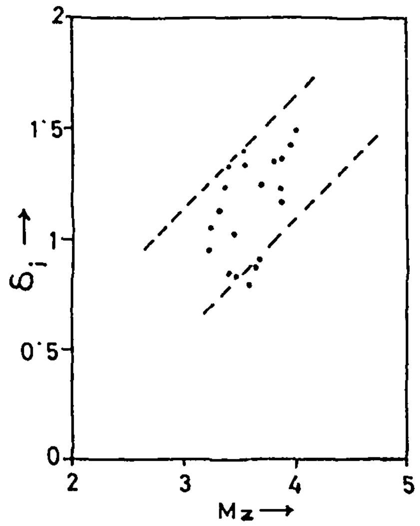

FIG: 9·4·4
Combination plots of Standard deviation Vs. Mean size of Barail sandstones
(After Folk & Ward, 1957)

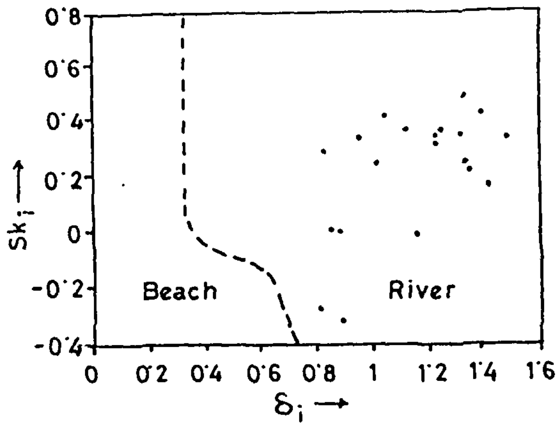

FIG: 9·5·1
Combination plots of Skewness Vs. Standard deviation of Barail sandstones (After Friedman, 1961)

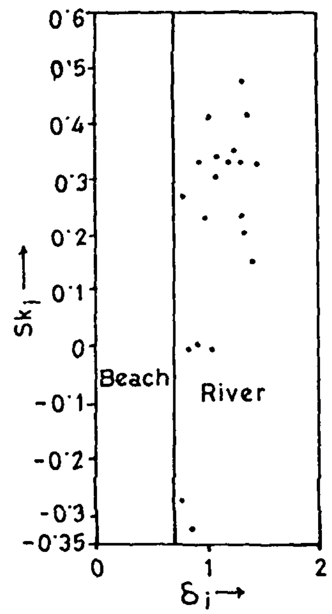

FIG: 9·5·2
Combination plots of Skewness Vs Standard deviation of Barail sandstones (After Moiola & Weiser, 1968)

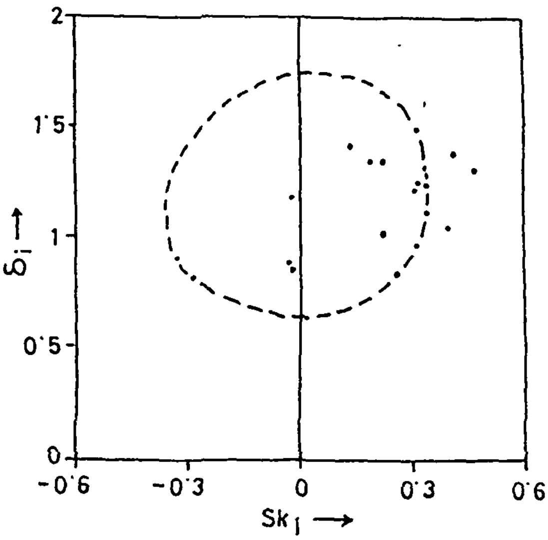

FIG: 9·5·3
Combination plots of Standard deviation Vs. Skewness of Barail sandstones (After Folk & Ward, 1957)

Sorting and skewness are both functions of mean size and thus bear a mathematical relationship with each other (Folk and Ward, 1957). These variables, plotted following Folk and Ward (1957), form a circle with most points falling to the right of the normal line of skewness (Fig. 9.5.3). The points falling on the left of the normal represent the negatively skewed sediments while the rest are near symmetrical to finely skewed. The scattering of plots indicate some variation in proportion of sand and silt modes.

Mean size Vs skewness :

The two parameters are plotted against each other for differentiation of river from beach environments following Friedman (1961). Most of the plots point to a river environment of deposition (Fig. 9.6.1).

Hough (1942) noted that sediments are more skewed with increasing fineness which is supported by Inman (1949). However, Pettijohn (1975) is of the opinion that this relationship may be slightly different in case of finer sediments. In bimodal sediments skewness is a function of grain size where the negative skewness is due to the dominance of a finer mode while the positive skewness is because of a coarser mode (Folk and Ward, 1957). The plots between these two parameters indicate a mixture of sand and silt modes and show that skewness values fall with decreasing mean size (Fig. 9.6.2).

Skewness Vs Kurtosis :

Scatter plots of skewness and kurtosis of the Barail sandstones, following the interrelationship of Friedman (1961), are shown in figure 9.7.1. Friedman assigned the "O-O"

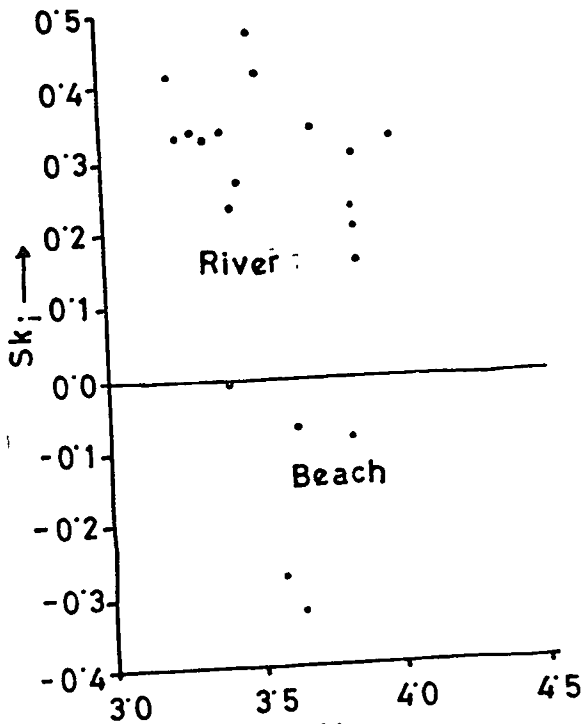

FIG. 9·6·1
Bivariate plots of Mean size Vs. Skewness of the Barail sandstones (After Friedman, 1961)

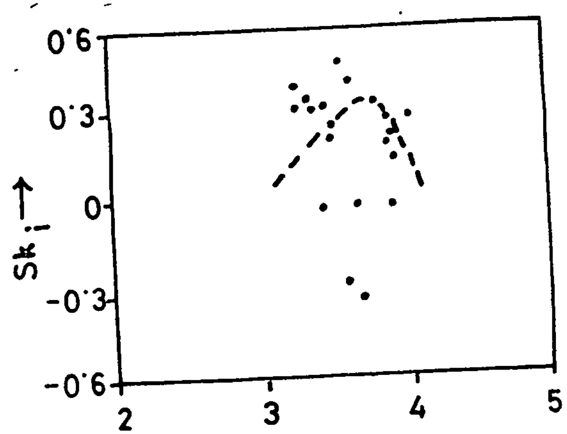

FIG. 9·6·2
Combination plots of Skewness Vs. Mean size of Barail sandstones (After Folk & Ward, 1957)

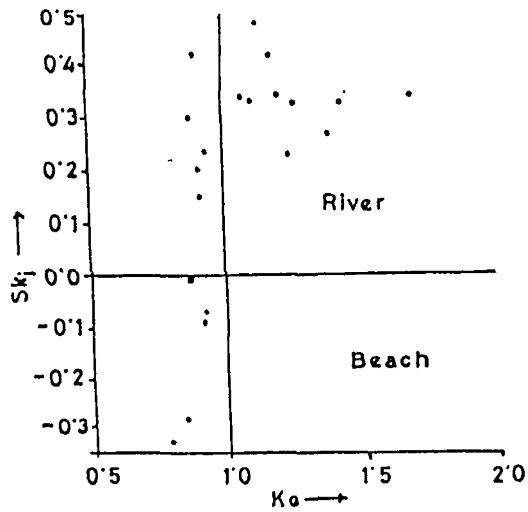

FIG: 9·7·1
Bivariate plots between Skewness and Kurtosis of the Barail sandstones (After Friedman, 1961)

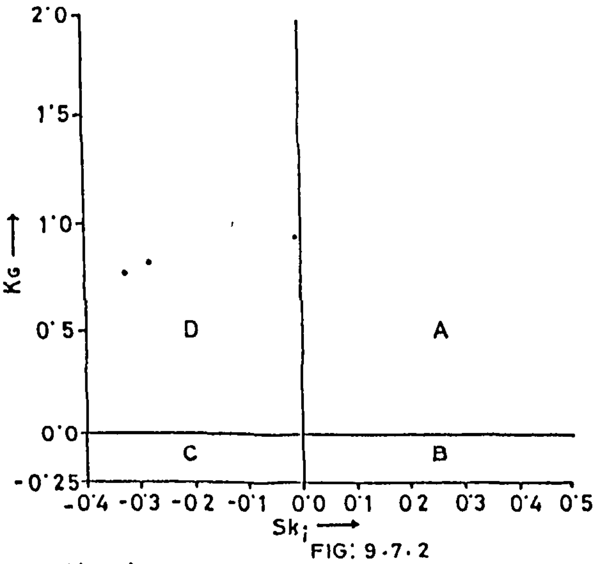

FIG: 9·7·2
Bivariate plots between Skewness and Kurtosis of the Barail sandstones. (After Thomas et al., 1972)

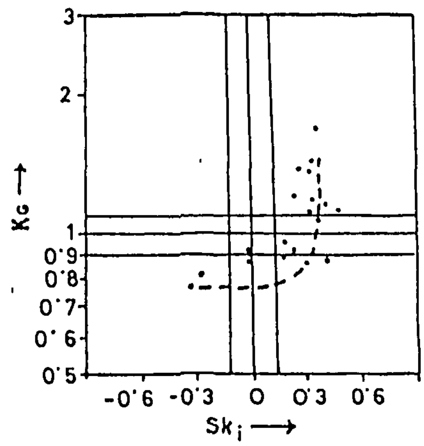

FIG: 9·7·3
Scatter plots of Kurtosis Vs. Skewness of Barail sandstones (After Folk & Ward, 1957)

skewness line as an environmental boundary between river and beach sediments. Most of the skewness-kurtosis plots indicate a river environment for the Barail sediments. Thomas et al. (1972) delineated four zones and designated them A, B, C and D. These zones relate to the intermixing of two or more populations with modification of the characteristic grain size symmetry and peakedness of the populations. These zones are related to the hydraulic energy that controls the sorting process. By plotting skewness against kurtosis (Fig. 9.7.2) following Thomas et al. (1972) it is found that the Barail sediments were subjected to moderate hydraulic energy pocesses.

Following Folk and Ward (1957), skewness is plotted against kurtosis (Fig. 9.7.3). The dispersal is fairly wide, to the right of the normal line of skewness. This scattering is due to separation between modes and the moderate sorting of the sediments.

Mean size Vs kurtosis :

Plots of these parameters after Folk and Ward (1957) take a sinusoidal trend (Fig. 9.8). With increasing grain size the sediments tend to become normal. With further increase they become leptokurtic and then platykurtic.

Standard deviation Vs kurtosis :

These two parameters, when plotted against each other following Folk and Ward (1957), result in the formation of an inverted 'V' (Fig. 9.9). The plots are scattered around the normal which is ascribed to the bimodality of the grain size population. The values of kurtosis suggest more or less moderate sorting of the two modes (Folk and Ward, 1957).

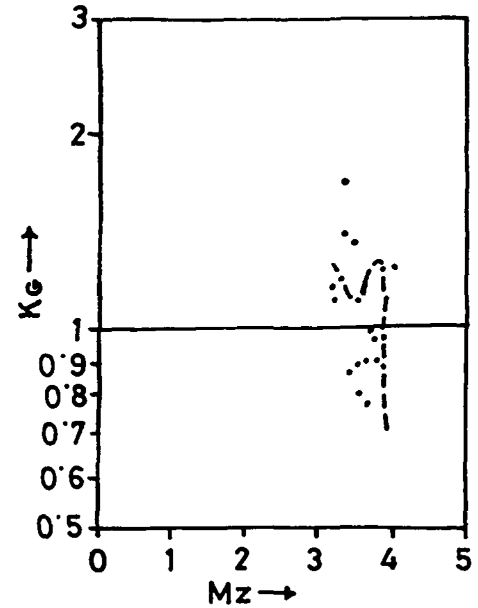

FIG: 9 · 8
Scatter plots of Kurtosis Vs. Mean size of Barail sandstones
(After Folk & Ward, 1957)

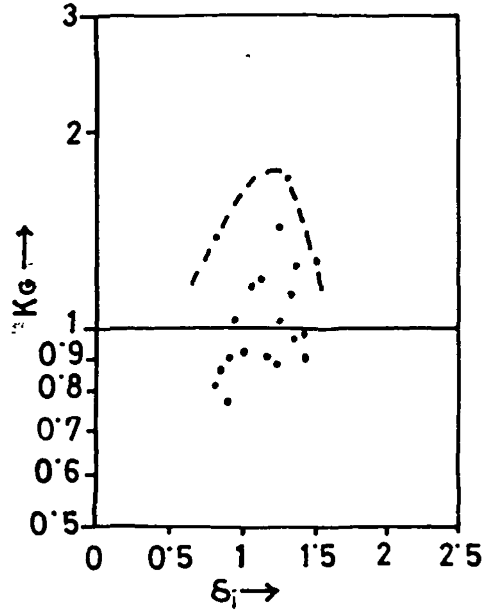

FIG: 9·9
Scatter plots of Kurtosis Vs. Standard deviation of Barail sandstones
(After Folk & Ward, 1957)

9.5. CM PATTERN :

C, the one percentile, and M, the median, range from 2643 to 3950 μ and 616 to 1267 μ respectively (Table 9.3). The pattern obtained on plotting C against M for the Barail sediments (Figs. 9.10.1 and 9.10.2) following Passega (1957, 1964), Passega and Byramjee (1969) and Reineck and Singh (1980) indicates that transportation was mostly in uniform suspension and partly as saltation. These deposits were probably laid down by rivers and turbidity currents.

The weight percentages of sediments finer than 125 (F), 31 (L) and 4 (A) μ are calculated following Passega and Byramjee (1969). The values of F, L and A range from 48.45 to 77.51, 1.36 to 22.40 and 0.11 to 4.58 respectively (Table 9.3). The FM, LM and AM plots are characteristically convex upwards (Fig. 9.11) which is due to transportation of the fine sediments in uniform suspension (Passega and Byramjee, 1969).

9.6. TEXTURAL CLASSIFICATION :

The Barail sandstones are made up of fine sand, silt and some clay. Sand ranges from 41.89 to 73.24%, silt from 25.28 to 55.71% and clay ranges from 0.44 to 6.34%. The average percentages of sand, silt and clay are 56.77, 40.62 and 2.58 respectively (Table 9.6). Plots of sand, silt and clay percentages in a triangular diagram (Fig. 9.12) following Folk (1954), show that the rocks are silty sandstones although a few come under the sandy-silt category.

9.7. SEDIMENTARY STRUCTURES :

Sedimentary structures are not common except for the abundance of fine parallel laminations. Small scale convolute

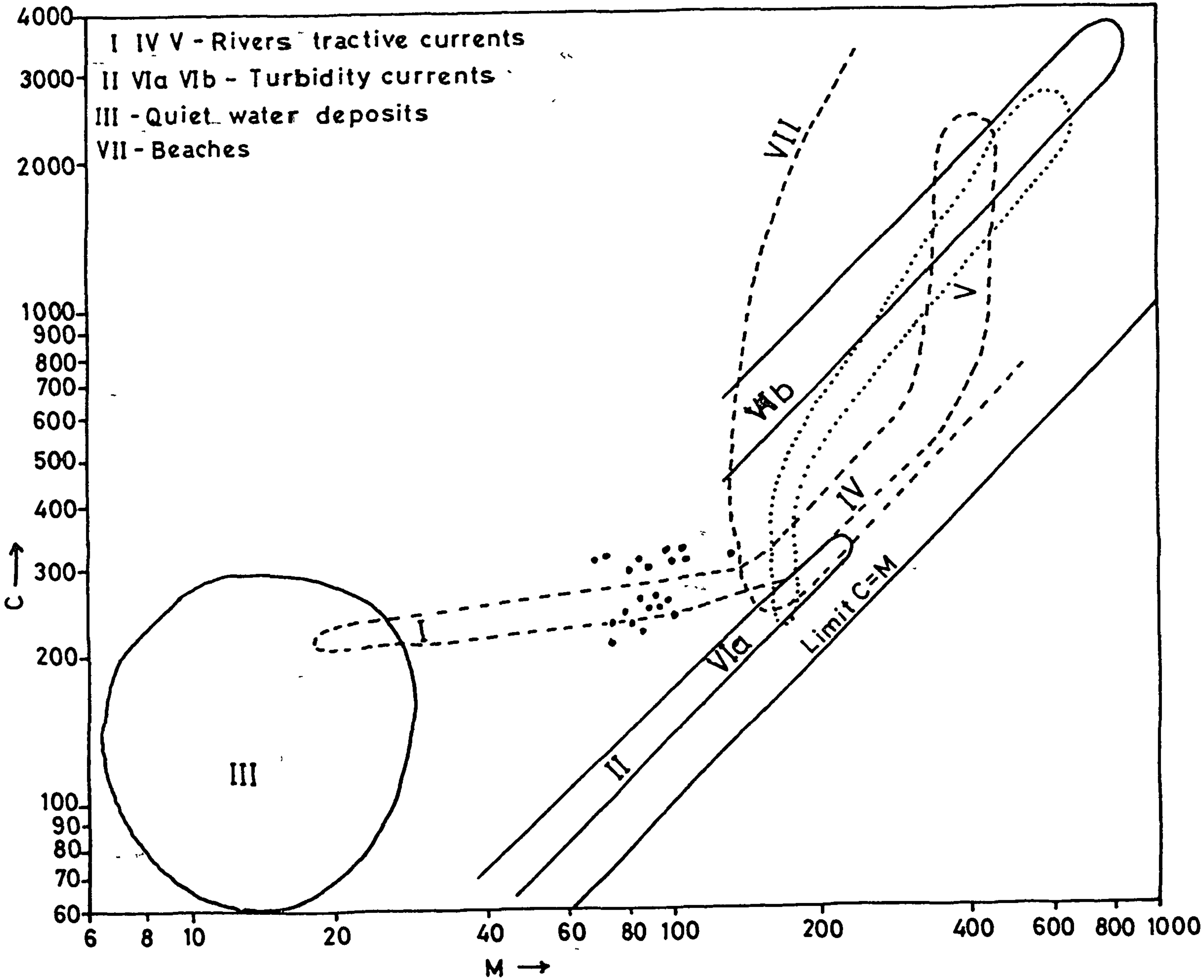

FIG: 9·10·1
CM Pattern of Barail sandstones
(After Passega, 1957)

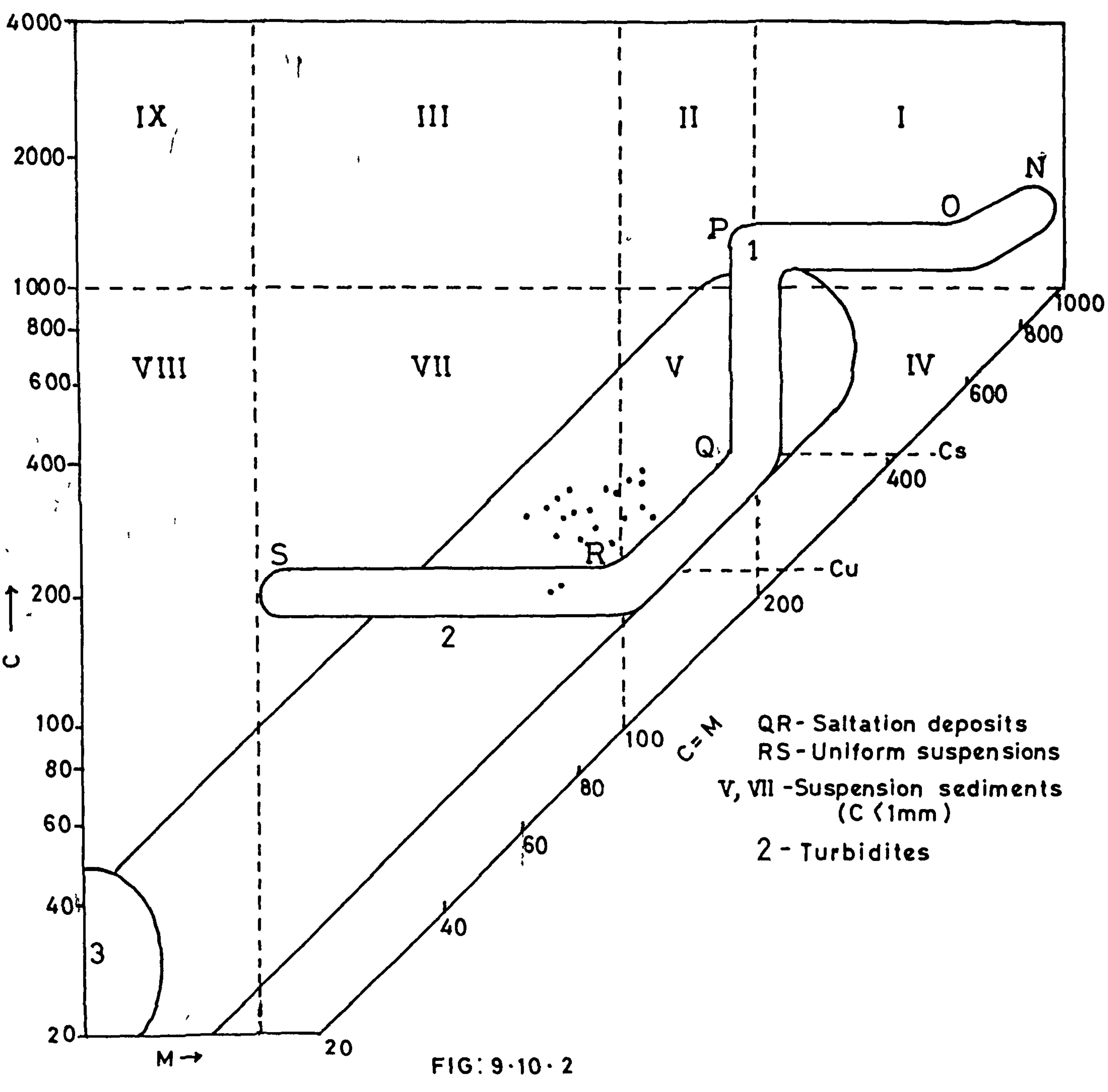

FIG: 9·10·2

CM Pattern of the Barail sandstones.
(After Passega, 1957, 1964; Passega and Byramjee, 1969; Reineck and Singh, 1980)

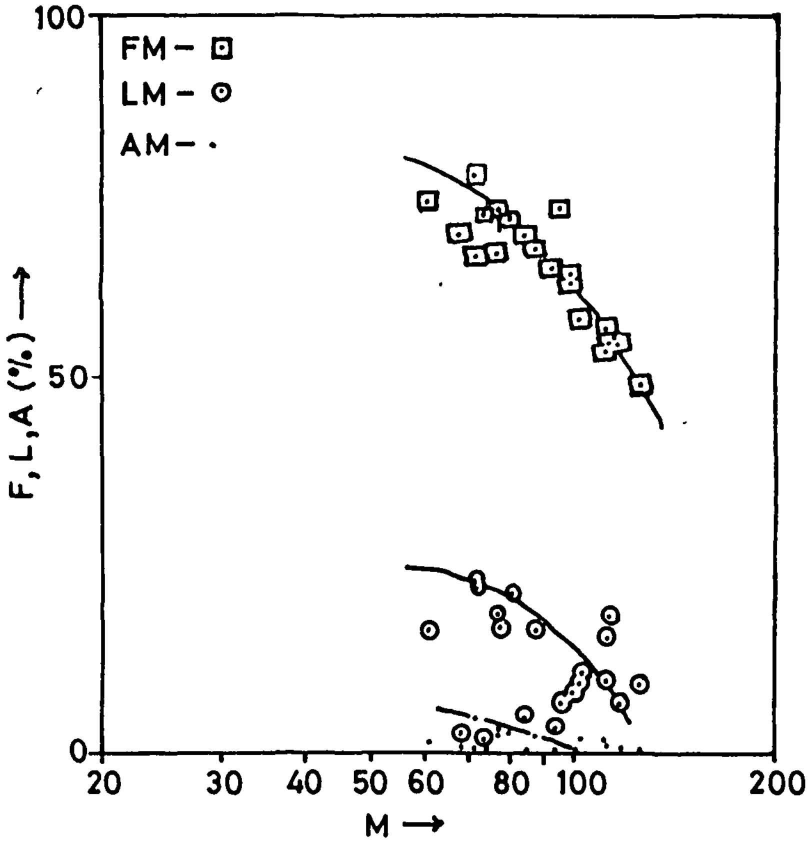

FIG: 9·11
FM, LM & AM diagrams of Barail Sandstones
(After Passega & Byramjee, 1969)

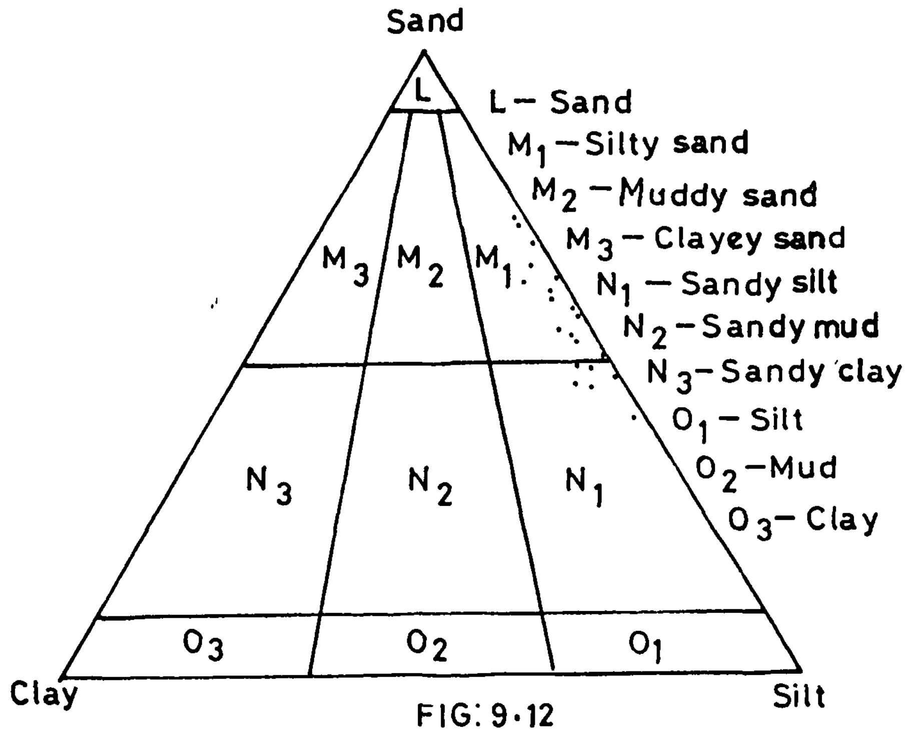

FIG: 9·12
Textural Classification of Barail sandstones
(After Folk, 1954)

Table 9.6

Textural classification of the Barail sandstones.

Sample No.	Textural components (Percentage)			Textural classification
	Sand	Silt	Clay	
B 1.	49.85	45.08	5.05	Sandy siltstone
B 7.	65.33	31.77	2.86	Silty sandstone
B 11.	62.56	31.96	5.44	Silty sandstone
B 22.	72.11	26.55	1.30	Silty sandstone
B 30.	54.19	42.54	3.25	Silty sandstone
B 34.	53.51	43.63	2.82	Silty sandstone
B 53.	60.79	36.58	2.59	Silty sandstone
B 65.	48.81	48.24	2.91	Sandy siltstone
B 69.	69.01	29.80	1.16	Silty sandstone
B 73.	46.03	49.63	4.30	Sandy siltstone
B 83.	55.00	40.82	4.15	Silty sandstone
B 87.	60.12	36.77	3.08	Silty sandstone
B 91.	56.80	42.73	0.45	Silty sandstone
B 92.	46.50	47.11	6.34	Sandy siltstone
B 93.	73.24	25.28	1.43	Silty sandstone
B 94.	58.24	41.27	0.46	Silty sandstone
B 95.	41.89	55.71	2.36	Sandy siltstone
B 96.	63.70	35.83	0.44	Silty sandstone
B 107.	47.45	51.83	0.69	Sandy siltstone
B 109.	50.25	49.21	0.50	Silty sandstone
Average	56.77	40.62	2.58	

laminations are also noted besides load casts and ripple marks. The Laisong Formation, the lowermost and only member of the Barail Group exposed in the area, is made up of massive, multi-layered sandstones at the base (Fig. 9.13.1) that are devoid of sedimentary structures.

Parallel laminations (Fig. 9.13.2) appear to be abundantly distributed throughout the Barail sandstones except in the massive ones. The laminations range in thickness from 0.5 to 2.0 mm. These laminations run parallel to the bedding planes.

The base of some of the Barail sandstones overlying shales exhibit load casts (Fig. 9.13.3) which are bulbous and irregular in shape.

The ripple marks (Fig. 9.13.4) noted are sinuous and asymmetric. Their wave lengths range between 5 and 6.5 cms. They have an average amplitude of 3 mm. The ripple indices vary from 16.66 to 21.66, averaging 19.16. According to Reineck and Wunderlich (1968), indices greater than 15 indicate current ripples.

Fig. 9.13.1

Massive, multi-layered Barail sandstones

Fig. 9.13.2

Laminated Barail sandstones

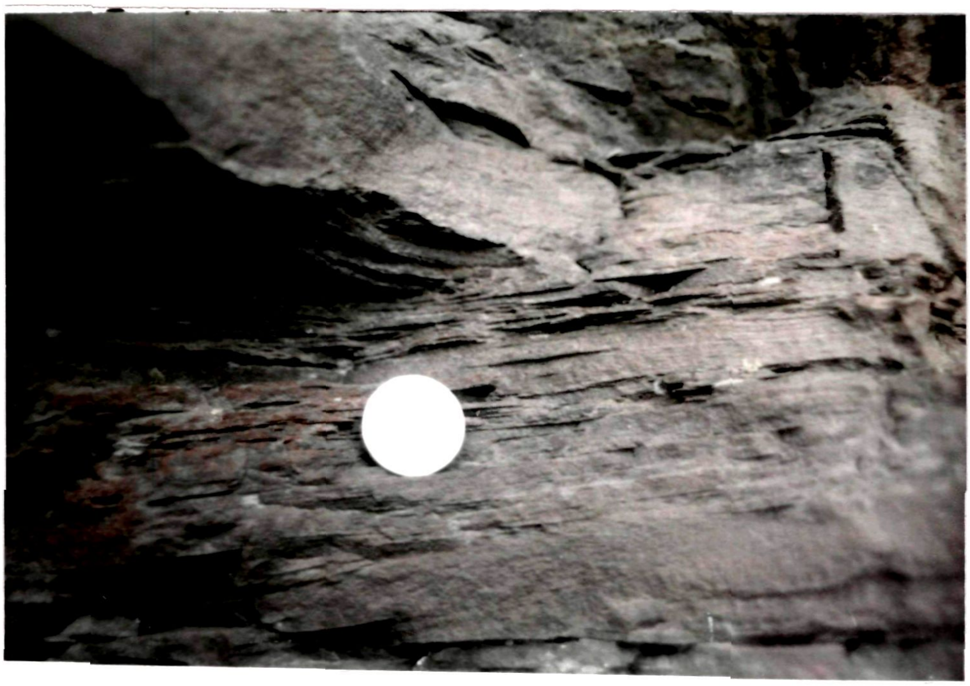

Fig. 9.13.3

Load casts in the Barail sandstones

Fig. 9.13.4

Ripple marks in the Barail sandstones

Panoramic view of Barail country

CHAPTER 10

HEAVY MINERALS

10.1. INTRODUCTION :

The heavy minerals are those of a higher density than the common rock forming minerals and have been derived from pre-existing rocks. They, being very stable and resistant to mechanical and chemical processes of rock disintegration, aid in establishing the erosional and tectonic history of basins and in an understanding of the lithology of the source rocks. An elaborate discussion is added in chapter 6.

For detailed heavy mineral studies twelve sandstone samples of the Barail Group are selected. The laboratory methods employed are described in chapter 3.

10.2. HEAVY MINERAL COMPOSITION :

The Barail sandstones contain the following heavy minerals in order of decreasing abundance - opaques, zircon, tourmaline, kyanite, epidote, garnet and rutile (Table 10.1).

Opaques :

The opaques (Fig. 10.1) include hematite and magnetite and are the dominant group, ranging from 85.11 to 88.80% and averaging 86.78% with a frequency of 8. Hematite occurs as dark brown grains whereas magnetite is found as black anhedral to subhedral grains.

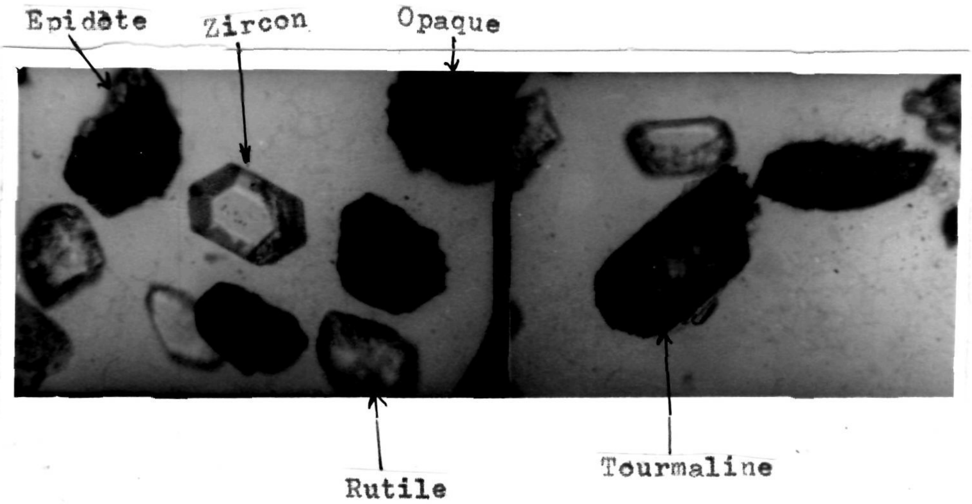

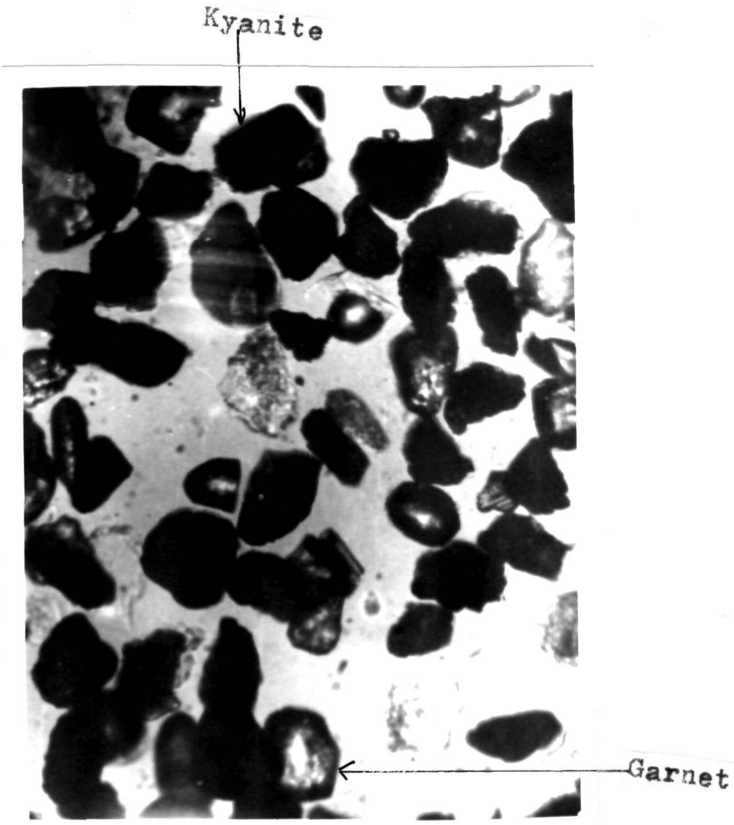

Fig.10.1

Table 10.1

Heavy mineral composition and frequency of the Barail sandstones.

Sample No.	Opaques	Zircon	Tourmaline	Rutile	Kyanite	Garnet	Epidote
B 1.	85.11 (8)	3.85 (3)	3.77 (3)	0.65 (1)	2.99 (3)	0.87 (1)	2.76 (3)
B 22.	85.19 (8)	3.35 (3)	4.16 (4)	0.44 (1*)	1.94 (2)	0.65 (1)	4.27 (4)
B 34.	88.47 (8)	3.17 (3)	2.73 (3)	0.30 (1*)	2.77 (3)	0.51 (1)	2.05 (3)
B 53.	86.42 (8)	3.45 (3)	3.31 (3)	0.36 (1*)	2.16 (3)	0.44 (1*)	3.86 (3)
B 65.	85.30 (8)	5.63 (4)	2.10 (3)	0.03 (1*)	4.07 (4)	0.27 (1*)	2.60 (3)
B 73.	86.13 (8)	4.48 (4)	2.62 (3)	0.19 (1*)	4.52 (4)	0.69 (1)	1.37 (2)
B 83.	88.80 (8)	2.18 (3)	3.51 (3)	0.31 (1*)	2.43 (3)	0.72 (1)	2.05 (3)
B 87.	87.21 (8)	3.32 (3)	3.37 (3)	0.21 (1*)	2.33 (3)	0.53 (1)	3.03 (3)
B 91.	85.27 (8)	4.63 (4)	2.99 (3)	0.27 (1*)	3.47 (3)	0.86 (1)	2.51 (3)
B 96.	88.55 (8)	2.97 (3)	3.02 (3)	0.34 (1*)	2.56 (3)	0.53 (1)	2.03 (3)
B 107.	87.09 (8)	3.98 (3)	2.66 (3)	0.22 (1*)	2.59 (3)	0.47 (1*)	2.99 (3)
B 109.	87.88 (8)	5.00 (4)	1.48 (2)	0.20 (1*)	2.33 (3)	0.46 (1*)	2.65 (3)
Average :	86.78	3.83	2.98	0.29	2.85	0.58	2.68

Note : Figures within parentheses indicate frequencies.

Zircon :

Zircon (Fig. 10.1) ranges from 2.18 to 5.63%, averaging 3.83% with a frequency ranging from 2 to 3. The majority of the grains are subangular to subrounded the remainder being angular and rounded. Most of the grains are colourless. The coloured *grains are weakly pleochroic and are straw yellow, pale pink and* pale brown. The grains of zircon show strong birefringence and high relief. The prismatic grains show parallel extinction while some grains exhibit zoning. Opaque and non-opaque minerals are common inclusions in zircon.

Tourmaline :

Tourmaline (Fig. 10.1) ranges from 1.48 to 4.16% and averages 3.01%. The frequency varies from 2 to 4. The grains are subangular to subrounded, most of them being elongated. The grains are variously coloured and range from brown to pink and green to blue. The pleochroic colours shown by the grains are brown and green. The tourmaline grains show more or less moderate relief and birefringence and some of them bear inclusions.

Kyanite :

The amount of kyanite (Fig. 10.1) ranges from 1.94 to 4.52%, averaging 2.85% with frequency ranging between 2 and 4. The grains, angular to subangular and showing a pale blue colour, are weakly pleochroic. They show moderate relief and birefringence and an oblique extinction.

Rutile :

Rutile (Fig. 10.1) averages 0.29% of the total heavy mineral composition and ranges from 0.03 to 0.65% with frequency ranging between 1* and 1. These grains are angular to subangular and are yellowish to red in colour with dark brown outlines. The relief shown by the grains is more or less high. The prismatic grains show a straight extinction.

Epidote :

Epidote (Fig. 10.1) ranges between 1.37 and 4.27% with an average of 2.68% and frequency ranging between 2 and 4. The grains are subangular to subrounded and are mostly pale yellow. The coloured grains show pale yellow to pale green pleochroic colours. The birefringence is strong and irregular fractures on the grains are common.

Garnet :

Garnet (Fig. 10.1), averaging 0.58%, ranges from 0.27 to 0.87% with frequency ranging from 1* to 1. Some of the grains show rhombic patterns and are more or less subrounded. They show a high relief and are mainly pale brown in colour. Fractures are seen in some of the grains.

The non-opaques to opaques ratios range between 0.13 and 0.17 (Table 10.2) with an average of 0.15. These ratios indicate multiple sources for these sediments. The distribution of the heavy minerals in the vertical section is shown in figure 10.2 and the frequency distribution is given in figure 10.3 (table 10.1).

10.3. Z.T.R. MATURITY INDEX :

The Z.T.R. maturity index reflects the maturity of the rocks (Hubert, 1962). The maturity index of the Barail sandstones ranges from 52.42 to 55.55, averaging 53.90 (Table 10.2).

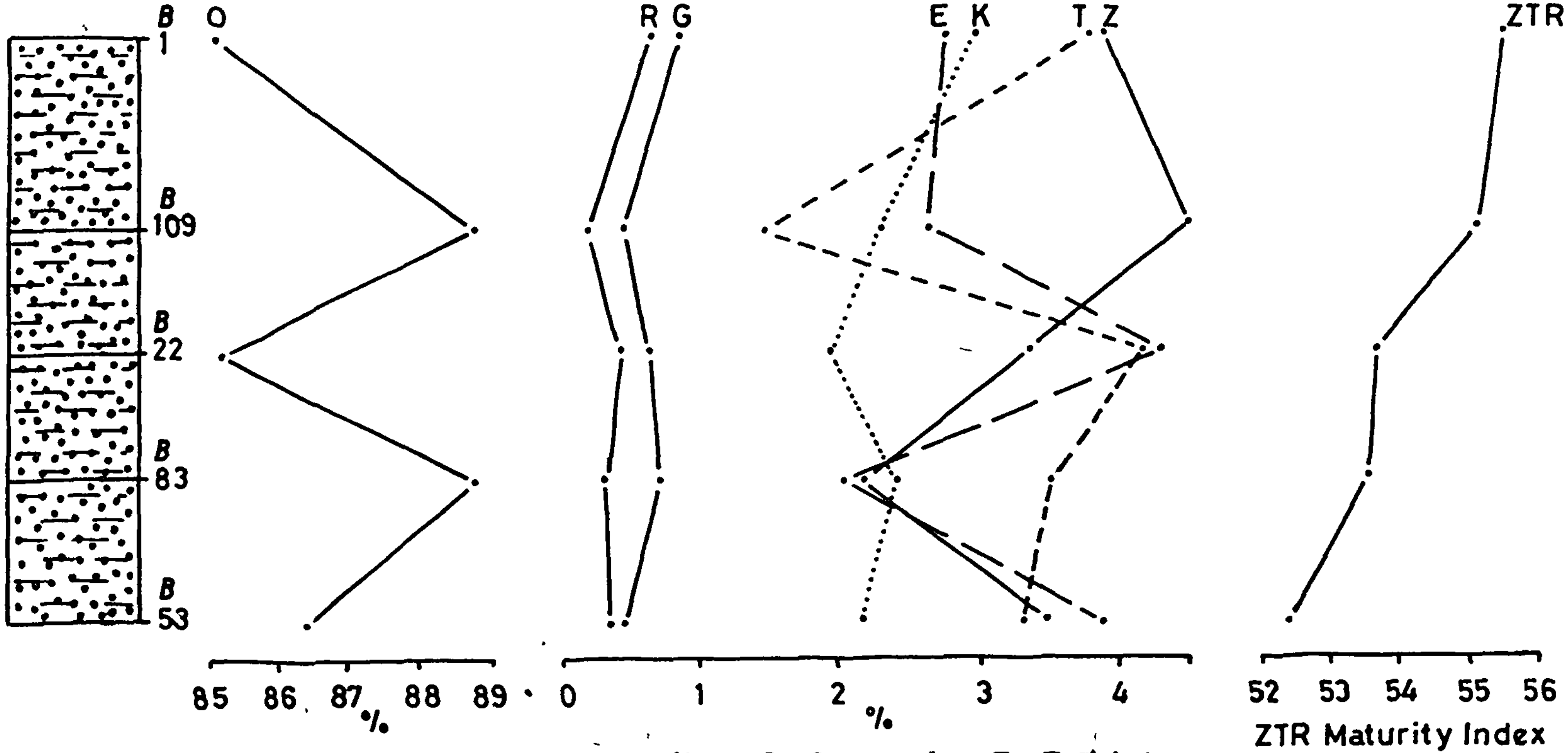

O-Opaque , R-Rutile , G-Garnet , E-Epidote,
K-Kyanite , T-Tourmaline , Z-Zircon.

FIG: 10 ·2

VERTICAL VARIATION OF HEAVY MINERALS AND ZTR MATURITY INDEX OF THE BARAIL SANDSTONES

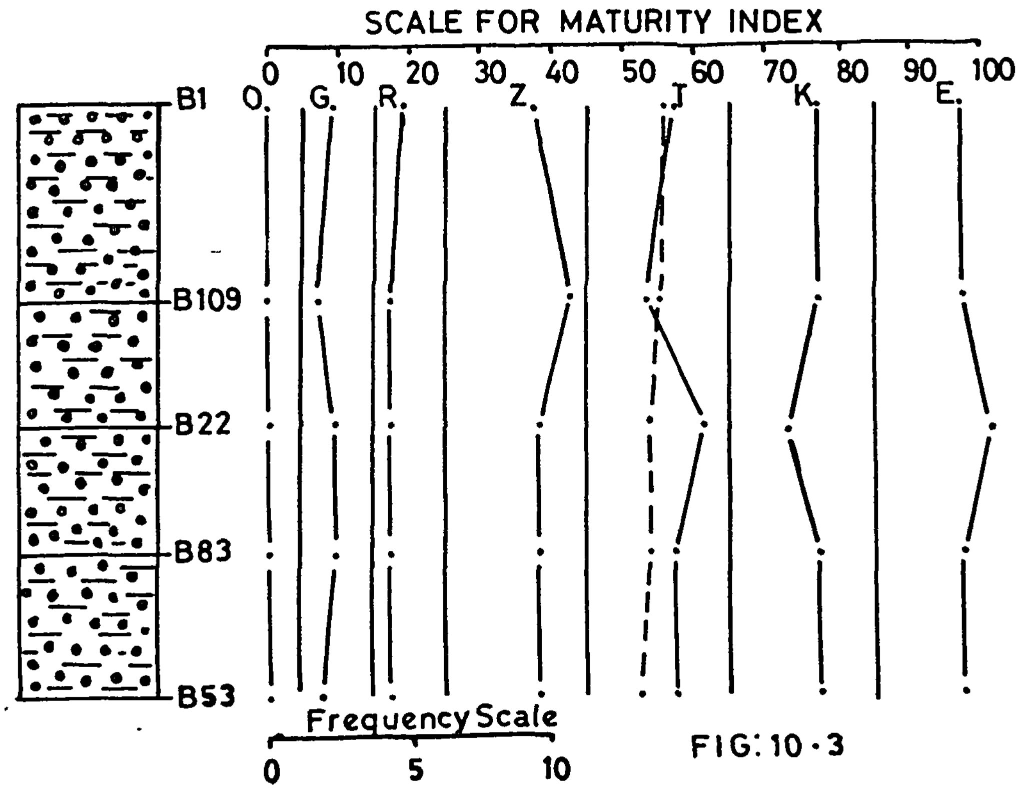

FIG: 10·3

O-Opaque , G- Garnet , R-Rutile , Z-Zircon

T-Tourmaline , K-Kyanite , E-Epidote

Mineral Axis

Mineral Frequency

Maturity Index

FREQUENCY DISTRIBUTION OF HEAVY MINERALS AND Z.T.R. MATURITY INDEX OF THE SANDSTONES OF THE BARAIL GROUP.

Table 10.2

Z.T.R. maturity index and non-opaque/opaque ratios of the Barail sandstones.

Sample No.	Recalculated percentages of zircon, tourmaline and rutile			Z.T.R. index	Non-opaque / opaque
	Zircon	Tourmaline	Rutile		
B 1.	25.86	25.32	4.37	55.55	0.17
B 22.	22.62	28.09	2.97	53.68	0.17
B 34.	27.49	23.68	2.60	53.77	0.13
B 53.	25.40	24.37	2.65	52.42	0.16
B 65.	38.30	14.29	0.20	52.79	0.17
B 73.	32.30	18.89	1.37	52.56	0.16
B 83.	19.46	31.34	2.77	53.57	0.13
B 87.	25.17	28.58	1.59	55.34	0.15
B 91.	31.43	20.30	1.83	53.56	0.17
B 96.	25.94	26.38	2.97	55.29	0.13
B 107.	30.83	20.60	1.70	53.13	0.15
B 109.	41.25	12.21	1.65	55.11	0.14
Average :	28.84	22.84	2.22	53.90	0.15

The maturity index, as seen in the vertical section (Fig. 10.3), shows a gradual increase towards the top.

10.4. QUANTIFICATION AND CORRELATION OF ZIRCON AND TOURMALINE DATA :

The average diameters of the zircon and tourmaline grains are calculated from which their mean sizes are obtained, as described in chapter 3. The mean size of zircon of the Barail sandstones is 0.107 while that of tourmaline is 0.108 (Tables 10.3.1 and 10.3.2).

The coefficient of correlation, a statistical measure, gives an idea as to whether there exists or not any correlation or mathematical dependence of any set of data upon another. Zircon of the Disang and Barail sandstones range in size from 0.04 to 0.16 mm. For purpose of correlation the coefficient of correlation for zircon is calculated and found to be -0.390 (Table 10.4.1). Tourmaline of the two groups show a narrower size range of 0.04 to 0.12 mm. The coefficient of correlation for this mineral is -0.891 (Table 10.4.2). The negative values of the coefficient of correlation indicate an inverse relation for both zircon and tourmaline data between the Disang and Barail Groups.

10.5. LENGTH AND BREADTH FREQUENCIES, AND ELONGATION RATIO FREQUENCIES OF ZIRCON AND TOURMALINE :

There exists variation in the length, breadth and elongation ratio frequencies distribution between these two groups of minerals, more so in the elongation ratio frequency.

The minimum and maximum length frequencies of 9 and 21% respectively of zircon lie in class intervals 0.030 to 0.070 and

Table 10.3.1

Mean size (M_z) of zircon of the Barail sandstones.

Class interval (Diameter in mm)	Class mid-point (m)	Frequency (f)	f x m	M_z
0.030 - 0.050	0.040	5	0.20	
0.050 - 0.070	0.060	5	0.30	
0.070 - 0.090	0.080	8	0.64	
0.090 - 0.110	0.100	5	0.50	0.107
0.110 - 0.130	0.120	11	1.32	
0.130 - 0.150	0.140	2	0.28	
0.150 - 0.170	0.160	9	1.44	
0.170 - 0.190	0.180	2	0.36	

$\Sigma f = 47 \quad \Sigma f \times m = 5.04$

$$M_z = \frac{\Sigma f \times m}{\Sigma f} = \frac{5.04}{47} = 0.107$$

Table 10.3.2

Mean size (M_z) of tourmaline of the Barail sandstones.

Class interval (Diameter in mm)	Class mid-point (m)	Frequency (f)	f x m	M_z
0.030 - 0.050	0.040	3	0.12	
0.050 - 0.070	0.060	5	0.30	
0.070 - 0.090	0.080	9	0.72	
0.090 - 0.110	0.100	8	0.80	0.108
0.110 - 0.130	0.120	10	1.20	
0.130 - 0.150	0.140	10	1.40	
0.150 - 0.170	0.160	6	0.96	

$\Sigma f = 51 \quad \Sigma f \times m = 5.50$

$$M_z = \frac{5.50}{51} = 0.108$$

Table 10.4.1

Coefficient of correlation of zircon of the sandstones of the Disang and Barail Groups.

Grain size (Diameter in mm)	Disang x	x^2	Barail y	y^2	xy
0.040	7	49	5	25	35
0.060	12	144	5	25	60
0.080	8	64	8	64	64
0.100	10	100	5	25	50
0.120	5	25	11	121	55
0.140	5	25	2	4	10
0.160	1	1	9	81	9
n = 7	Mx=6.86	$\Sigma x^2=408$	My=6.43	$\Sigma y^2=345$	xy=283

$$r = \frac{\sum(xy) - n.Mx.My}{\sqrt{\{\sum(x^2)-n(Mx)^2\}\ \{\sum(y^2)-n(My)^2\}}}$$

$$= \frac{283 - 7 \times 6.86 \times 6.43}{\sqrt{\{408-7\times(6.86)^2\}\ \{345-7\times(6.43)^2\}}}$$

$$= -0.390$$

Table 10.4.2

Coefficient of correlation of tourmaline of the sandstones of the Disang and Barail Groups.

Grain size (Diameter in mm)	Disang x	x^2	Barail y	y^2	xy
0.040	3	9	12	144	36
0.060	5	25	11	121	55
0.080	9	81	7	49	63
0.100	8	64	10	100	80
0.120	10	100	4	16	40
n = 5	Mx = 7	$\Sigma x^2=279$	My=8.8	$\Sigma y^2=430$	xy=274

$$r = \frac{274 - 5 \times 7 \times 8.8}{\sqrt{\{279-5 \times 49\}\ \{430 - 5 \times 77.44\}}}$$

$$= -0.891$$

0.170 and 0.190 mm respectively. The maxima of the frequency curve lies at 0.180 mm while the minima lies at 0.040 and 0.060 mm (Fig. 10.4.1, Table 10.5). The minimum and maximum breadth frequencies Of 2 and 28% respectively lie in class intervals 0.170 to 0.190 and 0.070 to 0.090 mm respectively. The maxima and minima of the breadth frequency curve lie at 0.080 and 0.180 mm respectively (Fig. 10.4.2, Table 10.5). The minimum and maximum elongation ratio frequency of 2 to 25% respectively of zircon of the Barail sandstones lie in class intervals 1.80 to 1.90 and 1.20 to 1.30 respectively. The maxima and minima of the elongation ratio frequency curve lie at 1.25 and 1.85 respectively (Fig. 10.4.3, Table 10.5).

Tourmaline shows a minimum and maximum length frequency of 4 and 25% respectively in class intervals 0.190 to 0.210 and 0.150 to 0.170 mm respectively. The maxima and minima of the frequency curve lie at 0.160 and 0.200 mm respectively (Fig. 10. 5.1, Table 10.6). The minimum and maximum breadth frequencies of 2 and 25% lie in class intervals 0.010 to 0.030 and 0.130 to 0.170, and 0.050 to 0.070 mm respectively. The maxima of the breadth frequency curve lies at 0.060 mm. The minima lies at 0.020, 0.140 and 0.160 mm (Fig. 10.5.2, Table 10.6). The minimum elongation ratio frequency of 2% lies in class intervals 1.80 to 2.00, 2.10 to 2.20 and 2.60 to 2.70 while the maximum of 15% lies in class interval 1.20 to 1.30. The maxima lies at 1.25 while the minima lies at 1.85, 1.95, 2.15 and 2.65 (Fig. 10.5.3, Table 10.6).

10.6. CATENAE OF ZIRCON AND TOURMALINE :

Smithson's diagram (1939) is followed for plotting lengths and breadths of zircon and tourmaline of the Barail Group. The pattern developed for zircon shows that the base lies very near the 1:1 line, the top lying on the 1:2 line.

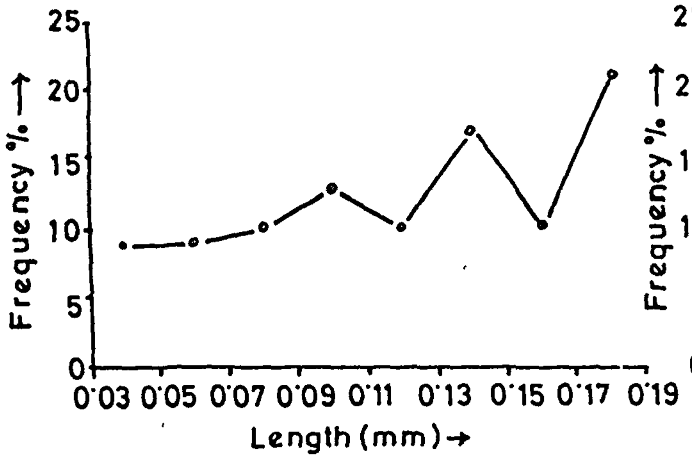

FIG: 10 · 4 · 1
Relationship between Length and frequency of Zircon of the sandstones of Barail Group

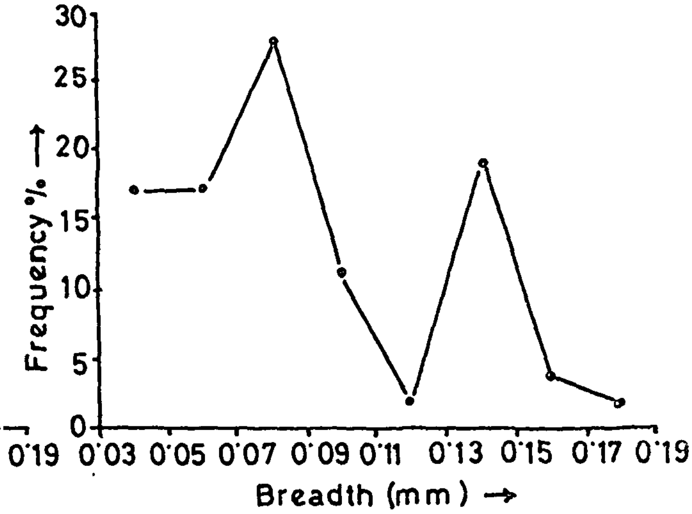

FIG: 10 · 4 · 2
Relationship between Breadth and frequency of Zircon of the sandstones of Barail Group

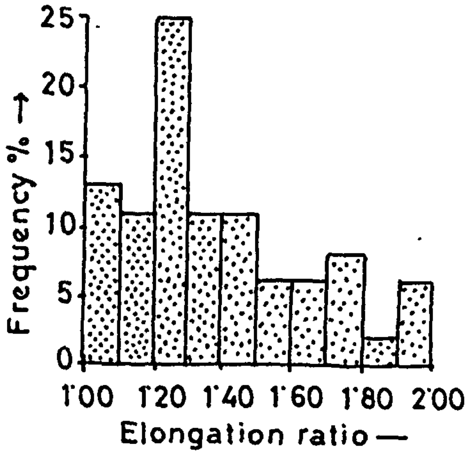

FIG: 10 · 4 · 3
Elongation ratio - frequency histogram of Zircon of the sandstones of Barail Group

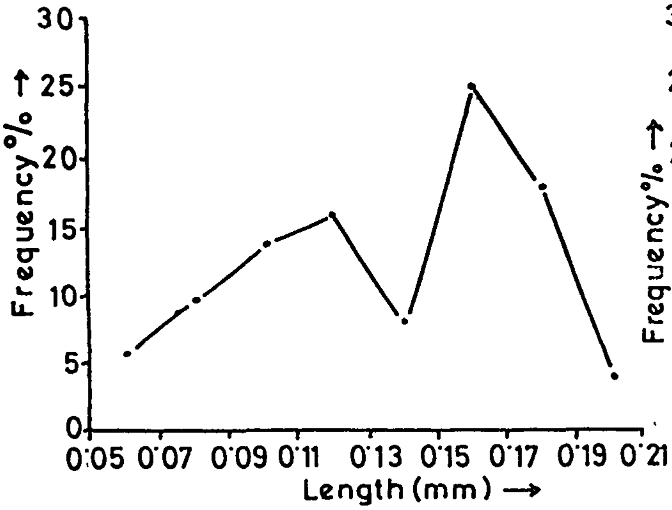

FIG: 10·5·1

Relationship between Length and Frequency of Tourmaline of the sandstones of Barail Group

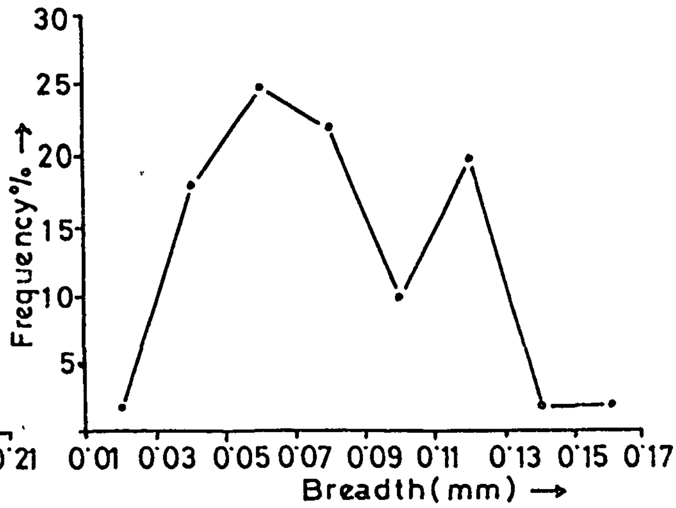

FIG: 10·5·2

Relationship between Breadth and Frequency of Tourmaline of the sandstones of Barail Group

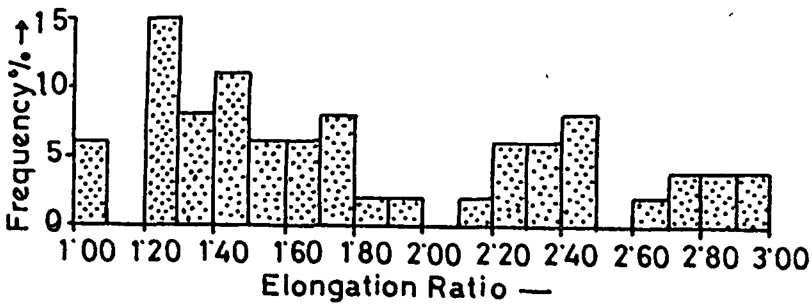

FIG: 10·5·3

Elongation ratio-frequency histogram of Tourmaline of the sandstones of Barail Group

Table 10.5

Length, breadth and elongation ratio frequency of zircon of the Barail sandstones.

Class interval	Length		Breadth		Class interval	Elongation	
	No. of grains	Frequency (%)	No. of grains	Frequency (%)		No. of grains	Frequency (%)
0.030-0.050	4	9	8	17	1.00-1.10	6	13
0.050-0.070	4	9	8	17	1.10-1.20	5	11
0.070-0.090	5	10	13	28	1.20-1.30	12	25
0.090-0.110	6	13	5	11	1.30-1.40	5	11
0.110-0.130	5	10	1	2	1.40-1.50	5	11
0.130-0.150	8	17	9	19	1.50-1.60	3	6
0.150-0.170	5	10	2	4	1.60-1.70	3	6
0.170-0.190	10	21	1	2	1.70-1.80	4	8
					1.80-1.90	1	2
					1.90-2.00	3	6

Table 10.6

Length, breadth and elongation ratio frequencies of tourmaline of the Barail sandstones.

Class interval	Length		Breadth		Class interval	Elongation	
	No. of grains	Frequency (%)	No. of grains	Frequency (%)		No. of grains	Frequency (%)
0.010-0.030	-	-	1	2	1.00-1.10	3	6
0.030-0.050	-	-	9	18	1.10-1.20	-	-
0.050-0.070	3	6	13	25	1.20-1.30	8	15
0.070-0.090	5	10	11	22	1.30-1.40	4	8
0.090-0.110	7	14	5	10	1.40-1.50	6	11
0.110-0.130	8	16	10	20	1.50-1.60	3	6
0.130-0.150	4	8	1	2	1.60-1.70	3	6
0.150-0.170	13	25	1	2	1.70-1.80	4	8
0.170-0.190	9	18	-	-	1.80-1.90	1	2
0.190-0.210	2	4	-	-	1.90-2.00	1	2
					2.00-2.10	-	-
					2.10-2.20	1	2
					2.20-2.30	3	6
					2.30-2.40	3	6
					2.40-2.50	4	8
					2.50-2.60	-	-
					2.60-2.70	1	2
					2.70-2.80	2	4
					2.80-2.90	2	4
					2.90-3.00	2	4

The concentration of points is thus clustered between 1:1 and 1:2 (Fig. 10.6). The pattern, in case of tourmaline, shows a wavy outline. The points are mainly clustered between 1:1 and 1:2 (Fig. 10.7). The catenae of both zircon and tourmaline are fan shaped and scattering of points are found to increase away from the points of origin of the coordinates.

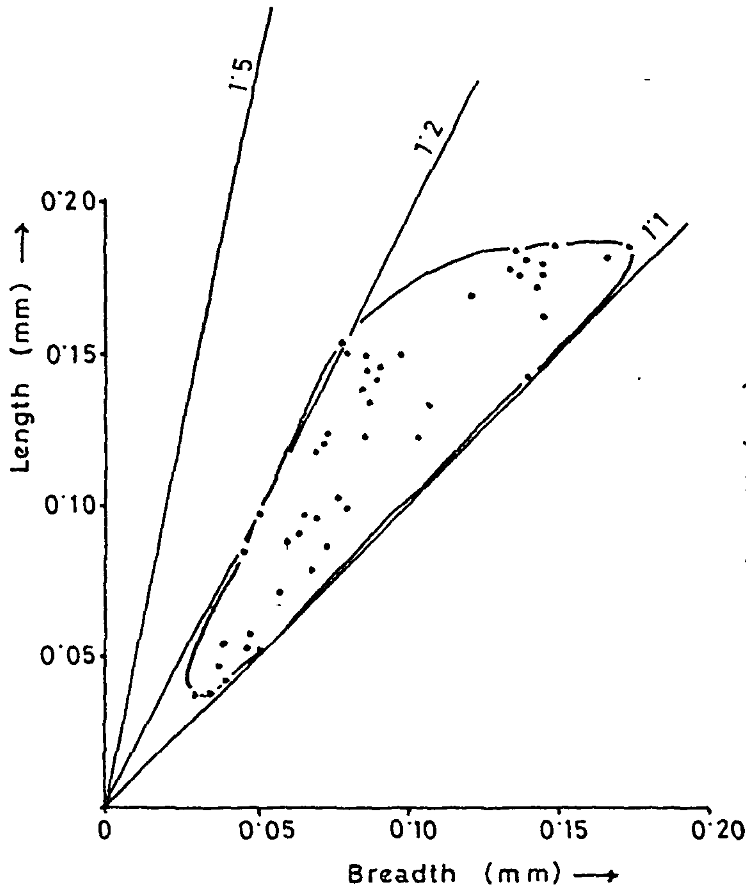

FIG: 10·6

Relationship between Length and Breadth of Zircon of the sandstones of the Barail Group.

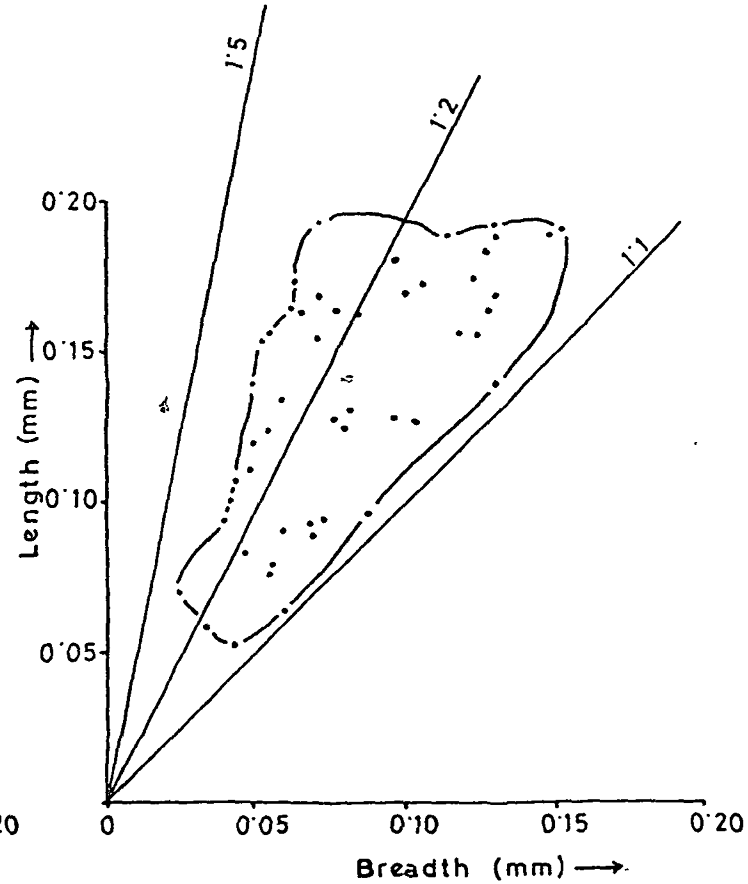

FIG: 10·7

Relationship between Length and Breadth of Tourmaline of the sandstones of the Barail Group.

CHAPTER 11

GEOCHEMISTRY

11.1. INTRODUCTION :

The geochemistry of the sandstones of the Barail Group is discussed in this chapter. For study purpose twenty samples are quantitatively analysed for the major oxides and four for the rare earth elements while ten are semi-quantitatively analysed for trace elements. The major oxides, REE and trace elements provide strong supporting evidences in unravelling the history of sediments when other techniques of study fail or are vague due to various reasons. The importance of geochemical studies is briefly discussed in chapter 7 and the methods of study are described in chapter 3.

11.2. MAJOR OXIDES :

The major oxides include SiO_2, TiO_2, Al_2O_3, Fe_2O_3, FeO, MnO, CaO, MgO, Na_2O, K_2O and P_2O_5 (Table 11.2.1). In percentage these oxides range from 60.52 to 90.40, 0.21 to 1.33, 3.92 to 13.29, 1.00 to 4.03, 0.54 to 5.76, $<$0.01 to 0.10, 0.30 to 4.65, 0.23 to 3.71, 0.12 to 1.04, 0.50 to 1.73 and 0.03 to 0.09 respectively. The average percentages are 74.39, 0.83, 8.91, 3.00, 2.23, 0.03, 1.35, 1.99, 0.62, 1.21 and 0.05 respectively. Values of Si, Al and FeT, calculated from SiO_2, Al_2O_3 and (Fe_2O_3+FeO) respectively, are shown in table 11.2.2. The distribution of these oxides in the vertical section is erratic as is shown in figure 11.2.1. in ascending order.

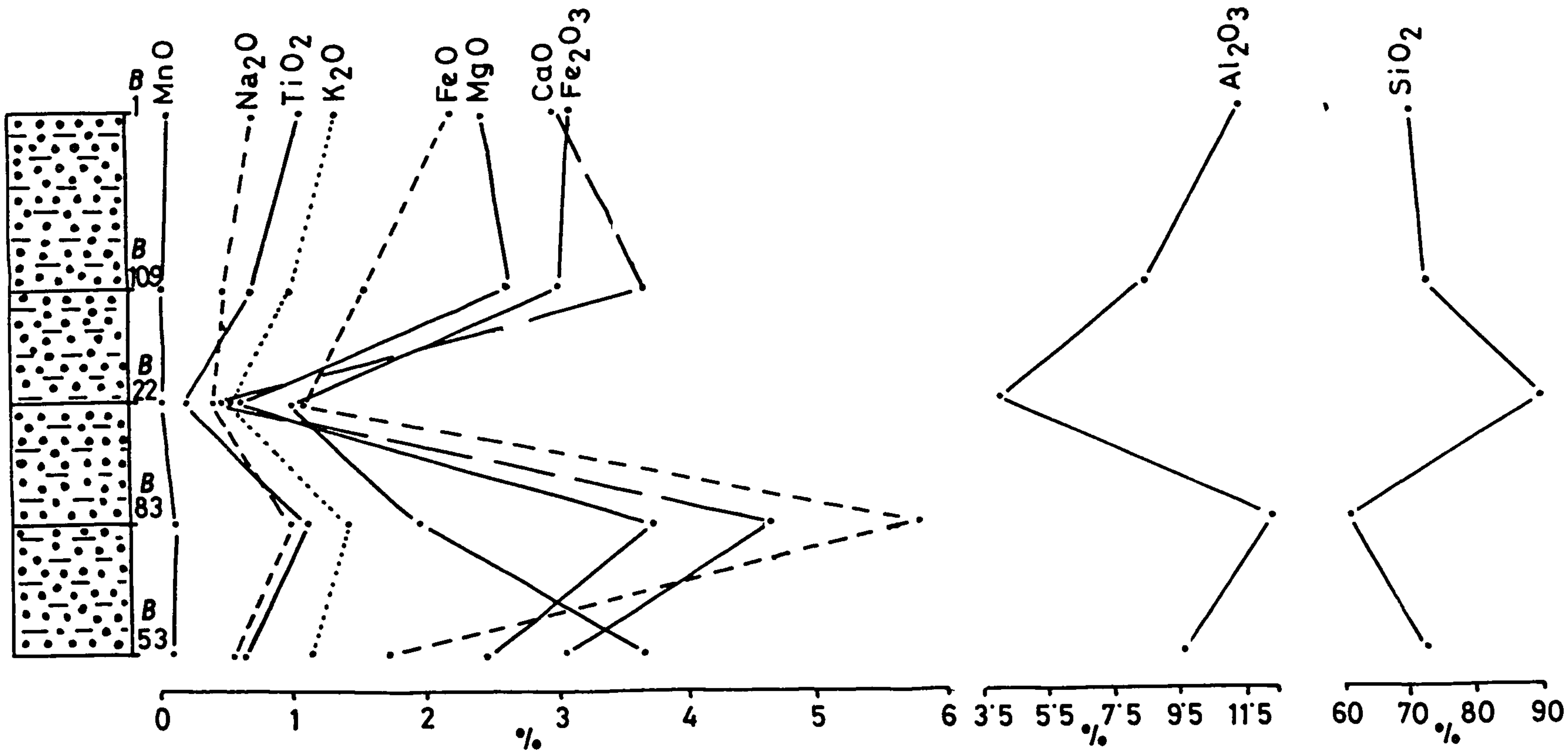

(Value of P_2O_5 < 0·05 % throughout)

FIG: 11·2·1

VERTICAL VARIATION OF MAJOR OXIDES OF THE BARAIL SANDSTONES

Table 11.2.1

Major oxide composition (percentage) of the sandstones of the Barail Group.

Sample No.	SiO_2	TiO_2	Al_2O_3	Fe_2O_3	FeO	MnO	CaO	MgO	Na_2O	K_2O	P_2O_5	L.O.I.
B 1.	70.08	1.06	11.27	3.05	2.16	0.06	2.94	2.38	0.72	1.30	<0.05	4.93
B 11.	81.34	0.57	8.38	1.82	1.62	<0.01	0.41	0.58	0.40	1.11	0.06	3.70
B 22.	89.50	0.21	3.92	1.00	1.08	0.01	0.46	0.59	0.43	0.50	<0.05	2.25
B 30.	73.46	0.64	9.47	3.85	2.76	0.02	0.52	2.47	0.97	1.05	0.05	4.74
B 34.	73.20	0.64	12.86	3.62	1.80	<0.01	0.34	0.71	0.41	1.54	0.08	4.79
B 45.	74.37	0.79	8.53	3.81	3.05	0.01	0.63	2.41	0.86	1.21	0.07	4.26
B 49.	73.13	0.91	8.69	3.72	2.56	0.03	0.71	2.33	0.77	1.18	0.07	5.97
B 53.	72.70	0.65	9.54	3.63	1.71	0.09	3.04	2.45	0.57	1.15	<0.05	4.42
B 61.	72.07	0.82	8.71	3.99	2.03	0.02	0.64	2.19	0.53	1.02	0.06	7.92
B 65.	70.68	1.22	13.29	1.85	4.50	<0.01	0.38	1.01	0.51	1.62	0.09	4.84
B 69.	70.33	0.71	9.36	4.01	2.69	0.03	0.68	2.63	0.95	1.32	<0.05	7.24
B 73.	71.70	0.71	8.97	3.78	1.82	0.08	2.51	2.44	0.61	1.21	<0.05	6.12
B 83.	60.52	1.10	12.19	1.94	5.76	0.10	4.65	3.71	1.04	1.41	<0.05	7.53
B 87.	69.13	1.33	10.01	4.03	2.51	<0.01	1.11	2.13	0.93	1.73	0.06	7.02
B 92.	90.40	0.85	3.99	1.01	0.54	<0.01	0.30	0.23	0.12	0.65	0.03	1.87
B 96.	86.12	0.65	6.15	1.22	1.08	<0.01	0.32	0.41	0.19	0.86	0.05	2.94
B 99.	70.26	1.02	9.26	3.86	1.77	0.03	1.69	3.16	0.78	1.59	<0.05	6.53
B 101.	69.53	1.11	9.37	3.33	2.03	0.06	1.26	2.79	0.57	1.33	<0.05	3.57
B 106.	80.55	0.93	6.08	3.51	1.73	<0.01	0.79	2.55	0.64	1.56	0.05	1.60
B 109.	72.74	0.70	8.17	2.98	1.53	<0.01	3.62	2.59	0.50	1.00	0.05	6.11
Average:	74.59	0.83	8.91	3.00	2.23	0.03	1.35	1.99	0.62	1.21	0.06	5.17

Table 11.2.2

Weight percentages and ratios of Si, Al and FeT (total iron) of the sandstones of the Barail Group.

Sample No.	Si	Al	FeT	Si :	FeT :	Al
B 1.	32.761	2.982	3.770	82.91	9.54	7.55
B 11.	38.024	2.217	2.489	88.99	5.82	5.19
B 22.	41.839	1.037	1.505	94.27	3.39	2.34
B 30.	34.306	5.010	4.835	77.71	10.94	11.83
B 34.	34.219	3.403	3.922	82.37	9.44	8.19
B 45.	34.730	4.512	5.033	78.45	11.36	10.19
B 49.	34.152	4.597	4.589	78.79	10.59	10.61
B 53.	33.985	2.524	3.864	84.18	9.51	6.25
B 61.	33.657	4.607	4.366	78.94	10.25	10.81
B 65.	33.041	3.517	4.595	80.18	11.15	8.67
B 69.	32.844	4.951	4.893	76.94	11.46	11.60
B 73.	33.484	4.745	4.056	79.20	9.58	11.21
B 83.	28.291	3.226	5.572	76.28	15.02	8.70
B 87.	32.284	5.295	4.767	76.24	11.26	12.49
B 92.	42.260	1.056	1.122	95.10	2.52	2.38
B 96.	40.259	1.627	0.941	94.00	2.20	3.80
B 99.	32.811	4.898	4.073	78.53	9.74	11.73
B 101.	32.470	4.959	3.905	78.54	9.46	12.00
B 106.	37.617	3.216	3.797	84.29	8.49	7.21
B 109.	34.004	2.162	3.263	86.24	8.27	5.49
Average :	34.852	3.527	3.768	82.60	9.00	8.40

11.2.1. RATIOS OF SOME OXIDES :

The ratios of some oxides of the Barail sandstones are shown in table 11.2.3. The TiO_2/Al_2O_3 ratios, ranging between 0.05 and 0.21, and averaging 0.10 indicate the presence of acidic and basic materials besides humid climatic conditions (Spears and Sotiriov, 1976). K_2O/Na_2O ratios, ranging between 1.08 and 5.41, and averaging 2.30, point to an exogeosynclinal environment of deposition (Middleton, 1960).

11.2.2. RELATIONSHIPS OF SOME OXIDES :

The values of (SiO_2+TiO_2), Al_2O_3 and the remaining oxides, excluding MnO and P_2O_5, are recalculated (Table 11.2.4) and used as end members in a ternary diagram (Fig. 11.2.2) following Kukal (1968) for rock nomenclature. Plots suggest that the sandstones be categorised as subgraywackes and graywackes. Following Herron (1988) log values of Fe_2O_3/K_2O ratios are plotted against those of SiO_2/Al_2O_3 (Fig. 11.2.3, Table 11.2.4) in a binary diagram. According to this scheme the sandstones may be termed litharenites and graywackes.

The percentages of CaO, Na_2O and K_2O (Fig. 11.2.4, Table 11.2.4) and that of Fe_2O_3, MgO and TiO_2 (Fig. 11.2.5, Table 11.2.4) are recalculated and plotted in ternary diagrams following Condie (1967). The diagrams suggest a granitic source for the sediments. SiO_2 percentages are plotted agaist those of total Al_2O_3, K_2O and Na_2O (Fig. 11.2.6) in a binary diagram following Suttner and Dutta (1986). Plots indicate that the paleoclimatic conditions were semi-humid to semi-arid.

The values of (Fe_2O_3+MgO), Na_2O and K_2O (Fig. 11.2.7, Table 11.2.4), recalculated and plotted in a ternary diagram

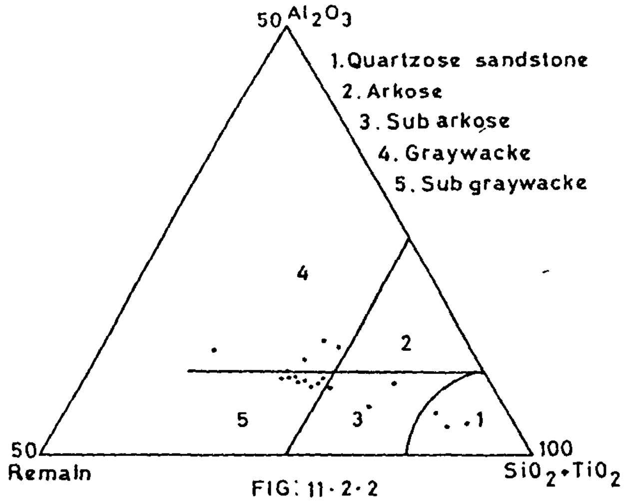

FIG: 11·2·2

Chemical composition of Barail sandstones expressed in the $SiO_2(+TiO_2)-Al_2O_3$-Remaining oxides triangle

(After Kukal, 1968)

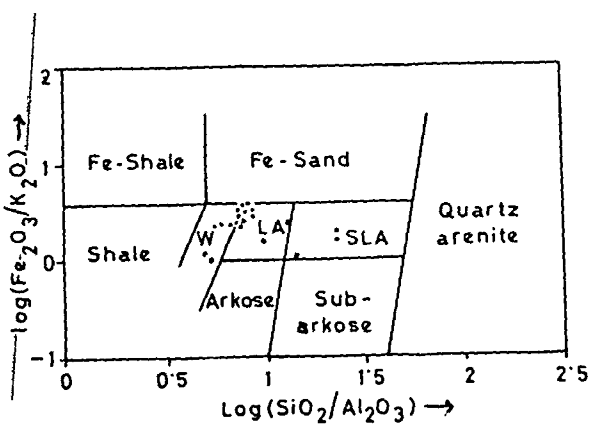

FIG: 11·2·3

W-Wacke LA-Litharenite SLA-Sublitharenite

Geochemical classification of the sandstones of the Barail Group.

(After Herron, 1988)

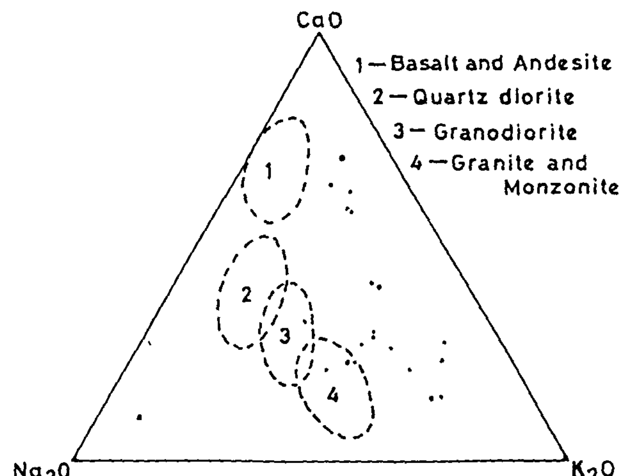

FIG: 11·2·4

Chemical composition of Barail sandstones in relation to Provenance

(After Condie, 1967)

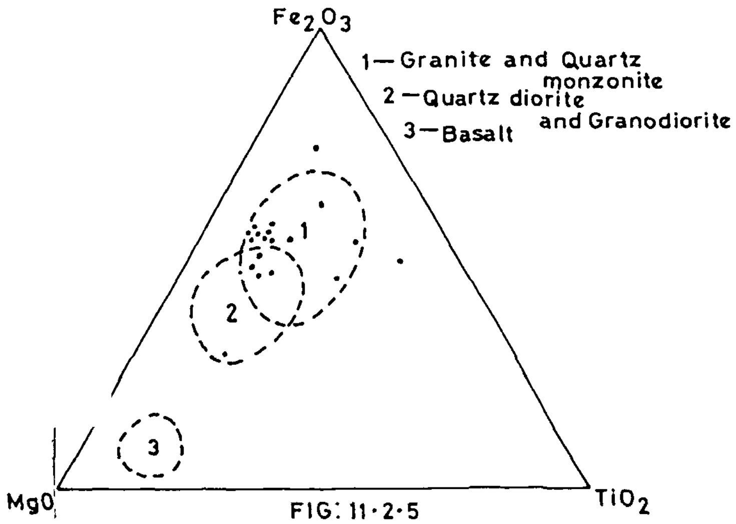

FIG: 11·2·5

Chemical composition of Barail sandstones in relation to Provenance (After Condie, 1967)

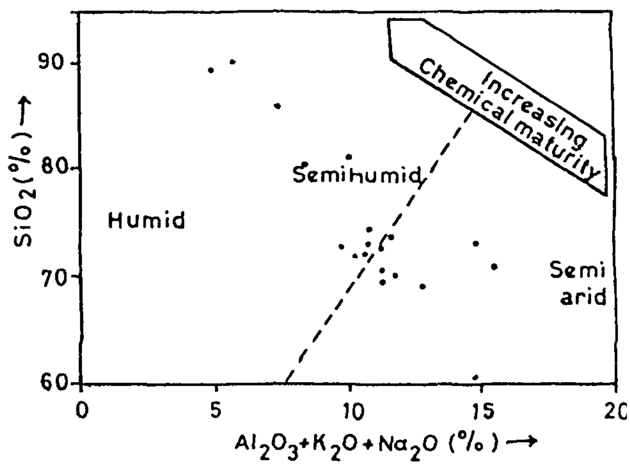

FIG: 11·2·6

Bivariate plots between SiO_2 and Total Al_2O_3, Na_2O and K_2O percentages of the Disang sandstones (After Suttner and Dutta, 1986)

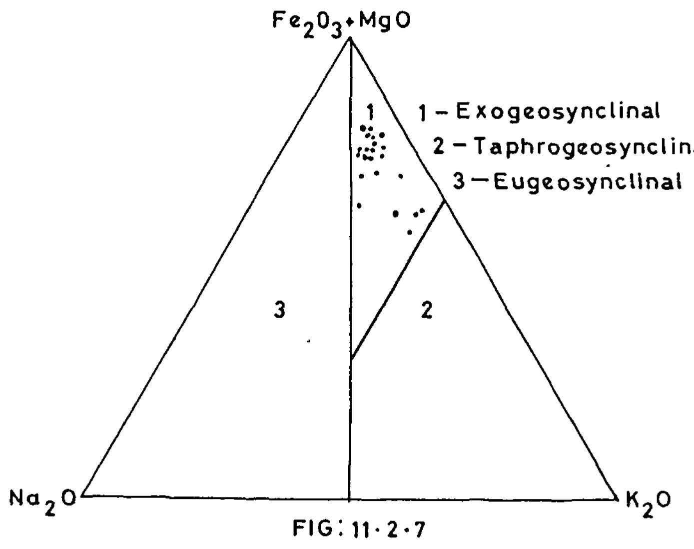

FIG: 11·2·7

Chemical composition of Barail sandstones in relation to Tectonic setting (After Blatt et al., 1980)

Table 11.2.3

Major oxide composition (volatile-free) and some ratios of the Barail sandstones.

Sample No.	SiO_2	TiO_2	Al_2O_3	Fe_2O_3	FeO	CaO	MgO	Na_2O	K_2O	A	B	C	D
B 1.	73.72	1.12	11.86	3.21	2.37	3.09	2.50	0.76	1.37	6.22	0.09	2.35	1.80
B 11.	84.46	0.59	8.70	1.89	6.54	0.43	0.60	0.41	1.57	9.71	0.07	1.64	2.77
B 22.	91.56	0.21	4.01	1.02	4.42	0.47	0.60	0.44	0.51	22.83	0.05	2.00	1.16
B 30.	72.12	0.67	9.94	4.04	2.90	0.55	2.59	1.02	1.10	7.76	0.07	3.67	1.08
B 34.	76.88	0.67	13.51	3.80	4.35	0.36	0.75	0.43	1.62	5.69	0.05	2.35	3.75
B 45.	77.68	0.83	8.91	3.98	3.19	0.66	2.52	0.90	1.26	8.72	0.09	3.15	1.41
B 49.	77.77	0.97	9.24	3.96	2.72	0.76	2.48	0.82	1.25	8.41	0.10	3.15	1.53
B 53.	76.06	0.68	9.98	3.80	6.59	3.18	2.56	0.60	1.20	7.62	0.07	3.16	2.01
B 61.	78.27	0.89	9.46	4.33	2.20	0.70	2.38	0.58	1.11	8.27	0.09	3.91	1.92
B 65.	74.27	1.28	13.97	1.94	2.37	0.40	1.06	0.53	1.70	5.32	0.09	1.14	3.17
B 69.	75.82	0.77	10.09	4.32	2.90	0.73	2.84	1.02	1.42	7.51	0.07	3.04	1.39
B 73.	76.37	0.76	9.55	4.03	1.94	2.67	2.60	0.65	1.29	7.99	0.08	3.12	1.98
B 83.	65.45	1.19	3.18	2.10	6.33	5.03	4.01	1.12	1.52	4.96	0.09	1.38	1.35
B 87.	74.35	1.43	10.77	4.33	2.70	1.19	2.29	1.00	1.86	6.91	0.13	2.33	1.86
B 92.	92.12	0.87	4.07	1.03	2.85	0.31	0.23	0.12	0.66	22.66	0.21	1.55	5.41
B 96.	88.70	0.67	6.33	1.26	3.36	0.33	0.42	0.19	0.88	14.00	0.11	1.42	4.52
B 99.	75.17	1.09	9.91	4.13	1.89	1.81	3.83	0.83	1.70	7.59	0.11	2.43	2.04
B 101.	76.05	1.21	10.25	3.64	2.22	1.38	3.05	0.62	1.45	7.42	0.12	2.50	2.33
B 106.	81.86	0.95	6.18	3.57	1.76	0.80	2.59	0.65	1.59	13.25	0.15	2.25	2.44
B 109.	77.47	0.75	8.70	3.17	5.75	3.86	2.76	0.53	1.06	8.90	0.09	2.98	2.00
Average:	78.56	0.88	9.43	3.17	3.46	1.43	2.11	0.66	1.30	9.59	0.10	2.48	2.30

A - SiO_2/Al_2O_3
B - TiO_2/Al_2O_3
C - Fe_2O_3/K_2O
D - K_2O/Na_2O

Table 11.2.4

Log values of some ratios and ratios among some major oxides of the Barail sandstones.

Sample No.	log (Fe_2O_3/K_2O)	log (SiO_2/Al_2O_3)	CaO :	Na_2O :	K_2O	Fe_2O_3 :	MgO :	TiO_2	Fe_2O_3 + MgO :	Na_2O	K_2O
B 1.	0.37	0.79	59.27	14.52	26.21	46.99	36.36	16.33	72.88	9.66	17.45
B 11.	0.21	0.99	21.35	20.83	57.81	61.28	19.53	19.19	61.38	10.23	28.39
B 22.	0.30	1.36	33.09	30.93	35.97	55.55	32.78	11.67	63.09	17.06	19.84
B 30.	0.56	0.89	20.47	38.19	41.34	55.32	35.49	9.19	75.78	11.63	12.59
B 34.	0.37	0.76	14.85	17.90	67.25	72.84	14.28	12.88	68.95	6.53	24.52
B 45.	0.50	0.94	23.33	31.85	44.81	54.35	34.38	11.27	75.03	10.37	14.59
B 49.	0.50	0.92	26.69	28.95	44.36	53.45	33.48	13.07	75.62	9.62	14.75
B 53.	0.50	0.88	63.86	11.97	24.16	53.94	36.40	9.66	77.95	7.31	14.74
B 61.	0.59	0.92	29.22	24.20	46.57	57.00	31.28	11.71	79.95	6.86	13.19
B 65.	0.06	0.73	15.14	20.32	64.54	45.34	24.75	29.90	57.31	10.22	32.46
B 69.	0.48	0.88	23.05	32.20	44.74	54.56	34.78	9.66	74.52	10.66	14.81
B 73.	0.49	0.90	57.97	14.09	27.94	54.54	35.21	10.24	77.36	7.59	15.05
B 83.	0.14	0.70	65.49	14.65	19.86	28.74	54.96	16.30	69.75	12.84	17.41
B 87.	0.37	0.84	29.44	24.67	45.89	53.80	28.44	17.76	69.84	10.54	19.61
B 92.	0.19	1.36	28.04	11.21	60.75	48.32	11.00	40.67	61.69	5.97	32.34
B 96.	0.15	1.15	23.36	13.87	62.77	52.81	17.75	29.44	60.82	7.09	32.09
B 99.	0.39	0.88	41.62	19.21	39.16	48.01	39.30	12.67	74.76	8.31	16.93
B 101.	0.40	0.87	39.87	18.04	42.09	46.06	38.59	15.35	76.31	7.11	16.58
B 106.	0.35	1.12	26.42	21.40	52.17	50.21	36.48	13.30	73.36	7.75	18.89
B 109.	0.47	0.95	70.70	9.66	19.53	47.53	41.31	11.16	78.78	7.07	14.14
Average :	0.37	0.86	35.66	20.93	43.41	52.03	31.89	16.08	71.26	9.22	19.52

following Blatt et al. (1980), suggest an exogeosynclinal environment of deposition. SiO_2 contents plotted against K_2O/Na_2O ratios (Fig. 11.2.8, Table 11.2.3) and SiO_2/Al_2O_3 ratios against that of K_2O/Na_2O ratios (Fig. 11.2.9, Table 11.2.3) following Roser and Korsch (1986) suggest a passive continental margin for the sandstones.

11.2.3. RELATIONSHIP OF SOME MAJOR ELEMENTS :

The values of Si, Al and FeT are recalculated to 100 percent and plotted in a ternary diagram (Fig. 11.2.10, Table 11.2.2) following Moore and Dennen (1970) for rock nomenclature. Following this method the Barail sandstones may be categorised as dominantly subgraywackes.

11.3. RARE EARTH ELEMENTS :

The sandstone samples are analysed for all the rare earth elements, viz., La, Ce, Pr, Nd, Pm, Sm, Eu, Gd, Tb, Dy, Ho, Er, Tm, Yb, Lu and Y (Table 11.3.1). In parts per million they range from 20 to 30, 38 to 64, 4.8 to 7.7, 19 to 29, 4 to 5.8, 0.63 to 1.10, 1.24 to 2.60, 0.15 to 0.41, 0.81 to 1.80, 0.21 to 0.30, 0.26 to 0.53, $<$0.05 to 0.08, 0.19 to 0.42, $<$0.04 to 0.09 and 0.45 to 7.80 respectively. The average contents in parts per million are 26.75, 51, 6.48, 27.25, 5.35, 0.92, 1.89, 0.27, 1.39, 0.25, 0.46, 0.07, 0.33, 0.05 and 3.67 respectively. The vertical distribution of the REE of the Barail sandstones, which is irregular, is shown in figure 11.3.1.

The chondrite normalised values of the REE and their patterns are shown in figure 11.3.2 and table 11.3.2. The REE distribution shows a steep LREE enriched-HREE depleted pattern (ΣLREE/ΣHREE - 21.78 to 30.00). Three samples show negative Eu anomalies (Eu/Eu^* - 0.79 to 0.88) whereas one sample shows a positive Eu anomaly (Eu/Eu^* - 1.14). The ΣREE content in the

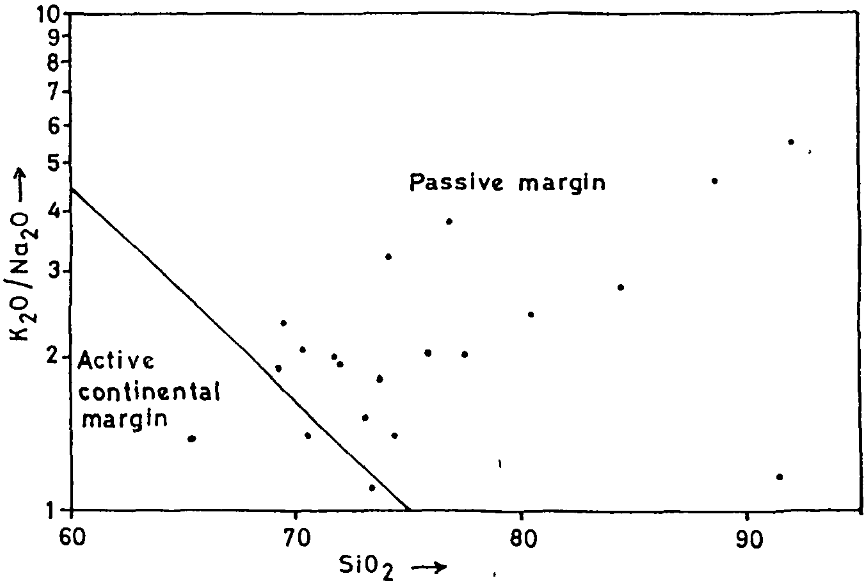

FIG: 11·2·8

Tectonic discrimination diagram for Barail sandstones

(After Roser & Korsch, 1986)

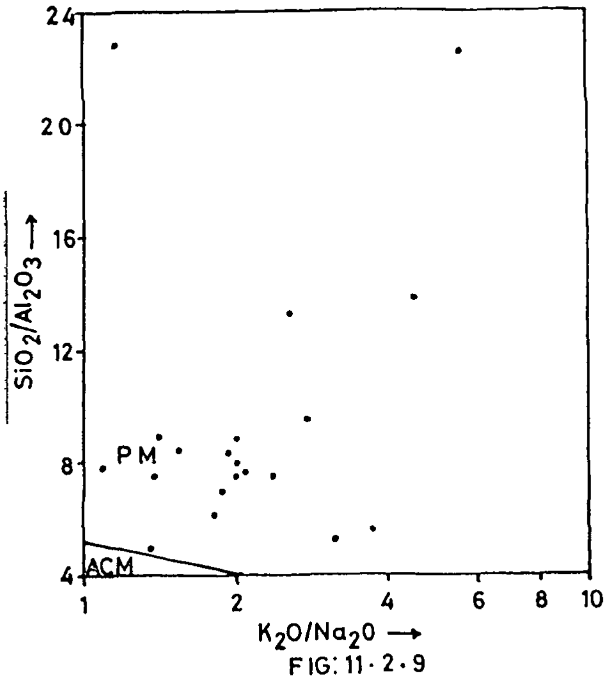

FIG: 11·2·9

Tectonic discrimination diagram for Barail sandstones

(After Roser & Korsch, 1986)

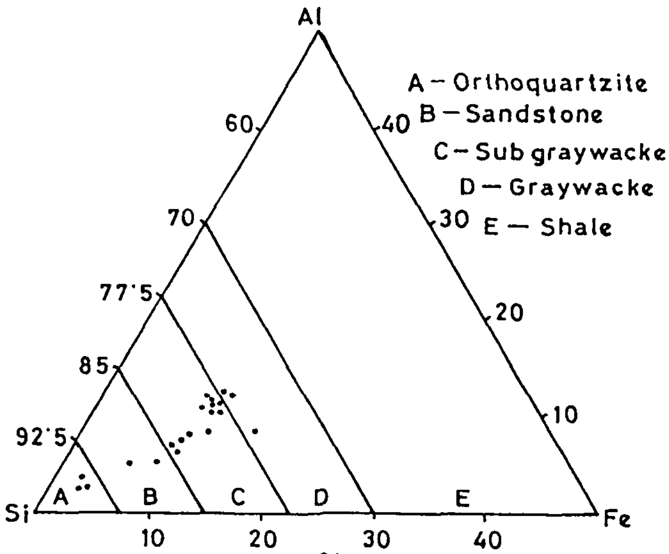

FIG: 11·2·10

Ternary plots of Si–Fe–Al of Barail sandstones

(After Moore & Dennen, 1970)

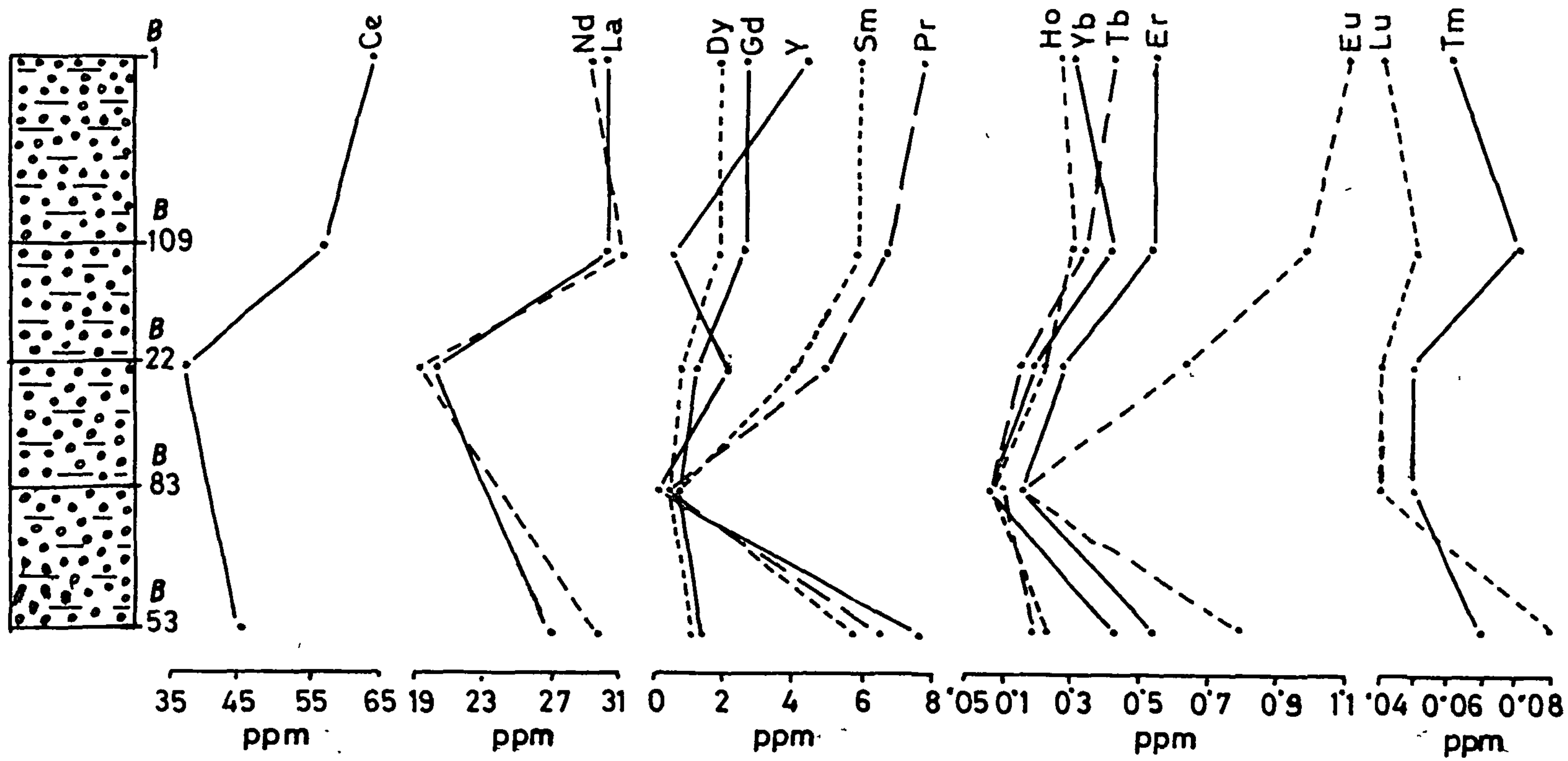

FIG: 11·3·1

VERTICAL VARIATION OF RARE EARTH ELEMENTS OF THE BARAIL SANDSTONES

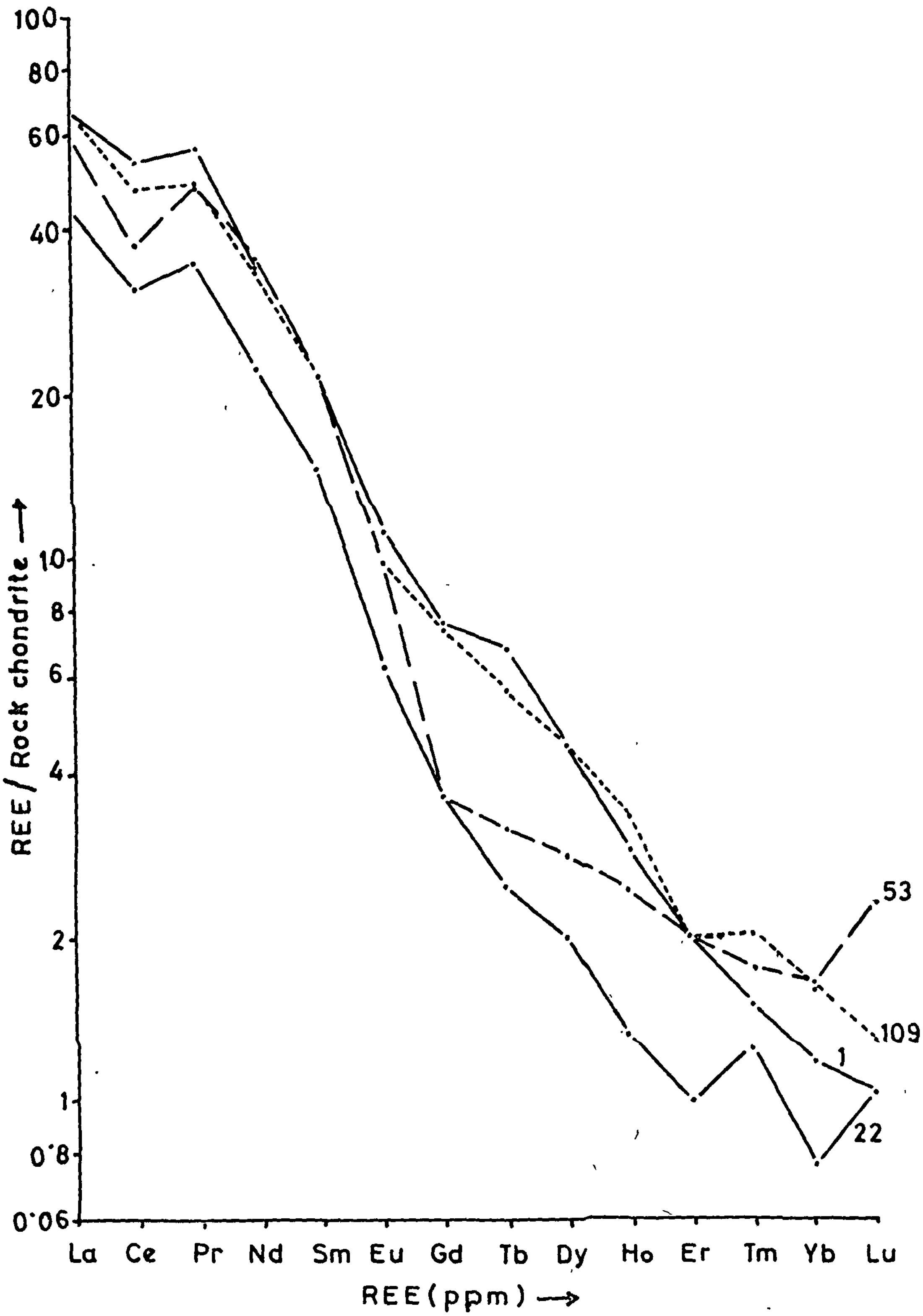

FIG: 11·3·2

Chondrite normalised REE pattern of the sandstones of the Barail Group

(After Evensen et al.,1978)

Table 11.3.1

Rare earth element composition and values of total LREE and HREE of the Barail sandstones.

Element	B 1	B 22	B 53	B 109	Average
La	30.00	20.00	27.00	30.00	26.75
Ce	64.00	38.00	45.00	57.00	51.00
Pr	7.70	4.80	6.70	6.70	6.48
Nd	29.00	19.00	30.00	31.00	27.25
Sm	5.80	4.00	5.80	5.80	5.35
Eu	1.10	0.63	0.98	0.98	0.92
Gd	2.60	1.24	1.24	2.48	1.89
Tb	0.41	0.15	0.19	0.34	0.27
Dy	1.80	0.81	1.14	1.80	1.39
Ho	0.26	0.21	0.22	0.30	0.25
Er	0.53	0.26	0.53	0.53	0.46
Tm	0.06	<0.05	0.07	0.08	0.07
Yb	0.30	0.19	0.42	0.41	0.33
Lu	<0.04	<0.04	0.09	0.05	0.05
Y	4.31	2.10	7.80	0.45	3.67
Total:	147.89	91.38	127.18	137.92	
La/Yb	100.00	105.26	64.29	73.17	
ΣLREE	136.50	85.20	114.50	130.50	
ΣHREE	6.00	2.86	3.90	5.99	

Table 11.3.2

Chondrite normalised REE values of the Barail sandstones.

Element	B 1	B 22	B 53	B 109	Average
La	65.217	43.478	58.696	65.217	58.152
Ce	53.333	31.667	37.500	47.500	42.500
Pr	56.204	35.036	48.905	48.905	47.262
Nd	34.118	22.352	35.294	36.471	32.059
Sm	21.481	14.815	21.481	21.481	19.814
Eu	11.111	6.364	9.899	9.899	9.318
Gd	7.600	3.647	3.647	7.294	5.547
Tb	6.833	2.500	3.167	5.667	4.542
Dy	4.500	2.025	2.850	4.500	3.469
Ho	2.921	1.348	2.472	3.371	2.528
Er	2.038	1.000	2.038	2.038	1.778
Tm	1.538	1.282	1.795	2.051	1.666
Yb	1.200	0.760	1.680	1.640	1.320
Lu	1.053	1.053	2.368	1.316	1.447
Eu/Eu*	0.88	0.88	1.14	0.79	0.92
Ce/Ce*	0.87	0.81	0.70	0.83	0.80

Barail sandstones appears to be high (89.28 to 143.59 ppm) and a strong negative Ce anomaly is noted (Ce/Ce^* - 0.70 to 0.87).

11.4. TRACE ELEMENTS :

The trace elements analysed are B, Mo, Ni, Co, V, Cr, Rb, Ga, Cd, Zn, and Zr (Table 11.4). In parts per million Ni ranges from <20 to 55, Co from <20 to 50, V from <10 to 50, Cr from <10 to 35, Cd from <20 to 55, Zn from 35 to 135 and Zr from 40 to 350. B and Rb are <20 ppm each while Mo and Ga are <10 ppm each in the Barail sandstones. On the average B, Mo, Ni, Co, V, Cr, Rb, Ga, Cd, Zn and Zr are <20, <10, 35, 26, 17, 18, < 20, <10, 35, 82 and 143 ppm respectively. Their distribution in the different lithounits in ascending order is shown in figure 11.4.1. As in the case of the major oxides and REE the trace elements are irregularly distributed.

11.4.1. RATIOS OF SOME TRACE ELEMENTS :

Certain ratios have been used successfully for determination of ventilation and Eh conditions in the depositional environment. Cr/V ratios range from 0.60 to 2.50 and average 1.24 (Table 11.4). The Ni/Co ratios range from 0.50 to 2.00 and average 1.26 (Table 11.4). These values, according to Dykpiv (1979), suggest good to moderate ventilation and lowering Eh conditions respectively.

11.4.2. RELATIONSHIPS OF SOME TRACE ELEMENTS :

Following Degens *et al*. (1957) percentages of B, Rb and Ga, recalculated and plotted (Fig. 11.4.2, Table 11.4) in a ternary diagram, indicate a marine environment of deposition. Also following Degens *et al*. (1957) pmm B is plotted against ppm Ga (Fig. 11.4.3) and ppm B against ppm Rb (Fig. 11.4.4) in binary

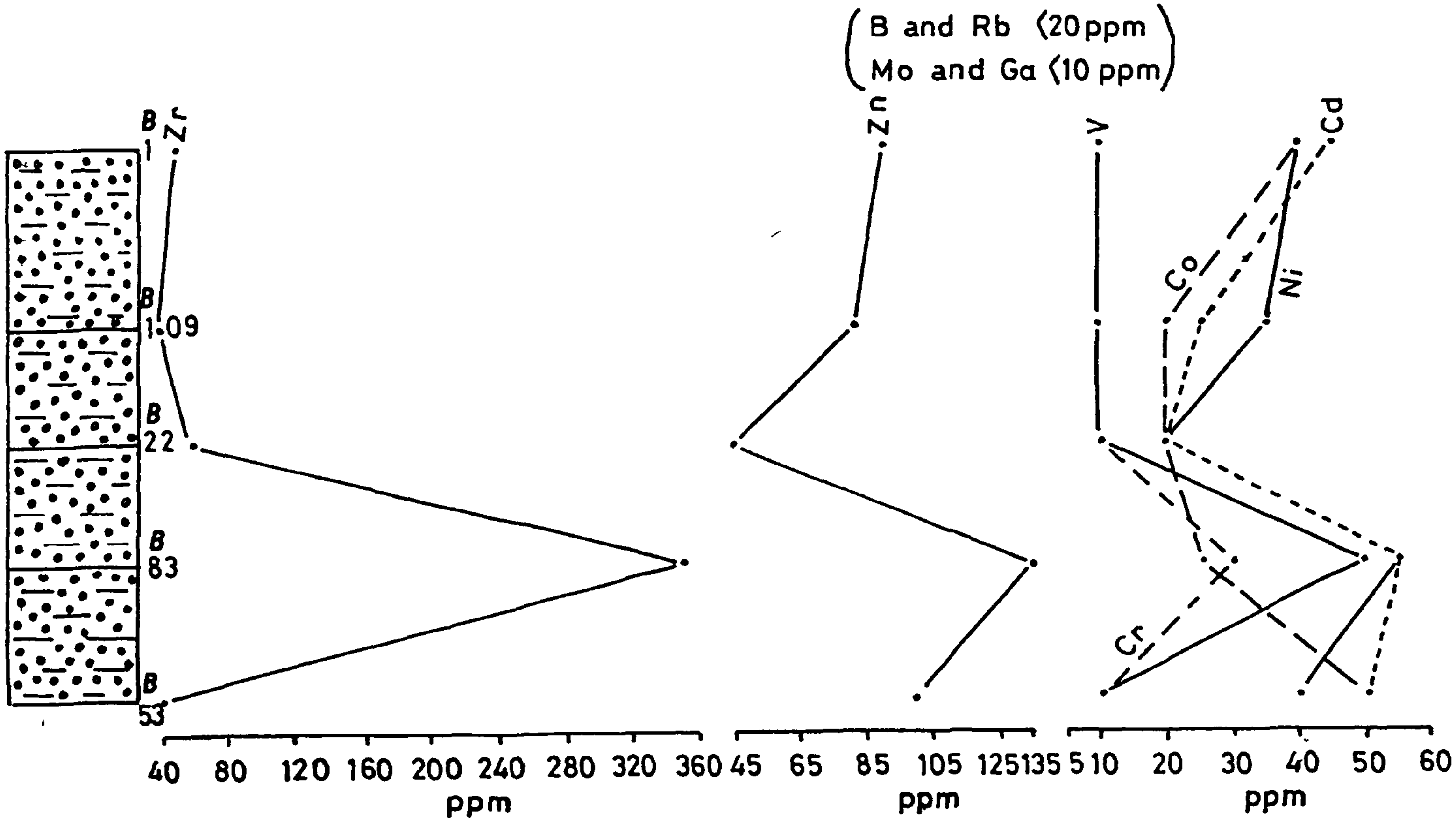

FIG: 11 · 4 · 1

VERTICAL VARIATION OF TRACE ELEMENTS OF THE BARAIL SANDSTONES

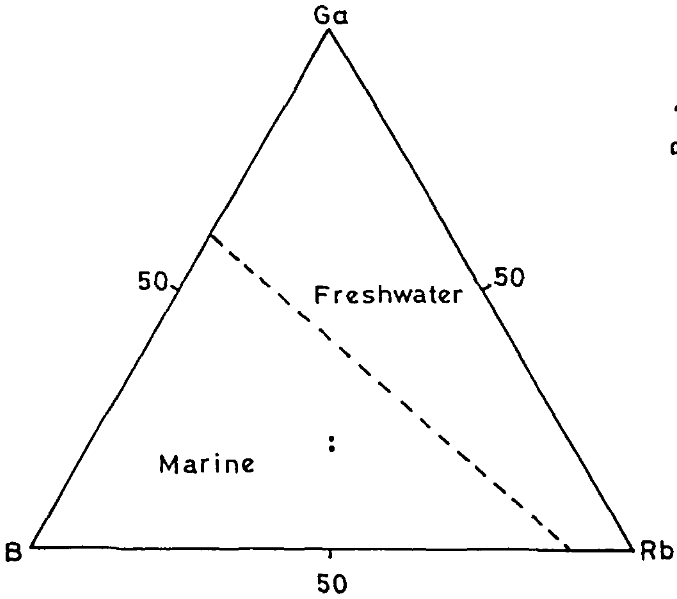

FIG: 11·4·2
Relationship among Ga, B and Rb in Barail sandstones

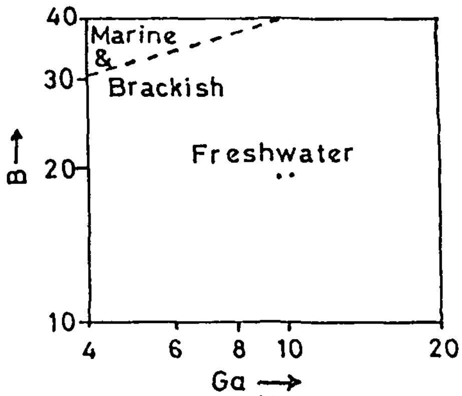

FIG: 11·4·3
Relationship between B & Ga(ppm) in Barail sandstones

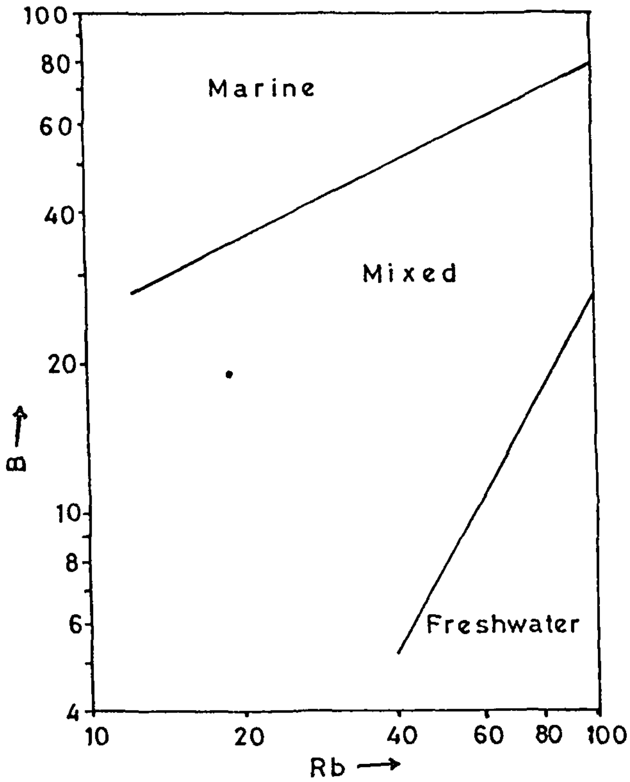

FIG: 11·4·4
Relationship between B & Rb (ppm) in Barail sandstones

Table 11.4

Trace element composition and some ratios of the Barail sandstones.

Sample No.	B	Mo	Ni	Co	V	Cr	Rb	Ga	Cd	Zn	Zr	Cr/V	Ni/Co
B 1.	< 20	<10	40	40	10	<10	<20	<10	45	90	50	0.95	1.00
B 11.	< 20	<10	30	20	10	20	<20	<10	20	60	200	2.00	1.50
B 22.	< 20	<10	< 20	<20	10	10	<20	<10	<20	45	60	1.00	1.00
B 34.	< 20	<10	40	20	15	15	<20	<10	55	110	160	1.00	2.00
B 53.	< 20	<10	40	50	<10	<10	<20	<10	50	100	40	1.00	0.80
B 65.	< 20	<10	40	25	25	35	<20	<10	50	90	160	1.40	1.60
B 83.	< 20	<10	55	25	50	30	<20	10	50	135	350	0.60	0.50
B 92.	< 20	<10	< 20	20	10	25	<20	<10	<20	35	200	2.50	0.97
B 96.	< 20	<10	30	20	20	20	<20	<10	20	80	170	1.00	1.50
B 109.	< 20	<10	35	20	<10	<10	<20	<10	25	80	40	1.00	1.75
Average	< 20	< 10	34.90	25.95	16.90	18.35	< 20	< 10	35.40	82.50	143	1.24	1.26

diagrams. These plots suggest fresh and mixed environments of deposition respectively for the Barail sandstones.

PART IV

CHAPTER 12

DISCUSSION AND CONCLUSION

12.1. DISANG GROUP :

The Disang sediments of the area around Botsa comprise thick sequences of shales with alternations of thin bedded sandstones and siltstones. The thickness of sandstones gradually increase towards the top. The Disangs of Nagaland, including those of the area under investigation, are categorised as a flysch facies (Directorate of Geology and Mining, Nagaland, 1978).

The flysch facies is argillaceous with rhythmic alternations of shales and thin bedded sandstones (Pettijohn, 1975) and is lithologically characterised by a facies uniformity with prevalence of clastic rocks. Flysch sediments are generally poor in fossils but contain sedimentary structures such as laminations, graded bedding, etc. They are deposited below the action of water waves by turbidity currents (Cicha et al., 1968). According to Dzulynski and Walton (1965), and Friedman and Sanders (1978) flysch are marine sediments with monotonous alternating layers of shales mudstones, siltstones and coarser sediments that form thick deposits which are laterally persistent.

The Disangs of Nagaland may be classed as dichronous, ranging from Maestrichtian to Thanetian, based on the finding of some Globotruncana sp. and Dandotiaspora dilata, the former by the Geological Survey of India (Dutta, 1993).

12.1.1. PROVENANCE :

The Disang sandstones contain non-undulose, undulose and polycrystalline quartz in different proportions. The non-undulose variety is considered as from an igneous source (Folk, 1968; Blatt et al, 1980). Undulose, (Folk, 1960; Blatt and Christie, 1963; Blatt, 1967; Waugh, 1970) and polycrystalline quartz (Blatt, 1967) suggest derivation of the sediments from a metamorphic terrain. Length-breadth ratios of quartz of the Disang sandstones point to igneous and metamorphic sources, the latter being dominant. According to Bokman (1962) quartz with ratios greater than 2 are most probably contributed from a metamorphic, terrain while the same with ratios less than 2 are probably of igneous origin. Phyllitic and slaty material present in the sandstones are indicative of a metamorphic origin (Mack, 1984). The occasional chert, fine grained sediments and polycrystalline quartz probably suggest recycling of the sediments. Relationships among quartz, feldspar and lithic fragments indicate a recycled orogen which was probably the source of the Disang sediments (Dickinson and Suczek, 1979).

The clay minerals detected in the Disang sandstones are illite and chlorite, a major fraction of which may be detrital. Illite is an igneous mineral while chlorite is considered a low-rank metamorphic (Grim, 1968). They are present in more or less equal amounts suggesting decrease of hydrolytic processes and increase in direct rock erosion at higher latitudes.

The polymodal nature of the grain-size curves may be attributed to multiple sources of the sediments (Visher, 1969). The range in median diameter values probably suggests changes in the provenance area during sedimentation. The heavy minerals present in the sediments also point to a mixed source. Pale yellow to brown tourmaline with prismatic forms are considered to be igneous minerals (Krynine, 1946); so also zircon

(Poldervaart, 1955). Epidote, garnet, pale brown tourmaline, rutile and kyanite are low to medium grade metamorphic minerals (Poldervaart, 1955; Heinrich, 1956; Folk, 1960; Pettijohn, 1975; Choudhury and Gill, 1981). The paucity of the heavy minerals suggest recycling of the sediments.

TiO_2/Al_2O_3 ratios of the sandstones indicate recycling and/or an acidic source. The Al and Fe contents of the Disang sandstones are much higher than those of the average clastic rocks. Excess Al in sediments is attributed to a granitic source while excess Fe to a basaltic one (Moore and Dennen, 1970). Triangular plots of CaO-Na_2O-K_2O and Fe_2O_3-MgO-TiO_2 after Condie (1967) also suggest granitic and basaltic provenances.

McLennan (1989) is of the view that Eu/Eu* ratios are good indicators of degree of intracrustal differentiation processes. The negative Eu/Eu* ratios of the Disang sandstones suggest moderate differentiation processes. The HREE-depleted patterns suggest a provenance of some Na-rich granitic rocks (Potter, 1978a, b), though contribution from a metamorphic terrain cannot be ruled out.

12.1.2. TRANSPORTATIONAL PROCESSES :

The Disang sediments of the Botsa area are mostly angular to subangular. Most of the quarts grains have length-breadth ratios greater than 2. These features suggest transportation of sediments over a short distance.

CM patterns indicate that the sediments of the Disang Group were transported as uniform and graded suspensions by turbidity currents. FM, LM and AM patterns of the finer sediments indicate that they are uniform suspension deposits. The presence of both uniform and graded suspension deposits indicate fluctuating current velocities (Passega, 1972, 1977). The range in median diameter values also suggest fluctuations in energy conditions in the sedimentary environment besides other changes in conditions of sedimentation (Rao, 1977; Venkatesh and Ray, 1981). Poor to moderate sorting, as in the case of the Disang sandstones, are indicative of variable and turbulent currents during deposition and little reworking (Wigely, 1961; Visher, 1969). Poorly sorted suspension populations indicate that the depositional basin was highly mobile which is attributed to turbulence created at depth due to incoming fresh waters laden with suspended sediments (Passega, 1972). Skewness values of these sandstones have a wide range and are mostly positive. According to Awasthi (1970) this indicates steady decrease of energy of the depositing agent. Unidirectional currents are responsible for positive skewness in sediments (Friedman, 1961; Martins, 1965). Coarse skewness values are attributed to high energy environments (Sahu, 1964). Great variation is noted in the percentages of suspension and saltation populations and in the positions of the truncation points of the saltation population which fall on the coarser sides of the curves. These are attributed to fluctuating current velocities and indicate that the combined hydraulic factors and bed roughness were variable. Much mixing is observed between the two populations which is due to variable energy conditions (Visher, 1969). Larger quantities of the suspension population suggest that the depositing medium had a high concentration of the same and that these sediments were rapidly deposited (Schumm, 1963) during the final phase of deposition when the velocity and buoyancy of flow were sufficiently reduced (Singh and Bhardwaj, 1991). Catenae of zircon and tourmaline indicate less attrition of the sediments and that they are water-laid. Discriminant function analyses suggest that fluvial and turbidity processes were responsible for transportation and deposition of the sediments.

Z.T.R. indices are indicative of rapid erosion, short transportation and quick deposition of the sediments. Parallel laminations noted in some of the sandstones owe their origin to fluctuations in current velocities in the depositional environment (Allen, 1970; Pettijohn, 1975). In turbidites they may originate due to deposition from a perfectly smooth, gradually decelerating suspension current (Kuenen, 1966).

12.1.3. DEPOSITIONAL ENVIRONMENTS :

The Disang sandstones contain some stable minerals. Stable minerals are indicators of a tectonically stable basin such as that of a passive continental margin (Folk, 1968). Chlorite and illite are constituents of a near-shore marine environment (Millot, 1942; Mason, 1966) where they form a stable pair at of a passive continental margin. This is an area of lowered rates of heat flow and reduced geothermal gradients as well as rapid subsidence and quick burial of terrigenous detritus and chemical sediments (Siever, 1979). The high concentration of K and Mg in sea water is a favourable factor for the formation of illite and chlorite (Grim, 1968).

Mean size-standard deviation, skewness-standard deviation and skewness-kurtosis plots indicate that the Disang sediments were deposited in a river environment. Studies of relationships between mean size and standard deviation indicate a rapidly sinking depositional basin with low tectonic uplift of the source (Inman, 1952; Cadigan, 1961). The sediments may belong to a lower deltaic plain environmental regime. Discriminant function analyses of these sandstones suggest that they were deposited in fluvial and shallow agitated marine environments.

SiO_2 Vs K_2O/Na_2O and SiO_2/Al_2O_3 Vs K_2O/Na_2O binary plots indicate a passive continental margin (Roser and Korsch, 1986). K_2O/Na_2O

ratios, which are greater than 1, are indicative of sediments deposited in plate interiors at passive margins (Bhatia, 1983) in exogeosynclinal environments (Middleton, 1960). Triangular plots of (Fe_2O_3 + MgO), Na_2O and K_2O also indicate an exogeosynclinal set-up. Exogeosynclinal sediments are deposited in a near-shore environment (Blatt et al., 1980) and are derived from older metamorphic and sedimentary sources (Middleton, 1960). According to White (1970) the marine environment is enriched in B. The B content in the Disang sandstones suggest such an environment. Ternary plots of B, Rb and Ga and binary diagrams of B and Ga, and B and Rb suggest marine, fresh water and mixed environments respectively (Degens et al., 1957). Ga is highly mobile in the biogeochemical cycle (Goldschmidt, 1954). Its low occurrence indicates inactivity in the biological process (Sinha and Singh, 1964).

The Disangs are poor in their fossil content though some pelecypods and gastropods have been recorded from the upper horizons of the same in the Botsa area (Mishra, 1988). The presence of these fossils suggest a shallow marine environment. However, no such fossil is recorded from the Upper Disangs of Upper Assam (Dutta, 1993).

The polycrystalline and strained quartz present in appreciable amounts in the Disang sediments are indicative of low mineralogical maturity (Blatt, 1967). The length-breadth ratios of quartz also suggest the same (Bokman, 1952). However, Cr/V ratios (Dykpiv, 1957) suggest good ventilation in the depositional environment.

The sandstones are found to be more enriched in K_2O than Na_2O and CaO. Further, the TiO_2/Al_2O ratios are higher than the average continental rocks. In granites K_2O is more or less equal to that of Na_2O and CaO. The relative enrichment of K_2O suggests chemical maturation (Middleton, 1960). The high TiO_2/

Al_2O_3 ratios also indicate the same (Spears and Sotiriov, 1976). The low Na/Al and Na/K ratios are indicative of graywackes (Pettijohn, 1957).

The negative Eu values suggest moderately deep-water anoxic conditions during deposition (Freyer, 1977). This is supported by the presence of pyrite in the Disang sediments. Ni/Co ratios suggest decreasing Eh conditions in the depositional basin (Dykpiv, 1979). Quartz-rich sandstones have low values of La/Yb ratios and ΣREE (Cullers et al., 1979). The Disang sandstones, however, show high values compared to the average sedimentary rocks. The average quartz-clay ratio of the Disang sandstones is as low as 1.3 but the La/Yb ratios and ΣREE is less. These abnormal results suggest that the Disang sandstones have suffered the "quartz-dilution effect". This is supported by the floating appearance of quartz on the matrix.

The Z.T.R. indices indicate poor to moderate maturity of the sediments. From petrographic and geochemical studies it may be concluded that the Disang sandstones of the Botsa area are graywackes to subgraywackes. These two rock types are characteristic of an exogeosynclinal environment. The cementing materials of these rocks include iron oxide, silica and calcium carbonate. The iron oxides are dominant while silica is scarce. The sandstones of this group of the Botsa area show the development of load casts in some sections. Their origin is attributed to differential loading of the underlying hydroplastic muds which cause vertical readjustment when sand sinks downwards with compensatory upward movement of mud (Pettijohn, 1975). Some concretions are also observed in the Disang sandstones. Concretions form by post-depositional solution and precipitation (Pettijohn, 1975).

12.1.4. DIAGENESIS :

The Disang sandstones show a series of alteration in mineralogical composition which may be grouped as early and post diagenetic. The precipitation of hematite as cement around the detritals and in-situ alteration of plagioclase are common early diagenetic features. Feldspars are altered to illite during diagenesis (Grim, 1968, Mack, 1978, Iman and Shaw, 1985) where the excess K of feldspars is held by the illites (Keller, 1964). The in-situ alteration of feldspar to illite is well established (Pettijohn, 1975). Chlorite, a common accessory detrital mineral of immature sands, may be an alteration product of primary micas. It replaces illite when diagenesis merges into metamorphism. Chlorite is a characteristic constituent of the microcrystalline matrix of graywackes (Selley, 1976). These clay minerals forming the matrix of the sandstones appear to have acted as barriers against the silica solutions from reaching the quartz grains and forming overgrowths (Heald and Laresse 1974). The sutured edges of the mica grains suggest the effect of pressure solution during deep-burial diagenesis.

12.2. BARAIL GROUP :

The Barail Group of rocks exposed in the area are made up of sandstones with thin intercalations of papery shales. Sedimentation of the Barails began with the deposition of massive , thick bedded, multi-layered sandstones (Sahu and Naik, 1988) over the Disangs without a hiatus followed by thin bedded ones. They represent a molasse facies (Directorate of Geology and Mining, Nagaland, 1978).

The molasse facies consists of deposits that have been produced due to extensive erosion of highlands after the final phase of an orogeny and deposited in marine, brackish or fresh-water environments. In these sediments laminations, ripple marks, etc. are common features (Cicha et al., 1968). Pettijohn (1975) considers molasse sediments as shallow-water deposits of deltas, closed bays or near-shore marshes which originate above wave base. These areas represent transitional environments which are made up mostly of recycled sediments with rock particles of sedimentary and low-grade metamorphic origin. The rock types of this environment are a mixture of graywackes, subgraywackes and quartzose sandstones (Kukal, 1968). According to Friedman and Sanders (1978) the molasse is a wedge-shaped body with shallow marine and non-marine strata, the sediments of which are derived due to erosion of older geosynclines, including flysch. The age of the Barail Group of rocks was considred as Oligocene (Mathur and Evans, 1964; Krishnan, 1968). However, Handique et al. (in Press), based on fossil evidence, opine that the Barails range from Late Eocene to Oligocene.

12.2.1. PROVENANCE :

The quartz types of the Barail sandstones include non-undulatory, undulatory, polycrystalline and reworked. Non-undulose variety of quartz, which are derived from igneous sources (Folk, 1968; Blatt et al., 1980), are most dominant in these sandstones. The undulose type is representative of a metamorphic source (Folk, 1960; Blatt and Christie, 1963; Blatt, 1967; Waugh, 1970). Polycrystalline quartz is also derived from a metamorphic terrain (Blatt, 1967). Length-breadth ratios of quartz, as deduced following Bokman (1952), indicate both igneous and metamorphic sources, the former proportionately greater. The presence of slaty and phyllitic materials indicate a low-grade metamorphic source (Mack, 1984) for the sediments. The presence of chert, some polycrystalline quartz and metasedimentary particles in sandstones, such as those of the Barails, suggests recycling of sediments from an orogenic source. Relationships of quartz, feldspar and lithic fragments also suggest the same (Dickinson and Suczek, 1979). Some of the coarser quartz grains of the Barail sandstones are well rounded and some have attained a high sphericity. These features, together with quartz detritals showing remnants of overgrowths suggest recycling (Lewis, 1984).

The Barail sediments contain illite and chlorite, a minor fraction of which may be original. According to Grim (1968) illite and chlorite are igneous and metamorphic minerals respectively. Their occurrence in similar proportions suggests more of direct erosion rather than weathering of the provenance.

The grain-size curves are bimodal and polymodal. Such curves indicate multiple sources of the sediments (Visher, 1969). Inconsistent median diameter values of these sandstones are probably due to changes in the provenance during sedimentation processes. The presence of heavy minerals like the opaques and zircon in the Barail sandstones suggest an igneous source (Poldervaart, 1955); so also yellow to brown prismatic tourmaline (Krynine, 1946). Pale brown tourmaline, epidote, garnet, rutile and kyanite indicate a low to medium grade metamorphic source (Poldervaart, 1955; Heinrich, 1956; Folk, 1960; Pettijohn, 1975; Choudhury and Gill, 1981). Their overall paucity suggests recycling of the sediments. TiO_2/Al_2O_3 ratios of the sediments suggest recycling and/or an acidic provenance. The Barail sediments are enriched in aluminium and Al-enriched sediments are derivatives of granitic sources (Moore and Dennen, 1970). A granitic source is inferred from the CaO-Na_2O-K_2O and Fe_2O_3-MgO-TiO_2 relations of Condie (1967). Studies made after McLennan (1989) of Eu/Eu* relationships suggest that intracrustal differentiation processes during the formation of the Barail sandstones were not as pronounced as they were for the Disangs. The Barail sandstones are depleted in HREE which, according to Potter (1978a, b), is a feature of Na-rich granitic derivatives.

12.2.2. TRANSPORTATIONAL PROCESSES :

The length-breadth ratios of quartz grains of the Barail Group suggest short transportation of the sediments. The subrounded to subangular nature of the fine quartz grains also suggest transportation over short distances. According to Plumley (1948) rounding in case of finer grains require longer transportation.

The sediments were transported in uniform and graded suspensions, most probably by fluvial processes. FM, LM and AM diagrams of the finer sediments indicate that they are uniform suspension deposits (Passega and Byramjee, 1969). Two or more populations together are indicative of fluctuating current velocities (Passega, 1972, 1977). The values of mean size, skewness and kurtosis are moderately wide-ranging which are also indicative of fluctuations in energy conditions or changes in conditions of sedimentation (Rao, 1977; Venkatesh and Ray, 1981). The sorting of the Barail sandstones is more or less moderate. This is attributed to little reworking due to turbulent currents during sedimentation (Wigely, 1961; Visher, 1969). Fine positively skewed sands, such as those of the Barails, indicate relatively calm and steadily decreasing energy state of the depositing medium (Awasthi, 1970). The positive skewness is also attributed to unidirectional currents (Friedman, 1961; Martins, 1965). The coarse skewness is indicative of a high energy environment (Sahu, 1964). The Barail sediments were probably deposited by rivers with fluctuating velocities. The variability in the truncation points, much mixing and variable percentages of the suspension and saltation populations are attributed to fluctuating currents which may exist due to bed roughness and hydraulic factors (Visher, 1969). The high concentrations of the suspension population suggest rapid dumping of the sediments (Schumm, 1963) during the final phase of deposition (Singh and Bhardwaj, 1991). Catenae of zircon and tourmaline indicate that these are water-laid deposits. In case of the Barails attritional processes were minimum. Discriminant function analyses of the sandstones suggest that fluvial and turbidity currents were responsible for transportation of the Barail sediments. However, from other studies it is suggested that fluvial processes were dominant.

The laminations that are common in the Barail sandstones indicate fluctuating energy conditions in the depositional environment (Allen, 1970; Pettijohn, 1975), though particles of equal weight, density and shape moving along the bottom also tend to segregate forming laminations (Kuenen, 1966). Ripples, though not very common, are noted. Fluctuating currents have probably not allowed their development. The ripple indices indicate moderate to high velocity currents (Reineck and Wunderlich, 1968). The ripples are sinous and asymmetric, suggesting unidirectional currents. The base of the Barails are noted for their massive, thick bedded, multi-layered sandstones. Beds of this nature owe their origin to very rapid sedimentation (Reineck and Singh, 1980).

12.2.3. DEPOSITIONAL ENVIRONMENTS :

The Barail sandstones contain an abundance of stable minerals which indicate a passive continental margin (Folk, 1968). Chlorite and illite form a stable pair in near-shore environments at these margins (Millot, 1942; Mason, 1966). A passive margin is a tectonically stable area with lowered rates of heat flow and low geothermal gradients. Here, subsidence is rapid while terrigenous detritus is quickly buried (Siever, 1979). The high contents of K and Mg in sea water may be a probable cause of the development of some of the illite and chlorite respectively (Grim, 1968) of the Barails. The occurrence of illite and chlorite in the Barails, which are most probably fresh-water sediments, is suggestive of transgression and regression.

Mean size-standard deviation, skewness-standard deviation and skewness-kurtosis relationships suggest that the Barail sediments were deposited in a river environment. These sediments were probably deposited in a deltaic area. Mean size-standard deviation relationships suggest that the depositional basin was rapidly subsiding with low tectonic uplift of the source (Inman, 1952; Cadigan, 1961). Discriminant function analyses of these sediments indicate shallow agitated marine and fluvial environments.

SiO_2 and K_2O/Na_2O, and SiO_2/Al_2O_3 and K_2O/Na_2O relationships (Roser and Korsch, 1986) indicate a passive continental margin for the Barail sediments. The K_2O/Na_2O ratios of these sediments are greater than 1. Such values suggest deposition in plate interiors at passive margins (Bhatia, 1983) in exogeosynclinal environments (Middleton, 1960). Triangular plots of (Fe_2O_3 + MgO), Na_2O and K_2O also indicate an exogeosynclinal set-up. Being derivatives of older metamorphic and sedimentary sources (Middleton, 1960) these sediments are deposited in a near-shore environment (Blatt *et al.*, 1980). The boron contents of the Barails point to a marine environment as according to White (1970) this environment is enriched in boron. Ternary plots of B, Rb and Ga also suggest the same whereas binary diagrams of B and Ga, and that of B and Rb suggest marine, fresh-water and mixed environments respectively (Degens *et al.*, 1957). Marine transgression is probably responsible for the anomalous boron contents in the Barail sandstones. According to Goldschmidt (1954) gallium is highly mobile in the biogeochemical cycle. Its low occurrence suggests lack of biological activity (Sinha and Singh, 1964).

The moderate maturity of the Barail sandstones is noted in that they contain minor proportions of polycrystalline and strained quartz (Blatt, 1967). Length-breadth ratios of quartz also suggest the same (Bokman, 1952). Cr/V ratios

(Dykpiv, 1979) suggest that conditions of ventilation at the depositional site was good.

The rocks under study are chemically mature as indicated by the relative enrichment of K_2O over Na_2O and CaO (Middleton, 1960) and high TiO_2/Al_2O_3 ratios (Spears and Sotiriov, 1976). Low values of Na/Al and Na/K are suggestive of graywackes (Pettijohn, 1975). The sandstones of the Barail Group contain siliceous and ferrugenous cements, the former dominant. These cements, however, are scarce in the finer sandstones.

The Eu/Eu* ratios show both negative and positive values which indicate anoxic and oxic conditions respectively during deposition (Freyer, 1977). The presence of limonite and lack of pyrite suggest that conditions in the depositional environment was an oxidising one. Such variations are probably due to a sloping basin floor or uneven basin configuration. Ni/Co ratios suggest lowering Eh conditions in the depositional basin (Dykpiv, 1979). Compared to the Disang sandstones the Barails have higher ΣREE contents which is attributed to the high zirconium content. The Z.T.R. indices suggest moderate maturity of these sediments.

Load casts, as noted in some of the Barail rocks, develop due to unequal loading over underlying plastic layers. Ripples develop in the initial stages of the lower flow regime in a near-shore environment where particle motion is rippled and depth of water uniform (Pettijohn, 1975).

The Barail sandstones may be classed as litharenites to sublitharenites. These rocks are typical of an exogeosynclinal environment (Dapples _et al._, 1953). Subgraywackes (litharenites) are shallow-water deposits.

12.2.4. DIAGENESIS :

Most of the illite of the Barail sandstones are probably diagenetic alteration products of the feldspars (Grim, 1968, Pettijohn, 1975; Mack, 1978; Imam and Shaw, 1985). The excess of potassium of the feldspars is held by the illites (Keller, 1964). Some of the chlorites are probably alteration products of the illites but mostly that of primary micas. According to Selley (1976) chlorite is a characteristic constituent of the microcrystalline matrix of graywackes. Overgrowths of quartz are lacking in the Barail sandstones which may be attributed to the illitic and chloritic matrix acting as barriers against silica solutions from reaching the quartz detritals (Heald and Laresse, 1974). Deep-burial diagenesis causing pressure solution is inferred from the sutured edges of the micas.

12.3. CONCLUSION :

The Disang rocks under study are graywackes to subgraywackes. The sediments were derived as a result of rapid erosion from orogenic sources where climatic conditions were semi-humid to semi-arid. The provenance include granitic, volcanic (probably basaltic), low to medium grade metamorphic and sedimentary terrains. The Disang sandstones are texturally classified as silty sands and comprise uniform and saltation populations. They were transported over a short distance in uniform and graded suspensions by fluvial and turbidity processes, the currents of which were mainly unidirectional and constantly fluctuating. The Disangs of the area were deposited in an exogeosynclinal set-up that belonged to a passive continental margin. Sedimentation took place in a shallow marine environment with probably an undulating floor and/or shallowing of the basin due to which both reducing and oxidising conditions prevailed. The maturity and sorting of the sediments representing a transitional facies is poor to moderate. Iron oxides, some silica and a little calcium carbonate form the cements. Diagenesis, due to deep burial of the sediments, has modified the original mineralogy.

Immediately after the Disangs were deposited sedimentation of the Barails began with the deposition of massive, thick, multi-layered sandstones followed by thinner beds. These sediments, litharenites to sublitharenites with silica as the dominant cement followed by a little iron oxides, were derived mainly from a granitic source and to a lesser extent from low-grade metamorphic terrains. From studies conducted it is inferred that these moderately sorted sediments are recycled. The Barail sandstones are texturally classified as silty sands and comprise uniform and saltation populations which were transported over a short distance in uniform and graded suspensions by fluvial processes and probably to a minor extent by turbidity currents. The transporting currents were more or less unidirectional and constantly fluctuating. These sediments were deposited in an exogeosynclinal set-up of a passive continental margin. The depositional environment was probably a delta where oxidising conditions were dominant. Transgression and regression probably took place during Barail sedimentation. Deep-burial diagenesis, to some extent, has changed the original mineralogy of the rocks.

BIBLIOGRAPHY

Allen, J.R.L., 1970, Physical processes of sedimentation : an introduction. Earth Science Series, no. **1**. London, George Allen and Unwin.

Argast, S. and Donnelly, T.W., 1987, The chemical discrimination of clastic sedimentary components. Jour. Sed. Pet., **57**, 813-823

Awasthi, A.K., 1970, Skewness as an environmental indicator in the Solani River System, Roorkee, India. Sed. Geol., **4**, 177-183.

Basset, J., Denney, R.C., Jeffery, G.H. and Mendhan, J., 1982, Vogels text book of quantitative inorganic analysis (including elementary instrumental analysis). Longmans.

Bhatia, M.R., 1983, Plate tectonics and geochemical composition of sandstones. Jour. Geol., **91**, 611-627.

Bhattacharyya, A.R., 1984, A quantitative appraisal of heavy minerals from the arenaceous rock formations of a part of Kumaon lesser Himalaya. In Srivastava, R.A.K.,ed., Current trends in Geology : Sedimentary geology of the Himalayas, **5**, 121-130.

Blatt, H., 1967, Provenance determination and recycling of sediments. Jour. Sed. Pet., 37, 1031-1044.

Blatt, H., and Christie, J.M., 1963, Undulatory extinction in quartz of igneous and metamorphic rocks and its significance in provenance study of sedimentary rocks. Jour. Sed. Pet., **33**, 559-579.

Blatt, H., Middleton, G.V. and Murray, F.C, 1980, Origin of sedimentary rocks, 2nd. ed. Englewood Cliffs, New Jersey, Prentice Hall.

Bokman, J., 1952, Clastic quartz particles as indices of provenance : Jour. Sed. Pet., **22**, 17-24.

Brunnschweiler, R.O., 1966, On the geology of Indo-Burma Ranges. Jour. Geol. Soc. Aus., **13**, 137-194.

Cadigan, R.A., 1961, Geological interpretation of grain-size distribution measurements of Colorado Plateau sedimentary rocks. Jour. Geol., **69**, 121-144.

Carver, R.E., ed., 1971, Procedures in sedimentary petrology. New York, Wiley-Interscience.

Chayes, F., 1949, A simple point counter for thin section analysis. Am. Min., **34**, 1-11.

Choudhuri, R.S. and Gill, G.T.S., 1981, Heavy mineral assemblage of Siwalik Group of Nepal Himalayas. Jour. Geol. Soc. Ind., **22**, 220-226.

Cicha, I., Thomé, P.S., Janoschek, R. and Prey, S., 1968, Problems of Flysch and Molasse complexes. Int. Geol. Cong. (23rd session), Prague.

Condie, K.C., 1967, Geochemistry of Early Precambrian Graywackes from Wyoming. Geochim. Cosmochim. Acta, **31**, 2136-2147.

Coryell, C.D., Chase, J.W. and Winchester, J.W., 1963, A procedure for geochemical interpretation of terrestrial rare earths abundance patterns. Jour. Geophy. Res., **68**, 559-566.

Crook, K.A.W., 1974, Lithogenesis and geotectonics : the significance of compositional variation in flysch arenites (graywackes). In Dott, R.H. and Shaver, R.H., ed., 1974, Modern and ancient geosynclinal sedimentation. Soc. Eco. Pal. Min., Sp. pub., **19**, 304-310.

Cullers, R.L., Choudhuri, S., Kilbane, N. and Koch, R., 1979, Rare earths in size fractions and sedimentary rocks of Pennsylvanian-Permian age from the mid-continent of the U.S.A. Geochim. Cosmochim. Acta, **43**, 1285-1302.

Dapples, E.C., Krumbein, W.C. and Sloss, L.C., 1953, Petrographic and lithologic attributes of sandstones. Jour. Geol., **61**, 291-317.

Degens, E.T., Williams, E.G. and Keith, W.F., 1957, Environmental studies of Carboniferous sediments. Part 1 : Geochemical criteria for differentiating marine from freshwater shales. Am. As. Pet. Geol. Bull., **41**, 2427-2455.

Dickinson, W.R., Beard, L.S., Brakenridge, G.R., Erjavac, J.A., Ferguson, R.C., Inman, K.E., Knepp, R.A., Lindberg, E.A. and Ryberg P.T., 1983, Provenance of North American Phanerozoic sandstones in relation to tectonic setting. Geol. Soc. Am. Bull., **94**, 222-235.

Dickinson, W.R. and Suczek, C.A., 1979, Plate tectonics and sandstone compositions. Am. As. Pet. Geol. Bull., **63**, 2164-2182.

Directorate of Geology and Mining, Nagaland, 1978, Miscellaneous Publications, no. **1**.

Doty, R.W. and Hubert, J.F., 1962, Petrography and paleogeography of the Warrenburg Channel Sandstone, Western Missourie. Sedimentology, **1**, 7-39.

Dutta, S.K., 1982, Tertiary stratigraphy of Upper Assam. Jour. Pal. Soc. Ind., Sp. pub., **1**, 65-83.

Dutta, S.K., 1993, Personal communication.

Dykpiv, H., 1979, Mineralogy and geochemistry of the Mesozoic sediments of AndØya, Northern Norway. Sed. Geol., **24**, 45-67. In Sarmah, R.N., 1983, Sedimentology and geochemistry of the sandstones of the Disang and Barail Groups, Kohima, Nagaland. Unpublished Ph.D. Thesis, Gauhati University.

Dzulynski, S. and Walton, E.K., 1965, Sedimentary features of flysch and graywackes. Developments in Sedimentology, no. **7**. Amsterdam, Elsevier.

Emery, K.O. and Stevenson, R.E., 1980, Laminated beach sands. Jour. Sed. Pet., **20**, 220-223.

Evans, P., 1932, Tertiary succession in Assam. Trans. Min. Geol. Inst. Ind., **27**, 155-260.

Evans, P., 1959, Stratigraphy and tectonics of the Assam Oil-field region. E.C.A.F.E. Symposium (1958), New Delhi.

Evans, P., 1964, The tectonic framework of Assam. Jour. Geol. Soc. Ind., **5**, 80-96.

Evans, P., Hayman, R.J. and Majeed, M.A., 1934, The graphical representation of heavy mineral analysis. Quar. Jour. Geol. Min. Met. Soc. Ind., **6**, 27-47.

Evensen, N.M., Hamilton, P.J. and O'Nions, R.K., 1978, Rare-earth abundances in chondritic meteorites. Geochim. Cosmochim. Acta, **42**, 1199-1212.

Fairbridge, R.W., ed., 1972, The encyclopedia of geochemistry and environmental sciences. Encyclopedia of Earth Science Series, no. **4**(A). New York, Van Nostrand Reinhold Co.

Folk, R.L., 1951, Stages of textural maturity in sedimentary rocks. Jour. Sed. Pet., **21**, 127-130.

Folk, R.L., 1954, The distinction between grain size and mineral composition in sedimentary rock nomenclature. Jour. Geol., **62**, 344-359.

Folk, R.L., 1960, Petrography and origin of the Tuscarora, Rose Hill and Keefer Formations, Lower and Middle Silurian of eastern West Virginia Jour. Sed. Pet., **30**, 1-58.

Folk, R.L., 1968, Petrology of sedimentary rocks. Austin, Texas, Hemphills.

Folk, R.L. and Ward, W.C., 1957, Brazos River Bar : a study in the significance of grain size parameters. Jour. Sed. Pet., **27**, 3-26.

Freyer, B.J., 1977, Rare earth evidence in iron formations for changing Precambrian oxidation states. Geochim. Cosmochim. Acta, **41**, 361-367.

Friedman, G.M., 1961, Distinction between dune, beach and river sands from their textural characteristics. Jour. Sed. Pet., **31**, 514-529.

Friedman, G.M., 1967, Dynamic processes and statistical parameters compared for size frequency distribution of beach and river sands. Jour. Sed. Pet., **37**, 327-354.

Friedman, G.M. and Sanders, J.E., 1978, Principles of sedimentology. New York, Wiley and Sons.

Geological Survey of India, 1975, Miscellaneous Publications, no. **30**.

Goldschmidt, V.M., 1954, Geochemistry. Oxford, Clarendon Press.

Goswami, D.N.D., 1960, Geology of Assam. Dept. of Pub., Univ. Gauhati.

Griffiths, J.C., 1951, Size versus sorting in some Caribbean sediments. Jour. Geol., **59**, 211-243.

Grim, R.E., 1968, Clay mineralogy, 2nd. ed. New York, McGraw-Hill.

Handique, G.K. and Dutta, S.K., 1980, A study of the Surma-Tipam Groups of Upper Assam Valley, south of Brahmaputra. Jour. Pal. Soc. Ind, **25**, 42-50.

Handique, G.K., Dutta, S.K. and Neog, A., (In Press), Stratigraphy, depositional environment and hydrocarbon prospect in Moran oil-field, Upper Assam. Birbal Sahni Centenary Volume, Lucknow.

Hayden, H.H., 1910, Some coal fields in North-eastern Assam. G.S.I. Rec., **40**, pt. 4.

Heald, M.T. and Laresse, R.E., 1973, The significance of the solution of feldspar in porosity development. Jour. Sed. Pet., **43**, 457-460.

Heinrich, E.W., 1956, Microscopic petrography. New York, McGraw-Hill.

Herron, M.M., 1988, Geochemical classification of terrigenous sands and shales from core or log data. Jour. Sed. Pet., **58**, 820-829.

Hough, J.L., 1942, Sediments of Cape Cod Bay, Massachussetts. Jour. Sed. Pet., **12**, 51-70.

Hubert, J.F., 1962, A zircon-tourmaline-rutile maturity index and the interdependence of the composition of heavy mineral assemblages with the gross composition and texture of sandstones. Jour. Sed. Pet., **32**, 440-450.

Iman, M.B. and Shaw, H.F., 1985, The diagenesis of Neogene clastic sediments from the Bengal Basin, Bangladesh. Jour. Sed. Pet., **55**, 665-671.

Indian Standards Institution, 1963, Methods of chemical analysis of quartzite and high silica sand. IS : 1917-1962.

Inman, D.L., 1949, Sorting of sediments in the light of fluid mechanics. Jour. Sed. Pet., **19**, 51-70.

Inman, D.L., 1952, Measures describing the size distribution of sediments. Jour. Sed. Pet., **22**, 125-145.

Jackson, K.C., 1970, Text book of lithology. New York, McGraw-Hill.

Keller, W.D., 1964, Processes of origin and alteration of clay minerals. Soil clay mineralogy. Chapel Hill, North Carolina, The University of North Carolina Press. In Grim, R.E., 1968, Clay mineralogy, 2nd. ed. New York, McGraw-Hill.

Krishnan, M.S., 1968, Geology of India and Burma, 5th. ed. London, Higginbothams.

Krumbein W.C. and Aberdeen, E., 1937, The sediments of Barataria Bay. Jour. Sed. Pet., **7**, 3-17.

Krumbein, W.C. and Pettijohn, F.J., 1938, Manual of sedimentary petrography. New York, Appleton Century Co.

Krumbein, W.C. and Sloss, L.L., 1963, Stratigraphy and sedimentation, 2nd. ed. San Francisco, W.H. Freeman and Co.

Krynine, P.D., 1946, The tourmaline group in sediments. Jour. Geol., **54**, 65-87.

Krynine, P.D., 1950, Microscopic morphology of quartz types. In Doty, R.W. and Hubert, J.F., 1962, Petrography and paleogeography of the Warrenburg Channel Sandstone, Western Missourie. Sedimentology, **1**, 7-39.

Kuenen, Ph.H., 1966, Experimental turbidite lamination in a circular flume. Jour. Geol., **74**, 523-545.

Kukal, Z., 1968, Origin, development and chemical classification of Early Paleozoic sandstones of Central Bohemia. Int. Geol. Cong. (23rd session), Prague, section **8**, 61-72.

Lewis, D.W., 1984, Practical sedimentology. Stroudsburg, Pennsylvania, Hutchinson Ross Publishing Co.

Mack, G.H., 1978, The survivability of labile, light mineral grains in fluvial, aeolian and littoral marine environments : the Permian Cutler and Cedar Mesa Formations, Moab, Utah. Sedimentology, **25**, 587-604.

Mack, G.H., 1984, Exceptions to the relationship between plate tectonics and sandstone composition. Jour. Sed. Pet., **54**, 212-220.

Majumder, T., Pal, J.C. and Das, S.B., 1980, Trace element study of banded iron formation and associated rocks of Orissa. G.S.I. Sp. Pub., no. **1**, 587-597.

Mallet, F.R., 1876, On the coal fields of Naga Hills bordering Lakhimpur and Sibsagar districts, Assam. G.S.I. mem., **12**, pt. 2.

Martins, L.R., 1965, Significance of skewness and kurtosis in environmental interpretation. Jour. Sed. Pet., **35**, 768-770.

Mason, B., 1966, Principles of Geochemistry, 3rd. ed. New York, John Wiley and Sons.

Mason, B. and Moore, C.B., 1982, Principles of Geochemistry, 4th ed. Wiley and Sons.

Mathur, L.P. and Evans, P., 1964, Oil in Inida. Int. Geol. Cong. (22nd session), N.Delhi.

McLennan, S.M., 1989, Rare earth elements in sedimentary rocks : influence of provenance and sedimentary processes. Rev. Min., **21**, 169-200.

McLennan, S.M. and Taylor, S.R., 1991, Sedimentary rocks and crustal evolution : tectonic setting and secular trends. Jour. Geol., **99**, 1-21.

Millot, G., 1942, Rélations entre la constitution et la genèse des roches sédimentaires argileuses. Géologie Appliquée et Prospection Minière, **2**. Nancy, France. In Grim, R.E., 1968, Clay mineralogy, 2nd. ed. New York, McGraw-Hill.

Middleton, G.V., 1960, Chemical composition of sandstones. Geol. Soc. Am. Bull., **71**, 1011-1026.

Migdisov, A.A., 1960, On the titanium/aluminium ratio in sedimentary rocks. Geochemistry, U.S.S.R. (English translation), **2**, 178-194.

Mishra, U.K., 1988, Palaeontological study of the Disang and Barail sediments in parts of Kohima district, Nagaland. G.S.I. Rec., **122**, 76-77.

Moiola, R.J. and Weiser, D., 1968, Textural parameters : an evaluation. Jour. Sed. Pet., **38**, 45-53.

Moore, B.R. and Dennen, W.H., 1970, A geochemical trend in silicon-aluminium ratios and the classification of clastic sediments. Jour. Sed. Pet., **40**, 1147-1152.

Oldham, R.D., 1883, Report on the geology of parts of Manipur and Naga Hills. G.S.I. Mem., **14**, pt. 4.

Owen, M.R., 1987, Hafnium content of detrital zircon : a new tool for provenance study. Jour. Sed. Pet., **57**, 824-830.

Page, H.G., 1955, Phi-millimeter conversion table. Jour. Sed. Pet., **25**, 285-292.

Pascoe, E.H., 1912, Traverse across Naga Hills of Assam, from Dimapur to neighbourhood of Saramati Peak. G.S.I. Rec., **13**, pt. 4.

Passega, R., 1957, Texture as a characteristic of clastic deposits. Am. As. Pet. Geol. Bull., **41**, 1952-1984.

Passega, R., 1964, Grain size representation by CM patterns as geological tool. Jour. Sed. Pet., **34**, 830-847.

Passega, R., 1972, Sediment sorting related to basin mobility and environment. Am. As. Pet. Geol. Bull., **56**, 2440-2450.

Passega, R., 1977, Significance of CM diagrams of sediments deposited by suspension. Sedimentology, **24**, 723-733.

Passega, R. and Byramjee, R., 1969, Grain size image of clastic deposits. Sedimentology, **13**, 223-252.

Pettijohn, F.J., 1957, Sedimentary rocks, 2nd. ed. New York, Harper and Row.

Pettijohn, F.J., 1975, Sedimentary rocks, 3rd ed. New York, Harper and Row.

Pettijohn, F.J., Potter, P.E. and Siever, R., 1973, Sand and sandstones. Heidelberg, Springer-Verlag.

Plumley, W.J., 1948, Black Hills terrace gravels : a study in sediment transport. Jour. Sed. Geol., **56**, 526-577.

Poldervaart, A., 1955, Zircon in rocks - 1 : sedimentary rocks. Am. Jour. Sc., **253**, 433-461.

Potter, P.E., 1978a, Significance and origin of big river sands. Jour. Geol., **86**, 13-33.

Potter, P.E., 1978b, Petrology and chemistry of modern big river sands. Jour. Geol., **86**, 423-449.

Rao, M.V., 1977, Provenance and sedimentation of Pakhals. Jour. Geol. Soc. Ind., **18**, 31-39.

Reineck, H.E. and Singh, I.B., 1980, Depositional sedimentary environments, 2nd. ed. Berlin, Springer-Verlag.

Reineck, H.E. and Wunderlich, F., 1968, Zur Unterscheidung von asymmetrischen Oszillationsrippeln und Strömungsrippeln. Senckenbergiana lethaea, **49**, 321-345. In Reineck H.E. and Singh, I.B., 1980, Depositional sedimentary environments, 2nd. ed. Berlin, Springer-Verlag.

Roser, B.P. and Korsch, R.J., 1986, Determination of tectonic setting of sandstone-mudstone suites using SiO_2 content and K_2O/Na_2O ratio. Jour. Geol., **94.**, 635-650.

Sahu, B.K., 1964, Depositional mechanisms from the size analysis of clastic sediments. Jour. Sed. Pet., **34**, 73-83.

Sahu, N.K. and Naik, K.K., 1988, Geology of the area around Tseminyu-Pughoboto, Kohima and Zunheboto districts, Nagaland, G.S.I. Rec., **122**, pt. 4, 16.

Sahu, N.K. and Venkataswamy, 1990, Systematic geological mapping around Chiephobozou and Jukuleqa areas of Kohima and Zunheboto districts, Nagaland. G.S.I. Rec., **123**, pt. 4, 62-53.

Schumm, S.A., 1963, Sinuosity of alluvial channels on the Great plains. Geol. Soc. Am. Bull., **74**, 1089-1100.

Schwab, F.L., 1975, Framework mineralogy and chemical composition of continental margin type sandstones. Geology, **3**, 487-490.

Selley, R.C., 1976, An introduction to sedimentology. London, Academic Press.

Siever, R., 1979, Plate tectonic controls in diagenesis. Jour. Geol., **87**, 127-155.

Singh, A. and Bhardwaj, B.D., 1991, Textural attributes, depositional processes and heavy mineral study of the Ganga sediments between Hardwar and Kachhla. Ind. Geol. As. Bull., **24**, 41-54.

Sinha, R.C. and Singh, R.M., 1964, Distribution and behaviour of trace elements during the diagenesis of Vindhyan sediments near Robertsganj, U.P., India. Int. Geol. Cong. (22nd session), New Delhi, pt. **15**, 205-225.

Sinha, N.K., Chatterjee, B.P. and Satsangi, P.P., 1982, Status of palaeontological researches in north-eastern region. G.S.I. Rec., **112**.

Smithson, F., 1939, Statistical methods in sedimentary petrology. Geol. Mag., **76**, 417-427.

Spears, D.A. and Sotiriov, R.K., 1976, Titanium in some Carboniferous sediments from Great Britain. Geochim. Cosmochim. Acta, **40**, 345-351.

Suttner, L.J., 1974, Sedimentary petrographic provinces : an evaluation. In Ross, C.A., ed., Paleogeographic provinces and provinciality. Soc. Eco. Pal. Min. Sp. pub., **21**, 25-84.

Suttner, L.J. and Dutta, P.K., 1986, Alluvial sandstone composition and palaeoclimate - 1 : framework mineralogy. Jour. Sed. Pet., **56**, 329-345.

Taylor, S.R., 1965, Application of trace element data to problems in petrology. In Physics and geochemistry of the earth - **6**, 133-272. Oxford, Pergammon Press.

Thomas, R.L., Kemp, A.L.W. and Lewis, W.M., 1972, Distribution, composition and characteristics of the surficial sediments of Lake Ontario. Jour. Sed. Pet., **42**, 68-84.

Twenhofel, W.H. and Tyler, S.A., 1941, Methods of study of sediments. New York, McGraw-Hill.

Van Andel, T.H., 1959, Reflections on the interpretation of heavy mineral analysis. Jour. Sed. Pet., **29**, 153-163.

Velbel, M.A., 1985, Mineralogically mature sandstones in accretionary prisms. Jour. Sed. Pet., **55**, 685-690.

Venkatarathnam, K. and Rao, A.T., 1968, Zircon from beach sands along east coast of India. Jour. Min. Soc. Ind, **9**, 20-29.

Venkatesh, K.V. and Ray, I., 1981, Grain size variation in the sediments off Tuticorin harbour, Tamil Nadu. Jour. Geol. Soc. Ind., **22**, 181-189.

Visher, G.S., 1969, Grain size distributions and depositional processes. Jour. Sed. Pet., **39**, 1074-1106.

Waugh, B., 1970, Petrology, provenance and silica diagenesis of the Penrith Sandstone (Lower Permian) of North-west England. Jour. Sed. Pet., **40**, 1226-1240.

Weaver, C.E., 1958, Geologic interpretation of argillaceous sediments, pts. 1 and 2. Am. As. Pet. Geol. Bull., **42**, 254-271. In Krumbein and Sloss, 1963, Stratigraphy and sedimentation, 2nd. ed. San Francisco, W.H. Freeman and Co.

Weaver, C.E., 1967, The significance of clay minerals in sediments. In : Fundamental aspects of petroleum geochemistry. Amsterdam, Elsevier Pub. Co., 37-76.

White, S.M., 1970, Mineralogy and geochemistry of continental shelf sediments off the Washington-Oregon coast. Jour. Sed. Pet., **40**, 38-54.

Wigley, R.L., 1961, Bottom sediments of Georges Bank. Jour. Sed. Pet., **31**, 165-188.

Wildeman, T.R. and Haskin, L.A., 1973, Rare earths in Precambrian sediments. Geochim. Cosmochim. Acta., **37**, 419-438.

Wilson, G.F. and Metre, W.B., 1953, Assam and Arakan. In : Science of petroleum, **6**, no. 1. London.